AD-A133 733 RESEARCH IN ADAPTIVE BEAMFORMING FOR SATELLITE COMMUNICATIONS(U) PENNSYLVANIA UNIV PHILADELPHIA F HABER ET AL. MAY 83 RADC-TR-83-54 F30602-81-K-0211 1/3

UNCLASSIFIED F/G 17/2 NL

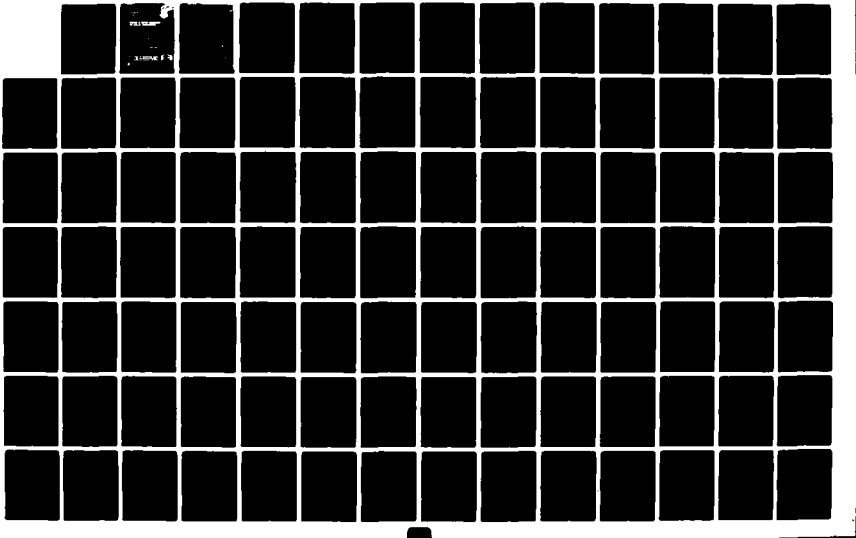

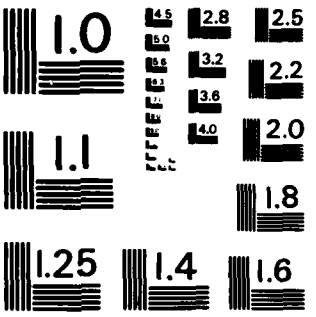

UNCLASSIFIED

SECURITY CLASSIFICATION OF THIS PAGE (When Data Entered)

REPORT DOCUMENTATION PAGE	READ INSTRUCTIONS BEFORE COMPLETING FORM
1. REPORT NUMBER: RADC-TR-83-54	2. GOVT ACCESSION NO.: AD-A133733
3. RECIPIENT'S CATALOG NUMBER:	
4. TITLE (and Subtitle): RESEARCH IN ADAPTIVE BEAMFORMING FOR SATELLITE COMMUNICATIONS	5. TYPE OF REPORT & PERIOD COVERED: Final Technical Report 1 Nov 81 - 31 Oct 82
	6. PERFORMING ORG. REPORT NUMBER: N/A
7. AUTHOR(s): Professor Fred Haber, Charles Bono, Professor Yeheskel Bar-Ness, Paul Chien-Chung Yeh	8. CONTRACT OR GRANT NUMBER(s): F30602-81-K-0211
9. PERFORMING ORGANIZATION NAME AND ADDRESS: University of Pennsylvania, 409 Franklin Building, 3451 Walnut Street, Philadelphia PA 19104	10. PROGRAM ELEMENT, PROJECT, TASK AREA & WORK UNIT NUMBERS: 62702F, 45196324
11. CONTROLLING OFFICE NAME AND ADDRESS: Rome Air Development Center (DCCR), Griffiss AFB NY 13441	12. REPORT DATE: May 1983
	13. NUMBER OF PAGES: 246
14. MONITORING AGENCY NAME & ADDRESS(if different from Controlling Office): Same	15. SECURITY CLASS. (of this report): UNCLASSIFIED
	15a. DECLASSIFICATION/DOWNGRADING SCHEDULE: N/A

16. DISTRIBUTION STATEMENT (of this Report)

Approved for public release; distribution unlimited.

17. DISTRIBUTION STATEMENT (of the abstract entered in Block 20, if different from Report)

Same

18. SUPPLEMENTARY NOTES

RADC Project Engineer: Walter J. Bushunow (DCCR)

19. KEY WORDS (Continue on reverse side if necessary and identify by block number)

Random Arrays	Pointing Vector
Satellite Antennas	LMS Interference Canceller
Spatial Filtering Algorithms	Steering Phase Error
Hybrid Arrays	Reference Generating Loop

20. ABSTRACT (Continue on reverse side if necessary and identify by block number)

The results of an investigation of adaptive interference cancelling techniques for use with satellite borne arrays of sensors are presented in the report. A "Hybrid Array" utilizing both a pointing vector and an internally generated reference is analyzed. The steady state and transient properties of the processor are presented showing speed of response, signal to interference plus noise ratio, and reduced sensitivity to pointing errors over schemes heretofore used.

DD FORM 1 JAN 73 1473 EDITION OF 1 NOV 65 IS OBSOLETE

UNCLASSIFIED

SECURITY CLASSIFICATION OF THIS PAGE (When Data Entered)

Also developed is the sensitivity to random amplitude and phase error in the pointing vector. A means by which the pointing vector can be obtained utilizing a pilot ground source is described and analyzed.

In addition, analyses are presented on improved methods using only an internally generated reference. One scheme is analyzed in which non-oscillatory weights are obtained even when an imperfect reference is generated. This analysis is carried out assuming no interference, paralleling earlier work on a related scheme in which oscillatory weights were obtained. A second analysis is presented on a method which corrects the cause for unstable weights. This anlaysis is carried out with desired signal, interference, and noise present.

TABLE OF CONTENTS

RESEARCH IN ADAPTIVE BEAMFORMING FOR SATELLITE COMMUNICATIONS

1. INTRODUCTION

Reported below are the results of a study carried out in the interval, November 1, 1981 - October 31, 1982 on adaptive beamforming and interference cancelling in large sparse satellite-borne arrays. The application in mind is the uplink of a communication satellite using beam-switching to ground users who may be close to potential interferers. In an earlier exploratory study, [1], the use of large sparse arrays was examined, giving their anticipated benefits and describing their problems. In brief, the array size is made large to put potential interferer on the quiescent pattern sidelobes where they can be suppressed effectively; it is made sparse to keep system complexity within bounds. Large size is usually attended by element position uncertainty so that forming accurate steering vectors toward desired sources becomes a problem; both, beam placement error and random error in forming the pointing vector phasors were anticipated. A processing system configuration, including alternative processing schemes was, nevertheless, found and this became the focus of the study reported here.

In section (2) below we present a technical summary of the study and its results. Detailed reports on which this summary is based are given in the Appendices of this document. Section 3 contains the conclusions and recommendations for further study.

2. TECHNICAL SUMMARY

2.1 Hybrid Array Analyses

The principal part of our work dealt with the properties of an array processing scheme which we term the "Hybrid Array". It is a

composite of the Howells-Applebaum processor which utilizes known direction of signal arrival, and the Widrow-Compton processor which uses a reference signal extracted from the incoming field through its known superimposed spread-spectrum code. This concept was arrived at by first supposing that rapid beam switching is achieved with a processor that utilizes pointing vector injection, then, recognizing that such arrays are highly sensitive to pointing vector errors, ways were sought to overcome the effect of such errors. The addition of a self-generating reference circuit which makes use of known signal structure, was conjectured to be one such way. An alternative scheme which bootstraps a pointing correction was also conceived, but remains to be analyzed. Analyses and simulations of the Hybrid Array were carried to determine its steady state and transient properties, and the improvement it provides when subjected to pointing error. The latter includes error in orienting the main beam toward the desired source, and independent phase errors in the pointing vector tending to defocus the main beam.

2.1.1 Steady State Behavior of Hybrid Array

Appendix A gives the results of the steady state analysis with the array processor shown in Figure 1, and the principal result shown in Figure 2. The latter shows the effect on the output signal to noise ratio (SNR) of adding the reference generating circuit to an Applebaum array in which the steering vector may be pointed off target. ρ is a measure of perfection of the reference generating circuit and ε is a measure of the pointing error. The loss in SNR with pointing error, and the decreasing sensitivity to pointing error as the reference generator approaches the ideal, is evident from these curves. With $\rho=1$, meaning that the reference generator perfectly matches the desired signal output so that the residue ε_f (see Figure 1) contains no signal, the effect of pointing error is

essentially the same as it would be in a focused nonadaptive array. The Applebaum Array which is a limiting case of the hybrid array with the lowest value of ρ is therefore poorer than the Hybrid Array for any pointing error.

Figures 4 through 8 of Appendix A show the results of computations carried out with a 7 element array comprised of non-uniformly spaced elements for a wide variety of conditions. The parameter F_s represents the amplitude and phase of the reference relative to the signal component entering the reference generator; $F_s=1$ is ideal. Typically, one might expect the reference amplitude to be a few percent away from ideal and several degrees off in phase. For such departures from ideal the curves all show a substantial reduction of sensitivity to pointing error over the Applebaum Array (the $F_s=0$ case). It should be noted that cases of multiple interferers and interference inside the main lobe of the quiescent array are included in these results.

The observed behavior can be explained by examining the analytical results. Without reference, the array processor treats the desired signal as interference when pointing is inaccurate. With perfect reference, the mechanism which marks the incoming signals for suppression (the covariance matrix of the array element outputs, less a constant times the covariance matrix of the desired signal alone) has the signal component removed by the action of the reference. As a consequence there is no tendency to suppress it when there is pointing error, though there is the normal loss that one would encounter in a miss-aimed conventional beamforming array. With imperfect reference, some vestige of signal remains in the suppression mechanism. The tendency to suppression is blunted but

not totally eliminated. The conclusion to be drawn form these results is that the Hybrid Array is a significant improvement over the directionally constrained array though it may fall short of ultimate perfection as it stands.

2.1.2 Transient Behavior of Hybrid Array

The results of analysis and simulation of the transient behavior of the Hybrid Array are given in Appendix B. Because there are two filters in the Hybrid Array, one in the sidelobe canceller weight setting loop and one in the reference generator, two coupled set of differential equations result. Both filters are assumed to be of first order in this analysis. By assuming that the weight setting loop is much slower than the reference generator, one set of equations can be solved without involving the other. The result is that a single set of first order linear differential equations with time variable coefficients is obtained for the time variable weights in the sidelobe canceller. Explicit solution of the output transient SINR for an N-element array remains to be carried out. We have however dealt more completely with the two-element array. The instantaneous values of the single complex weight was obtained in this case. From this, one can with some calculation determine the response as a function of time.

Simulations were carried out on the two-element array with $\lambda/2$ spacing assuming a signal and one interferer present. Results were obtained with and without noise. The signal was taken to be modulated with a spread spectrum code and the interference was taken to be a pure sinusoid. The array processor was assumed perfectly synchronized to the spectrum spreading code so that the transient behavior observed concerns only the response of

the weight setting loop and the reference generator. Runs were made with various sets of parameter values, input amplitudes, and pointing angles. Parameter values could be found with which convergence of the signal to interference (and noise, where applicable) ratio occurs in a fraction of the bit interval provided the pointing angle is not greatly in error. We found, for instance, that pointing errors up to 5^{o} could be tolerated but with a 20^{o} error convergence was slowed to the point where the output signal to interference ratio never reaches an adequate level.

In our simulations idealized signal pulses are used with zero rise time. Clearly the filter in the reference generator will not follow such an input so that at the beginning of each signal polarity reversal a substantial difference exists between signal input and output of the reference generator. This reflects itself as a sudden drop in signal to interference ratio of the array output. The processor overcomes this effect in less than half the pulse interval in the examples simulated, but this effect will reduce the receiver output quality. The loss can be overcome by an increase in transmitted power of the order of 3dB. Or, the weight obtained at the end of the first signal interval can be frozen for the duration of the transmission. The latter approach may, however, not be acceptable in the case of blinking interferers where nulls may have to be moved during the brief interval of a users on-time.

As a check on the analytical work, comparisons were made between the transient weight variation obtained by analysis and by simulation. The results matched very well suggesting that certain approximations used in the analysis are valid.

2.1.3 Effect of Random Errors in Pointing Vector on Steady State Behavior

In Appendix C an analysis is reported on the effect of random phase and amplitude errors on the steady state signal to interference plus noise ratio of the Hybrid Array. The analysis reported previously [1] on the effect of pointing error was concerned with correlated deviations in the phases of the pointing vector components which result in a shift of the direction of focus. This sort of error will occur where there is uncertainty in the signal arrival direction. For the case treated now the direction of arrival is assumed known correctly but the amplitudes and phases of the components of the pointing vector generated by the processor are assumed subject to independent errors. Such errors may be a consequence of circuit inadequacies, quantization errors when digital processing is done, and element position uncertainties. In section 2.2 below we will discuss an analysis of a method for estimating the pointing vector by calibrating to a pilot station then steering to the desired ground user. It is inevitable that this estimation procedure, like any other such procedure, is less than perfect and the principal point of that study is to find the error in the pointing phases so determined.

Results were obtained from which the SINR as a function of phase and amplitude standard deviations can be obtained; the reference generator quality parameter, F_s, and the number of elements, N, are principal parameters in the results. The analysis was carried out for a version of the Hybrid Array derived from a variant of the Applebaum Array in which the signal output magnitude is not constrained (See Figure 2 of Appendix C for this version; the version based on the constrained Applebaum Array is shown in Figure 1 of Appendix C.). Calculations were carried out

for the ratio of mean signal power output to mean noise power output (i.e., interference was not included) as a function of the standard deviation of amplitude and phase for arrays of 7, 30, and 100 elements and for values of F_s ranging from 1 (perfect reference) to 0 (no reference, identical to Applebaum Array). The results shown in Figures 3-8 of Appendix C were similar to those obtained for the case of error in pointing.

With no reference the loss of SNR is substantial and with perfect reference the loss is zero. With reference within 5% in amplitude and 10^{o} in phase the loss is generally small enough to be acceptable in the case of the 7 element array. Of great interest, though, is the effect of increasing the number of array elements. The sensitivity to the random errors increases with increases in number of array elements. In particular, in the case of a 30 element array, the loss is substantial unless the reference generator is close to perfect, or the errors in phase and amplitude are very small. We point out though that the improvement over the Applebaum Array is great in all cases of random pointing error.

Because the analysis was carried out for the unconstrained version of the Hybrid array (as shown in Figure 2 of Appendix C) we compared calculated results for SNR of the 7 element array for unconstrained and constrained versions (the latter as in Figure 1 of Appendix C). The differences were found to be only slight so that we are inclined to view the other results obtained as being approximately applicable to both arrays.

2.2 Pointing Vector Estimation

We examined a method for estimating the pointing vector to a desired source when interferers may be close to the desired source and the array element positions are not perfectly known. The procedure is based on the beamforming and scanning processes. The analysis of the method appears in Appendix D, below.

First, the array generates a pointing vector at the reference beacon by the use of a reflector antenna. The assumption is made that interferers are seen by this antenna only through its sidelobes and that sidelobe levels are reasonably low. The pointing vector is determined by correlating array outputs with the output of the reflector antenna. The vector obtained in this way has a bias caused by some residual interference at the reflector antenna output correlating with the interference at array element outputs. There is also a random component which is averaged out if the integration time is long enough. Analysis shows that both of these errors can be treated as random phase errors. For integration time long enough, the standard deviation of those random phase errors is about 5×10^{-4} radian if there is one interferer with the same power as the beacon source and if the sidelobe reduction is 30dB.

The second step is to steer the array from the beacon source to the desired ground source by using the information on angular displacement between them and the imperfect information on array element positions. The total error in the pointing vector aimed at a desired user is the sum of the error in beamforming and that in steering. For a seven element 10λ Hybrid Array with $F_s=0.95$ and SNR = 10 at input, the tolerance of element position is about 0.44λ for 1dB output SINR loss if the error in beamforming on the beacon is 5×10^{-4} radian. If the error induced in steering can be eliminated, the error of 5×10^{-4} radians causes a negligible loss in SINR for $F_s=0.95e^{-j10^{o}}$.

2.3 LMS Interference Canceller with Reference Generator

Appendix E contains an analysis of an LMS adaptive array processor which utilizes a self-generated reference only; that is, one which does not use direction of signal arrival information. An array processor to accomplish this is described by Compton (reference [3], Appendix E) and the problem of weight cycling encountered with this scheme is analyzed by DiCarlo and Compton (references [4], [5], Appendix E). We have here analyzed two variants of the Compton scheme both of which differ from the original in that one element is left unweighted and limiters in the reference generators are omitted. The difference between the two schemes analyzed here resides in how the reference generator is driven.

It is shown in Appendix E that simple and attainable conditions exist for the weights to converge to a constant value. Also, the SNR for the two schemes devised is obtained. In one scheme, where the reference generator is driven by the output of all array elements, the SNR turns out to be generally low - as low in some cases as the SNR of a single element. The other realization, in which the reference generator is driven by the output of the weighted elements only, the output SNR is the full value expected out of (N-1) coherently combined element outputs; N is the number of array elements.

We point out that the earlier analyses by DiCarlo and Compton and the analysis of Appendix E were carried out without interference present.

2.4 Effect of Interference on the Behavior of the LMS Array with Internally Generated Reference

As pointed out in section 2.3 above the published analyses on the subject of adaptive arrays with internally generated reference were carried out with a single signal and independent element noise only; that is, interference was not considered. In Appendix F the earlier analyses are extended to include interferers.

The array processing scheme of DiCarlo (reference [4] Appendix F) is assumed, along with the phase shift compensation scheme of Bar-ness (reference [3] Appendix F). The analytical difficulties which arise with interference present is associated with the greater complexity of the covariance matrix with more than one signal present. The covariance matrix of the multiple signals is of rank equal to the number of signals. The uncoupling of the resulting simultaneous differential equations presented difficulty though a transformation was found which made it possible to separate the effects of desired signal and interference.

It is here shown that the phase shift compensation is effective in the multiple interference case and that weight cycling can be avoided. The conditions to be satisfied though have not yet been found for the general case. One expects the conditions and the transient behavior of the array to be affected by the relative levels of the incoming signals and on their arrival directions. It was possible however to get an explicit condition for convergence in the case of a single interferer in addition to the desired signal.

Further work is to be done on the conditions for convergence in multiple interference as well as on convergence rates and achievable signal to interference plus noise ratios.

3. CONCLUSIONS AND RECOMMENDATIONS

We have seen that the Hybrid array processor is a substantial improvement in the steady state over an array using only direction of arrival information when systematic or random errors are encountered in the focusing phases and amplitudes. The transient analysis also suggests that if signal structure alone is used to drive the adaption process the response time will be greater than with the Hybrid Array. We point out that the Hybrid Array as described here does not suffer from the weight cycling problem associated with some processors which utilize known signal structure to self-generate a reference. Though we have not dealt with the problem of code aquisition time in this work it is to be noted that the use of a pointing vector, even an approximate one, insures a reasonably large signal component immediately from which the code aquisition circuit can more readily extract synchronizing information.

We have analyzed a pointing vector estimation method based on the use of a pilot source sufficiently out of the way of interferers. We have derived the estimation errors and with the pointing error sensitivity of the Hybrid processor, we have demonstrated feasibility of the scheme.

Finally, we have extended previous work on adaptive processing utilizing signal structure alone to self-generate a reference. Schemes were devised and analyzed which can be prevented from generating oscillating weights, and the behavior of such arrays in the presence of interfering sources has been analyzed.

The work carried out leads us to make a number of recommendations for further study.

While the Hybrid Array promises significant improvement over earlier schemes it depends on being able to generate a good reference. What is needed is either a mechanism for insuring that the self-generated reference is near perfect or a mechanism for correcting the steering vector. A possible circuit to accomplish this by the addition of another steering phase correction feedback loop for a two-element configuration had been conceived before [1]. Variants to accomplish this same end have been devised since then. These schemes should be further pursued. It may also be valuable to pursue methods of steering correction in one of the Applebaum arrays - that is, with processors which do not generate a reference internally. In addition, or as an alternative, ways should be devised for controlling the reference generator output through a feedback loop to minimize the signal component in the residue.

The improvements obtained with the Hybrid Array can be viewed as a consequence of utilizing more information about the desired signal than heretofore: the general problem of how to make optimal use of other bits of prior information is worth considering. For instance, approximate location of interferers, or their signal structure may also be known. There is also additional prior information regarding the desired signal which is potentially useful - the waveforms and error control codes used, for instance. This also leads to the question of how to design signals which will most effectively aid the array focusing mechanism.

We had originally adopted the view that the array size to be used would be sufficiently large to put potential interferers out of the main beam of the quiescent array pattern.

We have nevertheless obtained some computational results for the Hybrid Array assuming interferers well inside the beamwidth. Naturally, the SINR was found to be adversely affected. There is reason to expect that the SINR with main-beam interference is to some extent dependent on array element layout. The problem of element layout was one of the items considered originally by us but ruled out as a significant factor for large arrays with no main-beam interference. Since close interfers cannot be ruled out totally the effect of main-beam interference and its dependence on element layout ought to be considered.

The schemes with which we have dealt are all narrowband; that is, they utilize complex non-frequency dependent weights prior to element output combining. As long as the time displacement of signals seen by the different elements is small relative to the inverse of the signal bandwidth this method is satisfactory. For broadband signals, and/or for wavefronts arriving at angles very far off array broadside this may not be the case. Ways of extending the methods here described to wideband signals would be useful.

One of the principal advantages we see in arrays utilizing directional information in addition to signal structure information is the potential for high speed beam switching. We have verified fast convergence of the Hybrid Array with an interferer present in a particular location. However, the functioning of the array in a rapidly changing dynamic environment of multiple desired sources and dispersed blinking interferers requires further attention. One can imagine a simulation experiment with such a scenario. Also deserving attention for multiple access applications is the use of multiple directional constraints in which two or more simultaneous beams are focused.

REFERENCES

1. F. Haber, et al. "Applications of Self-Organizing Random Arrays to Communication Satellites". Report on Contract F30602-80-C-0230 with Interspec, Inc., Philadelphia, PA 19104. Rome Air Development Center report RADC-TR-81-248. Feb. 1982.

Appendix A

STEADY STATE BEHAVIOR OF HYBRID ARRAY

by

F. Haber, Y. Bar-ness, C. C. Yeh

Abstract

The steady state properties of an adaptive array utilizing prior knowledge of both approximate signal arrival direction and signal characteristics are here presented. The method combines the features of a directionally constrained array and one with a self-generated reference signal. Explicit results are obtained for output signal, interference, and noise powers assuming a single interferer is present. The inclusion of a self-generated reference circuit is shown to reduce the sensitivity to pointing error typical of arrays utilizing a zero order directional constraint, the improvement being a consequence of the reduction of the desired signal component fed back to the sidelobe cancelling circuit. A relationship between the degree of sensitivity reduction and the quality of the reference signal is developed. Results of computations of signal to interference plus noise ratios for a 7-element 10 wavelength non-uniformly spaced array as a function of pointing error are presented. These results show the behavior with one interferer inside and outside the beamwidth of the quiescent array, and with multiple interferers, for various degrees of perfection of the reference generating circuit. In all cases the computations confirm that the otherwise severe effects of small pointing errors are substantially reduced.

This research is supported by Rome Air Development Center under Contract No. F30602-81-K-0211.

AN ADAPTIVE INTERFERENCE CANCELLING ARRAY UTILIZING HYBRID TECHNIQUES

TABLE OF CONTENTS

INTRODUCTION

Adaptive arrays suitable for use in communication systems can be categorized according to the prior information utilized to distinguish desired from undesired signals. One scheme described by Applebaum and Chapman [1] is suited to point-to-point communication where direction of signal arrival is known; the directional information, through an input steering vector, constrains the array gain in this direction, maximally rejecting other, unwanted sources.* Another scheme, based on a concept by Widrow, et. al. [2] recognizes the desired signal via an externally supplied reference. For communication use, an extension of the latter was made by Compton, et. al. [3, 4] wherein the reference is internally generated utilizing some prior known signal structure information (e.g., the spread spectrum code superimposed on the signal).

One of the principal shortcomings of the first method, the directionally constrained method, is that small pointing errors result in large losses in the output signal to interference plus noise ratio (SINR). An analysis of this effect was made by Compton [5] and was reinforced by results obtained by us [6]. Unfortunately, pointing error is endemic in many applications where direction of arrival is ostensibly known. The second method is however not free of difficulties among which are problems relating to imperfect reference generation [7, 8]. Furthermore, one expects better transient response using the directionally constrained scheme because a substantial signal power becomes immediately available at the array output on injection of an approximately correct steering vector.

* With a constraint on the gain in a chosen direction the array is said to be zero order directionally constrained [1].

A comparison study of these two methods [9] suggested that the two can be made to complement one another and has led us to look at hybrid schemes which take advantage of both kinds of prior information--directionality and signal structure. We present below analyses and computational results of the steady state properties of one such scheme as defined in Figure 1. The array processor is represented in a form similar to that in Applebaum and Chapman [1, Figures 2 and 4] with the addition of a reference generating loop. We treat the case of narrow-band information bearing signals for both desired and undesired arrivals so that steering and nulling operations are carried out by control of amplitudes and phases of $\underline{s}$ and $\underline{y}$ respectively, at band center. Furthermore, we assume the reference generating circuit is operating in the synchronous mode with respect to the desired signal; the acquisition circuit for code timing is therefore not shown.

2. ANALYSIS

The array system under consideration is shown in Figure 1. Output signals from the array elements are represented by the complex vector

$$\underline{v}(t) = \alpha(t)\underline{s}_d + \sum_{j=1}^{J} \beta_j(t)\underline{s}_{Ij} + \underline{n}(t) \tag{1}$$

where $\underline{s}_d$ is the arrival phase vector of the desired signal comprised of N unit amplitude components, $\alpha(t)$ is its complex envelope; s_{Ij} is the arrival phase vector of the $j^{\underline{th}}$ interference signal, $\beta_j(t)$ is its complex envelope; and $\underline{n}(t)$ is the complex noise envelope vector, the components of which are assumed independent. If, for instance, the elements are arranged along the x-axis at positions x_i, $i = 1,2,\ldots N$, a desired signal arriving as a plane wave with its plane of arrival at an angle θ_d relative to the x-axis induces signal components

$$\alpha(t)s_{di} = \alpha(t)\exp(jkx_i\cos\theta_d),\ i = 1,2,\ldots N \tag{2}$$

in the array elements. $s_{di} = \exp(jkx_i\cos\theta_d)$ is the $i^{\underline{th}}$ unit amplitude component of $\underline{s}_d$. The rf wave at the $i^{\underline{th}}$ element is given by $v_i(t)\exp(j\omega t + \phi)$. The desired signal component at the i^{th} element, as represented by (2), has the carrier exponential suppressed.

The beamformer defined by the steering vector, $\underline{s}^*$ in Figure 1 generates an output given by the inner product of $\underline{s}^*$ and $\underline{v}$ given by (1); that is,

$$e_m = \underline{s}^{T*}\underline{v} \tag{3}$$

(the time variable in e_m and $\underline{v}$ is omitted but implied). The output of the

system is given by

$$e_o = e_m - \underline{y}^T \underline{u} \tag{4}$$

where $\underline{y}$ is the weight vector on the sidelobe canceller and

$$\underline{u} = A\underline{v} \tag{5}$$

A is an (N - 1) x N matrix of rank (N - 1) chosen such that $A\underline{s} = \underline{0}$; and, as a consequence, such that signals arriving with direction vector $\underline{s}$ do not contribute to $\underline{u}$. (3), (4), and (5) together give

$$e_o = \underline{s}^{T*}\underline{v} - \underline{y}^T A\underline{v} = (\underline{s}^* - A^T\underline{y})^T\underline{v} \tag{6}$$

Following Applebaum and Chapman [1] the equivalent weight vector $\underline{w}$ is defined by

$$e_o = \underline{w}^T\underline{v} \tag{7}$$

so that from (6)

$$\underline{w} = \underline{s}^* - A^T\underline{y} \tag{8}$$

Because of the way A is chosen this weight vector $\underline{w}$ insures the response in the direction of $\underline{s}$. That is, premultiplying (8) by $\underline{s}^T$ we have

$$\underline{s}^T\underline{w} = \underline{s}^T\underline{s}^* - \underline{s}^T A^T\underline{y} = N \tag{9}$$

In (9) we have used $\underline{s}^T\underline{A}^T\underline{y} = \underline{y}^T\underline{A}\underline{s} = 0$, and $\underline{s}^T\underline{s}^* = N$, the number of elements.

The weight vector of the sidelobe canceller is formed via a circuit which typically approximates the LMS algorithm using steepest descent search. In the steady state that weight vector is given by

$$\underline{y} = g\,\overline{\underline{u}^*(e_o - e_r)} \tag{10}$$

where e_r is the reference signal as identified in Figure 1 and g is the gain in the weight setting loop. The overbar stands for expected value.

The reference signal is assumed formed from the array output e_o by despreading using the desired signal's spread spectrum code, filtering, and respreading using the same code. In the process, interferers in whatever form they initially appear (i.e., wideband or narrowband) are reduced to a broadband low power spectral density noise. e_r is therefore viewed as being comprised of a component closely similar to the desired signal and a noise component, denoted n_r; that is,

$$e_r = F_s e_{od} + n_r \tag{11}$$

where e_{od} is the signal component of e_o and F_s is an operator representing the effect of the bandpass filter on the desired output signal component. We will specialize it in our work to a complex constant implying a phase and amplitude shift only.

Utilizing these preliminaries, the equivalent weight vector from which the output response is determined by (7), is shown in Appendix A to be given by (see A-12, A-13),

$$\underline{w} = \mu M_1^{-1} \underline{s}^* \tag{12}$$

where

$$M_1 = M - \overline{|\alpha|^2} F_s M_d \tag{13}$$

and

$$\mu = \frac{N}{\underline{s}^T M_1^{-1} \underline{s}^*} \tag{14}$$

M and M_d are defined by (15) and (16) below. When F_s=0 the hybrid array reduces to the conventional directionally constrained array and the weight vector as given by (12) reduces to $\underline{w} = \mu M^{-1} \underline{s}^*$.

We now examine the implications of the change brought about by inclusion of the reference generating circuit. From (1) we write for the covariance matrix of the inputs

$$M = \overline{\underline{v}^* \underline{v}^T} = \overline{|\alpha^2|} M_d + \sum_j \overline{|\beta_j^2|} M_{Ij} + M_n \tag{15}$$

where

$$M_d = \underline{s}_d^* \underline{s}_d^T \tag{16}$$

and

$$M_{Ij} = \underline{s}_{Ij}^* \underline{s}_{Ij}^T \tag{17}$$

$$M_n = \overline{\underline{n}^* \underline{n}^T} = \sigma_n^2 I \tag{18}$$

(15) is obtained using the assumed independence of all separately arriving signals (desired, undesired and noise) and the independence among the noise components. With M_1 as given by (13) we see that the effect of the self-generated reference signal is to alter the contribution of the desired signal component to the covariance matrix by a factor $(1-F_s)$. When $F_s = 1$, M_1 has, in fact, no component due to signal. We point out that the field environment is communicated to the array processor via the matrix

M in the conventional directionally constrained array. The tendency of the array processor is to suppress all signals recorded in the matrix M--except for the signal coming from the constraint direction defined by the steering vector $\underline{s}$. If $\underline{s}$ is different from the direction of the desired signal represented by $\underline{s}_d$ the processor deals with it as if it were an unwanted signal, suppressing it substantially even for small differences of angle. The effect of removing the desired signal contribution to M, or of reducing its influence on M by making F_s close to unity, is to reduce the tendency to suppression of the desired signal when $\underline{s}$ and $\underline{s}_d$ are not coincident. This may be seen most easily by imagining only a single signal present with arrival direction inherent in $\underline{s}_d$ and with $F_s = 1$. Then

$$M_1 = M_n = \sigma_n^2 I$$

and the weight vector is from (22)

$$\underline{w} = \underline{s}^* \tag{19}$$

The weight vector is identically that of a conventional beamformer and the desired signal will produce an output

$$e_{o(sig)} = \underline{s}_d^T \underline{s}^* \alpha \tag{20}$$

The pattern of $e_{o(sig)}$ as a function of angular difference between pointing vectors $\underline{s}_d$ and $\underline{s}$ will have the usual mainbeam beamwidth of approximately λ/ℓ where ℓ is the linear dimension of the array. We later show computational results bearing out this effect.

We now return to (12) for the purpose of putting it into a more explicit form in terms of the signal, interference, and noise components. The result will allow us to draw additional conclusions about the array behavior including the effect of imperfect elimination of the signal component from M. Using (13) and (15) we have, assuming a single interferer denoted $\beta(t)\underline{s}_I$,

$$M_1 = (1 - F_s)|\alpha^2|M_d + |\beta^2|M_I + \sigma_n^2 I$$

$$= \sigma_n^2[(1 - F_s)\gamma_d M_d + \gamma_I M_I + I] \tag{21}$$

where $\gamma_d = \overline{|\alpha^2|}/\sigma_n^2$ measures the SNR of the desired signal and $\gamma_I = |\beta^2|/\sigma_n^2$ measures the SNR of the undesired signal at each element. It is shown in Appendix B that the inverse of (21) is given by

$$M_1^{-1} = \frac{1}{\sigma_n^2}\left[I - \frac{(1-F_s)\gamma_d(\gamma_I N+1)M_d-(1-F_s)\gamma_d\gamma_I(M_dM_I+M_IM_d)+\gamma_I[(1-F_s)\gamma_d N+1)]M_I}{[(1-F_s)\gamma_d N+1](\gamma_I N+1)-(1-F_s)\gamma_d\gamma_I|\underline{s}_d^T\underline{s}_I^*|^2}\right] \tag{22}$$

To see the effect of imperfect reference generation we specialize (22) to the case of desired signal plus noise alone so that $\gamma_I = 0$. Then (22) becomes

$$M_1^{-1} = \frac{1}{\sigma_n^2}\left[I - \frac{(1 - F_s)\gamma_d M_d}{(1 - F_s)\gamma_d N + 1}\right] \tag{23}$$

The weight vector is then, using (12),

$$\underline{w} = \frac{\mu}{\sigma_n^2}\ [\underline{s}^* - k_1 M_d \underline{s}^*] \tag{24}$$

where

$$k_1 = \frac{(1 - F_s)\gamma_d}{(1 - F_s)\gamma_d N + 1} \tag{25}$$

The output signal to noise ratio is

$$\begin{aligned} SNR &= \frac{E[|\alpha \underline{s}_d^T(\underline{s}^* - k_1 M_d \underline{s}^*)|^2]}{E[|\underline{n}^T(\underline{s}^* - k_1 M_d \underline{s}^*)|^2]} \\ &= \gamma_d \frac{|\underline{s}_d^T(\underline{s}^* - k_1 M_d \underline{s}^*)|^2}{\|\underline{s}^* - k_1 M_d \underline{s}^*\|^2} \end{aligned} \tag{26}$$

$\|\cdot\|$ represents the norm of the vector inside the bars.

Making use of (16) and of the fact that $\underline{s}_d^T \underline{s}_d^* = N$ the numerator of the ratio in (26) becomes

$$|1 - k_1 N|^2 |\underline{s}_d^T \underline{s}^*|^2$$

and the denominator of that ratio becomes

$$N[1 + (|1 - k_1 N|^2 - 1)|\underline{s}_d^T \underline{s}^*|^2/N^2]$$

so that (26) can be written

$$SNR = \gamma_d \frac{|1 - k_1 N|^2 |\underline{s}_d^T \underline{s}^*|^2}{N[1 + (|1 - k_1 N|^2 - 1)|\underline{s}_d^T \underline{s}^*|^2/N^2]} \tag{27}$$

This result embodies both the degree of imperfect pointing and imperfect reference. For the case where the reference generator is perfect $k_1 = 0$ so that

$$SNR = \frac{\gamma_d}{N}|\underline{s}_d^T\underline{s}^*|^2 \tag{28}$$

The maximum of this quantity is obtained when pointing at $\underline{s}_d$ and in this case $|\underline{s}_d^T\underline{s}^*|^2 = |\underline{s}_d^T\underline{s}_d^*|^2 = N^2$ so that

$$SNR = N\gamma_d \tag{29}$$

an expected result.

For the case where $\underline{s}_d = \underline{s}$, but with imperfect reference (27) also gives

$$SNR = N\gamma_d$$

just as one would expect from perfect steering.

The pointing error is embodied in the quantity $|\underline{s}_d^T\underline{s}^*|^2$ which, as stated above, has a maximum value given by N^2 when $\underline{s}_d = \underline{s}$. A convenient indicator of pointing error is obtained by writing

$$|\underline{s}_d^T\underline{s}^*|^2 = (1 - \varepsilon)N^2 \tag{30}$$

with $0 \leq \varepsilon < 1$ being the measure of pointing error. Using (30) and, for brevity, denoting

$$|1 - k_1 N|^2 = \frac{1}{|(1 - F_s)\gamma_d N + 1|^2} = \rho \tag{31}$$

where k_1 is given by (25), (27) becomes

$$SNR = \gamma_d N\left[\frac{(1 - \varepsilon)\rho}{\varepsilon + (1 - \varepsilon)\rho}\right] \tag{32}$$

The right factor in brackets which we might term the normalized SNR shows how the SNR varies with pointing error as measured by ε, for degrees of imperfection in the reference signal as measured by ρ. We show in Figure 2 the behavior of that factor denoted by

$$r = \frac{(1 - \varepsilon)\rho}{\varepsilon + (1 - \varepsilon)\rho} \tag{33}$$

for ρ in the range (0.01, 1). The larger values of ρ represent closer tracking by the reference generator and vice-versa. We see here clearly the increasing sensitivity to pointing error as ρ gets smaller. If, for instance, $F_s = 0.9$, $N = 10$, $\gamma_d = 10$ we get $\rho = 10^{-2}$. It should be noted that with $F_s = 0$, i.e. when no reference is used, the corresponding value of ρ is about 10^{-4} implying greater pointing error sensitivity than for any of the cases shown in Fig. 2. These results are further confirmed in Section 3 where computations are carried out in the presence of both noise and interference.

For further insight into the behavior of the hybrid processor we examine the output signal to interference plus noise ratio (SINR) with an interferer present. We will, however, now assume a perfect reference; i.e., $F_s = 1$. The inverse covariance matrix given by (22) now becomes

$$M_1^{-1} = \frac{1}{\sigma_n^2}\left(I - \frac{\gamma_I M_I}{\gamma_I N + 1}\right) \tag{34}$$

and the weight vector is now

$$\underline{w} = \mu M_1^{-1}\underline{s}^* = \frac{\mu}{\sigma_n^2}\left(\underline{s}^* - k_2 M_I \underline{s}^*\right)$$

where

$$k_2 = \frac{\gamma_I}{\gamma_I N + 1} \tag{35}$$

Output signal (S_o), interference (I_o), and noise (N_o) are obtained by premultiplying (34) by $\alpha \underline{s}_d^T$, $\beta \underline{s}_I^T$, and $\underline{n}^T$, respectively. The output SINR is defined by

$$\text{SINR} = \frac{E(|S_o^2|)}{E(|I_o^2|) + E(|N_o|^2)} \tag{36}$$

The signal output power is

$$\begin{aligned} E(|S_o^2|) &= \frac{\mu^2}{\sigma_n^4} \overline{|\alpha^2|} |\underline{s}_d^T \underline{s}^* - k_2 \underline{s}_d^T \underline{s}_I^* \underline{s}_I^T \underline{s}^*|^2 \\ &= \frac{\mu^2 \overline{|\alpha^2|}}{\sigma_n^4} \{ |\underline{s}_d^T \underline{s}^*|^2 - 2k_2 \text{Re}[\underline{s}^{*T} \underline{s}_I)(\underline{s}_I^{*T} \underline{s}_d)(\underline{s}_d^{*T} \underline{s})] \\ &\quad + k_2^2 |(\underline{s}^{*T} \underline{s}_I)(\underline{s}_I^{*T} \underline{s}_d)|^2 \} \end{aligned} \tag{37}$$

If pointing is accurate so that $\underline{s} = \underline{s}_d$ (37) becomes

$$E(|S_o^2|) = \frac{\mu^2 \overline{|\alpha^2|}}{\sigma_n^4} (N^2 - 2k_2 N |\underline{s}_d^{*T} \underline{s}_I|^2 + k_2^2 |\underline{s}_d^{*T} \underline{s}_I|^4) \tag{38}$$

The noise output power is

$$\begin{aligned} E(|N_o|^2) &= \frac{\mu^2}{\sigma_n^4} E|\underline{n}^T (\underline{s}^* - k_2 \underline{s}_I^* \underline{s}_I^T \underline{s}^*)|^2 \\ &= \frac{\mu^2}{\sigma_n^2} [N - (2k_2 - k_2^2 N) |\underline{s}_I^T \underline{s}^*|^2] \end{aligned} \tag{39}$$

and the interference output power is

$$E(|I_o|^2) = \frac{\mu^2}{\sigma_n^4} \overline{|\beta^2|} |\underline{s}_I^T \underline{s}^* - k_2 \underline{s}_I^T \underline{s}_I^* \underline{s}_I^T \underline{s}^*|^2 \tag{40}$$

$$= \frac{\mu^2}{\sigma_n^4} \overline{|\beta^2|} (1 - k_2 N)^2 |\underline{s}_I^T \underline{s}^*|^2$$

Note from (35) if the interference to noise ratio γ_I and/or the number of elements N is large enough to make $\gamma_I N >> 1$, k_2 approaches 1/N. The output interference power as given by (40) is, in this case, strongly suppressed through the factor $(1 - k_2 N)$.

With accurate pointing (39) and (40) as well as (38) involve the quantity $|\underline{s}_d^{*T} \underline{s}_I|^2$, the inner product of the desired and undesired signal pointing vectors. If, for instance, the array elements were strung out along the x-axis with positions x_i,

$$|\underline{s}_d^{T*} \underline{s}_I|^2 = \left| \sum_{i=1}^{N} e^{jkx_i(\cos\theta_I - \cos\theta_d)} \right|^2 \tag{41}$$

where θ_I and θ_d are the undesired and desired signal arrival angles relative to array broadside and k is the wavenumber ($=2\pi/\lambda$). For a thinned array with the element positions x_i far apart in units of wavelength and with θ_I sufficiently different from θ_d, the sum in (41) is the vector sum of N arbitrarily oriented unit length phasors. With N large enough the squared length tends to be close to N.

If we take $|\underline{s}_d^{T*} \underline{s}_I|^2 = N$ and also take k_2 to be N^{-1} we get from (38)

$$E(|S_o^2|) = \frac{\mu^2 \overline{|\alpha^2|}}{\sigma_n^4} (N^2 - 2N + 1) = \frac{\mu^2 \overline{|\alpha^2|}}{\sigma_n^4} (N - 1)^2 \tag{42}$$

If k_2 had been zero, meaning there were no interference to suppress, the factor $(N - 1)^2$ in (42) would be replaced by N^2. As typically found, the suppression process causes a reduction in signal output power equal to that of a loss of one element.

Under the same assumptions, the noise output power is from (39)

$$E(|N_o|^2) = \frac{\mu^2}{\sigma_n^2} (N - 1) \tag{43}$$

Taking the view that the interference is totally suppressed, the output SINR is the same as the output SNR which is, using (42) and (43)

$$SNR = SINR = \frac{\overline{|\alpha^2|}}{\sigma_n^2} (N - 1) \tag{44}$$

More generally, the output SINR is given by substituting (37), (39), and (40) into (36).

3. COMPUTATIONAL RESULTS

Based on the results of Section 2, above, calculations of the steady-state output signal-to-interference plus noise ratio (SINR) were carried out assuming a linear array exposed to a desired signal and one or more undesired signals. The equivalent weight vector defined by (7) is given by

$$\underline{w} = \mu[(1 - F_s)\overline{|\alpha^2|}M_d + \sum_j \overline{|\beta_j^2|}M_{Ij} + M_n]^{-1}\underline{s}^* \tag{45}$$

(45) which is a composite of (12), (13), and (15), was used to calculate the equivalent weights and the corresponding mean square signal, noise, and interference outputs.

Figure 3(a) shows the the linear array element layout used for most of the computations. Seven elements were placed non-uniformly over an interval of 10 wavelenghts and a desired signal was assumed to be arriving broadside to the array. Computations of SINR were made for various deployments of interferers at various power levels relative to noise and signal. Since the behavior of a sparse array with arbitrarily selected element positions can be expected to depend on the particular realization of those positions, a second element layout as shown in Figure 3(b) was used to repeat a number of these computations. A sampling of the results obtained is presented below.

Of particular interest are the results shown in Figure 4 for the case of a desired signal arriving broadside to the array ($\theta_d = 90°$) and a single interferer arriving 5° off broadside. Signal, interference, and noise power are respectively 10 dB, 10dB, and 0 dB. The SINR versus pointing angle is shown for the case of an array with directional constraint only (the Applebaum-Chapman case) and for the hybrid array with varying degrees of perfection in the self-generated reference, i.e., with various F_s. With an ideal reference, i.e., $F_s = 1$, we see very little sensitivity to pointing

error (pointing error is pointing angle-90°), while with a directional constraint only, the pointing error sensitivity is extremely high. As the reference generating loop tends toward the ideal, the sensitivity decreases with reasonably tolerable levels achieved (3 dB loss in SINR for 0.5° pointing error) with moderate residual reference loop attenuation (5%) and phase shift (10°). Results not substantially dissimilar were obtained with the interference level raised to 20 dB with the alternative deployment of the array elements.

The interferer used to generate Figure 4 being 5° off broadside is outside the beamwidth of the quiescent array. By quiescent array we mean the array with adaption circuits inactive. In Figure 1 the quiescent output is e_m. The terms "beamwidth" and "mainbeam" will be used only in connection with the quiescent array. The behavior of the hybrid array with mainbeam interference is of interest and results of computations illustrating its properties under such a condition are shown in Figure 5. A single interferer is assumed 1° off broadside with all other conditions identical to those used to generate Figure 4. Interestingly, the sensitivity to pointing error of the array with directional constraint only, Figure 5(c), is not as severe as for the corresponding case of Figure 4 with the interferer off the mainbeam. The SINR in Figure 5 with correct pointing to the broadside signal is however about 8 dB less than for the case of interference off the mainbeam. This confirms a result obtained by Bar-Ness [9] in a comparison study of the two array processing methods which have been fused here into the Hybrid Array; the directionally constrained array is strongly affected by mainbeam interference. Figures 5(a) - 5(c) show the behavior of the Hybrid Array with ideal and non-ideal reference loop. The progressive increase in pointing error sensitivity is evident as the reference loop moves away from the ideal. The

SINR with correct pointing is seen however to be unchanged from that of the pure directionally constrained case. Sensitivity to interference level in the case of mainbeam interference is however more evident than in the case of off-mainbeam interference. In Figures 6 and 7 are shown results of computations with interference level of 20 dB and 0 dB relative to the noise level and with all other conditions identical to those of Figure 5. With 20 dB interference to noise ratio, Figure 6, the SINR with perfect pointing is slightly below (about 0.3 dB) that obtained with a 10 dB ratio. With 0 dB interference to noise ratio, Figure 7, the SINR with perfect pointing is above (about 2 dB) that obtained with a 10 dB ratio.

It should be noted that the dips in the SINR curves, Figures 5-7, do not occur at values of pointing angle equal to the respective interference arrival angles. Rather, as the level of interference is raised relative to that of the desired signal level the dip moves from a value somewhat above 88° to a value close to 89°, the actual interference arrival angle. This behavior appears to be a consequence of desired signal reduction induced by the interference and the effect of element noise. It should be noted that the multiple sidelobe canceller output, $\underline{u}^T\underline{y}$ in Figure 1, contains both signal and interference when pointing at an angle below 89°. Because signal and interference are angularly close to one another the output $\underline{u}^T\underline{y}$ which acts to cancel interference when pointing below 89° tends also to cancel signal. The signal and interference powers in the numerator and denominator, respectively, of the SINR both decrease. Because, for Figure 7, input interference and noise are taken to be of equal power, the output interference, being partly suppressed when pointing away from 89°, loses its effect on the SINR. The net SINR will therefore continue to decrease as the pointing angle moves further below 89°. The minimum actually observed occurs when the pointing angle becomes such that the cancelling effect of $\underline{u}^T\underline{y}$ on the desired signal goes through a maximum. When the undesired signal is large as in Figure 6 the SINR immediately below 89° is largely determined by signal and interference - not noise. Here, as the pointing angle moves below 89°, though both signal and interference may be decreasing, their ratio is increasing.

4. CONCLUSION

The Hybrid array processor analyzed here utilizes prior information on expected direction of signal arrival and on signal structure. It is a fusion of techniques using a directional constraint and a self-generated reference signal. It was here shown that the sensitivity to pointing error typical of (zero order) directionally constrained adaptive arrays is substantially reduced, the degree of reduction depending on the self-generating reference circuit. When the latter has unit gain and zero phase-shift the sensitivity is all but eliminated. With modest departures from these conditions there is still a significant improvement. In the particular case of a 10 wavelength linear array comprised of 7 non-uniformly spaced elements with a desired signal arriving broadside to the array and an interferer 5° off broadside, the output SINR falls off about 20 dB for a pointing error of 1/2° when no reference is used. On the other hand, with a reference generating circuit which tracks the amplitude of the desired signal within 5% and without phase shift the SINR is off by about 3 dB; with amplitude 5% off and a phase shift of 10° the SINR is off by about 8 dB. Improvements in sensitivity to pointing error are also observed when the interference is within the beamwidth of the quiescent array. However, such interference is observed to blunt the effect of pointing error even when no reference is used. The improvement with reference is therefore less dramatic in this case.

We have alluded to the advantage expected in transient response of this scheme over one which does not utilize the directional information. This is subject of another analysis and will be reported separately.

REFERENCES

1. S. P. Applebaum and D. J. Chapman, "Adaptive Arrays With Main Beam Constraints", IEEE Trans. on Antennas and Propagation", Vol. AP-24, No. 5, September 1976, pp. 650-662.

2. B. Widrow, J. McCool, and J. Ball, "The Complex LMS Algorithm", Proc. IEEE, Vol. 63, April 1975, pp. 719-20.

3. R. T. Compton, Jr., R. J. Huff, W. G. Swarner, and A. A. Ksienski, "Adaptive Arrays for Communication Systems: An Overview of Research at the Ohio State University", IEEE Trans. on Antennas and Propagation, Vol. AP-24, No. 5, September 1976, pp. 599-607.

4. R. T. Compton, Jr., "An Adaptive Array in Spread Spectrum Communication", Proc. IEEE, Vol. 66, March 1978, pp. 289-

5. R. T. Compton, Jr., "Pointing Accuracy and Dynamic Range in a Steered Beam Array", IEEE Trans. on Aerospace and Electronic Systems", Vol. AES-16, No. 3, May 1980, pp. 280-287.

6. F. Haber, P. C. C. Yeh, "Effect of Pointing Error on a Directionally Constrained Array", Valley Forge Research Center, University of Pennsylvania, Quarterly Report No. 36, February 15, 1981, pp. 34-44.

7. D. M. DiCarlo, "Reference Loop Phase Shift in an N-element Adaptive Array", IEEE Trans. on Aerospace and Electronic Systems, Vol. AES-15, No. , July 1979, pp. 576-582.

8. Y. Bar-Ness, "Eliminating Reference Loop Phase Shift Adaptive Array", IEEE Trans. on Aerospace and Electronic Systems, Vol. AES-18, No. 1, January 1982, pp. 115-123.

9. Y. Bar-Ness, "Comparing the Performance of Steered Beam and LMS Interference Cancellor", IEEE Trans. on Aerospace and Electronic Systems", Vol. AES-18, No. 4, July 1982 (tentative publication date).

10. A. P. Sage and J. L. Melsa, Estimation Theory with Applications to Communications and Control, McGraw-Hill, Inc., 1971, Appendix A.

APPENDIX A1 - EQUIVALENT WEIGHT VECTOR

We here extend the result obtained by Applebaum and Chapman [1] for a directionally constrained array, to the case of the Hybrid Array represented in Figure 1.

Using (3), (4) and (10) in the main text* and writing $\underline{u} = A\underline{v}$ we have

$$\underline{y} = g\,\overline{A^*\underline{v}^*(\underline{s}^{T*}\underline{v} - \underline{y}^T A\underline{v} - e_r)} \tag{A1-1}$$

$$= g[A^*M\underline{s}^* - A^*MA^T\underline{y} - A^*\overline{\underline{v}^* e_r}]$$

where M is the covariance matrix of inputs; that is

$$M = \overline{\underline{v}^*\underline{v}^T}$$

and it is positive definite (independent noise voltages are always assumed at the array elements).

To evaluate $\overline{\underline{v}^* e_r}$ (1) is rewritten

$$\underline{v}(t) = \alpha(t)\underline{s}_d + \underline{q}(t)$$

with $\underline{q}(t)$ representing all interference and noise components. Then using (6), replacing $\underline{v}$ with the signal part above we get

$$e_{od} = \alpha(\underline{s}^{*T} - \underline{y}^T A)\underline{s}_d \tag{A1-2}$$

From (11)

$$e_r = F_s\alpha(\underline{s}^{*T} - \underline{y}^T A)\underline{s}_d + n_r \tag{A1-3}$$

so that

*Equations in the main text will henceforth be recalled without further comment.

$$\overline{\underline{v}^* e_r} = \overline{(\alpha^* \underline{s}_d^* + \underline{q}^*)[F_s \alpha (\underline{s}^{*T} - \underline{y}^T A)\underline{s}_d + n_r]} \tag{A1-4}$$

$$= \overline{|\alpha|^2} F_s M_d (\underline{s}^* - A^T \underline{y})$$

where

$$M_d = \underline{s}_d^* \underline{s}_d^T \tag{A1-5}$$

is the covariance matrix corresponding to the desired signal direction vector and where we have assumed that $\underline{q}$, n_r and the desired signal are all uncorrelated. (Since n_r arises from $\underline{q}$ some dependence is apt to exist; it is here assumed negligible). Substituting (A1-4) into (A1-1) we get

$$\underline{y} = g[A^* M \underline{s}^* - A^* M A^T \underline{y} - \overline{|\alpha^2|} F_s A^* M_d (\underline{s}^* - A^T \underline{y})] \tag{A1-6}$$

$$= gA^*[M - \overline{|\alpha^2|} F_s M_d](\underline{s}^* - A^T \underline{y})$$

Premultiplying by A^T and using (8) we get

$$\underline{s}^* - \underline{w} = gA^T A^*[M - \overline{|\alpha^2|} F_s M_d]\underline{w} \tag{A1-7}$$

This result, from which the weight vector $\underline{w}$ can be obtained is in a form similar to that in Applebaum and Chapman [1, eq. (4)], the latter being obtained from (A1-7) with $F_s = 0$.

For the case $g >> 1$ we can also get from (A1-6)

$$A^*[M - \overline{|\alpha^2|}F_sM_d]\underline{w} \rightarrow \underline{0} \tag{A1-8}$$

Since $A\underline{s} = \underline{0}$, meaning that the $(N - 1)$ linearly independent N-dimensional row vectors of A are orthogonal to $\underline{s}$, the solution to (A1-8) must satisfy

$$[M - \overline{|\alpha^2|}F_sM_d]\underline{w} = \mu\underline{s}^*$$

or

$$\underline{w} = \mu[M - \overline{|\alpha^2|}F_sM_d]^{-1}\underline{s}^* \tag{A1-9}$$

where μ is an appropriate constant. From (9) we have

$$\underline{s}^T\underline{w} = N = \mu\underline{s}^T[M - \overline{|\alpha^2|}F_sM_d]^{-1}\underline{s}^* \tag{A1-10}$$

so that

$$\mu = \frac{N}{\underline{s}^T[M - \overline{|\alpha^2|}F_sM_d]^{-1}\underline{s}^*} \tag{A1-11}$$

and

$$\underline{w} = \mu M_1^{-1}\underline{s}^* = \frac{NM_1^{-1}\underline{s}^*}{\underline{s}^TM_1^{-1}\underline{s}^*} \tag{A1-12}$$

where

$$M_1 = M - \overline{|\alpha^2|}F_sM_d \tag{A1-13}$$

M_1 can be shown to be non-singular.

APPENDIX A2 - INVERSION OF THE COVARIANCE MATRIX

We obtain the inverse of the covariance matrix, M, of the array element output vector as given by (1) when a single interferer denoted $\beta(t)\underline{s}_I$ is present. M may be written (see (15)-(18))

$$M = \sigma_n^2[I_n + \gamma_d M_d + \gamma_I M_I] = \sigma_n^2 M_o. \tag{A2-1}$$

where $M_d = \underline{s}_d^* \underline{s}_d^T$, $M_I = \underline{s}_I^* \underline{s}_I^T$, I_n is an n by n identity matrix, and γ_d and γ_I are SNR's of desired signal and interference, respectively. M_d and M_I are positive semi-definite so that M is positive definite and therefore invertible.

For any two matrices A and B of dimension (n x r) and (r x n), respectively, if the inverse of $(I_n + AB)$ exists, then [10]

$$(I_n + AB)^{-1} = I_n - A(I_r + BA)^{-1}B \tag{A2-2}$$

I_r is an r x r identity matrix.

Eq. (A2-1) may be rewritten

$$M_o = I_n + \begin{bmatrix} \gamma_d \underline{s}_d^* & \gamma_I \underline{s}_I^* \end{bmatrix} \begin{bmatrix} \underline{s}_d^T \\ \underline{s}_I^T \end{bmatrix} \tag{A2-3}$$

and its inverse may be written

$$M_o^{-1} = \left\{ I + \begin{bmatrix} \gamma_d \underline{s}_d^* & \gamma_I \underline{s}_I^* \end{bmatrix} \begin{bmatrix} \underline{s}_d^T \\ \underline{s}_I^T \end{bmatrix} \right\}^{-1}$$

$$= I_n - \begin{bmatrix} \gamma_d \underline{s}_d^* & \gamma_I \underline{s}_I^* \end{bmatrix} \left\{ I_2 + \begin{bmatrix} \underline{s}_d^T \\ \underline{s}_I^T \end{bmatrix} \begin{bmatrix} \gamma_d \underline{s}_d^* & \gamma_I \underline{s}_I^* \end{bmatrix} \right\}^{-1} \begin{bmatrix} \underline{s}_d^T \\ \underline{s}_I^T \end{bmatrix} \qquad \text{(A2-4)}$$

where I_2 is a 2 x 2 identity matrix. The matrix factor in the second form of (A2-4) which is to be inverted gives

$$\left\{ I_2 + \begin{bmatrix} \underline{s}_d^T \\ \underline{s}_I^T \end{bmatrix} \begin{bmatrix} \gamma_d \underline{s}_d^* & \gamma_I \underline{s}_I^* \end{bmatrix} \right\}^{-1}$$

$$= \begin{bmatrix} N\gamma_d + 1 & \gamma_I \underline{s}_d^T \underline{s}_I^* \\ \gamma_d \underline{s}_I^T \underline{s}_d^* & N\gamma_I + 1 \end{bmatrix}^{-1}$$

$$= \frac{1}{\Delta} \begin{bmatrix} N\gamma_I + 1 & -\gamma_I \underline{s}_d^T \underline{s}_I^* \\ -\gamma_d \underline{s}_I^T \underline{s}_d^* & N\gamma_I + 1 \end{bmatrix}$$

where $\Delta = (N\gamma_d + 1)(N\gamma_I + 1) - \gamma_d\gamma_I|\underline{s}_d^T\underline{s}_I^*|^2$. Thus

$$M_o^{-1} = I_n - \frac{1}{\Delta}[\gamma_d\underline{s}_d^* \quad \gamma_I\underline{s}_I^*]\begin{bmatrix} N\gamma_d + 1 & -\gamma_I\underline{s}_d^T\underline{s}_I^* \\ -\gamma_d\underline{s}_I^T\underline{s}_d^* & N\gamma_d + 1 \end{bmatrix}\begin{bmatrix} \underline{s}_d^T \\ \underline{s}_I^T \end{bmatrix} \qquad \text{(A2-5)}$$

$$= I_n - \frac{1}{\Delta}[\gamma_d(N\gamma_I + 1)M_d - \gamma_d\gamma_I(M_dM_I + M_IM_d) + \gamma_I(N\gamma_d + 1)M_I]$$

Equation (22) in the text is obtained from this result by replacing γ_d by $\gamma_d(1 - F_s)$ and multiplying by $1/\sigma_n^2$ to give the inverse of the effective covariance matrix, M_1.

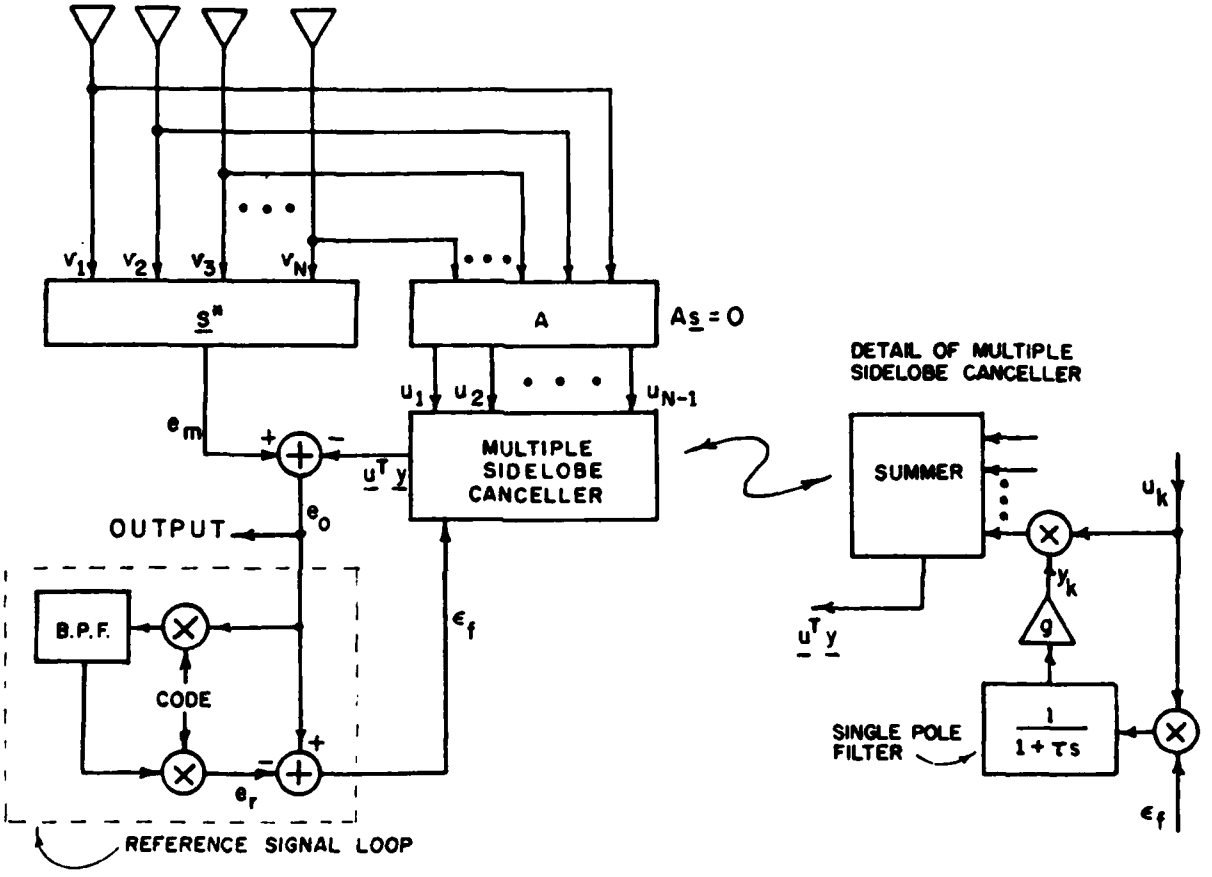

FIGURE 1. HYBRID ARRAY PROCESSOR

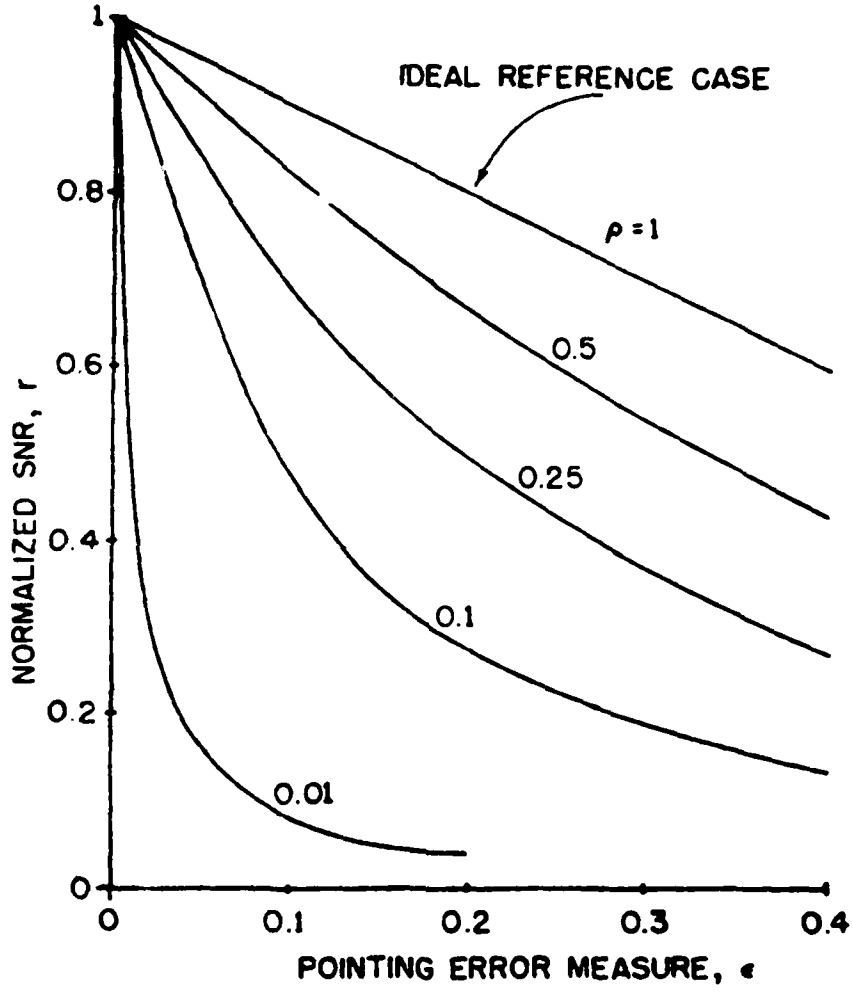

FIGURE 2. POINTING ERROR SENSITIVITY

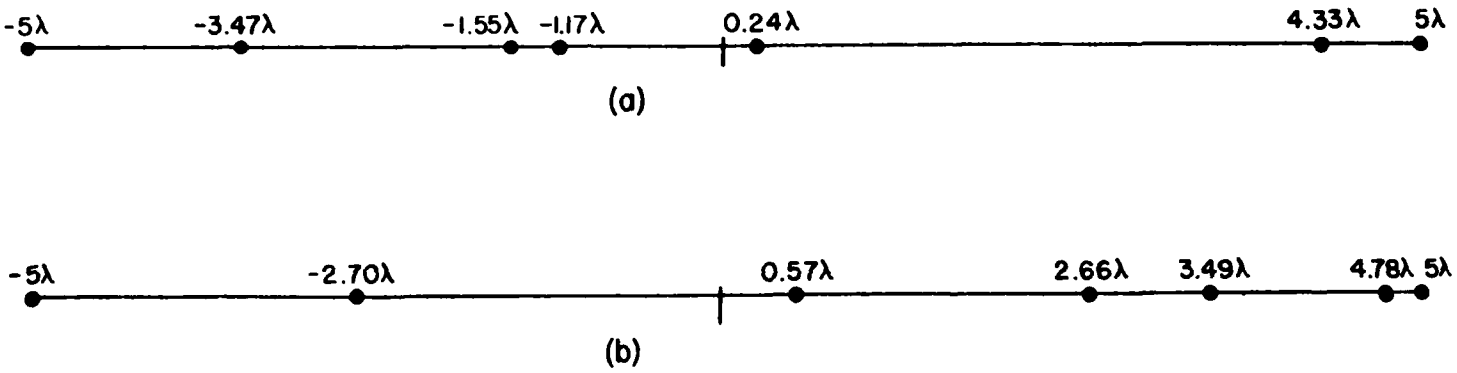

FIGURE 3. ARRAY ELEMENT LAYOUTS

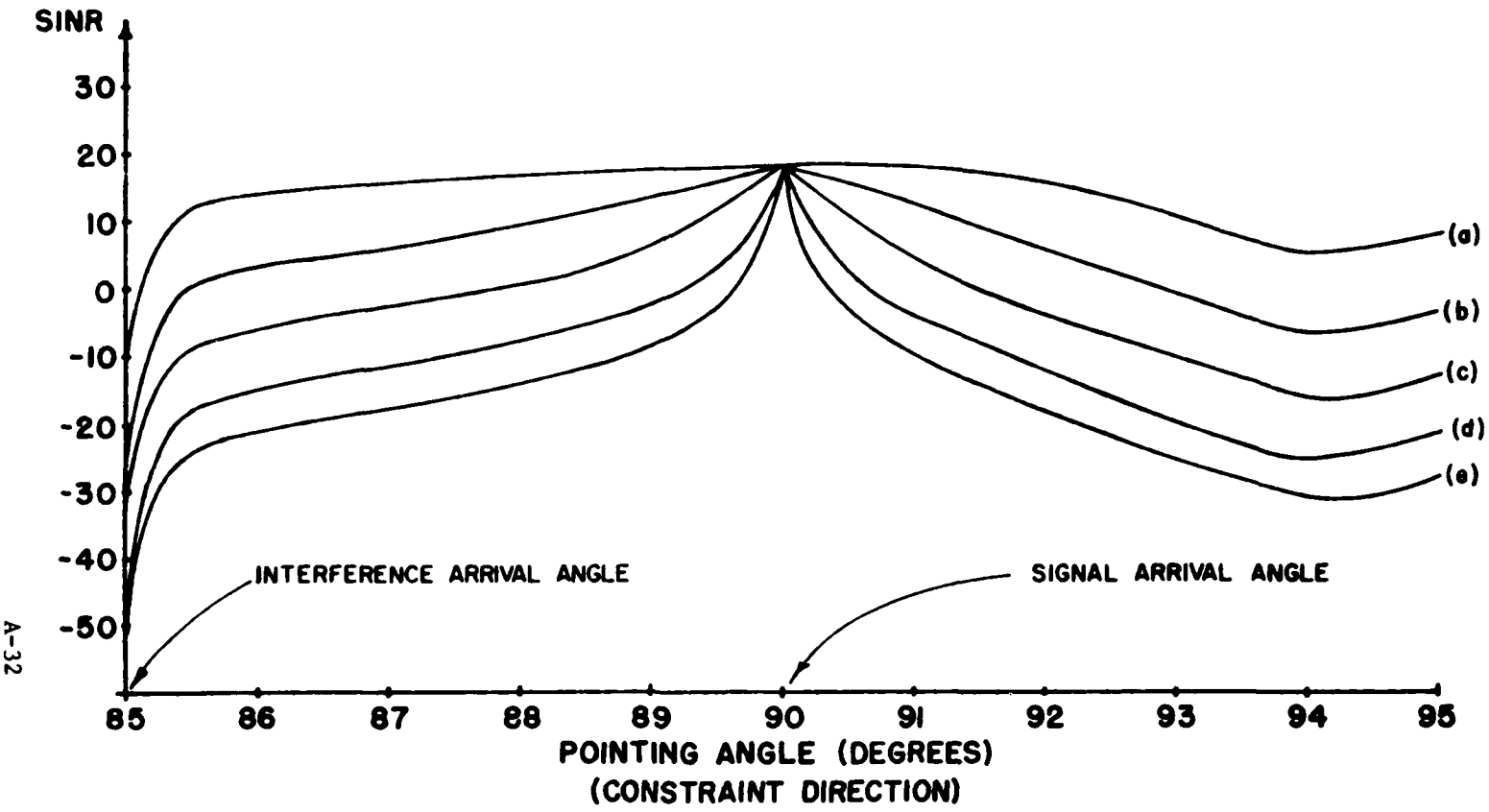

FIGURE 4. POINTING SENSITIVITY OF HYBRID ARRAY

7-element 10λ array; Signal, Interference power 10 dB relative to Noise power, Interferer at 85°

(a) $F_s = 1$, (b) $F_s = 0.95$, (c) $F_s = 0.95\exp(j10°)$,

(d) $F_s = 0.95\exp(j30°)$, (e) $F_s = 0.$

A-32

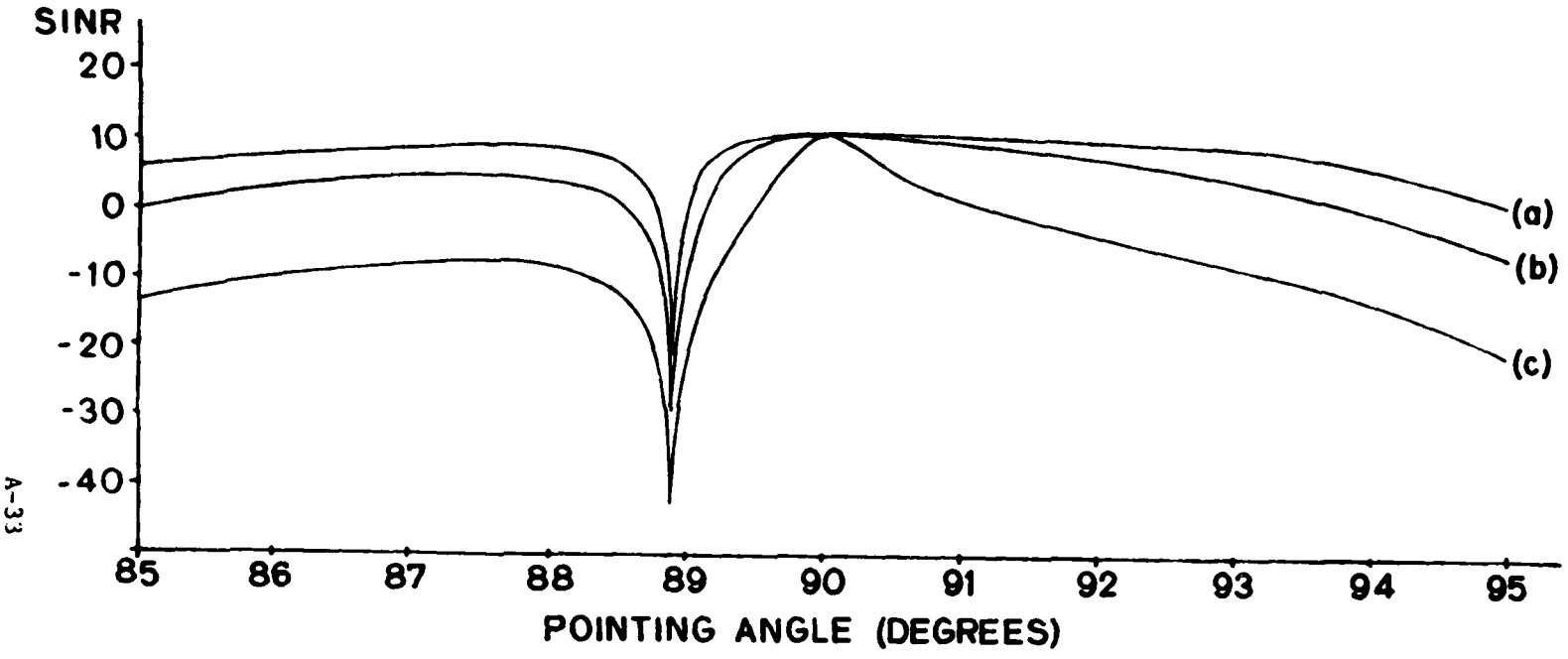

FIGURE 5. POINTING SENSITIVITY OF HYBRID ARRAY

7-element 10λ array; Signal, Interference power = 10 dB relative to Noise power, Interference at 89°.

(a) $F_s = 1$, (b) $F_s = 0.95\exp(-j10°)$,

(c) $F_s = 0$.

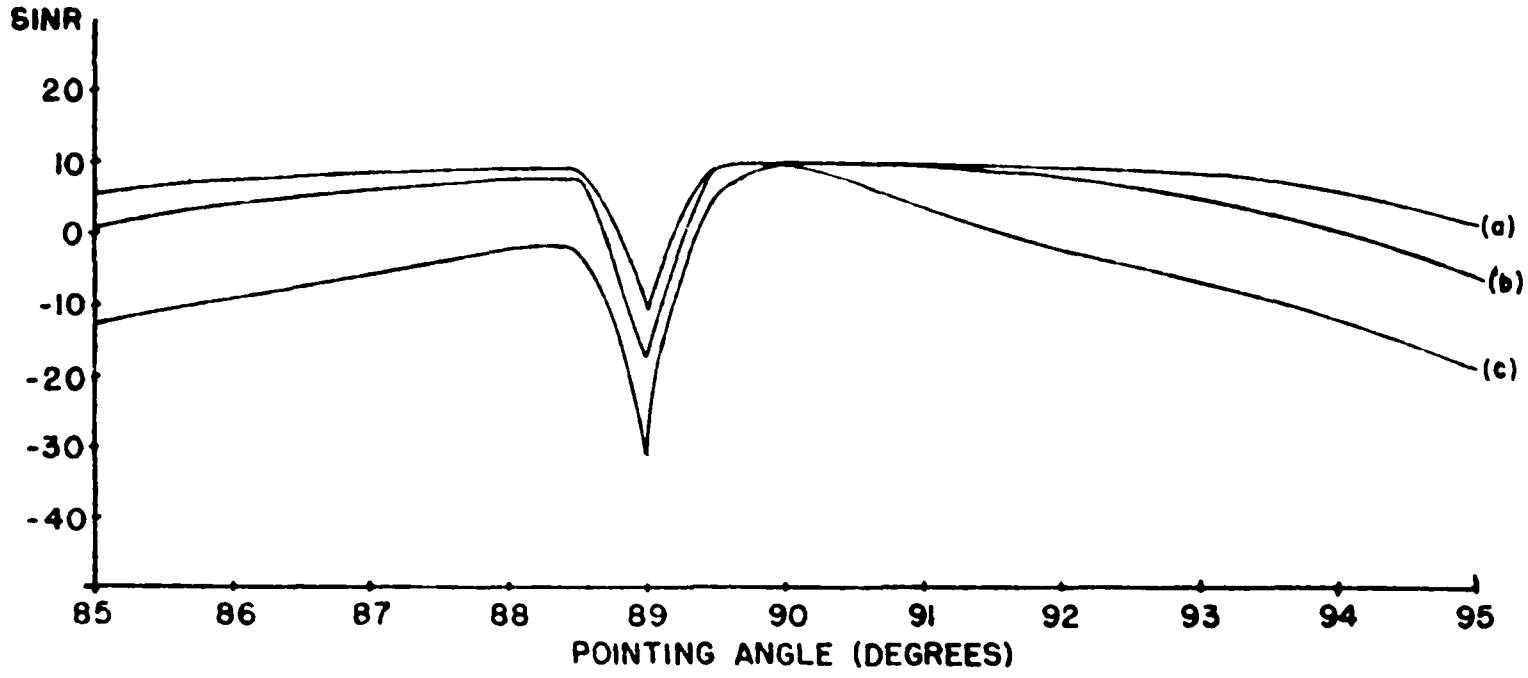

FIGURE 6. POINTING SENSITIVITY OF HYBRID ARRAY

7-element 10° array; Signal, Interference powers 10 dB and 20 dB, respectively, relative to noise, Interference at 89°.

(a) $F_s = 1$, (b) $F_s = 0.95\exp(-j10°)$, (c) $F_s = 0$

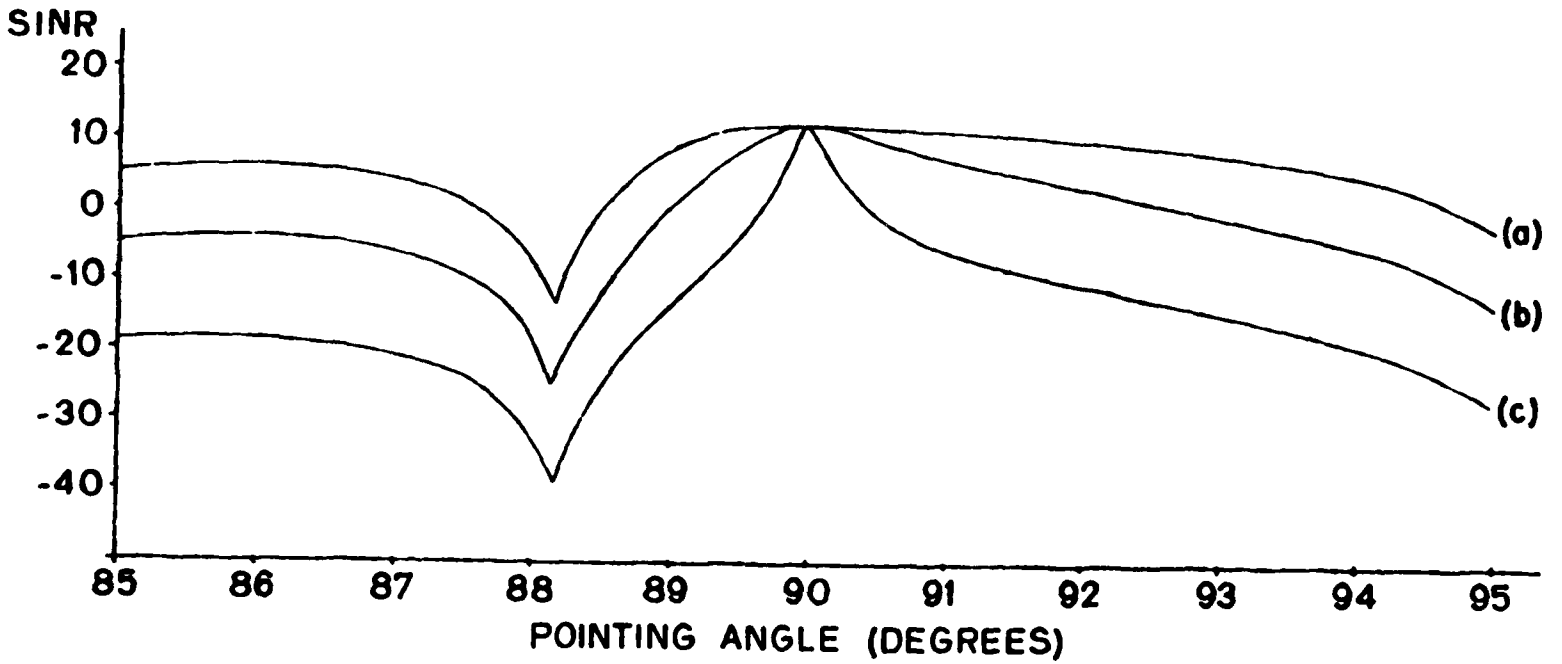

FIGURE 7. POINTING SENSITIVITY OF HYBRID ARRAY

7-element 10λ array; Signal, Interference powers 10 dB and 0 dB relative to Noise power, Interference at 89°.

(a) $F_s = 1$, (b) $F_s = 0.95\exp(-j10°)$, (c) $F_s = 0$.

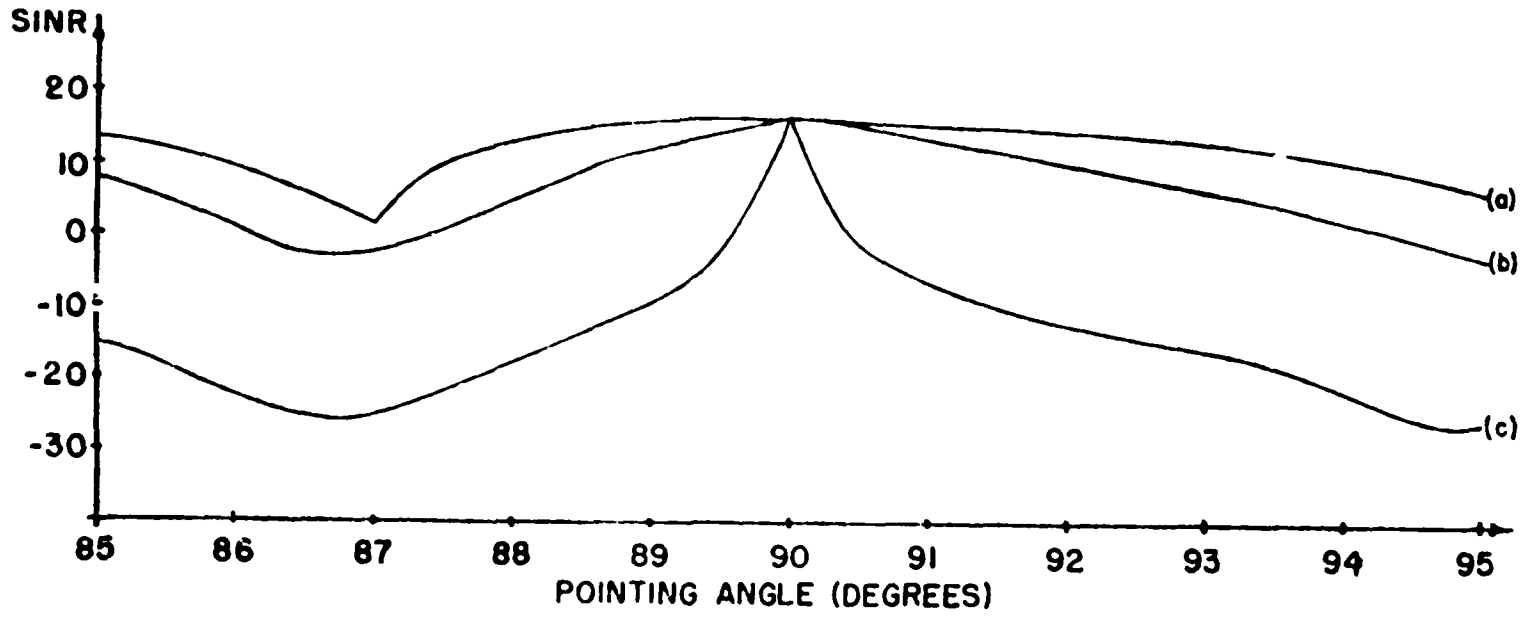

FIGURE 8. POINTING SENSITIVITY OF HYBRID ARRAY-MULTIPLE INTERFERERS

7-element 10° array; Signal, Interference powers 10 dB relative to Noise, Interferers at 37°, 65°, 127°, 190°, 253°.

(a) $F_s = 1$, (b) $F_s = 0.95$, (c) $F_s = 0$

List of Symbols - Appendix A

A	transformation matrix
$E[\ ]$	taking expectation of [ ]
e_m	output of the beamformer
e_o	array output
e_{od}	signal component of the array output
$e_o(sig)$	output desired signal of a beamformer
e_r	reference signal
F_s	operator representing the effect of the bandpass filter in the reference loop on the desired output signal component
g	gain in the weight setting loops
I	identity matrix
I_o	output interference
J	number of interferers
k	wave number
k_1	constant related to reference quality
k_2	constant related to interference to noise ratio
ℓ	linear dimension of the array
M	covariance matrix of array element outputs
M_1	equivalent covariance matrix
M^{-1}	inverse of M
M_d	covariance matrix corresponding to the desired signal direction vector
M_{ij}	covariance matrix corresponding to the j^{th} interferer direction vector
M_n	covariance matrix corresponding to noise
M_o	normalized covariance matrix
N	number of array elements
N_o	output noise

(Continued)

List of Symbols - Appendix A
(Continued)

n_r	noise component of the reference signal
$\underline{n}(t)$	complex noise envelope vector
$\underline{q}(t)$	interference and noise components of $\underline{v}(t)$
r	normal output signal to noise ratio = $SNR/\alpha_d N$
$R_e[\ ]$	real part of [ ]
$\underline{s}$	steering vector
$\underline{s}^*$	complex conjugate of $\underline{s}$
$\underline{s}_d$	arrival phase vector of the desired signal
s_{di}	the i^{th} unit amplitude component of $\underline{S}_d$
$\underline{s}_{ij}$	arrival phase vector of the j^{th} interferer
S_o	output signal
$\underline{s}^T$	transpose of $\underline{s}$
SINR	signal to interference plus noise ratio
SNR	signal to noise ratio
$\underline{u}$	input vector of the multiple sidelobe canceller
$v_i(t)$	output of the i^{th} array element
$\underline{v}(t)$	output vector of array elements
$\underline{w}$	equivalent weight vector
x_i	i^{th} array element position
$\underline{y}$	weight vector on the sidelobe canceller
$\alpha(t)$	desired signal waveform
$\overline{\lvert\alpha\rvert^2}$	power of $\alpha(t)$
$\overline{\lvert\beta_j\rvert^2}$	power of $\beta_j(t)$
$\beta_j(t)$	j^{th} interferer waveform
γ_d	signal to noise ratio at array elements

(Continued)

List of Symbols - Appendix A
(Continued)

γ_I	interference to noise ratio at array elements
Δ	determinant
ϵ	measure of pointing error
θ_d	arrival angle of the desired signal
θ_I	interferer arrival angle
λ	wavelength
μ	a constant
ρ	a constant related to reference quality
σ_n^2	noise power at array elements
ω	carrier frequency
$\overline{(\ )}$	expectation value of ( )
$\|\|\cdot\|\|$	norm

Appendix B

TRANSIENT RESPONSE OF THE HYBRID ARRAY

by

Chien-Chung Yeh

1. Analysis

We examine here the transient behavior of the Hybrid array. The circuit is that shown in Fig. 1 of Appendix A and the notation is also that of Appendix A. The input vector is written

$$\underline{V}(t) = \alpha(t)\underline{S}_d + \beta(t)\underline{S}_I + \underline{N}(t) \tag{1}$$

where $\alpha(t)$ and $\beta(t)$ are complex envelopes of desired and undesired signals respectively, $\underline{S}_d$ and $\underline{S}_I$ are their direction of arrival vectors, and $\underline{N}(t)$ is the random noise vector.

The output of the beamformer is

$$e_m(t) = \underline{V}^T(t)\underline{S}^* = \underline{S}^{*T}\underline{V}(t)$$

with $\underline{S}$ being the steering vector. We also have

$$\underline{U}(t) = A\,\underline{V}(t) \tag{2}$$

where $A\,\underline{S} = \underline{0}$. The sidelobe canceller generates $y_1(t) = \underline{Y}^T\underline{U}(t) = \underline{Y}^T A\,\underline{V}(t)$ so that

$$\begin{aligned} e_o(t) &= e_m - y_1(t) \\ &= (\underline{S}^* - A^T\underline{Y})^T\underline{V}(t) \end{aligned} \tag{3}$$

Define

$$e_o'(t) = e_o(t)g(t) \tag{4}$$

where $g(t)$ is the spreading code. $e_o'(t)$ is the array output with the

desired signal despread. The output, $e_{out}(t)$, of the bandpass filter assuming it to be a single pole with time constant τ_1 is given by

$$\tau_1 \frac{de_{out}(t)}{dt} + e_{out}(t) = e_o'(t) \tag{5}$$

The reference signal, $e_r(t)$, is obtained from $e_{out}(t)$ by respreading using the code g(t);

$$e_r(t) = e_{out}(t)g(t)$$

The residue feedback is

$$\begin{aligned} \varepsilon_f(t) &= e_o(t)-e_r(t) \\ &= [\underline{S}^*-A^T\underline{Y}(t)]^T\underline{V}(t) - e_{out}(t)g(t) \end{aligned} \tag{6}$$

For the weight control loop, we have

$$\tau_2 \frac{d\underline{Y}(t)}{dt} + \underline{Y}(t) = G\,\varepsilon(t)\,\underline{U}^*(t) \tag{7}$$

Substituting (3) and (4) into (5), we get

$$\tau_1 \frac{de_{out}(t)}{dt} + e_{out}(t) = [\underline{S}^* - A^T\underline{Y}(t)]^T\underline{V}(t)g(t) \tag{8}$$

We examine the transient response by assuming that the signal component in $\underline{V}(t)$ is a step function. Let

$$\alpha(t) = \begin{cases} \alpha g(t), & t \geq 0 \\ 0 & t < 0 \end{cases}$$

The foregoing may be viewed as the waveform seen with the first information digit received; the amplitude is α and the signal is modulated by

the spreading code g(t). Taking expectations on both sides of (8),

$$\tau_1 \frac{d\bar{e}_{out}(t)}{dt} + \bar{e}_{out}(t) = \overline{[\underline{S}^* - A^T\underline{Y}(t)]^T \underline{V}(t)g(t)} \tag{9}$$

It is reasonable to assume that the interference and noise are independent of the spreading code. Also in an adaptive array, the weights generally vary much more slowly than the input, i.e. the control loop bandwidth is much smaller than the bandwidth of $\underline{V}(t)$. See e.g. [1], where a similar argument is used on the independence of weight fluctuation and input. We therefore assume that to an adequate approximation the weights may be treated as being independent of $\underline{V}(t)$. (9) then becomes

$$\begin{aligned}\tau_1 \frac{d\bar{e}_{out}(t)}{dt} + \bar{e}_{out}(t) &= [\underline{S}^* - A^T\bar{\underline{Y}}(t)]^T \overline{\underline{V}(t)g(t)} \\ &= [\underline{S}^* - A^T\bar{\underline{Y}}(t)]^T \alpha\underline{S}_d\end{aligned} \tag{10}$$

Next, substituting (2) and (6) into (7), we have

$$\begin{aligned}\tau_2 \frac{d\underline{Y}(t)}{dt} + \underline{Y}(t) &= G\varepsilon(t)\underline{V}^*(t) \\ &= G\{[\underline{S}^* - A^T\underline{Y}(t)]^T\underline{V}(t) - e_{out}(t)g(t)\}A^*\underline{V}^*(t) \\ &= G\{A^*\underline{V}^*(t)\underline{V}^T(t)[S^* - A^T\underline{Y}(t)] - A^*\underline{V}^*(t)g(t)e_{out}(t)\}\end{aligned} \tag{11}$$

Taking expectations on both sides of (11) and using the same assumptions on independence we get

$$\begin{aligned}\tau_2 \frac{d\bar{\underline{Y}}(t)}{dt} + \bar{\underline{Y}}(t) &= G\{A^*\overline{\underline{V}^*(t)\underline{V}^T(t)}[\underline{S}^* - A^T\bar{\underline{Y}}(t)] \\ &\quad - A^*\overline{\underline{V}^*(t)g(t)e_{out}(t)}\}\end{aligned} \tag{12}$$

Since $e_{out}(t)$ is the output of a narrowband L.P.F. or B. P. F., as compared to the spreading code chip rate, it should be admissible to treat it as approximately independent of the product of $\underline{V}(t)$ and $g(t)$. That is, we can assume $\underline{V}^*(t)g(t) = \alpha\underline{S}_d^* + \underline{N}_1(t)$ and $e_{out}(t) = \alpha\underline{S}_d^* + \underline{N}_2(t)$ with the fluctuation components $\underline{N}_1(t)$ and $\underline{N}_2(t)$ essentially independent. Thus (12) becomes

$$\tau_2 \frac{d\underline{Y}(t)}{dt} + \bar{\underline{Y}}(t) = G\{A^*M[\underline{S}^* - A^T\bar{\underline{Y}}(t)] - A^*\overline{\underline{V}^*(t)g(t)} \cdot \bar{e}_{out}(t)$$

$$= G\{A^*M[\underline{S}^* - A^T\bar{\underline{Y}}(t)] - A^*\alpha\underline{S}_d^*\bar{e}_{out}(t)\} \qquad (13)$$

where

$$M = \overline{\underline{V}^*(t)\underline{V}^T(t)}$$

$$= \alpha^2\underline{S}_d^*\underline{S}_d^T + \beta^2\underline{S}_I^*\underline{S}_I^T + \sigma_n^2 I \qquad (14)$$

with

$$\alpha^2 = \overline{|\alpha^2(t)|}$$

$$\beta^2 = \overline{|\beta^2(t)|}$$

$$\sigma_n^2 I = \overline{\underline{N}^*(t)\underline{N}^T(t)}$$

(13) can be arranged as

$$\tau_2 \frac{d\bar{\underline{Y}}(t)}{dt} = -(I + GA^*MA^T)\bar{\underline{Y}}(t) + G[A^*M\underline{S}^* - A^*\alpha\underline{S}_d^*\bar{e}_{out}(t)] \qquad (15)$$

(10) and (15) are coupled sets of linear equations which are to be solved. As they stand they are tedious to solve. However with the following approximation a manageable result is obtained. Assume that τ_1 is small.

τ_2 is large and G is moderate so that $\bar{e}_{out}(t)$ varies much faster than $\underline{\bar{Y}}(t)$. Then in (10) we may treat $\underline{\bar{Y}}(t)$ as a constant and get the solution of $\bar{e}_{out}(t)$ as

$$\bar{e}_{out}(t) = \alpha[\underline{S}^* - A^T\underline{\bar{Y}}(t)]^T\underline{S}_d(1-e^{-\frac{t}{\tau_1}}) \tag{16}$$

Substituting (16) into (15),

$$\tau_2\frac{d\underline{\bar{Y}}(t)}{dt} = -\{I + G[A^*MA^T - A^*\alpha^2\underline{S}_d^*\underline{S}_d^T A^T(1-e^{-\frac{t}{\tau_1}})]\}\underline{\bar{Y}}(t)$$
$$+ GA^*[M - \alpha^2\underline{S}_d^*\underline{S}_d^T(1 - e^{-\frac{t}{\tau_1}})]\underline{S}^* \tag{17}$$

In the following we look at the physical meaning and justification of (17). First, if the reference loop were infinitely responsive, τ_1 would have to be near zero and (10) would reduce to $\bar{e}_{out}(t) = \alpha[\underline{S}^* - A^T\underline{\bar{Y}}(t)]^T\underline{S}_d$. This substituted into (15) would give

$$\tau_2\frac{d\underline{\bar{Y}}(t)}{dt} = -[I + GA^*(\beta^2\underline{S}_I^*\underline{S}_I^T + \sigma_n^2 I)A^T]\underline{\bar{Y}}(t)$$
$$+GA^*(\beta^2\underline{S}_I^*\underline{S}_I^T + \sigma_n^2 I)\underline{S}^* \tag{18}$$

this result is embodied in (17); note that if t is large enough so that $e^{-t/\tau_1} \simeq 0$ (17) becomes identical to (18). Next, we know that without the reference loop, the weight equation would be

$$\tau_2\frac{d\underline{\bar{Y}}(t)}{dt} = -(I + GA^*MA^T)\underline{\bar{Y}}(t) + GA^*M\underline{S}^* \tag{19}$$

With $t \simeq 0$, $e^{-\frac{t}{\tau_1}} \simeq 1$, so that (17) turns out to be

$$\tau_2\frac{d\underline{\bar{Y}}(t)}{dt} = -(I + GA^*MA^T)\underline{\bar{Y}}(t) + GA^*M\underline{S}^*$$

It is the same as (19).

To summarize, when $t \approx 0$, the output of the reference loop is very small and the weight equation is similar to that without the reference loop. For t large enough, the output of the reference loop reaches its steady state value and the array works as if we have a perfect reference loop. (17) may therefore turn out to a good approximation.

It should be pointed out that an information bearing waveform $\alpha(t)$ will be comprised of a random sequence of positive and negative steps. Even after the initial transient there will be signal related feedback in ε_f resulting from inability of the reference loop to instantaneously follow signal changes. These will affect the weight control loop even though the interference input to the weight control loop and the signal residue on ε_f are statistically uncorrelated.

For G large enough such that I can be ignored compared to GA^*MA^T, (17) reduces to

$$\tau_2 \frac{d\underline{\bar{Y}}(t)}{dt} = - G[A^*MA^T - A^*\alpha^2\underline{S}_d^*\underline{S}_d^TA^T(1 - e^{-\frac{t}{\tau_1}})]\underline{\bar{Y}}(t) + GA^*[M-\alpha^2\underline{S}_d^*\underline{S}_d^T(1 - e^{-\frac{t}{\tau_1}})]\underline{S}^* \quad (20)$$

The solution of (17) for the case of a two element array is carried out in the following. For a two element array, $\underline{\bar{Y}}(t)$ is a scalar. Therefore (17) is a first order linear differential equation. We divide both sides of (17) by τ_2 and rearrange it to give

$$\frac{d\bar{y}(t)}{dt} + \{\frac{1}{\tau_2} + \frac{G}{\tau_2}[A^*(\beta^2\underline{S}_I^*\underline{S}_I^T + \sigma_n^2I)A^T + A^*\alpha^2\underline{S}_d^*\underline{S}_d^TA^Te^{-\frac{t}{\tau_1}}]\}\bar{y}(t) = \frac{G}{\tau_2}A^*[(\beta^2\underline{S}_I^*\underline{S}_I^T + \sigma_n^2I) + \alpha^2\underline{S}_d^*\underline{S}_d^Te^{-\frac{t}{\tau_1}}]\underline{S}^* \quad (21)$$

From the theory of ordinary differential equations, the solution of

$$\frac{dy(t)}{dt} + f(t)y(t) = r(t) \tag{22}$$

is

$$y(t) = e^{-h(t)} \left[\int_o^t e^{h(t')} r(t')dt' + C \right] \tag{23}$$

where

$$h(t) = \int_o^t f(t')dt' \tag{24}$$

and C is a constant. (21) is exactly in the same form as (22) with

$$f(t) = \frac{1}{\tau_2} + \frac{G}{\tau_2} \left[A^* (\beta^2 \underline{S}_I {}^* \underline{S}_I {}^T + \sigma_n {}^2 I) + \alpha^2 \underline{S}_d {}^* \underline{S}_d {}^T A^T e^{-\frac{t}{\tau_1}} \right] \tag{25}$$

and

$$r(t) = \frac{G}{\tau_2} \left[(\beta^2 \underline{S}_I {}^* \underline{S}_I {}^T + \sigma_n {}^2 I) + \alpha^2 \underline{S}_d {}^* \underline{S}_d {}^T e^{-\frac{t}{\tau_1}} \right] \tag{26}$$

Using (24) and (25), we get

$$\begin{aligned} h(t) &= \int_o^t \{ \frac{1}{\tau_2} + \frac{G}{\tau_2} \left[A^* (\beta^2 \underline{S}_I {}^* \underline{S}_I {}^T + \sigma_n {}^2 I) A^T + A^* \alpha^2 \underline{S}_d {}^* \underline{S}_d {}^T A^T e^{-\frac{t'}{\tau_1}} \right] \} dt' \\ &= \left[\frac{1}{\tau_2} + \frac{G}{\tau_2} A^* (\beta^2 \underline{S}_I {}^* \underline{S}_I {}^T + \sigma_n {}^2 I) A^T \right] t \\ &\quad + \frac{G}{\tau^2} A^* \alpha^2 \underline{S}_d {}^* \underline{S}_d {}^T A^T \tau_1 (1 - e^{-\frac{t}{\tau_1}}) \end{aligned} \tag{27}$$

The constant C in (23) is determined by the initial condition. If we let $\bar{y}(0) = 0$, then

$$C = \bar{y}(0) = 0$$

Therefore, the solution of (21) is

$$\bar{y}(t) = e^{-h(t)} \int_0^t e^{h(t')} r(t')dt \tag{28}$$

with h(t) and r(t) given by (27) and (26), respectively.

2. SIMULATION RESULTS

The behavior of a two element array with $\lambda/2$ spacing as shown in Figure 1, was simulated. The desired signal was assumed to be spread in spectrum with an information sequence of 100 bps generated by a seven digit shift register and a code sequence of 10K bps generated by a 10 digit shift register. The desired signal arrival angle was assumed to be at broadside, i.e. $\theta_d = 90°$ and the interferer was assumed to be a pure carrier arriving from, $\theta_I = 45°$, in phase with one of the two binary signal alternatives.

In the first part, we assume that there is no noise and the SIR is measured at e_o. The SIR is defined as the ratio of squares magnitudes of the samples of the desired signal and interference at each time. The signal power and interference power are assumed the same and are chosen to be 100. The steering angle, θ, ranges from 90^o to 70^o. G was chosen such that $G\beta^2 >> 1$. τ_1 was chosen such that the bandwidth of the reference loop is about the same or several times the information bandwidth of the desired signal. τ_2 was chosen so that the control loop bandwidth is much smaller than the information bandwidth. Simulation was done at baseband.

Figure 2 is the result of simulation with $\theta = 90°$, $G = 10$, and $\tau_2 = 4$; τ_1 is a parameter. Two values are chosen for τ_1:

$$\frac{1}{200\pi} \quad \text{and} \quad \frac{1}{1000\pi}$$

For the first one, the bandwidth of the reference loop is the same as the information bandwidth. For the second, the reference loop has bandwidth five times the information bandwidth. The results show that the response with $\tau_1 = \frac{1}{200\pi}$ fluctuates more than with $\tau_1 = \frac{1}{1000\pi}$ but both have the same convergence speed. At t=0; the initial value of the controlled weight y was set to zero, and the output SIR is about 7 dB. When t increasing to half the information bit duration, the SIR increases to about 40 dB. At the end of the first information bit, the SIR is about 60 dB. However, as the polarity of the information bit changes, the SIR decreases drastically and then starts to increase, again.

An explanation of Fig. 2 is given in the following. The weight y is controlled by the correlation of ε_f and U^*. With correct pointing, U contains only interference. Let S and I denote desired signal and interference respectively. U can be written

$$U = I_u \tag{29}$$

The feedback is

$$\varepsilon_f = e_o - e_r \tag{30}$$

e_o can be written

$$e_o = S_o + I_o \tag{31}$$

e_r can be approximated by

$$e_r = S_r + N_r \tag{32}$$

where N_r is a noise term resulting from interference not totally eliminated by the reference loop filter. Substituting (31) and (32) into

(30), we get

$$\epsilon_f = (S_o - S_r) + I_o - N_r \tag{33}$$

Using (29) and (33), we have

$$\epsilon_f U^* = (S_o - S_r)\, I_U^* + I_o I_U^* - N_r I_U^*$$

$$= S_f I_U^* + I_o I_U^* - N_r I_U^* \tag{34}$$

where $S_f = S_o - S_r$.

In (34) the term $I_o I_U^*$ drives y to cancel the interference, and the terms $S_f I_U^*$ and $N_r I_U^*$ make the weight fluctuate. The fluctuation of the weight increases as S_f or G increases.

The desired signal component of the feedback decreases during the transient as the bandwidth of the reference loop increases. That is why the response for $\tau_1 = \frac{1}{200\pi}$ is more noisy than that for $\tau_1 = \frac{1}{1000\pi}$. However, increasing the bandwidth of the reference loop also increases the noise component, N_r, in the feedback. There is a trade-off between decreasing S_f and increasing N_r.

The drastic drop in SIR as the polarity of the information bit changes is caused by the delay of the reference loop. The waveforms of S_o, S_r and S_f during the transition time are shown below.

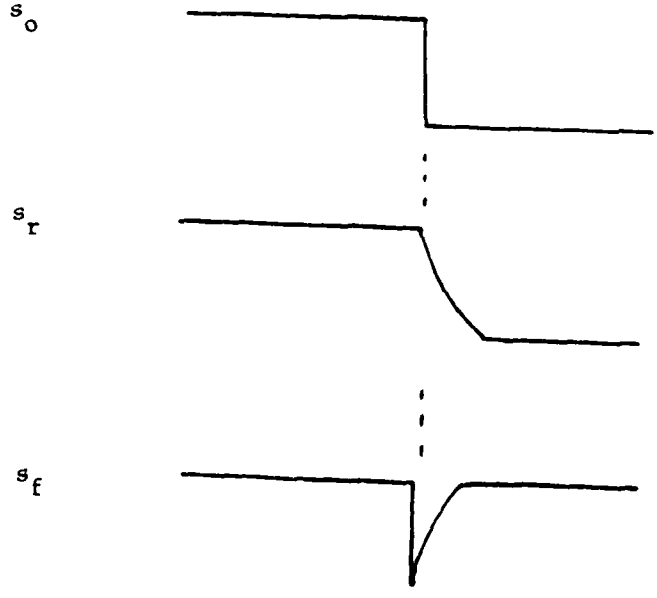

When the polarity changes, there is a spike in S_f. In the short interval of its duration, the term $S_f I_U^*$ drives the weight away from its ideal value and the SIR decreases drastically.

It should be pointed out that if the desired signal power is much smaller than the interference, the weights will not be so effected by the signal when its polarity changes.

The convergence speed is controlled by G and τ_2. Increasing G or decreasing τ_2 will increase the convergence speed. In Fig. 3 convergence rates for G = 30 and G = 10 are compared. Since the fluctuation increases as G increases, τ_1 was chosen to be $\frac{1}{1000\pi}$ to reduce the fluctuation. The results show that the response for G = 30 is about three times faster than that for G = 10 as expected, and reaches steady state in about one half the duration of an information bit.

We kept G = 30, $\tau_1 = \frac{1}{1000\pi}$ and $\tau_2 = 4$, but changed the pointing angle to see the effect of pointing error. Four steering angles were chosen, namely, $\theta = 90°$, which is the correct angle, 89°, 85° and 70°. Results are shown in Fig. 4. With 5° of pointing error, the array is able to work well and reaches steady state in about half an information bit, though there is some degration at steady state. However, for $\theta = 70°$, the convergence speed is relatively slow and can not reach steady state within the first information bit.

The slow rise in SIR when pointing at 70° requires explanation. For a large pointing error, the desired signal component in U is not small. This signal component will correlate with the signal component in the feedback making the signal component into the reference generator time varying. The apparent effect is to significantly increase the convergence time. This indicates that knowledge of the direction of the desired signal, or a reasonable approximation to it, can be used to significantly reduce weight convergence time.

Simulation of a two element Applebaum array was also carried out by setting e_r to zero. Results show that the fluctuation in response is much larger than that of the Hybrid array. The reason for this is that the signal component in the feedback is very large in the case of the Applebaum array while the signal component of the feedback is largely eliminated by the reference loop in the case of the Hybrid array. We have seen that the fluctuation increases as S_f increases. In order to reduce the fluctuation, we have to decrease G or increase τ_2. This, however, will make the convergence speed of the Applebaum array much slower than that of the Hybrid array.

We next added random noise to the simulation described above. In addition we took the output point to be the point identified as e_{out} in Fig. 1 and determined the SINR here. First the array element signal power, interference power, and noise power were taken to be 1, 100, and 1, respectively. Since the spreading ratio is 100 to 1, without adaption the output signal and interference have about the same power and are 20 dB higher than the noise. With G = 10, $\tau_1 = \frac{1}{200\pi}$ and $\tau_2 = 4$, four pointing angles, 90°, 89°, 85° and 70° were chosen to carry out the simulations. Results are shown in Fig. 5. It can be seen that with 5° of pointing error the loss is not much. Within half an information bit, the array can null the interference such that its power is much smaller than noise and the SINR depends on the signal to noise ratio. Therefore the SINR is about 20 dB which is the signal to noise ratio at the input. However, for $\theta = 70°$, the convergence speed is relative slow. But the array catches up quickly after the first information bit.

It is worth noting that since the signal power at the array elements is chosen to be much less than the interference, the weight is not much effected by the information bit polarity reversals. There is a drop in instantaneous SINR as the polarity changes since the signal falls to zero at this time but the weight is apparently not seriously affected.

We then simulated the case when signal power, interference power, and noise power are 100, 100 and 1, respectively. The values of G, τ_1, τ_2 and pointing angles used are the same as those in Fig. 5. Simulation results are shown in Fig. 6. We see that with 5° of pointing error, the array can achieve 40 dB SINR, which is determined by the signal to noise ratio at the input, within half an information bit. For pointing at $\theta = 70°$, the response is slow and is not able to null the interference below noise within one information bit. As the polarity of the information bit changes the weight is driven away from its original value because the signal has the same power as the interference at the array input.

To justify the assumptions made in analyzing the transient response, the controlled weight obtained from (28) of the work on transient response is compared with the weight obtained from the simulations. Only the imaginary parts are compared; the real parts are very close to zero. Results are shown in Fig. (7) and (8). The values of G, τ_1, and τ_2 are the same for both figures, which are G = 10, $\tau_1 = \frac{1}{200\pi}$ and $\tau_2 = 4$. The signal and interference arrival angles are, $\theta_d = 90°$ and $\theta_I = 45°$ respectively. Fig. 7 shows the results of the noise free case with pointing angle at $\theta = 89°$. Curve a is the theoretical results from (28) and curve b is the simulation results. These two curves match very well. Curve C is the theoretical results when we assume that $\tau_1 = 0$, i.e. the reference

loop is ideal. Figure 8 shows the results for the case in which the signal power, interference power, and noise power are 100, 100, and 1, respectively, and θ is 85^{o}. Curves a and b here also match very well. We therefore conclude that the theoretical results are based on reasonable approximations.

References

1. L. E. Brennan, E. L. Pugh, I. S. Reed "Control Loop Noise in Adaptive Array Antennas" IEEE Trans. on Aerospace and Electronic Systems AES 7 No. 2 March 1971, pp 254-262.

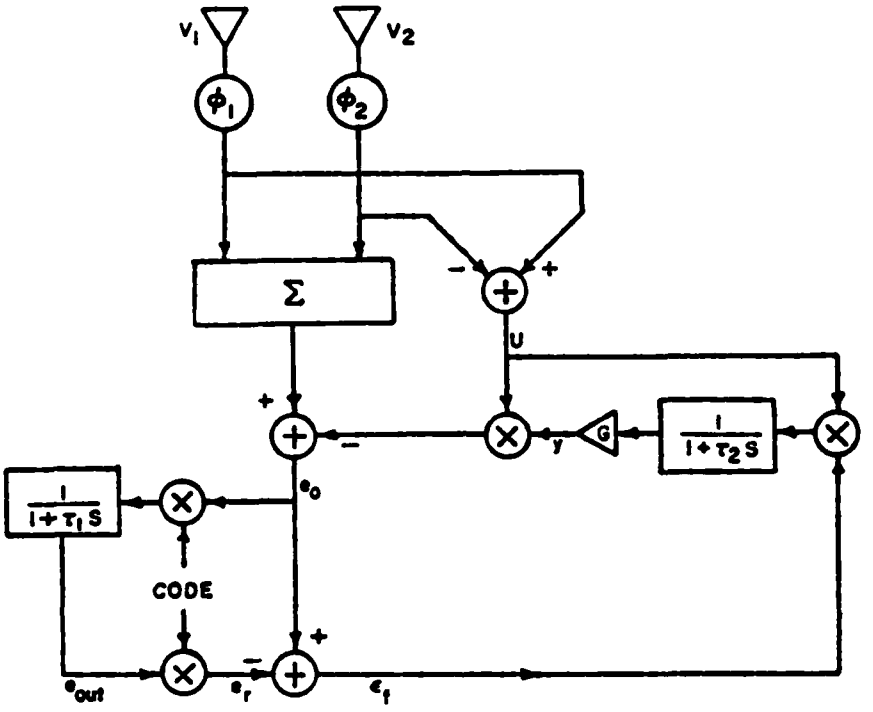

FIGURE 1 Two Element Hybrid Array

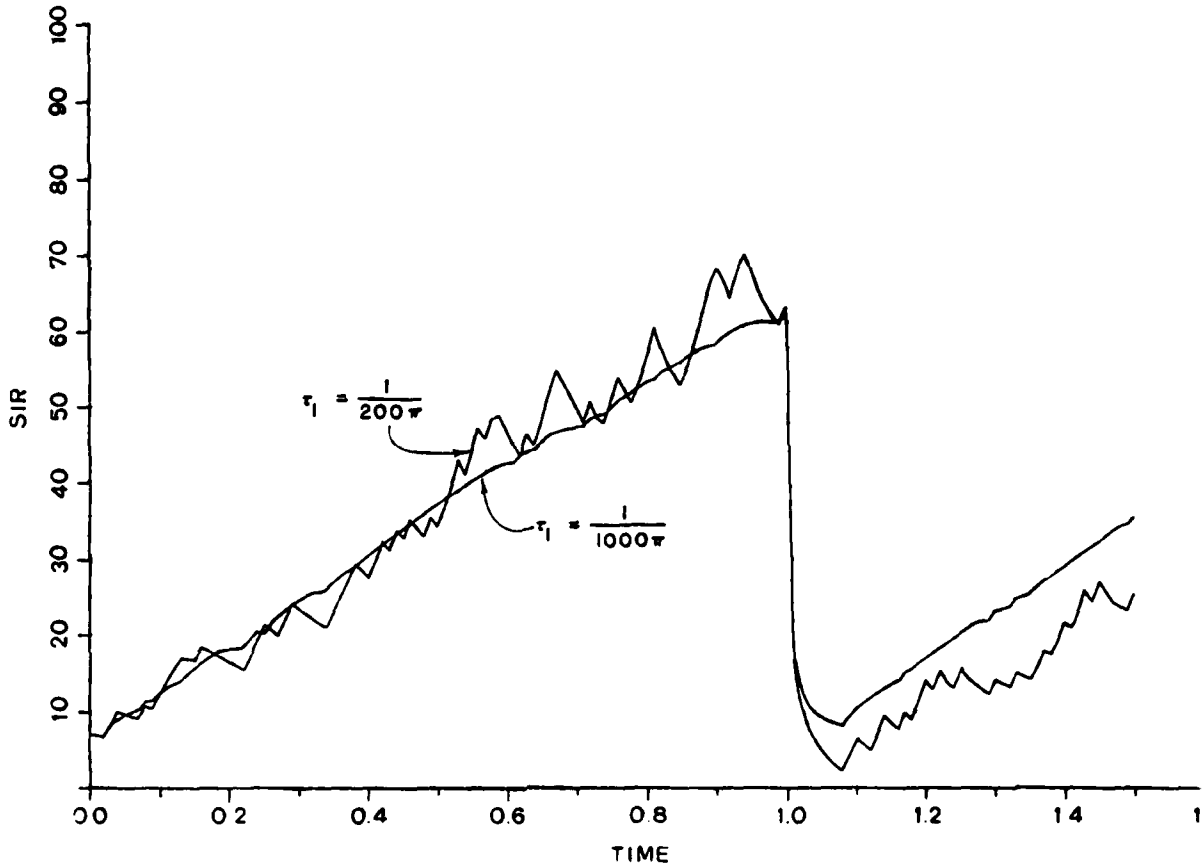

FIGURE 2 Transient Response - Hybrid Array Noiseless Case

Signal Power 20dB Interference Power 20dB

$\theta_d = 90^\circ$, $\theta_I = 45^\circ$, $\theta = 90^\circ$, $G = 10$, $\tau_2 = 4$

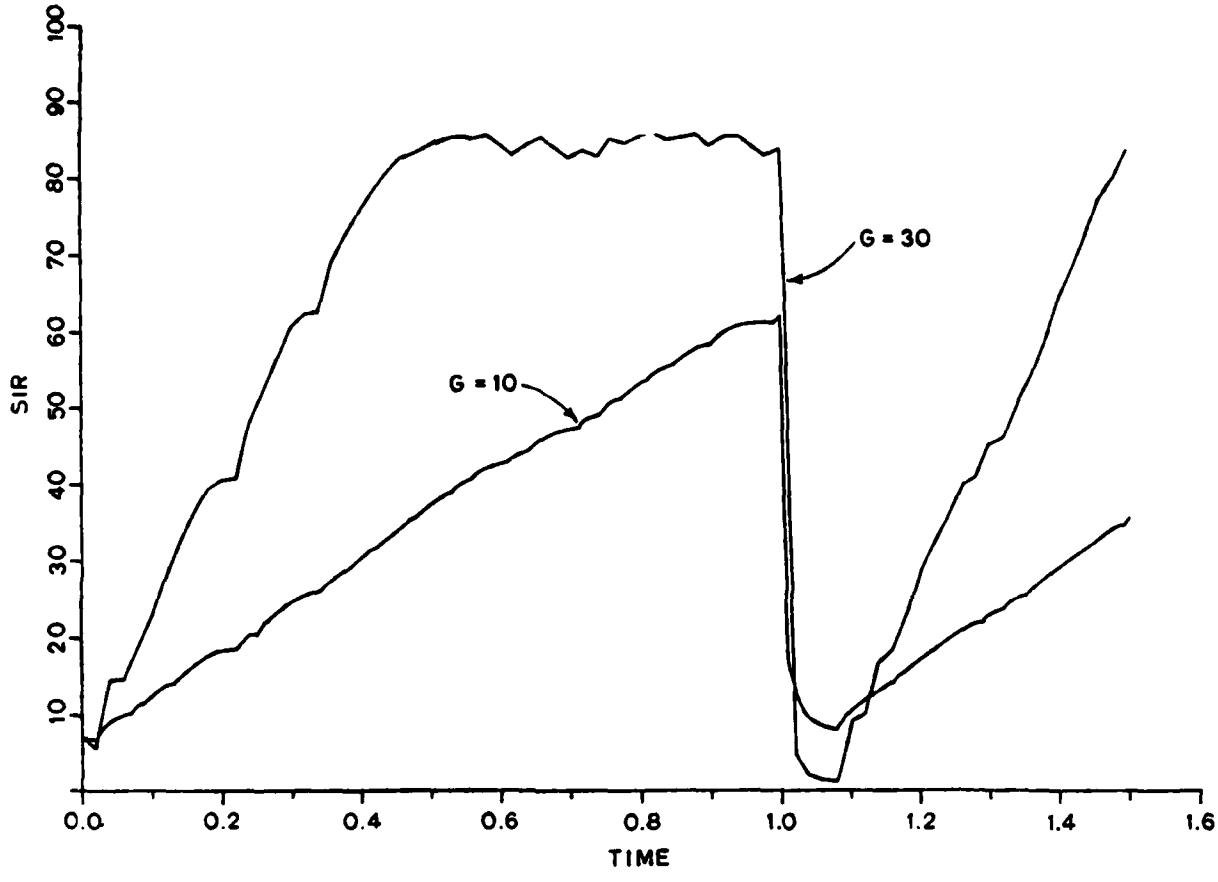

FIGURE 3 Transient Response - Hybrid Array Noiseless Case

Signal Power 20dB Interference Power 20dB

$\theta_d = 90^o$, $\theta_I = 45^o$, $\theta = 90^o$, $\tau_1 = \frac{1}{1000\pi}$, $\tau_2 = 4$

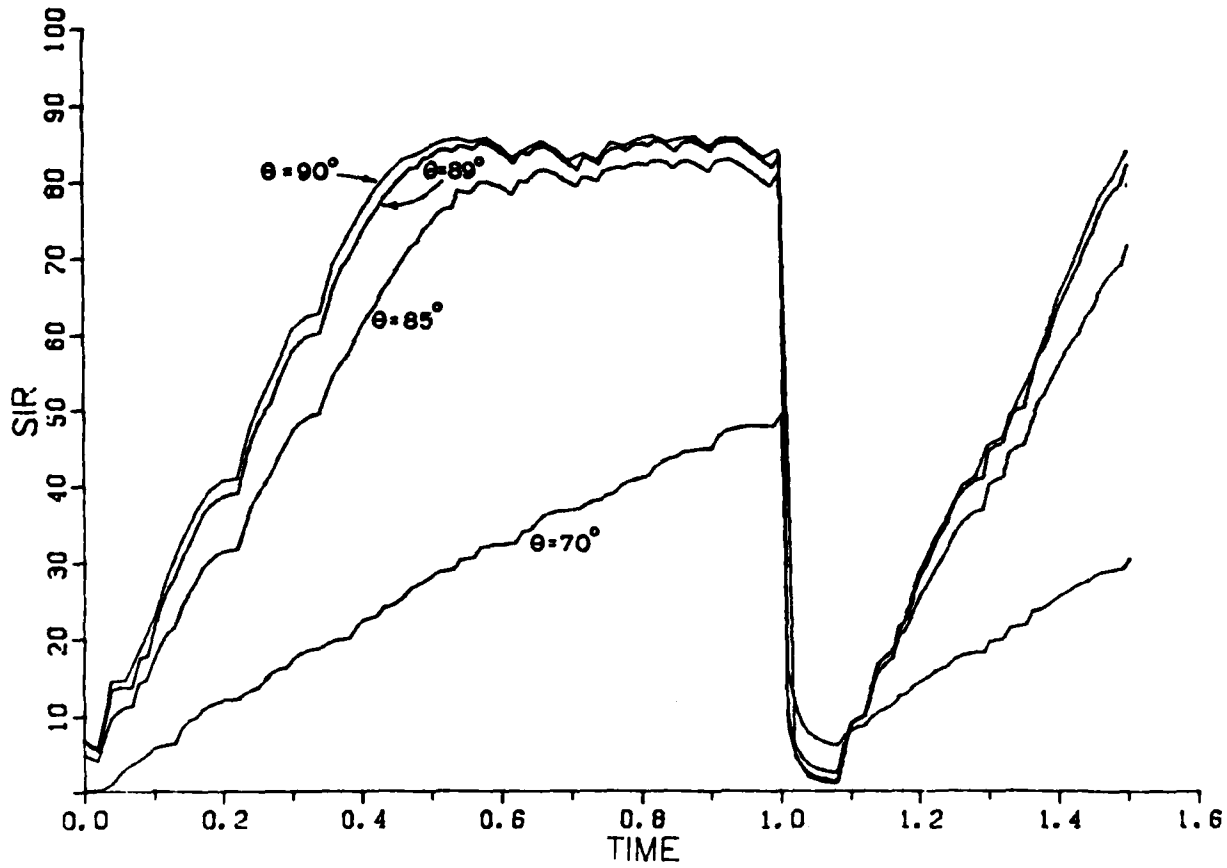

FIGURE 4 Transient Response - Hybrid Array Noiseless Case
Signal Power 20dB Interference Power 20dB
$\theta_d = 90^\circ$, $\theta_I = 45^\circ$, G = 30, $\tau_1 = \frac{1}{1000\pi}$, $\tau_2 = 4$

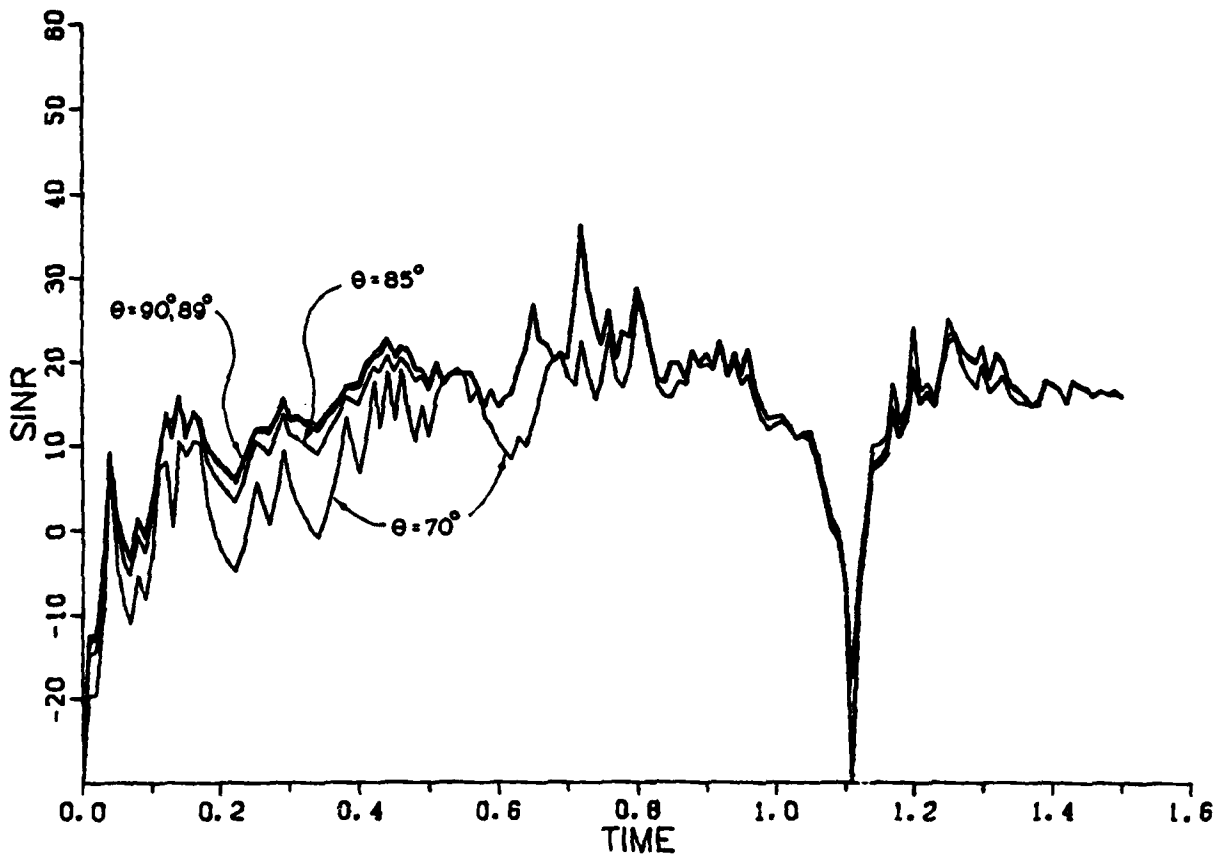

FIGURE 5 Transient Response - Hybrid Array

Signal Power 0dB Interference Power 20dB

Noise Power 0dB

$\theta_d = 90^\circ$, $\theta_I = 45^\circ$, G = 10, $\tau_1 = \frac{1}{200\pi}$, $\tau_2 = 4$

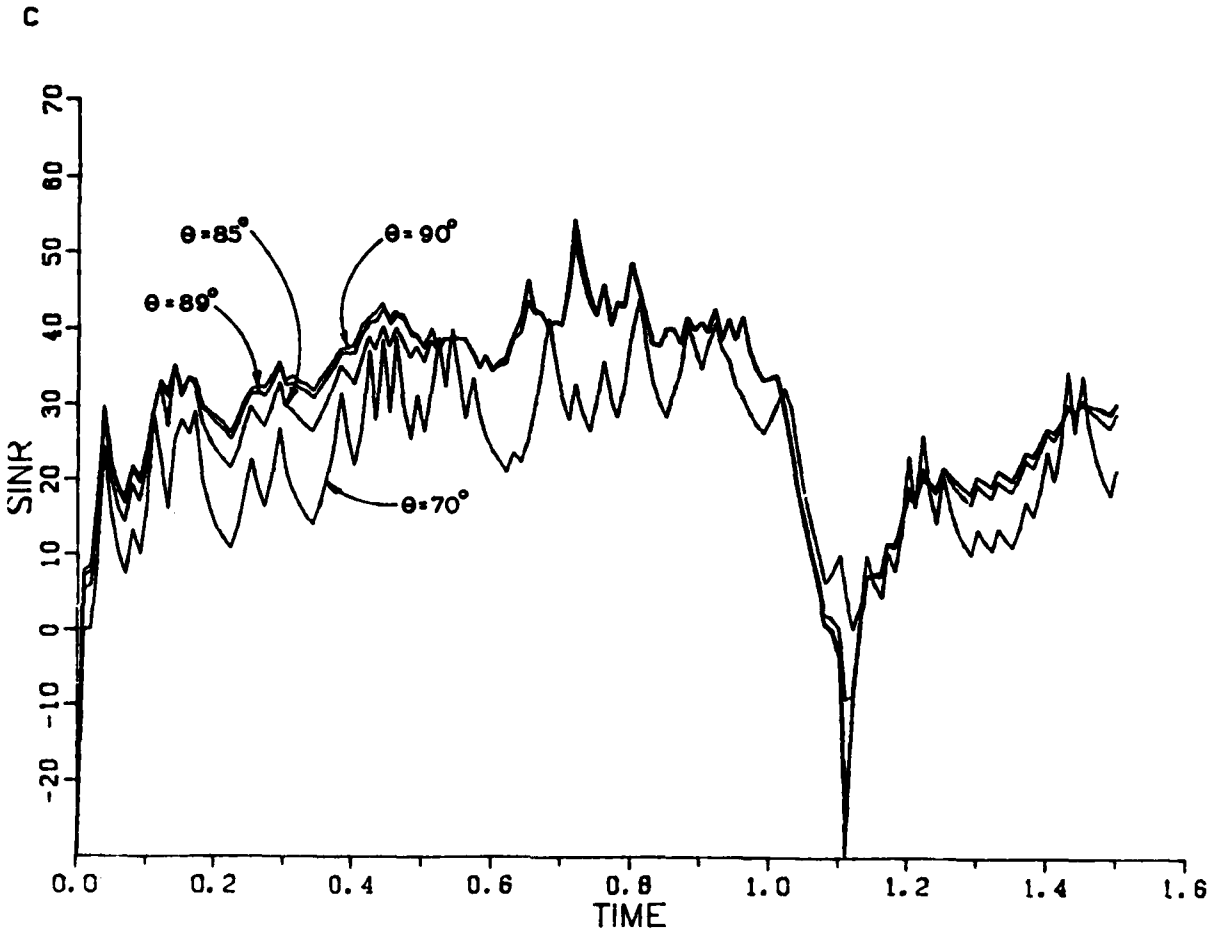

FIGURE 6 Transient Response - Hybrid Array

Signal Power 20dB Interference Power 20dB

Noise Power 0dB

$\theta_d = 90^\circ$, $\theta_I = 45^\circ$, G = 10, $\tau_1 = \frac{1}{200\pi}$, $\tau_2 = 4$

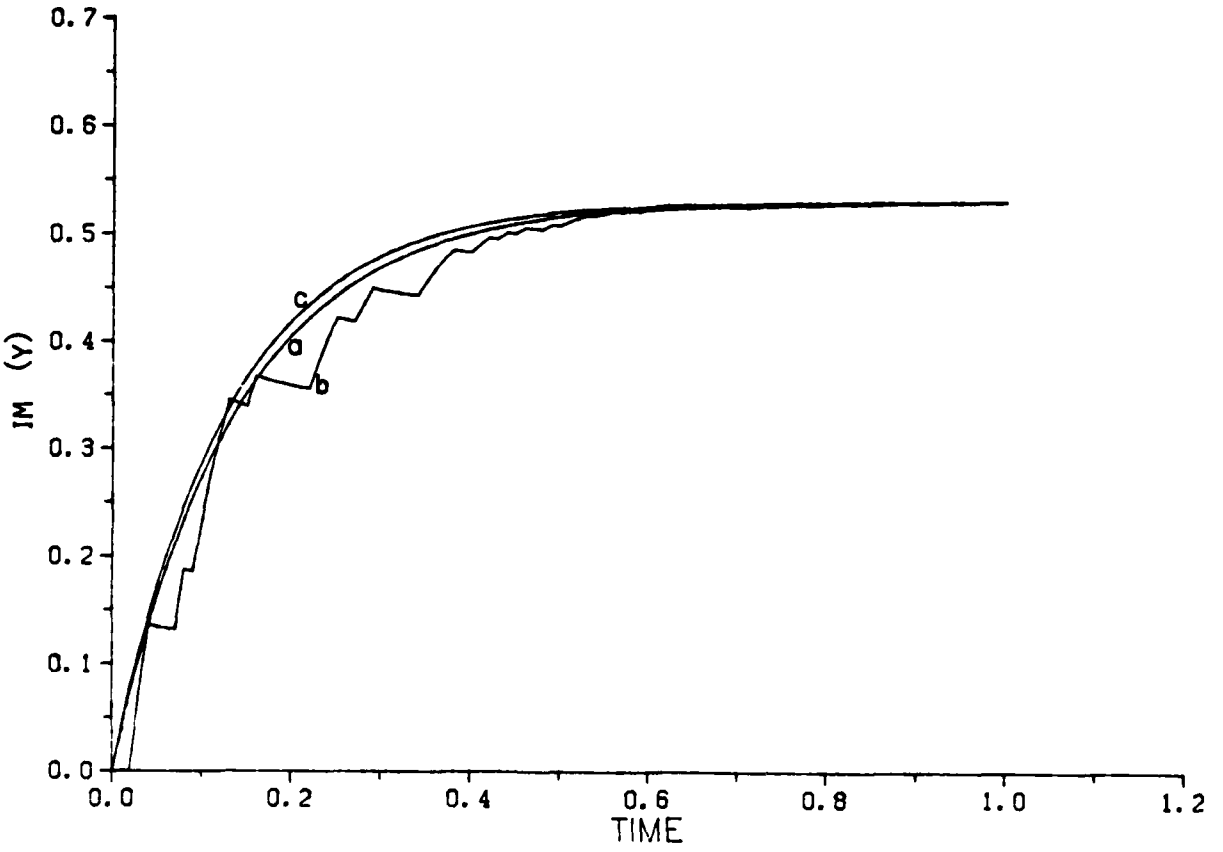

FIGURE 7 Weight Transient - Hybrid Array Noiseless Case

Signal Power 20dB Interference Power 20dB

$\theta_d = 90^o$, $\theta_I = 45^o$, $\theta = 89$, $G = 10$, $\tau_1 = \frac{1}{200\pi}$, $\tau_2 = 4$

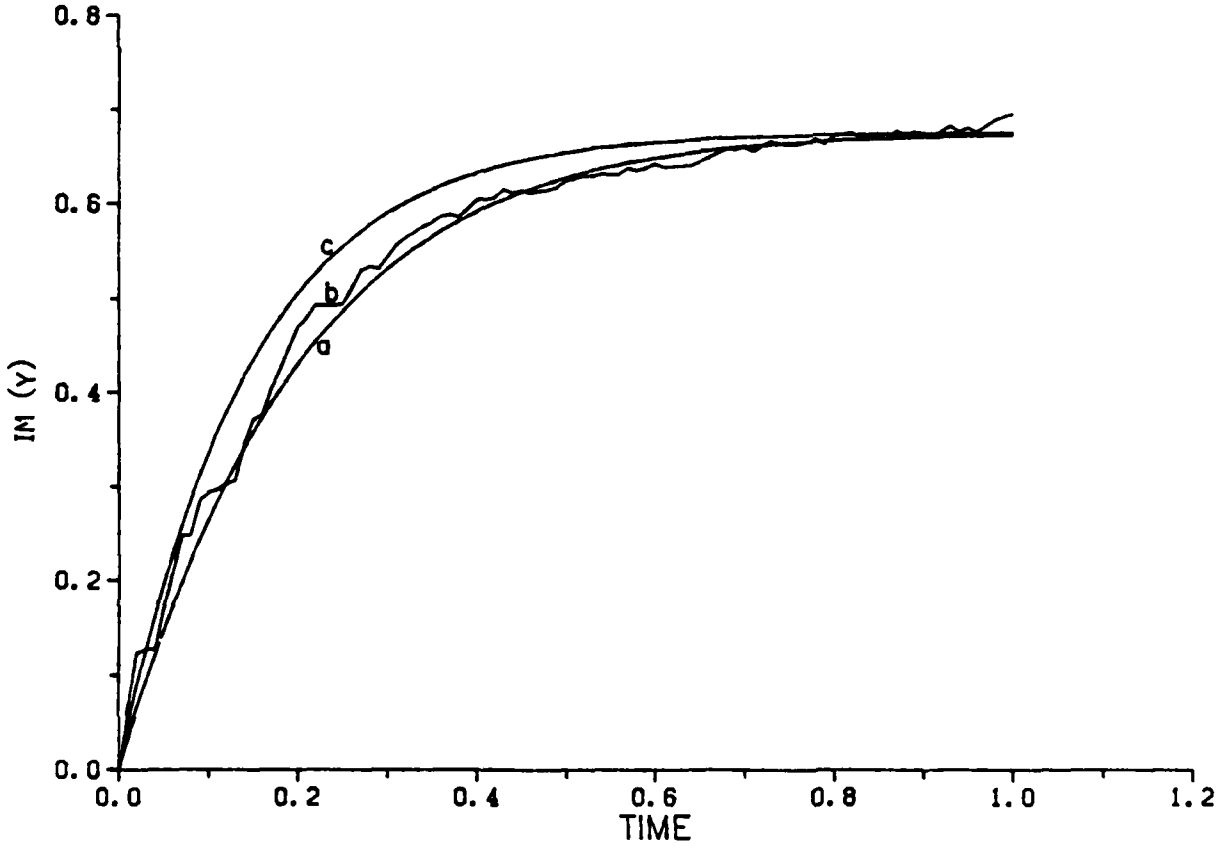

FIGURE 8 Weight Transient - Hybrid Array

Signal Power 20dB Interference Power 20dB

Noise Power 0dB

$\theta_d = 90^\circ$, $\theta_I = 45^\circ$, $\theta = 85^\circ$, G = 10, $\tau_1 = \frac{1}{200\pi}$,

$\tau_2 = 4$

List of Symbols - Appendix B

A	transformation matrix
B.P.F.	band pass filter
$e_m(t)$	beamformer output
$e_o(t)$	array output
$e_o'(t)$	array output with desired signal despread
$e_{out}(t)$	output of the band pass filter
$e_r(t)$	reference signal
G	gain of the weight control loops
g(t)	spreading code
h(t)	time function as defined in text
I	identity matrix
I_o	interference component of e_o
I_u	interference component of U
L.P.F.	low pass filter
M	covariance matrix
N_r	noise component of e_r
$\underline{N}(t)$	input noise vector
$\underline{N}_1(t)$	noise vector
$\underline{N}_2(t)$	noise vector
r(t)	time function as defined in text
$\underline{S}$	steering vector
$\underline{S}_d$	arrival phase vector of the desired signal
$\underline{S}_I$	arrival phase vector of the interferer
S_o	desired signal component of e_o
S_r	desired signal component of e_r

(continued)

List of Symbols - Appendix B
(Continued)

$\underline{S}^*$	complex conjugate of $\underline{S}$
$\underline{U}(t)$	input vector to the sidelobe canceller
$\underline{V}(t)$	vector of array element outputs
$\underline{V}^T$	transpose of $\underline{V}$
$\underline{Y}$	sidelobe canceller weights
$y_1(t)$	sidelobe canceller output
α	amplitude of the desired signal
α^2	desired signal power at array elements
$\alpha(t)$	desired signal waveform
β^2	interference power at array elements
$\beta(t)$	interferer waveform
$\varepsilon_f(t)$	residue feedback
θ	steering angle
θ_d	desired signal arrival angle
θ_I	interferer arrival angle
σ_n^2	noise power at array elements
τ_1	time constant of the reference loop
τ_2	time constant of the weight control loops

Appendix C

EFFECTS OF RANDOM AMPLITUDE AND STEERING PHASE ERRORS ON THE BEHAVIOR OF THE HYBRID ARRAY

Chien - Chung Yeh and Fred Haber

The adaptive array processor proposed by Applebaum [1] uses prior information on the direction of signal arrival, through a steering vector. A different system realization which constrains the processor to maintain constant gain of the main beam is later described by Applebaum and Chapman [2]. Ideally, both systems achieve maximum signal to interference plus noise ratio. For application to communication, both systems are very sensitive to the accuracy of the steering vector [3,4]. To overcome this shortcoming, a Hybrid array processing technique has been proposed for point-to-point spread spectrum communication [5]. It has been shown that the hybrid processor is much less sensitive to error of the expected direction of signal arrival.

In addition to the error caused by imperfectly information of the direction of signal arrival, the steering vector might be subject to random phase errors arising from uncertainties in element positions or as a consequence of quantization. In addition the system might introduce random amplitude errors on the array element outputs prior to processing, arising from circuit disimilarities. An analysis of effect of random errors in the steering vector in the Applebaum array has been given by Compton [6]. Here we study the effect of phase and amplitude perturbations on the performance of Hybrid array for both the gain constrained and the non-constrained processors. The two versions of Hybrid array based on the Applebaum arrays with and without gain constraint are shown in Figures 1 and 2, respectively. The analysis assumes

narrow band desired and undesired signals and a reference generating circuit which has achieved perfect spread spectrum chip synchronism with respect to the desired signal. The analyses and computational results are presented below.

Analysis:

Consider an N-element linear array with random gain error c_n, n=1, 2, .. N, on each element. The c_n's are all assumed to be random variables with zero mean and variance σ_c^2. The output signal of the array elements may be represented by the complex vector

$$\underline{V}'(t) = C\underline{V}(t) \tag{1}$$

where C is an N x N diagonal matrix with elements $1+c_1$, $1+c_2$, ... $1+c_N$ on the diagonal, and $\underline{V}(t)$ is the output vector of the array elements without random gain error. $\underline{V}(t)$ is represented by

$$V(t) = \alpha(t)\underline{S}_d + \sum_{j=1}^{J} \beta_j(t)\underline{S}_{Ij} + \underline{N}(t) \tag{2}$$

where $\underline{S}_d$ is the arrival phase vector of the desired signal comprised of N unit amplitude components, $\alpha(t)$ is its complex envelope; $\underline{S}_{Ij}$ is the arrival phase vector of the jth interference signal, $\beta_j(t)$ is its complex envelope; and $\underline{N}(t)$ is the complex noise envelope vector, the components of which are assumed independent with power σ_n^2. If, for instance, the elements are arranged along the X axis at positions x_n, n=1, 2, .. N, the ith component of the arrival phase vector of a desired signal arriving as a plane wave at an angle θ_d relative to the X-axis is $s_{d_n} = \exp(jkx_n\cos\theta_d)$.

A steering vector intended for signals with arrival angle θ but with random phase error can be written

$$\underline{S} = \begin{bmatrix} e^{jkx_1\cos\theta} \cdot e^{j\phi_1} \\ e^{jkx_2\cos\theta} \cdot e^{j\phi_2} \\ \vdots \\ e^{jkx_N\cos\theta} \cdot e^{j\phi_N} \end{bmatrix} = \begin{bmatrix} s_1 \\ s_2 \\ \vdots \\ s_N \end{bmatrix} \tag{3}$$

where ϕ_n, n=1, 2, ...N are random errors. We will assume the latter to be i.i.d. random variables $N(0,\sigma_\phi^2)$. From (3), the mean value of $\underline{S}$ is

$$\bar{\underline{S}} = \overline{e^{j\phi}} \cdot \begin{bmatrix} e^{jkx_1\cos\theta} \\ e^{jkx_2\cos\theta} \\ \vdots \\ e^{jkx_N\cos\theta} \end{bmatrix}$$

$$= e^{-\sigma_\phi^2/2} \underline{S}_o \tag{4}$$

since $\overline{e^{j\phi}} = e^{-\sigma_\phi^2/2}$, and where

$$\underline{S}_o = \begin{bmatrix} e^{jkx_1\cos\theta} \\ e^{jkx_2\cos\theta} \\ \vdots \\ e^{jkx_N\cos\theta} \end{bmatrix} = \begin{bmatrix} s_{o1} \\ s_{o2} \\ \vdots \\ s_{oN} \end{bmatrix} \tag{5}$$

is the steering vector without random errors. Equation (4) shows the steering vector $\underline{S}$ is not biased; the constant $e^{-\sigma_\phi^2/2}$ does not matter.

With array output vector $\underline{V}'$, and steering vector $\underline{S}$, the Hybrid array with constrained mainbeam gain, as shown in Fig. 1, results in equivalent steady state weights [5]

$$\underline{W}' = \mu M_1'^{-1}\underline{S}^* \tag{6}$$

so that

$$e_o = \underline{V}'^T\underline{W}' \tag{7}$$

The time variable is omitted but implied. In (6), the random variable μ and matrix M_1' are given by

$$\mu = \frac{N}{S^T M_1'^{-1}\underline{S}^*} \tag{8}$$

and

$$M_1' = CM_1C \tag{9}$$

where

$$M_1 = (1-F_S)\overline{|\alpha^2|}\,\underline{S}_d^*\underline{S}_d^T + \sum_{j=1}^{J}\overline{|\beta_j^2|}\,\underline{S}^*_{Ij}\underline{S}^T_{Ij} + \sigma_n^2 I \tag{10}$$

with F_s being the complex reference loop gain. (Note that if F_s is complex, M_1 is not Hermitian). Substituting (6) and (9) into (7) we have

$$e_o = \mu\underline{V}'^T C^{-1}M_1^{-1}C^{-1}\underline{S}^* \tag{11}$$

using (1), (11) comes out to be

$$e_o = \mu\underline{V}^T M_1^{-1}C^{-1}\underline{S}^* \tag{12}$$

Define the equivalent weight vector W such that

$$e_o = \underline{V}^T\underline{W} \tag{13}$$

Therefore, $\underline{W} = \mu M_1^{-1}C^{-1}\underline{S}^*$ (14)

Substituting (9) into (8), we have

$$\mu = \frac{N}{\underline{S}^T C^{-1} M_1^{-1} C^{-1} \underline{S}^*} \tag{15}$$

For the nonconstrained Hybrid array processor shown in Fig. 2, the equivalent weight vector is, as shown in Appendix A,

$$\underline{W} = M_1^{-1} C^{-1} \underline{S}^* \tag{16}$$

The average SINR can be defined as the average value of the SINR treated as a random variable which is a function of the random gain and phase errors. With this definition the average SINR of these two system realizations are the same. However, it is difficult to get, by analysis, an explicit expression for the average so defined. For analysis it is easier to determine the separate averages of the power of signal, interference, and noise, then to form the SINR using these averages. For the nonconstrained processor, such separate calculations are especially easy since μ is one. We therefore use this approach below, setting μ to unity. To insure that the SINR so determined is meaningful we also carry out an average SINR calculation by simulation using both definitions, and we find the difference between the two quite small. Thus we conclude that the SINR obtained by the analytical technique we have chosen, closely matches the SINR according to the first definition, and apply to both realizations of the Hybrid array.

By setting u to be one, the average output signal power is

$$\begin{aligned} P_d &= \overline{(\alpha \underline{S}_d^T \underline{W})(\alpha \underline{W}^T \underline{S}_d)^*} \\ &= \overline{|\alpha^2| \underline{S}_d^T M_1^{-1} C^{-1} \underline{S}^* \underline{S}^T C^{-1} M_1^{-1T^*} \underline{S}_d^*} \\ &= \overline{|\alpha^2|} \underline{S}_d^T M_1^{-1} \, \overline{C^{-1} \underline{S}^* \underline{S}^T C^{-1}} \, M_1^{-1T^*} \underline{S}_d^* \end{aligned} \tag{17}$$

$\overline{C^{-1}\underline{S}^{*}\underline{S}^{T}C^{-1}}$ in (17) is examined in the following. Since C is a diagonal matrix, C^{-1} is

$$C^{-1} = \begin{bmatrix} \frac{1}{1+c_1} & & 0 \\ & \frac{1}{1+c_2} & \\ 0 & & \ddots \; \frac{1}{1+c_N} \end{bmatrix} \tag{18}$$

For $c_n << 1$, n=1, 2, ...N. (18) can be approximated by

$$C^{-1} = \begin{bmatrix} 1-c_1 & & 0 \\ & 1-c_2 & \\ 0 & & \ddots \; 1-c_N \end{bmatrix} \tag{19}$$

To calculate $C^{-1}\underline{S}^{*}\underline{S}^{T}C^{-1}$, take the expectation with respect to random phase error first.

$$\overline{(C^{-1}\underline{S}^{*}\underline{S}^{T}C^{-1})}_{\phi} = C^{-1}\,\overline{\underline{S}^{*}\underline{S}^{T}}\,C^{-1} \tag{20}$$

We examine $\underline{S}^{*}\underline{S}^{T}$ in (20)

$$\overline{\underline{S}^{*}\underline{S}^{T}} = \begin{bmatrix} s_1^{*} \\ s_2^{*} \\ \vdots \\ s_N^{*} \end{bmatrix} \begin{bmatrix} s_1 & s_2 & \cdots & s_N \end{bmatrix}$$

$$= \begin{bmatrix} 1 & \overline{e^{j\phi}}^{2}\, e^{jk(x_2-x_1)\cos\theta} & \\ \overline{e^{j\phi}}^{2}\cdot e^{jk(x_1-x_2)\cos\theta} & 1 & \\ \vdots & & \\ \overline{e^{j\phi}}^{2}\, e^{jk(x_1-x_N)\cos\theta} & & 1 \end{bmatrix}$$

(equation continued on next page)

$$= e^{-\sigma_\phi^2} \begin{bmatrix} 1 & e^{jk(x_2-x_1)\cos\theta} & \\ e^{jk(x_1-x_2)\cos\theta} & 1 & \\ \vdots & & \\ e^{jk(x_1-x_N)\cos\theta} & & 1 \end{bmatrix} + (1-e^{-\sigma_\phi^2})I \tag{21}$$

Using (5), (21) comes out to be

$$\overline{\underline{S}\,\underline{S}^{*T}} = e^{-\sigma_\phi^2}\,\underline{S}_o\,\underline{S}_o^{*T} + (1-e^{-\sigma_\phi^2})I \tag{22}$$

Comparing (22) with (4), we see that $(1-e^{-\sigma_\phi^2})I$ in (22) is contributed by the self-correlated term, which is similar to the variance. Substituting (22) into (20), we have

$$\overline{(C^{-1}\underline{S}^{*}\underline{S}^{T}C^{-1})_\phi} = e^{-\sigma_\phi^2}\,C^{-1}\underline{S}_o^{*}\underline{S}_o^{T}C^{-1} + (1-e^{-\sigma_\phi^2})C^{-1}C^{-1} \tag{23}$$

Then, taking the expectation with respect to the random gain error,

$$\overline{C^{-1}\underline{S}^{*}\underline{S}^{T}C^{-1}} = e^{-\sigma_\phi^2}\,\overline{C^{-1}\underline{S}_o^{*}\underline{S}_o^{T}C^{-1}} + (1-e^{-\sigma_\phi^2})\overline{C^{-1}C^{-1}} \tag{24}$$

We examine $\overline{C^{-1}\underline{S}_o^{*}\underline{S}_o^{T}C^{-1}}$ in (24).

$$C^{-1}\underline{S}_o^{*} = \begin{bmatrix} (1-c_1)s_{o1}^{*} \\ (1-c_2)s_{o2}^{*} \\ \vdots \\ (1-c_N)s_{oN}^{*} \end{bmatrix} \tag{25}$$

$$\underline{S}_o^T C^{-1} = \left[(1-c_1)s_{o1}\ (1-c_2)s_{o2}\ \ldots (1-c_N)s_{oN}\right] \tag{26}$$

Using (25) and (26), we have

$$C^{-1}\underline{S}_o^*\underline{S}_o^T C^{-1} = \begin{bmatrix} (1-c_1)^2 & (1-c_1)(1-c_2)s_{o1}^* s_{o2} & \cdots \\ (1-c_1)(1-c_2)s_{o1}s_{o2}^* & (1-c_2)^2 & \\ & & (1-c_3)^2 \\ & & \ddots \\ (1-c_1)(1-c_N)s_{o1}s_{oN}^* & & (1-c_N)^2 \end{bmatrix} \tag{27}$$

The expectation of (27) is therefore

$$\overline{C^{-1}S_o^* S_o^T C^{-1}} = \begin{bmatrix} 1+\sigma_c^2 & s_{o1}^* s_{o2} & \cdots & s_{o1}^* s_{oN} \\ s_{o1}s_{o2}^* & 1+\sigma_c^2 & & \\ & & & \\ s_{o1}s_{oN}^* & & & 1+\sigma_c^2 \end{bmatrix}$$

$$= \underline{S}_o^* \underline{S}_o^T + \sigma_c^2 I \tag{28}$$

$\overline{C^{-1}C^{-1}}$ in (24) is

$$\overline{C^{-1}C^{-1}} = \begin{bmatrix} (1-c_1)^2 & & \\ & (1-c_2)^2 & \\ & & (1-c_N)^2 \end{bmatrix}$$

$$= (1+\sigma_c^2)I \tag{29}$$

Substituting (28) and (29) into (24), we have

$$\overline{C^{-1}\underline{S}^*\underline{S}^T C^{-1}} = e^{-\sigma_\phi^2}(\underline{S}_o^*\underline{S}_o^T + \sigma_c^2 I) + (1-e^{-\sigma_\phi^2})(1+\sigma_c^2)I$$

$$= e^{-\sigma_\phi^2}\underline{S}_o^*\underline{S}_o^T + (1-e^{-\sigma_\phi^2})I + \sigma_c^2 I \tag{30}$$

Substituting (30) into (17), we have

$$P_d = |\overline{\alpha^2}|\Big[e^{-\sigma_\phi^2}\underline{S}_d^T M_1^{-1}\underline{S}_o^*\underline{S}_o^T M_1^{-1T^*}\underline{S}_d^* + (1-e^{-\sigma_\phi^2})\underline{S}_d^T M_1^{-1}M_1^{-1T^*}\underline{S}_d^* + \sigma_c^2\underline{S}_d^T M_1^{-1}M_1^{-1T^*}\underline{S}_d^*\Big] \tag{31}$$

Similarly, the average interference output power is

$$P_I = \overline{\Big(\sum_{j=1}^{J}\beta_j\underline{S}_{Ij}^T\underline{W}\Big)\Big(\sum_{j'=1}^{J}\beta_{j'}\underline{W}^T\underline{S}_{Ij'}\Big)^*}$$

$$= \sum_{j=1}^{J}|\beta_j^2|\Big[e^{-\sigma_\phi^2}\underline{S}_{Ij}^T M_1^{-1}\underline{S}_o^*\underline{S}_o^T M_1^{-1T^*}\underline{S}_{Ij}^* + (1-e^{-\sigma_\phi^2})\underline{S}_{Ij}^T M_1^{-1}M_1^{-1T^*}\underline{S}_{Ij}^* + \sigma_c^2\underline{S}_{Ij}^T M_1^{-1}M_1^{-1T^*}\underline{S}_{Ij}^*\Big] \tag{32}$$

The average noise power is

$$P_n = \overline{(\underline{N}^T\underline{W})(\underline{W}^T\underline{N})^*}$$

$$= \overline{\underline{N}^T M_1^{-1}C^{-1}\underline{S}^*\underline{S}^T C^{-1}M_1^{-1T^*}\underline{N}^*} \tag{33}$$

In (33), we take the expectation with respect to the random gain and phase errors first, giving

$$P_{n_{\phi c}} = \underline{N}^T M_1^{-1} C^{-1} \underline{S}^* \underline{S}^T C^{-1} M_1^{-1T^*} \underline{N}^*$$

$$= \underline{N}^T M_1^{-1} [e^{-\sigma_\phi^2} \underline{S}_o^* \underline{S}_o^T + (1-e^{-\sigma_\phi^2}) I + \sigma_c^2 I] M_1^{-1T^*} \underline{N}^*$$

$$= e^{-\sigma_\phi^2} \underline{N}^T M_1^{-1} \underline{S}_o^* \underline{S}_o^T M_1^{-1T^*} \underline{N}^* + (1-e^{-\sigma_\phi^2}) \underline{N}^T M_1^{-1} M_1^{-1T^*} N^*$$

$$+ \sigma_c^2 \underline{N}^T M_1^{-1} M_1^{-1T^*} \underline{N}^*$$

$$= e^{-\sigma_\phi^2} \underline{S}_o^T M_1^{-1T^*} \underline{N}^* \underline{N}^T M_1^{-1} \underline{S}_o^* + (1-e^{-\sigma_\phi^2}) \underline{N}^T M_1^{-1} M_1^{-1T^*} \underline{N}^*$$

$$+ \sigma_c^2 \underline{N}^T M_1^{-1} M_1^{-1T^*} \underline{N}^* \qquad (34)$$

Then, we take the expectation with respect to the noise random variables giving

$$P_n = e^{-\sigma_\phi^2} \underline{S}_o^T M_1^{-1T^*} \overline{\underline{N}^* \underline{N}^T} M_1^{-1} \underline{S}_o^* + (1-e^{-\sigma_\phi^2}) \overline{\underline{N}^T M_1^{-1} M_1^{-1T^*} \underline{N}^*}$$

$$+ \sigma_c^2 \overline{\underline{N}^T M_1^{-1} M_1^{-1T^*} \underline{N}^*}$$

$$= \sigma_n^2 e^{-\sigma_\phi^2} \underline{S}_o^T M_1^{-1T^*} M_1^{-1} \underline{S}_o^* + \sigma_n^2 (1-e^{-\sigma_\phi^2}) \text{Trace} [M_1^{-1} M_1^{-1T^*}]$$

$$+ \sigma_n^2 \sigma_c^2 \text{Trace} \left[M_1^{-1} M_1^{-1T^*} \right] \qquad (35)$$

Note that the quadratic form $\overline{\underline{N}^T M_1^{-1} M_1^{-1T^*} \underline{N}^*}$ reduces to $\sigma_n^2 \text{Trace} \left[M_1^{-1} M_1^{-1T^*} \right]$ because the noise terms are independent with each other.

Discussion:

If there is only random gain error, i.e. $\sigma_\phi = 0$, (31), (32) and (35) turn out to be

$$P_d = \overline{|\alpha^2|} \underline{S}_d^T M_1^{-1} \underline{S}_o^* \underline{S}_o^T M_1^{-1T^*} \underline{S}_d^* + \overline{|\alpha^2|} \sigma_c^2 \underline{S}_d^T M_1^{-1} M_1^{-1T^*} \underline{S}_d^* \qquad (36)$$

$$P_I = \sum_{j=1}^{J} |\overline{\beta_j^2}| \, \underline{S}_{Ij}^T M_1^{-1} \underline{S}_o^* \underline{S}_o^T M_1^{-1T^*} \underline{S}_{Ij}^*$$

$$+ \sum_{j=1}^{J} |\overline{\beta_j^2}| \sigma_c^2 \underline{S}_{Ij}^T M_1^{-1} M_1^{-1T^*} \underline{S}_{Ij}^* \qquad (37)$$

and

$$P_n = \sigma_n^2 \underline{S}_o^T M_1^{-1T^*} M_1^{-1} \underline{S}_o^* + \sigma_n^2 \sigma_c^2 \text{Trace}[M_1^{-1} M_1^{-1T^*}] \qquad (38)$$

The first term on the right hand side of each of the equations (36), (37) and (38) is the output power without random errors. The second term in each is contributed by random amplitude error and increases as σ_c^2 increasing.

If there is only random phase error, i.e. $\sigma_c^2 = 0$, (31), (32) and (35) become

$$P_d = |\overline{\alpha^2}| e^{-\sigma_\phi^2} \underline{S}_d^T M_1^{-1} \underline{S}_o^* \underline{S}_o^T M_1^{-1T^*} \underline{S}_d^*$$

$$+ |\overline{\alpha}|^2 (1-e^{-\sigma_\phi^2}) \underline{S}_d^T M_1^{-1} M_1^{-1T^*} \underline{S}_d^* \qquad (39)$$

$$P_I = \sum_{j=1}^{J} |\overline{\beta_j^2}| \, [e^{-\sigma_\phi^2} \underline{S}_{Ij}^T M_1^{-1} \underline{S}_o^* \underline{S}_o^T M_1^{-1T^*} \underline{S}_{Ij}^*$$

$$+ \sum_{j=1}^{J} |\overline{\beta_j^2}| (1-e^{-\sigma_\phi^2}) \underline{S}_{Ij}^T M_1^{-1} M_1^{-1T^*} \underline{S}_{Ij}^* \qquad (40)$$

and

$$P_n = \sigma_n^2 e^{-\sigma_\phi^2} \underline{S}_o^T M_1^{-1T^*} M_1^{-1} \underline{S}_o^* + \sigma_n^2 (1-e^{-\sigma_\phi^2}) \text{Trace}[M_1^{-1} M_1^{-1T^*}] \qquad (41)$$

The first term on the right hand side of each of the equations (39), (40) and (41) is similar to each of the corresponding terms on the right of (36), (37) and (38) except for the factor $e^{-\sigma_\phi^2}$. As the phase variance increases, these terms which represent the mean steering vector decrease. At the same time, the second term on the right of each of the equations (39), (40) and (41), containing the factor $(1-e^{-\sigma_\phi^2})$, increases from zero. We point out that the assumption of normally distributed phase errors implies errors with σ_ϕ less than, say, $\pi/2$.

To see explicitly how the signal is effected by the random gain and phase errors, let us assume that there is no interference. Then,

$$M_1 = (1-F_s)|\overline{\alpha^2}|\underline{S}_d^* \underline{S}^T + \sigma_n^2 I \tag{42}$$

Using the matrix inversion lemma, we have

$$M_1^{-1} = \frac{1}{\sigma_n^2}\left[I - \frac{(1-F_s)\gamma_d \underline{S}_d^* \underline{S}_d^T}{(1-F_s)\gamma_d N + 1}\right] \tag{43}$$

with

$$\gamma_d = \frac{|\overline{\alpha^2}|}{\sigma_n^2}$$

Assume that there is only random error, so that $\underline{S}_o = \underline{S}_d$. It is shown in the Appendix B that substituting (43) into (31) and (35), we get the results shown in (44), (45) and (46), below.

$$P_d = \frac{|\overline{\alpha^2}| e^{-\sigma_\phi^2} N^2}{\sigma_n^4 |(1-F_s)\gamma_d N+1|^2} + \frac{|\overline{\alpha^2}|(1-e^{-\sigma_\phi^2})N}{\sigma_n^4 |(1-F_s)\gamma_d N+1|^2} + \frac{|\overline{\alpha^2}|\sigma_c^2 N}{\sigma_n^4 |(1-F_s)\gamma_d N+1|^2} \tag{44}$$

$$P_n = \frac{\sigma_n^2 e^{-\sigma_\phi^2} N}{\sigma_n^4 |(1-F_S)\gamma_d N+1|^2} + \frac{\sigma_n^2 (1-e^{-\sigma_\phi^2})\{\gamma_d N(N-1)[|1-F_s|^2 \gamma_d N+2-2R_e F_s]+N}{\sigma_n^4 |(1-F_s)\gamma_d N+1|^2} + \frac{\sigma_n^2 \sigma_c^2 \{\gamma_d N(N-1)[|1-F_s|^2 \gamma_d N+2-2R_e F_s]+N\}}{\sigma_n^4 |(1-F_s)\gamma_d N+1|^2} \tag{45}$$

where $R_e F_s$ is defined as the real part of F_s. The signal-to-noise ratio is then

$$SNR = \frac{\gamma_d e^{-\sigma_\phi^2} N + \gamma_d (1-e^{-\sigma_\phi^2}) + \gamma_d \sigma_c^2}{e^{-\sigma_\phi^2} + (1-e^{-\sigma_\phi^2} + \sigma_c^2)\{\gamma_d (N-1) \cdot [|1-F_s|^2 \gamma_d N + 2 - 2R_e F_s] + 1\}} \tag{46}$$

In the following we separately discuss the effect of random phase error in the steering vector and the effect of random gain error.

First we assume that there is only random phase error. Then (46) reduces to

$$SNR = \frac{\gamma_d e^{-\sigma_\phi^2} N + \gamma_d (1-e^{-\sigma_\phi^2})}{1 + (1-e^{-\sigma_\phi^2}) \gamma_d (N-1) [|1-F_s|^2 \gamma_d N + 2 - 2R_e F_s]} \tag{47}$$

Two special cases are of interest. With $F_s = 1$, the reference signal is ideal and we have from (47)

$$SNR = \gamma_d e^{-\sigma_\phi^2} N + \gamma_d (1-e^{-\sigma_\phi^2}) \tag{48}$$

Degradation of SNR for this case is the same as that for a conventional beamforming array.

For $F_s = 0$, we have the Applebaum array for which (47) gives

$$SNR = \frac{\gamma_d e^{-\sigma_\phi^2} N + \gamma_d (1-e^{-\sigma_\phi^2})}{1 + (1-e^{-\sigma_\phi^2}) \gamma_d (N-1)(\gamma_d N + 2)} \tag{49}$$

Equations (47) - (49) are shown plotted in Figures 3 - 5 for N = 7, 30 and 100 respectively, with F_s as family parameter. The improvements obtained with the Hybrid array over the Applebaum array are here evident. It should be noted, though, that with increasing N the effect of a given phase error variance also increases.

Computer simulation was also carried out for a seven element 10λ array without interference with results as shown in Table 1. Six combinations of F_s and σ_ϕ were simulated, each with 100 samples of random phase errors. The third column in Table 1 was obtained by computing the SNR for each random phase sample then averaging over the 100 samples. The average SNR in the fourth column is the ratio of average signal power to average noise power when μ equals one. The last column is the results of theoretical computation based on equations (47) - (49). The difference between the third and the fourth column is small. For the Hybrid array with F_s close to one, they are almost the same. From these results we conclude that the simulation sample used for the fourth column is adequate, and that the similarity of results in the third and fourth columns suggests that the SNR calculated as a ratio of averages and as an average of ratios are not appreciably different.

If there is only random gain error, (46) reduces to

$$SNR = \frac{\gamma_d N + \gamma_d \sigma_c^2}{1+\sigma_c^2\{\gamma_d(N-1)[|1-F_s|^2\gamma_d N+2-2R_e F_s]+1\}} . \tag{50}$$

With $F_s = 1$, we have from (50)

$$SNR = \frac{\gamma_d N+\sigma_c^2\gamma_d}{1+\sigma_c^2} \tag{51}$$

AD-A133 733 RESEARCH IN ADAPTIVE BEAMFORMING FOR SATELLITE COMMUNICATIONS(U) PENNSYLVANIA UNIV PHILADELPHIA F HABER ET AL. MAY 83 RADC-TR-83-54 F30602-81-K-0211

2/3

UNCLASSIFIED F/G 17/2 NL

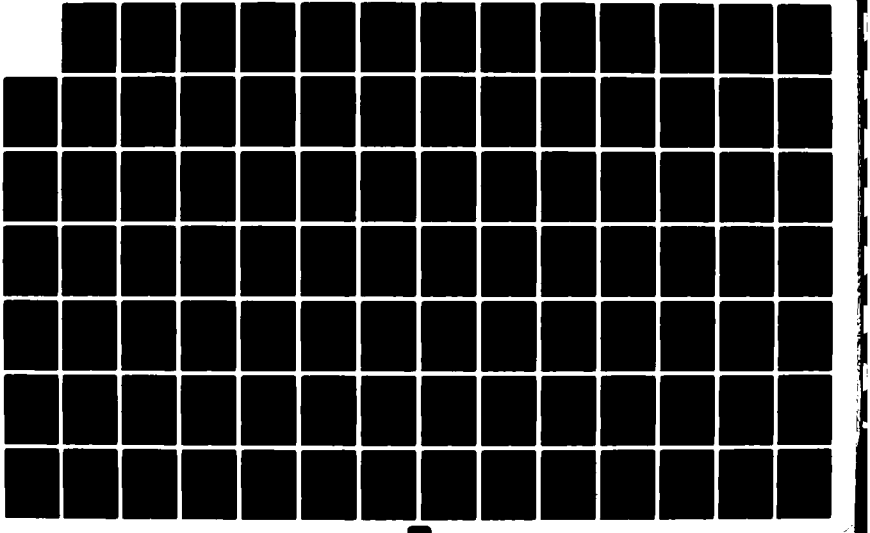

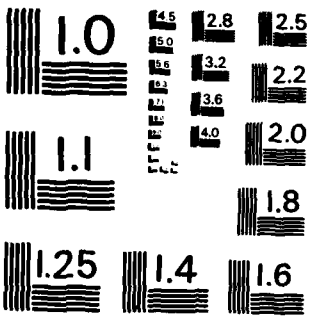

MICROCOPY RESOLUTION TEST CHART
NATIONAL BUREAU OF STANDARDS - 1963 - A

Degradation is the same as that for a conventional beamforming array.

For $F_s = 0$, (50) becomes

$$SNR = \frac{\gamma_d N+\gamma_d \sigma_c^2}{1+\sigma_c^2[\gamma_d(N-1)(\gamma_d N+2)+1]} \tag{52}$$

Equation (50) - (52) are shown plotted in Figures 6 - 8. The Hybrid array is much less sensitive to the random gain error than the Applebaum array.

Computer simulation was again carried out for the same array geometry. Results, as shown in Table 2, show the number of samples is adequate and SNR calculated by two definitions are close.

Fs	σ_ϕ	Average of Each SNR Sampled	Average Signal Power Over Average Noise Power	Computation Based on (47) - (49)
1.0	5°	18.42	18.42	18.42
$0.95e^{-j10°}$	5°	15.39	15.22	15.29
0.0	5°	3.73	3.00	3.14
1.0	10°	18.33	18.33	18.34
$0.95e^{-j10°}$	10°	11.52	11.08	11.19
0.0	10°	-2.20	-2.96	-2.82

TABLE 1
Simulation of 7 element 10λ Hybrid Array with Random Phase Errors.

Fs	σ_c	Average of Each SNR Sampled	Average Signal Power Over Average Noise Power	Computation Based on (50) - (52)
1.0	0.025	18.45	18.45	18.45
$0.95e^{-j10°}$	0.025	18.08	18.07	18.09
0	0.025	13.03	12.66	12.77
1.0	0.05	18.44	18.44	18.44
$0.95e^{-j10°}$	0.05	17.15	17.10	17.15
0	0.05	8.22	7.56	7.73

TABLE 2
Simulation of 7 element 10λ Hybrid Array with Random Amplitude Errors.

REFERENCES

[1] S. P. Applebaum, "Adaptive Arrays," IEEE Trans. on Antennas and Propagation, Vol. AP-24, No. 5, September 1976.

[2] S. P. Applebaum and D. J. Chapman, "Adaptive Arrays with Main Beam Constraints," IEEE Trans. on Antennas and Propagation, Vol. AP-24, No. 5, September 1976.

[3] R. T. Compton Jr., "Pointing Accuracy and Dynamic Range in a Steered Beam Array," IEEE Trans. on Aerospace and Electronic Systems, Vol. AES-16, No. 3, May 1980.

[4] F. Haber, P.C.C. Yeh, "Effect of Pointing Error on a Directionally Constrained Array," Valley Forge Research Center, University of Pennsylvania, Quarterly Progress Report No. 36, February 15, 1981.

[5] F. Haber, Y. Bar-Ness and C. C. Yeh, "An Adaptive Interference Cancelling Array Utilizing Hybrid Techniques," Appendix in this Report.

[6] R.T. Compton Jr., "The Effect of Random Steering Vector Errors in the Applebaum Adaptive Array," IEEE Trans. on Aerospace and Electronic Systems, Vol. AES-18, No. 5, September 1982.

LIST OF FIGURE CAPTIONS

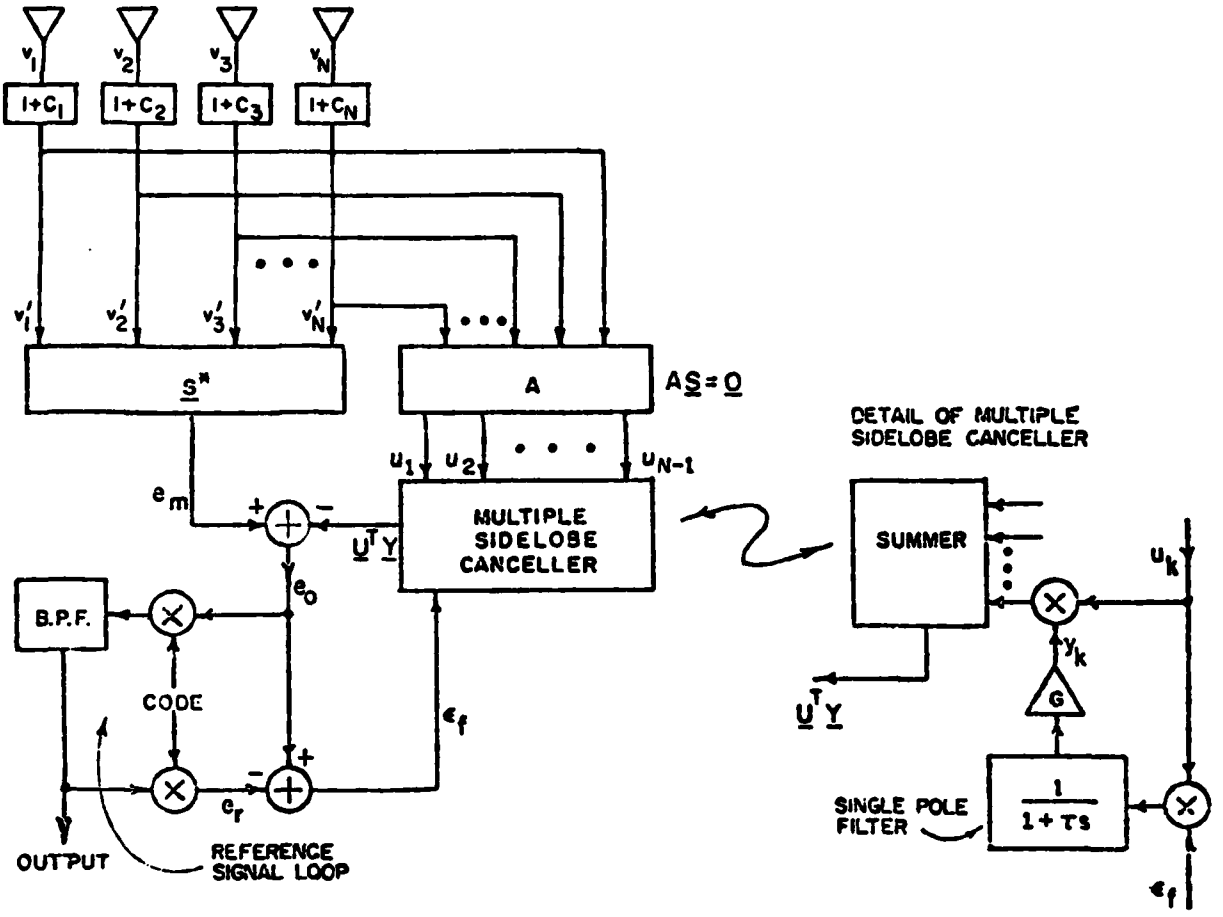

Figure 1 Constrained Hybrid Array Processor

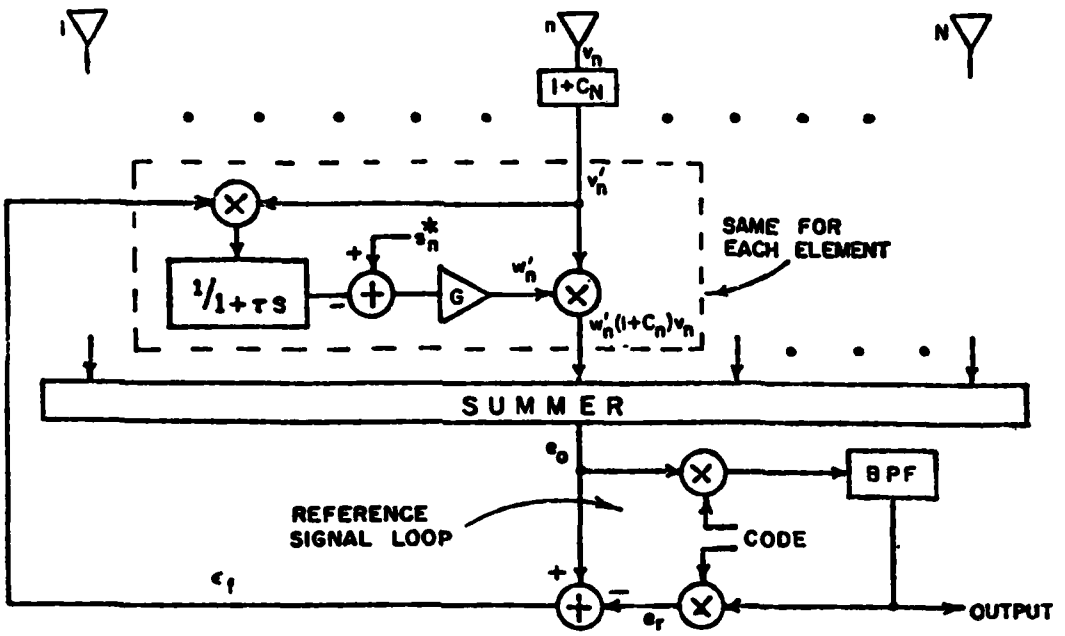

Figure 2 Nonconstrained Hybrid Array Processor

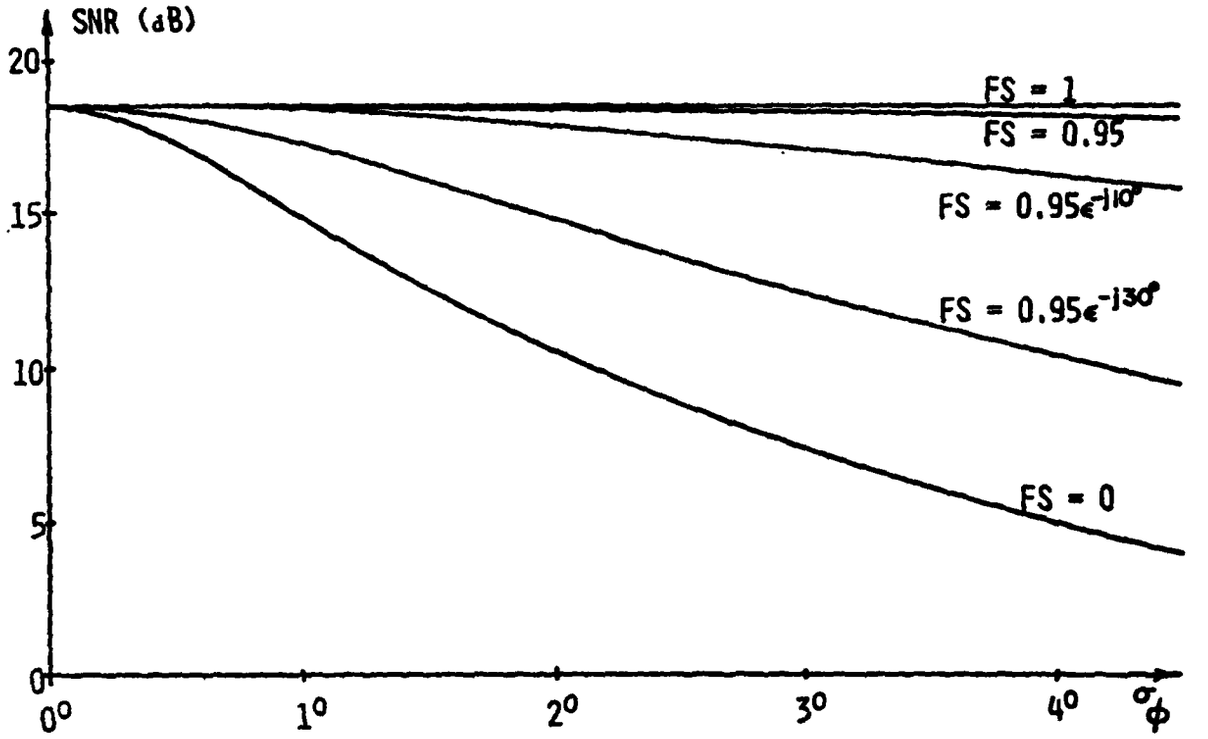

Figure 3 Sensitivity to Random Phase Errors

N = 7

γ_d = 10

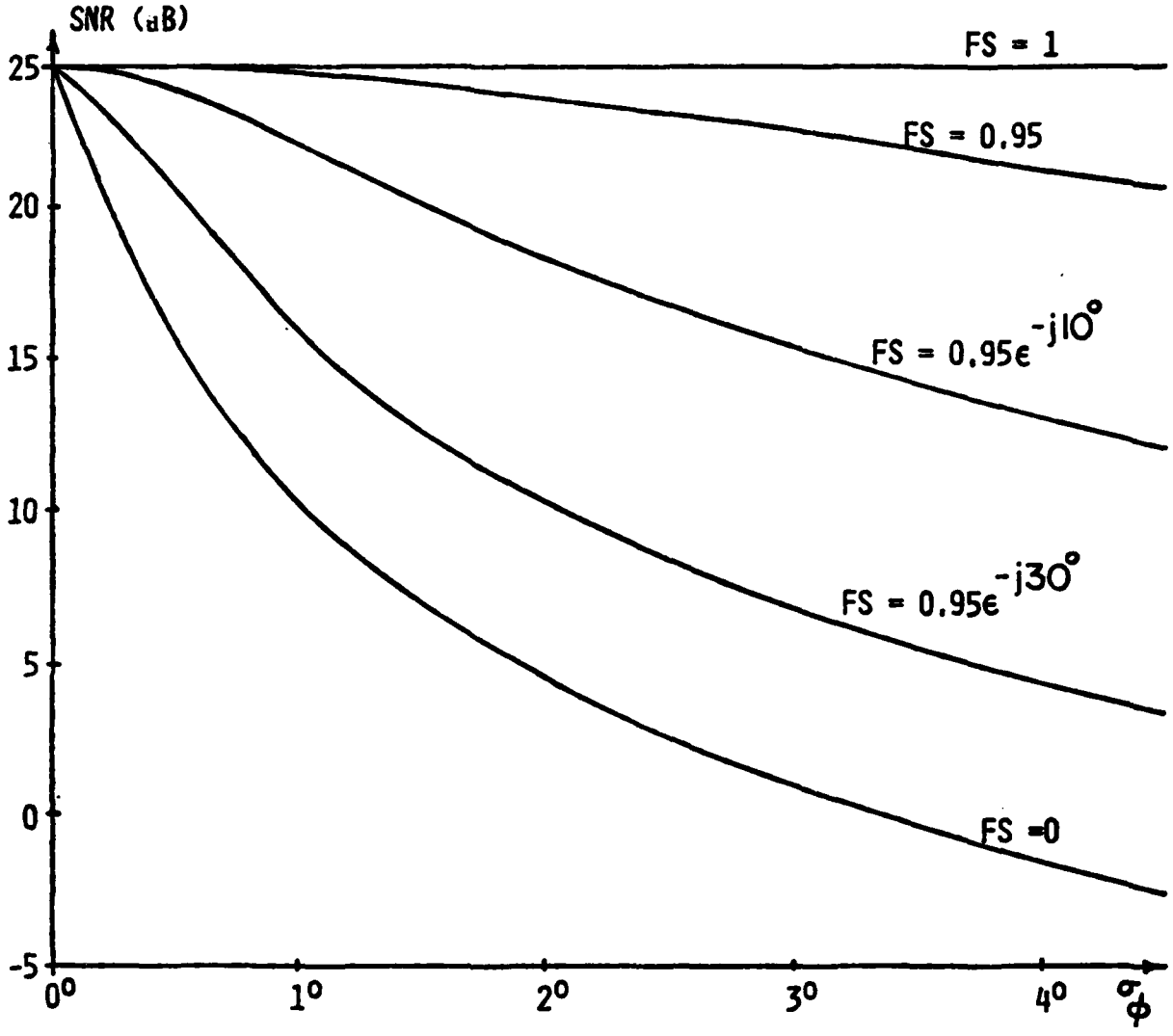

Figure 4 Sensitivity to Random Phase Errors

N = 30

γ_d = 10

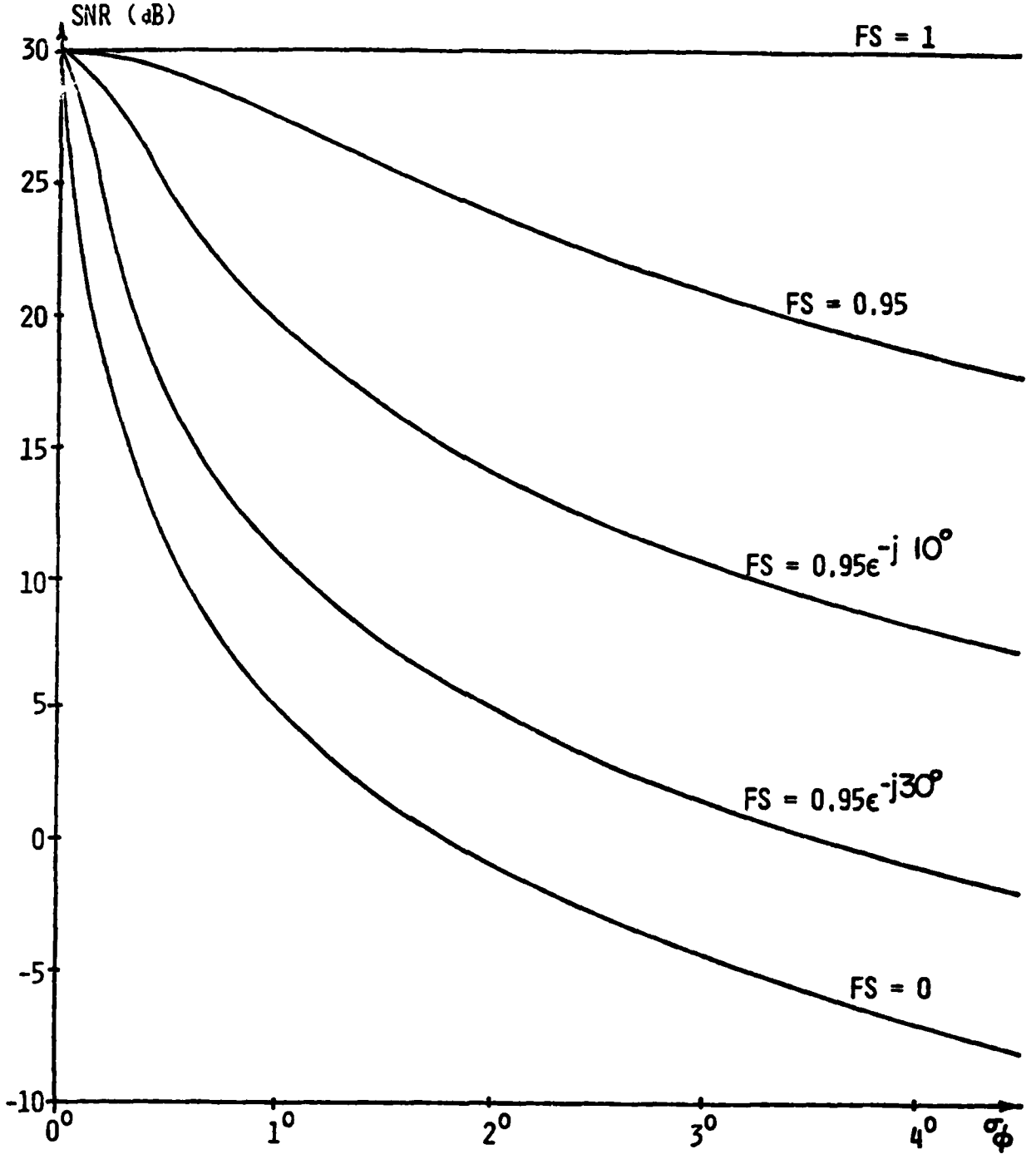

Figure 5 Sensitivity to Random Phase Errors

N = 100

γ_d = 10

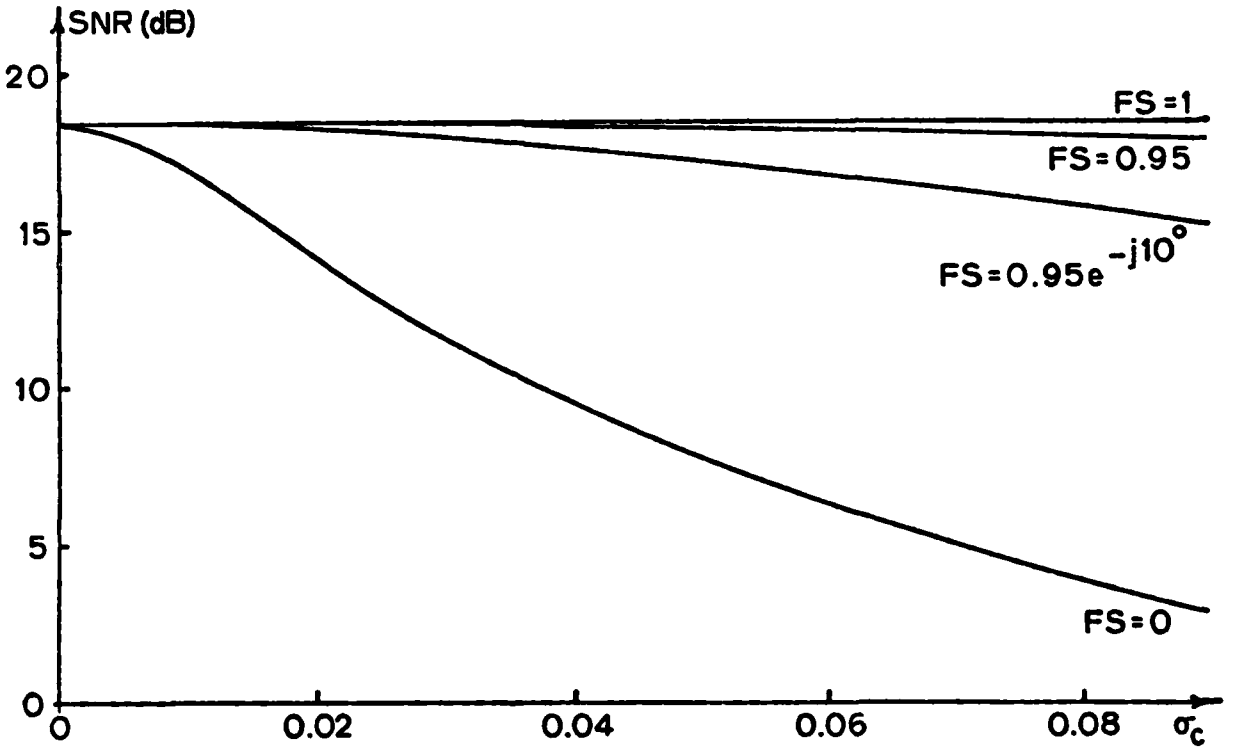

Figure 6 Sensitivity to Random Amplitude Errors

N = 7

γ_d = 10

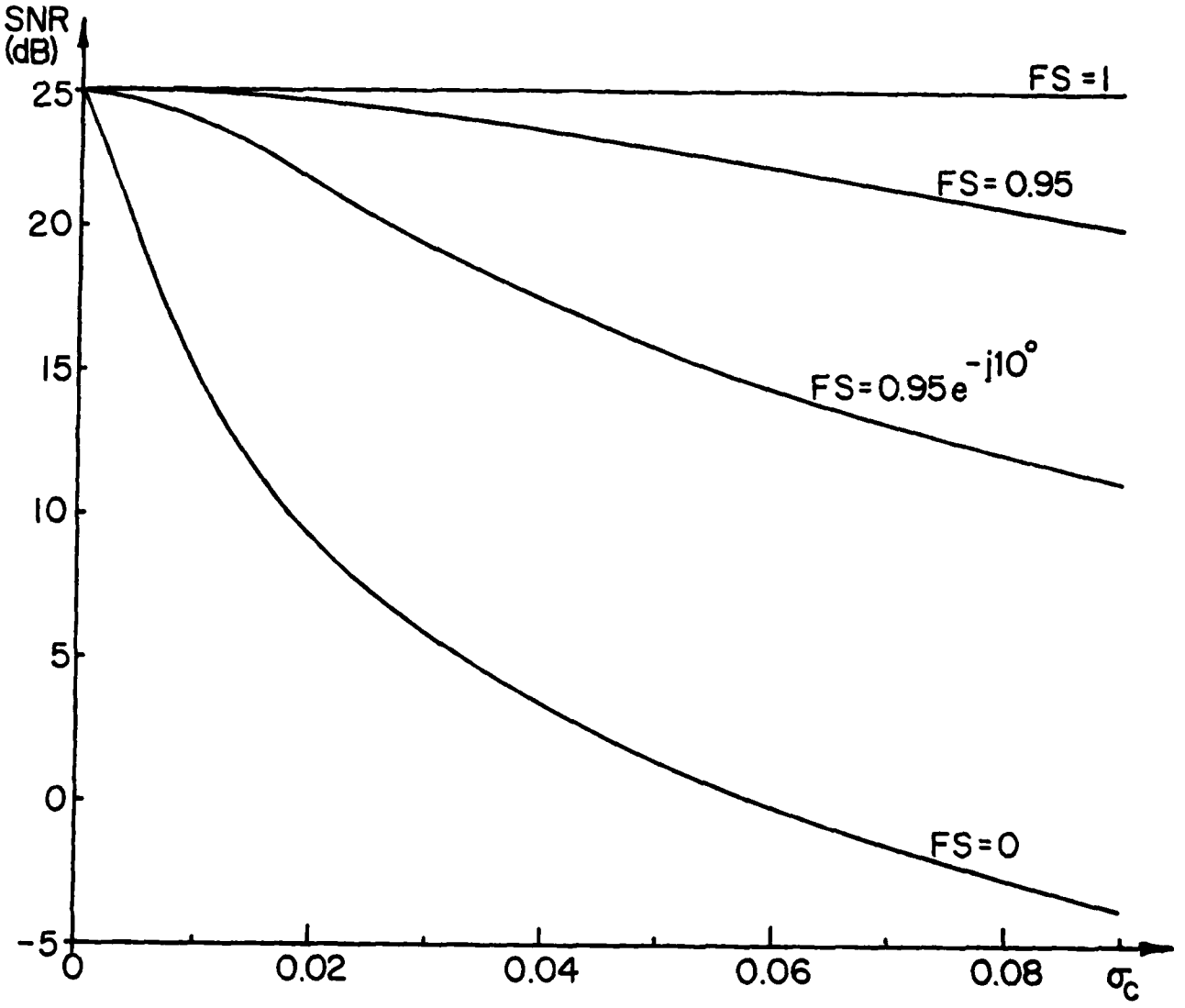

Figure 7 Sensitivity to Random Amplitude Errors

N = 30

γ_d = 10

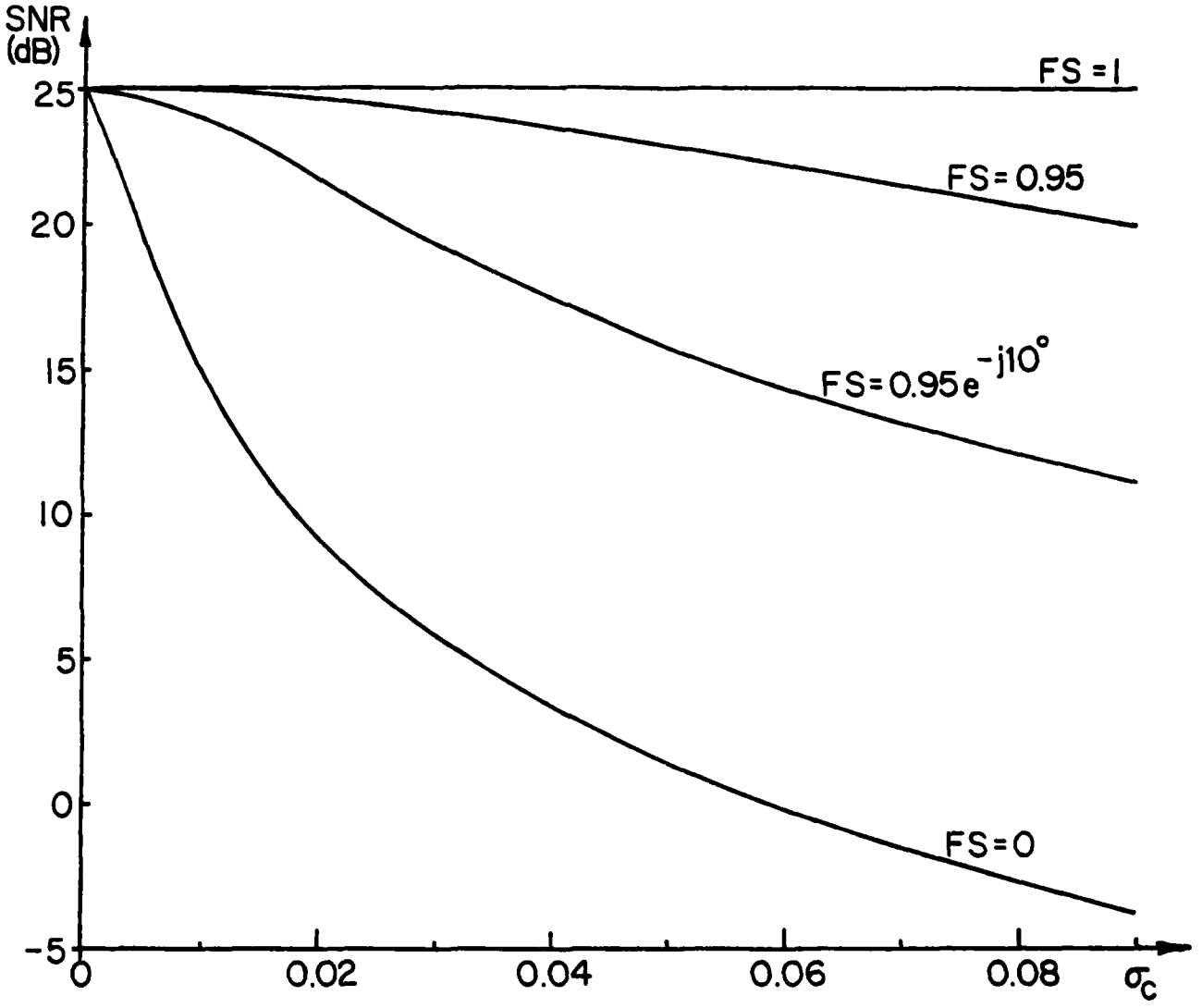

Figure 7 Sensitivity to Random Amplitude Errors

N = 30

γ_d = 10

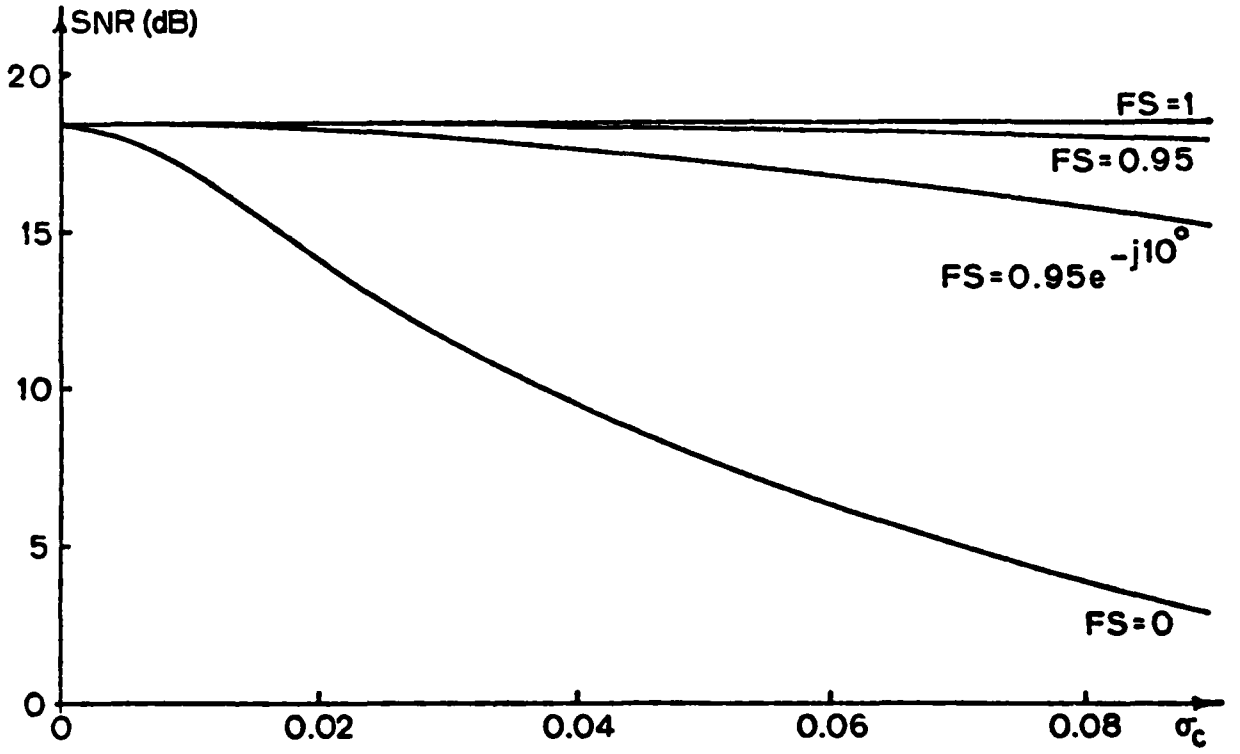

Figure 6 Sensitivity to Random Amplitude Errors

N = 7

γ_d = 10

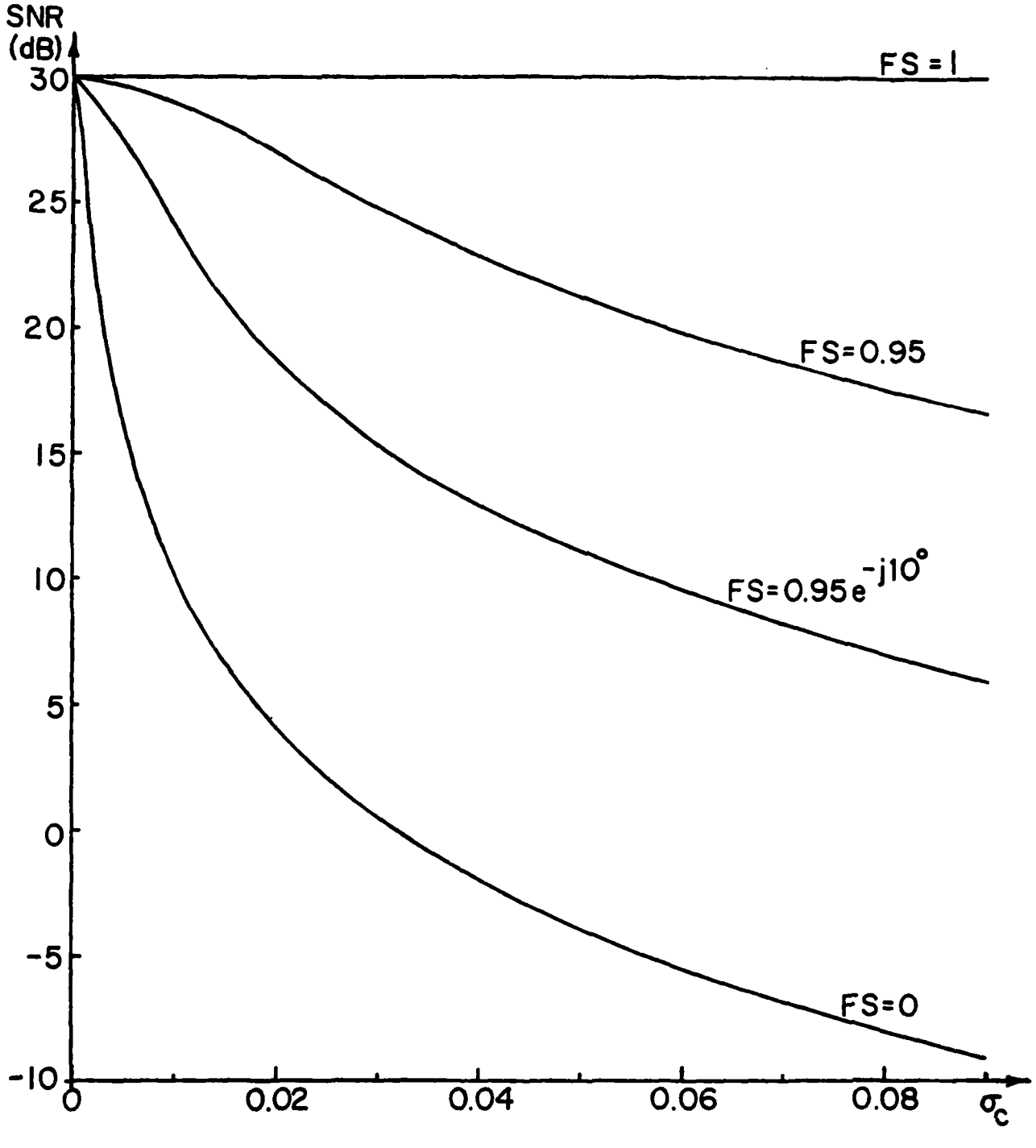

Figure 8 Sensitivity to Random Amplitude Errors

N = 100

γ_d = 10

Appendix C1

The equivalent weight vector of a nonconstrained Hybrid array shown in Fig. 2 is derived in the following. The steady state control loop equation for G large enough is

$$\overline{\underline{V}'^{*}(e_o - e_r)} = \underline{S}^{*} \tag{C1-1}$$

where

$$e_o = \underline{V}'^{T}\underline{W}' = \underline{V}^{T}C\underline{W}' \tag{C1-2}$$

and

$$e_r = F_s \alpha \underline{S}_d^{T} C\underline{W}' + n_r \tag{C1-3}$$

Using (C1-1) and (C1-2) we have

$$\overline{C\underline{V}^{*}\underline{V}^{T}C\underline{W}'} - \overline{C\underline{V}^{*}e_r} = \underline{S}^{*} \tag{C1-4}$$

Using (C1-3) $\overline{\underline{V}^{*}e_r}$ in (C1-4) is

$$\overline{\underline{V}^{*}e_r} = \overline{\underline{V}^{*}(F_s \alpha \underline{S}_d^{T} C\underline{W}' + n_r)} = F_s \overline{|\alpha^2|}\,\underline{S}_d^{*}\underline{S}_d^{T}C\underline{W}' \tag{C1-5}$$

Substituting (C1-5) into (C1-4), we have

$$\overline{C\underline{V}^{*}\underline{V}^{T}\underline{W}'} - CF_s \overline{|\alpha^2|}\,\underline{S}_d^{*}\underline{S}_d^{T}C\underline{W}' = \underline{S}^{*} \tag{C1-6}$$

(C1-6) can be written as

$$CM_1C\underline{W}' = \underline{S}^{*} \tag{C1-7}$$

Therefore

$$\underline{W}' = C^{-1}M_1^{-1}C^{-1}\underline{S}^{*} \tag{C1-8}$$

The equivalent weight vector $\underline{W}$ is defined such that

$$e_o = \underline{V}^{T}\underline{W} \tag{C1-9}$$

From (C1-2) and (C1-9), we have

$$\underline{W} = C\underline{W}' = M_1^{-1}C^{-1}\underline{S}^{*} \tag{C1-10}$$

Appendix C2

We work out an example to see explicitly how the desired signal is effected by the random gain and phase errors. Assume that there are only desired signal and noise. M_1 reduces to

$$M_1 = (1-F_s)\overline{|\alpha^2|}\underline{S}_d^*\underline{S}_d^T+\sigma_n^2 I \tag{C2-1}$$

The inverse of M_1 can be obtained by using the matrix inversion lemma, which gives

$$M_1^{-1} = \frac{1}{\sigma_n^2}\left[I- \frac{(1-F_s)\gamma_d \underline{S}_d^* \underline{S}_d^T}{(1-F_s)\gamma_d N+1}\right] \tag{C2-2}$$

with $\gamma_d = \dfrac{\overline{|\alpha^2|}}{\sigma_n^2}$.

Assume that there are only random errors, so that $\underline{S}_o = \underline{S}_d$. (31) and (35) comes out to be

$$\begin{aligned} P_d = {} & \overline{|\alpha^2|}e^{-\sigma_\phi^2}\underline{S}_d^T M_1^{-1}\underline{S}_d^*\underline{S}_d^T M_1^{-1T^*}\underline{S}_d^* \\ & + \overline{|\alpha^2|}(1-e^{-\sigma_\phi^2})\underline{S}_d^T M_1^{-1}M_1^{-1T^*}\underline{S}_d^* \\ & + \overline{|\alpha^2|}\sigma_c^2\underline{S}_d^T M_1^{-1}M_1^{-1T^*}\underline{S}_d^* \end{aligned} \tag{C2-3}$$

and

$$\begin{aligned} P_n = {} & \sigma_n^2 e^{-\sigma_\phi^2}\underline{S}_d^T M_1^{-1T^*}M_1^{-1}\underline{S}_d^*+\sigma_n^2(1-e^{-\sigma_\phi^2})\mathrm{Trace}[M_1^{-1}M_1^{-1T^*}] \\ & + \sigma_n^2\sigma_c^2\mathrm{Trace}[M_1^{-1}M_1^{-1T^*}] \end{aligned} \tag{C2-4}$$

Parts of (C2-3) are evaluted below using (C2-2). Thus

$$\underline{S}_d^T \underline{M}_1^{-1} \underline{S}_d^* \underline{S}_d^T \underline{M}_1^{-1T^*} \underline{S}_d^* = (\underline{S}_d^T \underline{M}_1^{-1} \underline{S}_d^*)(\underline{S}_d^T \underline{M}_1^{-1} \underline{S}_d^*)^{T^*}$$

$$= |\underline{S}_d^T \underline{M}_1^{-1} \underline{S}_d^*|^2$$

$$= \left|\frac{1}{\sigma_n^2} \underline{S}_d^T \left[I - \frac{(1-F_s)\gamma_d \underline{S}_d^* \underline{S}_d^T}{(1-F_s)\gamma_d N + 1}\right] \underline{S}_d^*\right|^2$$

$$= \left|\frac{1}{\sigma_n^2} \left[N - \frac{(1-F_s)\gamma_d N^2}{(1-F_s)\gamma_d N+1}\right]\right|^2$$

$$= \frac{N^2}{\sigma_n^4 \left|(1-F_s)\gamma_d N+1\right|^2} \qquad \text{(C2-5)}$$

and also

$$\underline{S}_d^T \underline{M}_1^{-1} \underline{M}_1^{-1T^*} \underline{S}_d^* = \frac{1}{\sigma_n^4} \underline{S}_d^T \left[I - \frac{(1-F_s)\gamma_d \underline{S}_d^* \underline{S}_d^T}{(1-F_s)\gamma_d N + 1}\right]$$

$$\cdot \left[I - \frac{(1-F_s)\gamma_d \underline{S}_d^* \underline{S}_d^T}{(1-F_s)\gamma_d N + 1}\right]^{T^*} \underline{S}_d^*$$

$$= \frac{1}{\sigma_n^4} \left[\underline{S}_d^T - \frac{(1-F_s)\gamma_d N \underline{S}_d^T}{(1-F_s)\gamma_d N+1}\right] \cdot \left[\underline{S}_d^* - \frac{(1-F_s)^* \gamma_d N \underline{S}_d^*}{(1-F_s)^* \gamma_d N + 1}\right]$$

$$= \frac{1}{\sigma_n^4} \frac{\underline{S}_d^T}{(1-F_s)\gamma_d N+1} \cdot \frac{\underline{S}_d^*}{(1-F_s)^* \gamma_d N+1}$$

$$= \frac{N}{\sigma_n^4 \left|(1-F_s)\gamma_d N+1\right|^2} \qquad \text{(C2-6)}$$

Substituting (C2-5) and (C2-6) into (C2-3) we have

$$P_d = \frac{|\overline{\alpha^2}| e^{-\sigma_\phi^2 N^2}}{\sigma_n^4 |(1-F_s)\gamma_d N+1|^2} + \frac{|\overline{\alpha^2}| (1-e^{-\sigma_\phi^2})N}{\sigma_n^4 |(1-F_s)\gamma_d N+1|^2}$$

$$+ \frac{|\overline{\alpha^2}| \sigma_c^2 N}{\sigma_n^4 |(1-F_s)\gamma_d N+1|^2} \qquad \text{(C2-7)}$$

Parts of (C2-4) are next evaluated. Thus

$$\underline{S}_d^T M_1^{-1T^*} M_1^{-1} \underline{S}_d^* = \frac{1}{\sigma_n^4} \underline{S}_d^T [I - \frac{(1-F_s)\gamma_d \underline{S}_d^* \underline{S}_d^T}{(1-F_s)\gamma_d N+1}]^{T^*}$$

$$\cdot \; [I - \frac{(1-F_s)\gamma_d \underline{S}_d^* \underline{S}_d^T}{(1-F_s)\gamma_d N + 1}] \underline{S}_d^*$$

$$= \frac{1}{\sigma_n^4} [\underline{S}_d^T - \frac{(1-F_s)^* \gamma_d N \underline{S}_d^T}{(1-F_s)^* \gamma_d N+1}][\underline{S}_d^* - \frac{(1-F_s)\gamma_d N \underline{S}_d^*}{(1-F_s)\gamma_d N+1}]$$

$$= \frac{1}{\sigma_n^4} \cdot \frac{\underline{S}_d^T}{(1-F_s)^* \gamma_d N+1} \cdot \frac{\underline{S}_d^*}{(1-F_s)\gamma_d N+1}$$

$$= \frac{N}{\sigma_n^4 |(1-F_s)\gamma_d N+1|^2} \qquad \text{(C2-8)}$$

and also

$$\text{Trace}[M_1^{-1}M_1^{-1^{T*}}] = \frac{1}{\sigma_n^4}\text{Trace}[I - \frac{(1-F_s)\gamma_d \underline{S}_d^* \underline{S}_d^T}{(1-F_s)\gamma_d N + 1}$$

$$- \frac{(1-F_s)^*\gamma_d \underline{S}_d^* \underline{S}_d^T}{(1-F_s)^*\gamma_d N + 1} + \frac{|1-F_s|^2\gamma_d^2 N \underline{S}_d^* \underline{S}_d^T}{|(1-F_s)\gamma_d N + 1|^2}]$$

$$= \frac{1}{\sigma_n^4}[N - \frac{(1-F_s)\gamma_d N}{(1-F_s)\gamma_d N+1} - \frac{(1-F_s)^*\gamma_d N}{(1-F_s)^*\gamma_d N+1}$$

$$+ \frac{|1-F_s|^2\gamma_d^2 N^2}{|(1-F_s)\gamma_d N+1|^2}]$$

$$= \frac{1}{\sigma_n^4|(1-F_s)\gamma_d N+1|^2}\{N[|1-F_s|^2\gamma_d^2 N^2+(1-F_s)^*\gamma_d N$$

$$+ (1-F_s)\gamma_d N+1]-[|1-F_s|^2\gamma_d^2 N^2 + (1-F_s)\gamma_d N]$$

$$- [|1-F_s|^2\gamma_d^2 N^2+(1-F_s)^*\gamma_d N] + |1-F_s|^2\gamma_d^2 N^2\}$$

$$= \frac{\gamma_d N(N-1)[|1-F_s|^2\gamma_d N+2-2R_eF_s]+N}{\sigma_n^4|(1-F_s)\gamma_d N+1|^2} \qquad \text{(C2-9)}$$

where R_eF_s is the real part of F_s.

Substituting (C2-8) and (C2-9) into (C2-4), we have

$$P_n = \frac{\sigma_n^2 e^{-\sigma_\phi^2 N}}{\sigma_n^4|(1-F_s)\gamma_d N+1|^2}$$

$$+ \frac{\sigma_n^2(1-e^{-\sigma_\phi^2})\{\gamma_d N(N-1)[|1-F_s|^2\gamma_d N+2-2R_eF_s]+N\}}{\sigma_n^4|(1-F_s)\gamma_d N+1|^2}$$

$$+ \frac{\sigma_n^2\sigma_c^2\{\gamma_d N(N-1)[|1-F_s|^2\gamma_d N+2-2R_eF_s]+N\}}{\sigma_n^4|(1-F_s)\gamma_d N+1|^2} \qquad \text{(C2-10)}$$

From (C2-7) and C2-10), the output SNR is

$$SNR = \frac{P_d}{P_n}$$

$$= \frac{|\overline{\alpha^2}|e^{-\sigma_\phi^2}N^2+|\overline{\alpha^2}|(1-e^{-\sigma_\phi^2})N+|\overline{\alpha^2}|\sigma_c^2 N}{\sigma_n^2 e^{-\sigma_\phi^2}N+\sigma_n^2(1-e^{-\sigma_\phi^2}+\sigma_c^2)\{\gamma_d N(N-1)]|1-F_s|^2\gamma_d N+2-2R_e F_s]+N\}}$$

$$= \frac{\gamma_d e^{-\sigma_\phi^2}N+\gamma_d(1-e^{-\sigma_\phi^2})+\gamma_d\sigma_c^2}{e^{-\sigma_\phi^2}+(1-e^{-\sigma_\phi^2}+\sigma_c^2)\{\gamma_d(N-1)[|1-F_s|^2\gamma_d N+2-2R_e F_s]+1\}} \qquad \text{(C2-11)}$$

List of Symbols - Appendix C

C	diagonal matrix with elements $1 + c_n$, $n = 1, \ldots N$
c_n	random gain error on the n^{th} array element
e_o	array output
e_r	reference signal
F_s	complex loop gain
G	gain of the weight control loops
I	identity matrix
k	wave number
M_1	equivalent covariance matrix
N	number of array elements
n_r	noise component of reference signal
$\underline{N}(t)$	noise vector of array output
P_d	average output signal power
P_I	average output interference power
P_n	average output noise power
$R_e F_s$	real part of F_s
$\underline{S}$	steering vector with random phase errors
$\underline{S}_d$	arrival phase vector of the desired signal
$\underline{S}_{Ij}$	arrival phase vector of the j^{th} interferer
s_n	n^{th} component of $\underline{S}$
$\underline{S}_o$	steering vector without random phase errors
s_{on}	n^{th} component of $\underline{S}_o$
μ	weight factor; a random variable here
$\underline{V}(t)$	array output vector without random gain error
$\underline{V}'(t)$	array output vector with random gain error
$\underline{W}$	equivalent weight vector

(Continued)

List of Symbols - Appendix C
(Continued)

$\underline{W}'$	weight vector defined by $e_o = \underline{V}'^T\underline{W}'$
x_n	position of the n^{th} array element
$\alpha(t)$	desired signal waveform
$\beta_j(t)$	j^{th} interferer waveform
γ_d	signal to noise ratio at array elements
θ	steering angle
θ_d	desired signal arrival angle
σ_c^2	variance of random gain error
σ_n^2	noise power at array elements
σ_ϕ^2	variance of the random phase errors
ϕ_n	random phase error on the n^{th} element

Appendix D

ESTIMATION OF THE POINTING VECTOR

by

Chien - Chung Yeh and Fred Haber

We deal here with the problem of deriving an array pointing vector aimed at a desired source assuming that the environment may contain an interferer emitter angularly close to the desired source. We suppose that a reference station forms part of the system that station providing system management, information on ground source location, synchronizing signals, and also capable of serving as a beacon for organizing the array. The scenario assumed is shown in Figure 1. The array shown in the figure and utilized in the analysis is linear though there is no intention to limit the approach to linear arrays.

The procedure to be examined is based on a two-step process. First the array will generate a pointing vector aimed at the reference beacon. This vector is determined by correlating array outputs with the output of a reflector antenna with good sidelobe reduction properties. Then, with given information on angular displacement between beacon and desired ground source, the array will steer this vector, aiming it at the desired ground source. The objective is to get a reasonably accurate pointing vector toward the desired ground station in the presence of strong nearby interference and without the requirement of extremely accurate knowledge of array element locations.

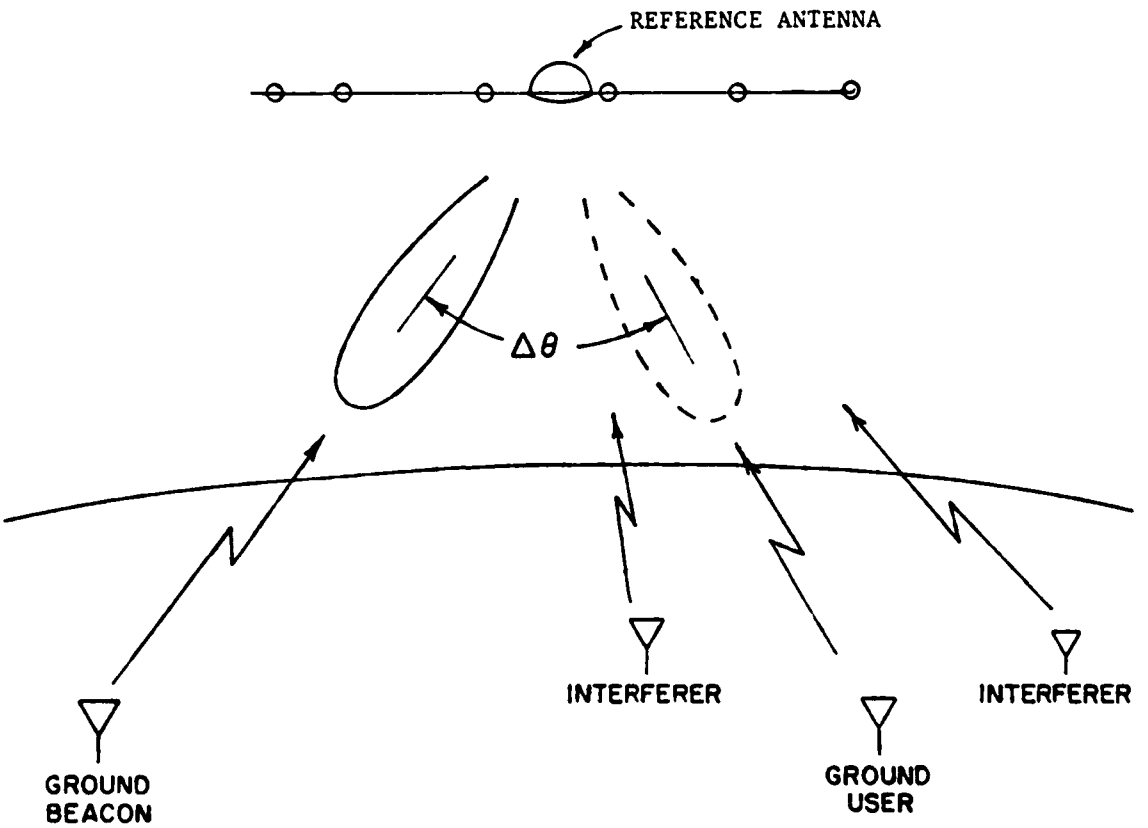

FIGURE 1

Array Scenario

1. Estimation of Beacon Pointing Vector.

With the arrangement suggested in Figure 1, assume an N element linear array with element positions x_1, x_2, ... x_N, and a directive reference antenna, though a planar array is likely to be used in applications, the concept is more easily pursued using a linear deployment. At this stage the desired ground source is assumed off. The beacon signal arrival direction is denoted θ_b and that of the interferer is denoted θ_i. The inputs of the array elements, which are denoted by $x_1(t)$, $x_2(t)$, ... $x_N(t)$, can be expressed as

$$x_n(t) = \alpha(t)e^{j\phi_b}e^{jkx_n\cos\theta_b} + \beta(t)e^{j\phi_i}e^{jkx_n\cos\theta_i} + n_n(t) \qquad (1)$$

where $\alpha(t)$ is the beacon signal waveform, $\beta(t)$ is the interferer waveform, ϕ_b is the electrical angle of the beacon signal at the origin, ϕ_i is the electrical angle of the interferer at the origin and $n_n(t)$ is the noise, $\alpha(t)$, $\beta(t)$, $n_n(t)$, ϕ_b, and ϕ_i are assumed to be independent.

The reference from the directive reference antenna is

$$r(t) = a\alpha(t)e^{j\phi_b} + b\beta(t)e^{j\phi_i} + n_r(t) \qquad (2)$$

where a and b are complex numbers representing the gains of the reference antenna to signal and interferer. The vector of array element inputs is

$$\underline{X}(t) = \begin{bmatrix} x_1(t) \\ x_2(t) \\ \vdots \\ x_N(t) \end{bmatrix}$$

$$= \alpha(t)e^{j\phi_b}\begin{bmatrix} e^{jkx_1\cos\theta_b} \\ e^{jkx_2\cos\theta_b} \\ \vdots \\ e^{jkx_N\cos\theta_b} \end{bmatrix} + \beta(t)e^{j\phi_i}\begin{bmatrix} e^{jkx_1\cos\theta_i} \\ e^{jkx_2\cos\theta_i} \\ \vdots \\ e^{jkx_N\cos\theta_i} \end{bmatrix} + \begin{bmatrix} n_1(t) \\ n_2(t) \\ \vdots \\ n_N(t) \end{bmatrix}$$

$$= \alpha(t)e^{j\phi_b}\underline{S}_b + \beta(t)e^{j\phi_i}\underline{S}_I + \underline{N}(t) \tag{3}$$

where

$$\underline{S}_b = \begin{bmatrix} e^{jkx_1\cos\theta_b} \\ \vdots \\ e^{jkx_N\cos\theta_b} \end{bmatrix} \tag{4}$$

is the signal phase vector

$$\underline{S}_I = \begin{bmatrix} e^{jkx_1\cos\theta_i} \\ \vdots \\ e^{jkx_N\cos\theta_i} \end{bmatrix} \tag{5}$$

is the interference phase vector and

$$\underline{N}(t) = \begin{bmatrix} n_1(t) \\ n_2(t) \\ \vdots \\ n_N(t) \end{bmatrix} \tag{6}$$

is the noise vector.

The vector $\underline{S}_b$ is pointing vector we wish to estimate and we consider the estimator $\hat{\underline{S}}_b$ defined by

$$\hat{\underline{S}}_b = \frac{1}{T} \int_o^T \underline{X}(t)\, r^*(t)dt$$

$$= \frac{1}{T} \int_o^T \left[\alpha(t)e^{j\phi_b}\underline{S}_b + \beta(t)e^{j\phi_i}\underline{S}_I + \underline{N}(t)\right] \cdot \left[a\alpha(t)e^{j\phi_b} + b\beta(t)e^{j\phi_i} + n_r(t)\right]^* dt. \tag{7}$$

(7) can be written as

$$\hat{\underline{S}}_b = \frac{1}{T}\int_o^T a^*\alpha^2(t)\underline{S}_b dt + \frac{1}{T}\int_o^T b^*\beta^2(t)\underline{S}_I dt$$

$$+ \frac{1}{T}\int_o^T \left\{\alpha(t)e^{j\phi_b}\underline{S}_b[b^*\beta(t)e^{-j\phi_i} + n_r^*(t)]\right.$$

$$+ \beta(t)e^{j\phi_i}\underline{S}_I\left[a^*\alpha(t)e^{-j\phi_b} + n_r^*(t)\right]$$

$$\left. + \underline{N}(t)\left[a^*\alpha(t)e^{-j\phi_b} + b^*\beta(t)e^{-j\phi_i} + n_r^*(t)\right]\right\} dt. \tag{8}$$

The mean and variance of the estimator all now examined. The expectation of the first term on the right hand side of (8) is

$$A_1 = \frac{1}{T} a^*\underline{S}_b \int_o^T \left\langle \alpha^2(t)\right\rangle dt$$

$$= a^*\alpha^2\underline{S}_b \tag{9}$$

where

$$\langle \alpha^2(t) \rangle = \alpha^2.$$

The expectation of the second term is

$$A_2 = \frac{1}{T} b^* \underline{S}_I \int_o^T \langle \beta^2(t) \rangle \, dt$$

$$= b^* \beta^2 \underline{S}_I \tag{10}$$

where

$$\langle \beta^2(A) \rangle = \beta^2.$$

The expectation of the third term is

$$A_3 = \frac{1}{T} \int_o^T \Big\{ \langle \alpha(t) \rangle \langle e^{j\phi_b} \rangle \underline{S}_b \left[b^* \langle \beta(t) \rangle \langle e^{-j\phi_i} \rangle + \langle n_r^*(t) \rangle \right]$$

$$+ \langle \beta(t) \rangle \langle e^{j\phi_i} \rangle \underline{S}_I \left[a^* \langle \alpha(t) \rangle \langle e^{-j\phi_b} \rangle + \langle n_r^*(t) \rangle \right]$$

$$+ \langle \underline{N}(t) \rangle \left[a^* \langle \alpha(t) \rangle \langle e^{-j\phi_b} \rangle + b^* \langle \beta(t) \rangle \langle e^{-j\phi_i} \rangle + \langle n_r^*(t) \rangle \right] \Big\} dt. \tag{11}$$

It is assumed that the beacon signal is a zero mean time continuous, binary polarity reversal waveform and the interferer is monochromatic at the carrier frequency of the signal. Then

$$\langle \alpha(t) \rangle = 0$$
$$\langle \beta(t) \rangle = \beta \tag{12}$$

The phases ϕ_b and ϕ_i are uniformly distributed between [0, 2π], so that

$$\langle e^{j\phi_b} \rangle = 0$$

$$\langle e^{j\phi_i} \rangle = 0 \tag{13}$$

and the noises are zero mean so that

$$\langle n_r(t) \rangle = 0$$

$$\langle \underline{N}(t) \rangle = \underline{0} \tag{14}$$

with (12), (13), and (14)

$$A_3 = 0. \tag{15}$$

From (9), (10), and (15), the expectation of $\hat{\underline{S}}_b$ is

$$\langle \hat{\underline{S}}_b \rangle = a^* \alpha^2 \underline{S}_b + b^* \beta^2 \underline{S}_I \tag{16}$$

The second turn on the right represents a pointing bias which should be kept small relative to the first term. That is we will want to make $|b^* \beta^2 / a^2 \alpha^2| << 1$ to avoid significant bias error. We now turn to the variance of the estimator $\hat{\underline{S}}_b$. For two vectors $\underline{A}$ and $\underline{B}$ with

$$\underline{A} = \begin{bmatrix} a_1 \\ a_2 \\ \vdots \\ a_N \end{bmatrix} \quad \text{and} \quad \underline{B} = \begin{bmatrix} b_1 \\ b_2 \\ \vdots \\ b_N \end{bmatrix},$$

define

$$\underline{AB} \triangleq \begin{bmatrix} a_1 b_1 \\ a_2 b_2 \\ \vdots \\ a_N b_N \end{bmatrix}. \tag{17}$$

With this definition, the variance of $\hat{\underline{S}}_b$ can be written as

$$\text{Var}\,[\hat{\underline{S}}_b] = \langle(\hat{\underline{S}}_b - \langle\hat{\underline{S}}_b\rangle)(\hat{\underline{S}}_b - \langle\hat{\underline{S}}_b\rangle)^*\rangle \tag{18}$$

where * means the complex conjugate. From (16), (9) and (10), $\langle\hat{\underline{S}}_b\rangle$ can be expressed as

$$\langle\hat{\underline{S}}_b\rangle = \frac{1}{T}\int_o^T a^*\langle\alpha^2(t)\rangle\,\underline{S}_b dt + \frac{1}{T}\int_o^T b^*\langle\beta^2(t)\rangle\underline{S}_I dt. \tag{19}$$

Since it is assumed that the signal is a binary code sequence and the interferer is monochromatic,

$$\langle\alpha^2(t)\rangle = \alpha^2(t) = \alpha^2$$
$$\langle\beta^2(t)\rangle = \beta^2(t) = \beta^2 \tag{20}$$

Substitute (20) into (19),

$$\langle\hat{\underline{S}}_b\rangle = \frac{1}{T}\int_o^T a^*\alpha^2(t)\underline{S}_b dt + \frac{1}{T}\int_o^T b^*\beta^2(t)\underline{S}_I dt. \tag{21}$$

From (8) and (21),

$$\hat{\underline{S}}_b - \langle\hat{\underline{S}}_b\rangle = \frac{1}{T}\int_o^T \Big\{\alpha(t)e^{j\phi_b}\underline{S}_b\left[b^*\beta(t)e^{-j\phi_i} + n_r^*(t)\right]$$
$$+ \beta(t)e^{j\phi_i}\underline{S}_I\left[a^*\alpha(t)e^{-j\phi_b} + n_r^*(t)\right]$$
$$+N(t)\left[a^*\alpha(t)e^{-j\phi_b} + b^*\beta(t)e^{-j\phi_i} + n_r^*(t)\right]\Big\}\,dt$$
$$= \frac{1}{T}\int_o^T \alpha(t)e^{j\phi_b}\underline{S}_b b^*\beta(t)e^{-j\phi_i}dt$$
$$+ \frac{1}{T}\int_o^T \beta(t)e^{j\phi_i}\underline{S}_I a^*\alpha(t)e^{-j\phi_b}dt$$

$$+\frac{1}{T}\int_o^T\left[\alpha(t)e^{j\phi_b}\underline{S}_b+\beta(t)e^{j\phi_i}\underline{S}_I\right]n_r^*(t)dt$$

$$+\frac{1}{T}\int_o^T\underline{N}(t)\left[a^*\alpha(t)e^{-j\phi_b}+b^*\beta(t)e^{-j\phi_i}+n_r^*(t)\right]dt \qquad (22)$$

Substitute (22) into (18)

$$\text{Var}\left[\hat{\underline{S}}_b\right]=\left\langle\left(\hat{\underline{S}}_b-\left\langle\hat{\underline{S}}_b\right\rangle\right)\left(\hat{\underline{S}}_b-\left\langle\hat{\underline{S}}_b\right\rangle\right)^*\right\rangle$$

$$=\left\langle\left\{\frac{1}{T}\int_o^T\alpha(t)e^{j\phi_b}\underline{S}_b b^*\beta(t)e^{-j\phi_i}dt\right.\right.$$

$$+\frac{1}{T}\int_o^T\beta(t)e^{j\phi_i}\underline{S}_I a^*\alpha(t)e^{-j\phi_b}dt$$

$$+\frac{1}{T}\int_o^T\left[\alpha(t)e^{j\phi_b}\underline{S}_b+\beta(t)e^{j\phi_i}\underline{S}_I\right]n_r^*(t)dt$$

$$\left.+\frac{1}{T}\int_o^T\underline{N}(t)\left[a^*\alpha(t)e^{-j\phi_b}+b^*\beta(t)e^{-j\phi_i}+n_r^*(t)\right]dt\right\}$$

$$\cdot\left\{\frac{1}{T}\int_o^T\alpha(t)e^{-j\phi_b}\underline{S}_b^* b\beta(t)e^{j\phi_i}dt\right.$$

$$+\frac{1}{T}\int_o^T\beta(t)e^{-j\phi_i}\underline{S}_I^* a\alpha(t)e^{j\phi_b}dt$$

$$+\frac{1}{T}\int_o^T\left[\alpha(t)e^{-j\phi_b}\underline{S}_b^*+\beta(t)e^{-j\phi_i}\underline{S}_I^*\right]n_r(t)dt$$

$$\left.+\frac{1}{T}\int_o^T\underline{N}^*(t)\left[a\alpha(t)e^{j\phi_b}+b\beta(t)e^{j\phi_i}+n_r(t)\right]dt\right\}\Big\rangle$$

$$(1) \quad = \left\langle \frac{1}{T^2} \int_o^T \alpha(t) e^{j\phi_b} \underline{S}_b b^* \beta(t) e^{-j\phi_i} dt \cdot \int_o^T \alpha(t') e^{-j\phi_b} \underline{S}_b^* b \beta(t') e^{j\phi_i} dt' \right\rangle$$

$$(2) \quad + \left\langle \frac{1}{T^2} \int_o^T \beta(t) e^{j\phi_i} \underline{S}_I a^* \alpha(t) e^{-j\phi_b} dt \cdot \int_o^T \beta(t') e^{-j\phi_i} \underline{S}_I^* a \alpha(t') e^{j\phi_b} dt' \right\rangle$$

$$(3) \quad + \left\langle \frac{1}{T^2} \int_o^T \alpha(t) e^{j\phi_b} \underline{S}_b b^* \beta(t) e^{-j\phi_i} dt \cdot \int_o^T \beta(t') e^{-j\phi_i} \underline{S}_I^* a \alpha(t') e^{j\phi_b} dt' \right\rangle$$

$$(4) \quad + \left\langle \frac{1}{T^2} \int_o^T \beta(t) e^{j\phi_i} \underline{S}_I a^* \alpha(t) e^{-j\phi_b} dt \cdot \int_o^T \alpha(t') e^{-j\phi_b} \underline{S}_b^* b \beta(t') e^{j\phi_i} dt' \right\rangle$$

$$(5) \quad + \left\langle \frac{1}{T^2} \int_o^T \left[\alpha(t) e^{j\phi_b} \underline{S}_b + \beta(t) e^{j\phi_i} \underline{S}_I \right] n_r^*(t) dt \right.$$

$$\left. \cdot \int_o^T \left[\alpha(t') e^{-j\phi_b} \underline{S}_b^* + \beta(t') e^{-j\phi_i} \underline{S}_I^* \right] n_r(t') dt' \right\rangle$$

$$(6) \quad + \left\langle \frac{1}{T^2} \int_o^T \underline{N}(t) \left[a^* \alpha(t) e^{-j\phi_b} + b^* \beta(t) e^{-j\phi_i} + n_r^*(t) \right] dt \right.$$

$$\left. \cdot \int_o^T \underline{N}^*(t') \left[a \alpha(t') e^{j\phi_b} + b \beta(t') e^{j\phi_i} + n_r(t') \right] dt' \right\rangle$$

$$(7) \quad + \left\langle \frac{1}{T^2} \left[\int_o^T \alpha(t) e^{j\phi_b} \underline{S}_b b^* \beta(t) e^{-j\phi_i} dt + \int_o^T \beta(t) e^{j\phi_i} \underline{S}_I a^* \alpha(t) e^{-j\phi_b} dt \right] \right.$$

$$\cdot \left\{ \int_o^T \left[\alpha(t') e^{-j\phi_b} \underline{S}_b^* + \beta(t') e^{-j\phi_i} \underline{S}_I^* \right] n_r(t') dt' \right.$$

$$\left. \left. + \int_o^T \underline{N}^*(t') \left[a \alpha(t') e^{j\phi_b} + b \beta(t') e^{j\phi_i} + n_r(t') \right] dt' \right\} \right\rangle$$

$$(8)\quad +\left\langle \frac{1}{T^2}\left\{ \int_o^T \left[\alpha(t)e^{j\phi_b}\underline{S}_b + \beta(t)e^{j\phi_i}\underline{S}_I\right] n_r^*(t)dt \right.\right.$$

$$\left.\left. + \int_o^T \underline{N}(t)\left[a^*\alpha(t)e^{-j\phi_b} + b^*\beta(t)e^{-j\phi_i} + n_r^*(t)\right] dt\right\}\right.$$

$$\left. \cdot \left[\int_o^T \alpha(t')e^{-j\phi_b}\underline{S}_b^* b\beta(t')e^{j\phi_i}dt' + \int_o^T \beta(t')e^{-j\phi_i}\underline{S}_I^* a\alpha(t')e^{j\phi_b}dt'\right]\right\rangle$$

$$(9)\quad +\left\langle \frac{1}{T^2} \int_o^T \left[\alpha(t)e^{j\phi_b}\underline{S}_b + \beta(t)e^{j\phi_i}\underline{S}_I\right] n_r^*(t)dt \right.$$

$$\left. \cdot \int_o^T \underline{N}^*(t')\left[a\alpha(t')e^{j\phi_b} + b\beta(t')e^{j\phi_i} + n_r(t')\right] dt'\right\rangle$$

$$(10)\quad +\left\langle \frac{1}{T^2} \int_o^T \underline{N}(t)\left[a^*\alpha(t)e^{-j\phi_b} + b^*\beta(t)e^{-j\phi_i} + n_r^*(t)\right] dt \right.$$

$$\left. \cdot \int_o^T \left[\alpha(t')e^{-j\phi_b}\underline{S}_b^* + \beta(t')e^{-j\phi_i}\underline{S}_I^*\right] n_r(t')dt'\right\rangle \qquad (23)$$

No Noise Case:

In practice, the signal is designed to be much larger than the noise. It would be reasonable to assume that the noise is zero. Then, only the first four terms on the right hand side of (23) are not zero.

The first term, in (23), is

$$\left\langle \frac{1}{T^2} \int_o^T \int_o^T \alpha(t)\alpha(t')|b|^2 \underline{I}_1 \beta(t)\beta(t')dt\, dt' \right\rangle$$

$$= \frac{1}{T^2} \int_o^T \int_o^T \left\langle \alpha(t)\alpha(t') \right\rangle \beta^2 |b|^2 \underline{I}_1 dt\, dt' \qquad (24)$$

where $\underline{I}_1 \triangleq \begin{bmatrix} 1 \\ 1 \\ 1 \end{bmatrix}$ is an N x 1 all 1's vector. $\alpha(t)$ is a binary code sequence of rectangular chips with random and equiprobable amplitudes $\pm \alpha$.

It can be shown for such a waveform

$$\langle\alpha(t)\alpha(t')\rangle = \begin{cases} \alpha^2\left[1 - \frac{|t - t'|}{\tau}\right] & \text{for } |t - t'| \leq \tau \\ 0 & \text{otherwise} \end{cases} \tag{25}$$

For $T >> \tau$ (24) can be approximated to be

$$\frac{1}{T^2}\int_{t'=0}^{T}\int_{t=0}^{T}\langle\alpha(t)\alpha(t')\rangle\beta^2|b|^2\underline{I}_1 dtdt'$$

$$\simeq \frac{1}{T^2}\int_{t'=0}^{T}\int_{t=t'-\tau}^{t'+\tau}\alpha^2\left[1-\frac{|t-t'|}{\tau}\right]\beta^2|b|^2\underline{I}_1 dtdt'$$

$$= \frac{1}{T^2}\int_{t'=0}^{T}\alpha^2\tau\beta^2|b|^2\underline{I}_1 dt'$$

$$= \frac{1}{T}\alpha^2\tau\beta^2|b|^2\underline{I}_1 \tag{26}$$

Similarly, the second term in (23) is

$$\left\langle\frac{1}{T^2}\int_{t'=0}^{T}\int_{t=0}^{T}\beta(t)\beta(t')\underline{I}_1|a|^2\alpha(t)\alpha(t')dtdt'\right\rangle$$

$$= \frac{1}{T^2}\int_{t'=0}^{T}\int_{t=0}^{T}\beta^2|a|^2\langle\alpha(t)\alpha(t')\rangle\underline{I}_1 dtdt'$$

$$\simeq \frac{1}{T^2}\int_{t'=0}^{T}\beta^2\tau|a|^2\alpha^2\underline{I}_1 dt'$$

$$= \frac{1}{T}\alpha^2\tau\beta^2|a|^2\underline{I}_1 \tag{27}$$

The third term is

$$<\frac{1}{T^2}\int_{t'=0}^{T}\int_{t=0}^{T} ab^{*}\underline{S}_b\underline{S}_I^{*}e^{j2\phi_b}e^{-j2\phi_i}\alpha(t)\alpha(t')\beta(t)\beta(t')dtdt'>$$

$$=\frac{1}{T^2}\int_{t'=0}^{T}\int_{t=0}^{T} ab^{*}\underline{S}_b\underline{S}_I^{*}<e^{j2\phi_b}><e^{-j2\phi_i}><\alpha(t)\alpha(t')>\beta^2dtdt'$$

$$=\underline{0} \tag{28}$$

because

$$<e^{j2\phi_b}> = <e^{-j2\phi_i}> = 0.$$

Similarly, the fourth term is

$$<\frac{1}{T^2}\int_{t'=0}^{T}\int_{t=0}^{T} a^{*}b\underline{S}_b^{*}\underline{S}_I e^{j2\phi_b}e^{j2\phi_i}\alpha(t)\alpha(t')\beta(t)\beta(t')dtdt'>$$

$$=\frac{1}{T^2}\int_{t'=0}^{T}\int_{t=0}^{T} a^{*}b\underline{S}_b^{*}\underline{S}_I<e^{-j2\phi_b}><e^{j2\phi_i}><\alpha(t)\alpha(t')>\beta^2dtdt'$$

$$=\underline{0} \tag{29}$$

Substituting (26), (27), (28) and (29) into (23), $\mathrm{Var}[\hat{\underline{S}}_b]$ for the no noise case is

$$\mathrm{Var}[\hat{\underline{S}}_b] = \frac{1}{T}\alpha^2\tau\beta^2|b|^2\underline{I}_1 + \frac{1}{T}\alpha^2\tau\beta^2|a|^2\underline{I}_1 \tag{30}$$

where

$|a|$ = amplitude of signal at reference antenna output relative to element signal level

$|b|$ = amplitude of interference at antenna output relative to element interference level

τ = PN sequence chip width

T = integration duration

$\alpha^2/2$ = signal power at each element

$\beta^2/2$ = interference power at each element

Example:

We obtain numerical values for the estimator bias in the no noise case. Assume at the inputs of array elements the signal is 10dB lower than the interference, and at the reference from the dish antenna the signal is 20dB higher than the interference; i.e. the antenna gain is 30dB. Thus

$$\beta^2 = 10\alpha^2$$

$$|a|^2\alpha^2 = 100|b|^2\beta^2$$

so that

$$|a|^2 = 1000|b|^2$$

From (16)

$$\langle \hat{\underline{S}}_b \rangle = a^*\alpha^2\underline{S}_b + b^*\beta^2\underline{S}_I$$

$$= a^*\alpha^2\left[\underline{S}_b + \frac{b^*\beta^2}{a^*\alpha^2}\underline{S}_I\right]$$

where

$$\frac{|b^*\beta^2|}{|a^*\alpha^2|} = \frac{1}{\sqrt{10}}$$

The biasing error vector is $1/\sqrt{10}$ of the desired pointing vector magnitude. This may not be good enough. If at the inputs of array elements the signal is the same as the interference (a condition which is not unreasonable if the pilot source is a fixed station capable of substantial power) and the antenna gain is 30dB.

$$\alpha^2 = \beta^2$$

and

$$|a|^2 = 1000|b|^2$$

$$\langle \hat{\underline{S}}_b \rangle = a^* \alpha^2 [\underline{S}_b + \frac{b^* \beta^2}{a^* \alpha^2} \underline{S}_I]$$

where

$$\frac{|b^* \beta^2|}{|a^* \alpha^2|} = \frac{1}{10\sqrt{10}}$$

This ratio is much better though we would advise using a dish with better than 30dB mainlobe to sidelobe ratio to get even greater suppression of the bias term.

With Noise:

Let the power spectral density of the noise at each array element be denoted $\phi_n(f)$ and assume it to be as shown below

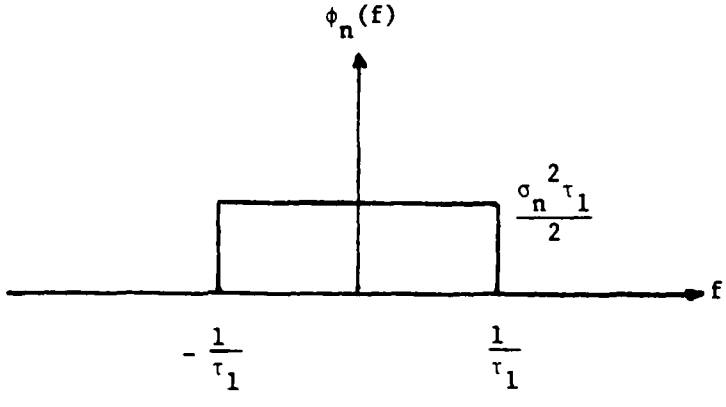

Let the power spectral density of noise at the dish antenna be denoted $\phi_r(f)$ and assume it as shown below

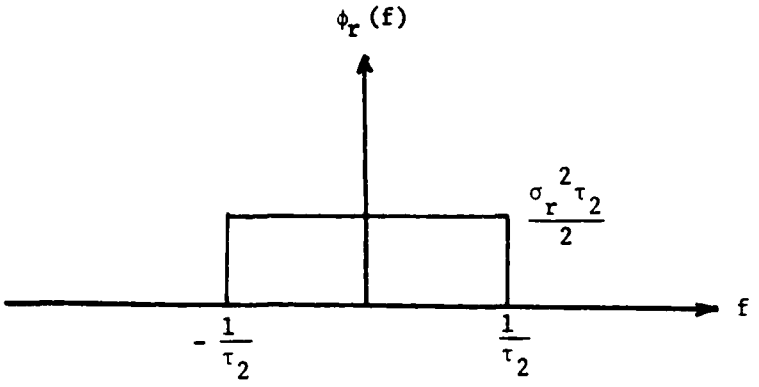

τ_1 and τ_2 are much smaller than τ, the P-N sequence chip width. The autocorrelation functions of the noise inputs are, respectively

$$R_n(t) = E[n_n(u)n_n^*(u+t)]$$

$$= \int_{-\infty}^{\infty} \phi_n(f) e^{j2\pi ft} df$$

$$= \sigma_n^2 \frac{\sin \frac{2\pi t}{\tau_1}}{\frac{2\pi t}{\tau_1}} \tag{31}$$

and

$$R_r(t) = E[n_r(u)n_r^*(u+t)]$$

$$= \int_{-\infty}^{\infty} \phi_r(f) e^{j2\pi ft} df$$

$$= \sigma_r^2 \frac{\sin \frac{2\pi t}{\tau_2}}{\frac{2\pi t}{\tau_2}} \tag{32}$$

The variance of $\hat{\underline{S}}_b$ is given in (23). Here the first four terms are the same as those for the no noise case, which are given in (26), (27), (28) and (29). The fifth term in (23) is

$$<\frac{1}{T^2}\int_o^T [\alpha(t)e^{j\phi_b}\underline{S}_b + \beta(t)e^{j\phi_i}\underline{S}_I]n_r^*(t)dt$$

$$\cdot \int_o^T [\alpha(t')e^{-j\phi_b}\underline{S}_b^* + \beta(t')e^{-j\phi_i}\underline{S}_I^*]n_r(t')dt'>$$

$$= \frac{1}{T^2}\int_{t'=0}^T \int_{t=0}^T <\alpha(t)\alpha(t')><n_r(t')n_r^*(t)>\underline{I}_1 dtdt'$$

$$+ \frac{1}{T^2}\int_{t'=0}^T \int_{t=0}^T <\beta(t)\beta(t')><n_r(t')n_r^*(t)>\underline{I}_1 dtdt' \qquad (33)$$

substituting (25), (31) and (32) into (33) and using $T >> \tau$, (33) can be approximated by

$$\frac{1}{T^2}\int_{t'=0}^T \int_{t=t'-\tau}^{t'+\tau} \alpha^2[1-\frac{|t-t'|}{\tau}]\sigma_r^2 \frac{\sin\frac{2\pi(t-t')}{\tau_2}}{\frac{2\pi(t-t')}{\tau_2}}\underline{I}_1 dtdt'$$

$$+ \frac{1}{T^2}\int_{t'=0}^T \int_{t=0}^T \beta^2\sigma_r^2 \frac{\sin\frac{2\pi(t-t')}{\tau_2}}{\frac{2\pi t-t')}{\tau_2}}\underline{I}_1 dtdt' \qquad (34)$$

Examining the two terms in (34) separately, the first term is

$$\frac{1}{T^2}\int_{t'=0}^{\lambda} \int_{t=t'-\tau}^{t'+\tau} \alpha^2[1-\frac{|t-t'|}{\tau}]\sigma_r^2 \frac{\sin\frac{2\pi(t-t')}{\tau_2}}{\frac{2\pi(t-t')}{\tau}}\underline{I}_1 dtdt'$$

$$= \frac{1}{T^2}\int_{t'=0}^{T}\int_{t=-\tau}^{\tau}\alpha^2\left[1-\frac{|t|}{\tau}\right]\sigma_r^2\frac{\sin\frac{2\pi t}{\tau_2}}{\frac{2\pi t}{\tau_2}}\underline{I}_1 dt dt'$$

$$= \frac{1}{T}\int_{t=-\tau}^{\tau}\alpha^2\left[1-\frac{|t|}{\tau}\right]\sigma_r^2\frac{\sin\frac{2\pi t}{\tau_2}}{\frac{2\pi t}{\tau_2}}\underline{I}_1 dt$$

$$= \frac{2}{T}\int_{0}^{\tau}\alpha^2\left[1-\frac{t}{\tau}\right]\sigma_r^2\frac{\sin\frac{2\pi t}{\tau_2}}{\frac{2\pi t}{\tau_2}}\underline{I}_1 dt \qquad (35)$$

In the second term of (34) let t-t' = u and t' = ν, giving

$$\frac{1}{T^2}\int_{t'=0}^{T}\int_{t=0}^{T}\beta^2\sigma_r^2\frac{\sin\frac{2\pi(t-t')}{\tau_2}}{\frac{2\pi(t-t')}{\tau_2}}\underline{I}_1 dt dt'$$

$$= \frac{1}{T^2}\int_{u=-T}^{0}\int_{\nu=-u}^{T}\beta^2\sigma_r^2\frac{\sin\frac{2\pi u}{\tau_2}}{\frac{2\pi u}{\tau_2}}\underline{I}_1 d\nu du$$

$$+ \frac{1}{T^2}\int_{u=0}^{T}\int_{\nu=0}^{T-u}\beta^2\sigma_r^2\frac{\sin\frac{2\pi u}{\tau_2}}{\frac{2\pi u}{\tau_2}}\underline{I}_1 d\nu du$$

$$= \frac{2}{T^2}\int_{0}^{T}(T-u)\beta^2\sigma_r^2\frac{\sin\frac{2\pi u}{\tau_2}}{\frac{2\pi u}{\tau_2}}\underline{I}_1 du \qquad (36)$$

From (35) and (36), the fifth term in (23) can be replaced by the approximate equivalent

$$\frac{2}{T}\int_{0}^{\tau}\alpha^2\left[1-\frac{t}{\tau}\right]\sigma_r^2\frac{\sin\frac{2\pi t}{\tau_2}}{\frac{2\pi t}{\tau_2}}\underline{I}_1 dt$$

$$+ \frac{2}{T^2} \int_0^T (T - t)\beta^2 \sigma_r^2 \frac{\sin\frac{2\pi t}{\tau_2}}{\frac{2\pi t}{\tau_2}} \underline{I}_1 dt \tag{37}$$

Similarly, the sixth term is

$$< \frac{1}{T^2} \int_0^T \underline{N}(t)[a^* \alpha(t) e^{-j\phi_b} + b^* \beta(t) e^{-j\phi_i} + n_r^*(t)]dt$$

$$\cdot \int_0^T \underline{N}^*(t')[a\alpha(t') e^{j\phi_b} + b\beta(t') e^{j\phi_i} + n_r(t')]dt' >$$

$$= \frac{1}{T^2} \int_{t'=0}^T \int_{t=0}^T <\underline{N}(t)\underline{N}^*(t')> |a|^2 <\alpha(t)\alpha(t')> dtdt'$$

$$+ \frac{1}{T^2} \int_{t'=0}^T \int_{t=0}^T <\underline{N}(t)\underline{N}^*(t')> |b|^2 <\beta(t)\beta(t')> dtdt'$$

$$+ \frac{1}{T^2} \int_{t'=0}^T \int_{t=0}^T <\underline{N}(t)\underline{N}^*(t')> <n_r^*(t) n_r(t')> dtdt'$$

$$\approx \frac{1}{T^2} \int_{t'=0}^T \int_{t=-\tau}^{\tau} |a|^2 \alpha^2 [1 - \frac{|t|}{\tau}] \sigma_n^2 \frac{\sin\frac{2\pi t}{\tau_1}}{\frac{2\pi t}{\tau_1}} \underline{I}_1 dtdt'$$

$$+ \frac{1}{T^2} \int_{t'=0}^T \int_{t=0}^T |b|^2 \beta^2 \sigma_n^2 \frac{\sin\frac{2\pi(t-t')}{\tau_1}}{\frac{2\pi(t-t')}{\tau_1}} \underline{I}_1 dtdt'$$

$$+ \frac{1}{T^2} \int_{t'=0}^T \int_{t=0}^T \sigma_n^2 \sigma_r^2 \frac{\sin\frac{2\pi(t-t')}{\tau_1} \cdot \sin\frac{2\pi(t-t')}{\tau_2}}{4\pi^2 \frac{(t-t')^2}{\tau_1 \tau_2}} \underline{I}_1 dtdt'$$

$$= \frac{2}{T}\int_0^{\tau} |a|^2\alpha^2[1-\frac{t}{\tau}]\sigma_n^2 \frac{\sin\frac{2\pi t}{\tau_1}}{\frac{2\pi t}{\tau_1}} \underline{I}_1 dt$$

$$+ \frac{2}{T^2}\int_0^{T} (T-t)|b|^2\beta^2\sigma_n^2 \frac{\sin\frac{2\pi t}{\tau_1}}{\frac{2\pi t}{\tau_1}} \underline{I}_1 dt$$

$$+ \frac{2}{T^2}\int_0^{T} (T-t)\sigma_n^2\sigma_r^2 \frac{\sin\frac{2\pi t}{\tau_1}\sin\frac{2\pi t}{\tau_2}}{\frac{(2\pi t)^2}{\tau_1\tau_2}} \underline{I}_1 dt \qquad (38)$$

The 7th, 8th, 9th and 10th terms in (23) are zero because of the independence of the random variables representing signal and interference phase. Substituting (26), (27), (37) and (38) into (23), we have

$$\mathrm{Var}[\hat{\underline{S}}_b] = \frac{1}{T}\alpha^2\tau\beta^2(|a|^2 + |b|^2)\underline{I}_1$$

$$+ \frac{2}{T}\int_0^{\tau} \alpha^2[1-\frac{t}{\tau}]\sigma_r^2 \frac{\sin\frac{2\pi t}{\tau_2}}{\frac{2\pi t}{\tau_2}} \underline{I}_1 dt$$

$$+ \frac{2}{T^2}\int_0^{T} (T-t)\beta^2\sigma_r^2 \frac{\sin\frac{2\pi t}{\tau_2}}{\frac{2\pi t}{\tau_2}} \underline{I}_1 dt$$

$$+ \frac{2}{T}\int_0^{\tau} |a|^2\alpha^2[1-\frac{t}{\tau}]\sigma_n^2 \frac{\sin\frac{2\pi t}{\tau_1}}{\frac{2\pi t}{\tau_1}} \underline{I}_1 dt$$

$$+ \frac{2}{T^2}\int_0^{T} (T-t)|b|^2\beta^2\sigma_n^2 \frac{\sin\frac{2\pi t}{\tau_1}}{\frac{2\pi t}{\tau_1}} \underline{I}_1 dt$$

$$+\frac{2}{T^2}\int_0^T (T-t)\sigma_n^2\sigma_r^2 \frac{\sin\frac{2\pi t}{\tau_1}\sin\frac{2\pi t}{\tau_2}}{\frac{(2\pi t)^2}{\tau_1\tau_2}} \underline{I}_1 dt \tag{38a}$$

To simplify (38a) somewhat assume the rf bandwidths of array elements and reference antenna equal so that $\tau_1 = \tau_2 << \tau$, we then have

$$\mathrm{Var}[\hat{\underline{S}}_b] = \frac{1}{T}\alpha^2\tau\beta^2(|a|^2 + |b|^2)\underline{I}_1$$

$$+\frac{2}{T}\int_0^\tau \alpha^2(\sigma_r^2 + |a|^2\sigma_n^2)(1-\frac{t}{\tau}) \frac{\sin\frac{2\pi t}{\tau_1}}{\frac{2\pi t}{\tau_1}} \underline{I}_1 dt$$

$$+\frac{2}{T^2}\int_0^T \beta^2(\sigma_r^2 + |b|^2\sigma_n^2)(T-t) \frac{\sin\frac{2\pi t}{\tau_1}}{\frac{2\pi t}{\tau_1}} \underline{I}_1 dt$$

$$+\frac{2}{T^2}\int_0^T (T-t)\sigma_n^2\sigma_r^2 \frac{\sin^2\frac{2\pi t}{\tau_1}}{(\frac{2\pi t}{\tau_1})^2} \underline{I}_1 dt \tag{39}$$

To examine (39), the second term on the right hand side of (39) is

$$\frac{2}{T}\int_0^\tau \alpha^2(\sigma_r^2 + |a|^2\sigma_n^2)(1-\frac{t}{\tau}) \frac{\sin\frac{2\pi t}{\tau_1}}{\frac{2\pi t}{\tau_1}} \underline{I}_1 dt$$

$$= \frac{2}{T}\alpha^2(\sigma_r^2 + |a|^2\sigma_n^2)\underline{I}_1 \int_0^\tau \frac{\sin\frac{2\pi t}{\tau_1}}{\frac{2\pi t}{\tau_1}} dt$$

$$- \frac{2}{T} \alpha^2 (\sigma_r^2 + |a|^2 \sigma_n^2) \frac{1}{2\pi} I_1 \frac{\tau_1}{\tau} \int_0^{\tau} \frac{2\pi t}{\tau_1} dt \tag{39a}$$

In (39a), two integral terms are examined below

$$\int_0^{\tau} \frac{\sin \frac{2\pi t}{\tau_1}}{\frac{2\pi t}{\tau_1}} dt$$

$$= \frac{\tau_1}{2\pi} \int_0^{\frac{2\pi\tau}{\tau_1}} \frac{\sin x}{x} dx$$

$$\simeq \frac{\tau_1}{2\pi} \int_0^{\infty} \frac{\sin x}{x} dx$$

$$= \frac{\tau_1}{4} \tag{39b}$$

The other integral term is

$$\int_0^{\tau} \sin \frac{2\pi t}{\tau_1} dt = 0 \tag{39c}$$

for $\tau = m\tau_1$, m is a integer. The second term in (39a) will also be negligible for other values of τ provided that $\tau >> \tau_1$. Substituting (39b) and (39c) into (39a), the second term on the right hand side of (39) is

$$\frac{2}{T}\int_0^{\tau}\alpha^2(\sigma_r^2+|a|^2\sigma_n^2)(1-\frac{t}{\tau})\frac{\sin\frac{2\pi t}{\tau_1}}{\frac{2\pi t}{\tau_1}}\ \underline{I}_1\ dt$$

$$=\frac{\tau_1}{2T}\ \alpha^2\ (\sigma_r^2+|a|^2\sigma_n^2)\ \underline{I}_1 \qquad (40)$$

The third term on the right hand side of (39) is

$$\frac{2}{T^2}\int_0^{T}\beta^2(\sigma_r^2+|b|^2\sigma_n^2)(T-t)\frac{\sin\frac{2\pi t}{\tau_1}}{\frac{2\pi t}{\tau_1}}\ \underline{I}_1\ dt$$

$$=\frac{2}{T^2}\ \beta^2(\sigma_r^2+|b|^2\sigma_n^2)T\ \underline{I}_1\ \int_0^{T}\frac{\sin\frac{2\pi t}{\tau_1}}{\frac{2\pi t}{\tau_1}}\ dt$$

$$-\frac{2}{T^2}\ \beta^2(\sigma_r^2+|b|^2\sigma_n^2)\ \frac{\tau_1}{2\pi}\ \underline{I}_1\int_0^{T}\sin\frac{2\pi t}{\tau_1}\ dt \qquad (41)$$

In (41) $\int_0^{T}\sin\frac{2\pi t}{\tau_1}\ dt=0$ as specified by (39c), (41) then reduces to

$$\frac{2}{T^2}\int_0^{T}\beta^2(\sigma_r^2+|b|^2\sigma_n^2)(T-t)\frac{\sin\frac{2\pi t}{\tau_1}}{\frac{2\pi t}{\tau_1}}\ \underline{I}_1\ dt$$

$$=\frac{2}{T}\ \beta^2(\sigma_r^2+|b|^2\sigma_n^2)\ \underline{I}_1\ \frac{\tau_1}{2\pi}\int_0^{T}\frac{\sin\frac{2\pi t}{\tau_1}}{\frac{2\pi t}{\tau_1}}\ d(\frac{2\pi t}{\tau_1})$$

$$\simeq\frac{\tau_1}{\pi T}\beta^2(\sigma_r^2+|b|^2\sigma_n^2)\underline{I}_1\ \int_0^{\infty}\frac{\sin x}{x}\ dx$$

$$= \frac{\tau_1}{2T} \beta^2(\sigma_r^2 + |b|^2\sigma_n^2)\underline{I}_1 \tag{42}$$

The fourth term on the right hand side of (39) will be approximated by an upper bound, as follows:

$$\frac{2}{T^2} \int_o^T (T-t)\sigma_n^2\sigma_r^2 \frac{\sin^2 \frac{2\pi t}{\tau_1}}{\left(\frac{2\pi t}{\tau_1}\right)^2} \underline{I}_1 \, dt$$

$$< \frac{2}{T} \sigma_n^2\sigma_r^2 \underline{I}_1 \int_o^T \frac{\sin^2 \frac{2\pi t}{\tau_1}}{\left(\frac{2\pi t}{\tau_1}\right)^2} dt$$

$$= \frac{2}{T} \sigma_n^2\sigma_r^2 \underline{I}_1 \frac{\tau_1}{2\pi} \int_o^{\frac{2\pi T}{\tau_1}} \frac{\sin^2 x}{x^2} dx$$

$$\simeq \frac{\tau_1}{\pi T} \sigma_n^2\sigma_r^2 \underline{I}_1 \int_o^\infty \frac{\sin^2 x}{x^2} dx$$

$$= \frac{\tau_1}{2T} \sigma_n^2\sigma_r^2 \underline{I}_1 \tag{43}$$

Substituting (40), (42) and (43) into (39), we get our approximation for $\mathrm{Var}[\hat{\underline{S}}_b]$.

$$\mathrm{Var}[\hat{\underline{S}}_b] \simeq \frac{\tau}{T} \alpha^2\beta^2(|a|^2 + |b|^2)\underline{I}_1$$

$$+ \frac{\tau_1}{2T} \alpha^2(\sigma_r^2 + |a|^2\sigma_n^2)\underline{I}_1$$

$$+ \frac{\tau_1}{2T} \beta^2(\sigma_r^2 + |b|^2\sigma_n^2)\underline{I}_1$$

$$+ \frac{\tau_1}{2T} \sigma_n^2\sigma_r^2 \underline{I}_1 \tag{44}$$

To examine the estimated $\hat{\underline{S}}_b$ more thoroughly, we go back to (8). (8) can be written as

$$\hat{\underline{S}}_b = \frac{1}{T}\int_o^T a^*\alpha^2(t)\underline{S}_b dt + \frac{1}{T}\int_o^T b^*\beta^2(t)\underline{S}_I dt$$

$$+ \underline{S}_b \frac{1}{T}\int_o^T \alpha(t)e^{j\phi_b}[b^*\beta(t)e^{-j\phi_i} + n_r^*(t)]dt$$

$$+ \underline{S}_I \frac{1}{T}\int_o^T \beta(t)e^{j\phi_i}[a^*\alpha(t)e^{-j\phi_b} + n_r^*(t)]dt$$

$$+ \frac{1}{T}\int_o^T \underline{N}(t)[a^*\alpha(t)e^{-j\phi_b} + b^*\beta(t)e^{-j\phi_i} + n_r^*(t)]dt \qquad (45)$$

The 2nd, 3rd and 4th terms in (45) are zero mean with variance not zero when T is finite. However, the 2nd and 3rd terms can be written as $C_1\underline{S}_b$ and $C_2\underline{S}_I$ respectively where C_1 and C_2 are uncorrelated random variables. So the 2nd term contains signal information and the 3rd term contains interferance information. The 4th term is random fluctuation.

From (44) the variance contributed by the 4th term of (45) is

$$\sigma_{rf}^2 \simeq \frac{\tau_1}{2T}\alpha^2|a|^2\sigma_n^2 + \frac{\tau_1}{2T}\beta^2|b|^2\sigma_n^2$$

$$+ \frac{\tau_1}{2T}\sigma_n^2\sigma_r^2 \qquad (46)$$

(45) can be written

$$\hat{\underline{S}}_b = (a^*\alpha^2 + C_1)\underline{S}_b + (b^*\beta^2 + C_2)\underline{S}_I + \begin{bmatrix} u_1 e^{jw_1} \\ u_2 e^{jw_2} \\ \vdots \\ u_N e^{jw_N} \end{bmatrix} \tag{47}$$

In (47), $u_1, u_2, \ldots u_N$ are independent random variables with zero mean and variance

$$\sigma_{u_1}^2 = \sigma_{u_2}^2 = \ldots = \sigma_{u_N}^2 = \sigma_{rf}^2. \tag{48}$$

$w_1, w_2, \ldots w_N$ are independent random variables uniformly distributed between $[0, 2\pi]$. The u_n's are independent of the w_n's.

From (44) and (45) we can see that the variance of C_1 is

$$\sigma_{C_1}^2 = \frac{\tau}{T}\alpha^2\beta^2|b|^2 + \frac{\tau_1}{2T}\alpha^2\sigma_r^2 \tag{49}$$

and the variance of C_2 is

$$\sigma_{C_2}^2 = \frac{\tau}{T}\beta^2\alpha^2|a|^2 + \frac{\tau_1}{2T}\beta^2\sigma_r^2 \tag{50}$$

Since the standard deviation of C_1 is much smaller than $|a^*\alpha^2|$, C_1 can be ignored in (47). Thus we have

$$\hat{\underline{S}}_b \approx a^*\alpha^2\left(\underline{S}_b + \frac{b^*\beta^2 + C_2}{a^*\alpha^2}S_I + \begin{bmatrix} \frac{u_1}{a^*\alpha^2} e^{jw_1} \\ \vdots \\ \frac{u_N}{a^*\alpha^2} e^{jw_N} \end{bmatrix}\right) \tag{51}$$

The constant $a^*\alpha^2$ may be dropped. (51) becomes

$$\hat{\underline{S}}_b = \underline{S}_b + \frac{b^* \beta^2 + C_2}{a^* \alpha^2} \underline{S}_I + \begin{bmatrix} v_1 e^{jw_1} \\ \cdot \\ \cdot \\ \cdot \\ v_N e^{jw_N} \end{bmatrix} \tag{52}$$

where $v_N = \frac{u_N}{a^* \alpha^2}$ is a r.v. with zero mean and variance

$$\sigma_{v_N}^2 = \frac{\sigma_{u_N}^2}{|a|^2 \sigma^4}$$

$$= \frac{1}{|a|^2 \alpha^4} \left[\frac{\tau_1}{2T} \alpha^2 |a|^2 \sigma_n^2 + \frac{\tau_1}{2T} \beta^2 |b|^2 \sigma_n^2 \right.$$

$$\left. + \frac{\tau_1}{2T} \sigma_n^2 \sigma_r^2 \right] \tag{53}$$

2. Scanning from Beacon to Ground Station.

We now turn to the problem of steering the beacon phase vector to the direction of the ground station. From (16) we have

$$\langle \hat{\underline{S}}_b \rangle = \underline{S}_b + \frac{b^* \beta^2}{a^* \alpha^2} \underline{S}_I \tag{54}$$

$\underline{S}_b$ and $\underline{S}_I$ are beacon and interferer phase vector, respectively. α^2 and β^2 are the power of beacon and interferer. a and b are complex numbers representing the voltage gain of the dish antenna on beacon signal and interferer, respectively.

To examine (54) more thoroughly, define

$$\gamma = \gamma_{Re} + j\gamma_{Im} \triangleq \frac{b^* \beta^2}{a^* \alpha^2} \tag{55}$$

Then,

$$\langle \hat{\underline{S}}_b \rangle = \underline{S}_b + \gamma \underline{S}_I \ . \tag{56}$$

It is reasonable to assume that beacon and interferer have the same order of power and that the dish antenna has a 30 dB mainlobe to sidelobe ratio i.e. $\alpha^2 \approx \beta^2$ and $\frac{|a|^2}{|b|^2} \approx 10^3$. Then $|\gamma|$ is in the order of $10^{-3/2}$. From (5b),

$$\langle \hat{\underline{S}}_b \rangle = \begin{bmatrix} e^{jkx_1\cos\theta_b} + \gamma e^{jkx_1\cos\theta_i} \\ e^{jkx_2\cos\theta_b} + \gamma e^{jkx_2\cos\theta_i} \\ \vdots \\ e^{jkx_N\cos\theta_b} + \gamma e^{jkx_N\cos\theta_i} \end{bmatrix} \tag{57}$$

where θ_b and θ_i are beacon and interferer directions.

To see the phase of the nth element of $\langle \hat{\underline{S}}_b \rangle$ we write

$$e^{jkx_n\cos\theta_b} + \gamma e^{jkx_n\cos\theta_i}$$

$$= e^{jkx_n\cos\theta_b}[1 + \gamma e^{jkx_n(\cos\theta_i - \cos\theta_b)}]. \tag{58}$$

The term in brackets of (58) is

$$1 + \gamma e^{jk\alpha_n(\cos\theta_i - \cos\theta_b)}$$

$$= 1 + \alpha_{Re}\cos[kx_n(\cos\theta_i - \cos\theta_b)] - \gamma_{Im}\sin[kx_n(\cos\theta_i - \cos\theta_b)]$$

$$+ j\{\gamma_{Re}\sin[kx_n(\cos\theta_i - \cos\theta_b)] + \gamma_{Im}\cos[kx_n(\cos\theta_i - \cos\theta_b)]\} \quad (59)$$

$$= A_n e^{j\psi_n}$$

The phase term ψ_n is what we are interested in and is specified by

$$\tan\psi_n = \frac{\gamma_{Re}\sin[kx_n(\cos\theta_i - \cos\theta_b)] + \gamma_{Im}\cos[kx_n(\cos\theta_i - \cos\theta_b)]}{1+\gamma_{Re}\cos[kx_n(\cos\theta_i - \cos\theta_b)] - \gamma_{Im}\sin[kx_n(\cos\theta_i - \cos\theta_b)]} \quad (60)$$

For $|\gamma|<<1$, (60) can be approximated by

$$\tan\psi_n \simeq \gamma_{Re}\sin[kx_n(\cos\theta_i - \cos\theta_b)] + \gamma_{Im}\cos[kx_n(\cos\theta_i - \cos\theta_b)] \quad (61)$$

Since $\tan\psi_n$ is small, $\tan\psi_n \simeq \psi_n$.

$$\psi_n \simeq \gamma_{Re}\sin[kx_n(\cos\theta_i - \cos\theta_b)] + \gamma_{Im}\cos[kx_n(\cos\theta_i - \cos\theta_b)] \quad (62)$$

From (58) and (59), the nth element of $\langle\hat{\underline{S}}_b\rangle$ is

$$e^{jkx_n\cos\theta_b} + \gamma e^{jkx_n\cos\theta_i} = A_n e^{j(kx_n\cos\theta_b + \psi_n)} \quad (63)$$

The normalized mean value of the estimated beacon phase vector is therefore

$$\langle\hat{\underline{S}}_b\rangle = \begin{bmatrix} e^{j(kx_1\cos\theta_b + \psi_1)} \\ e^{j(kx_2\cos\theta_b + \psi_2)} \\ \vdots \\ e^{j(kx_N\cos\theta_b + \psi_N)} \end{bmatrix} \quad (64)$$

In (64), $\psi_1, \psi_2, \ldots \psi_N$ are phase errors. (62) shows that ψ_n is correlated with $kx_n\cos\theta_b$ which is the correct pointing phase. However ψ_n is more like a random phase error as the following example shows. The phase error of the nth element as given by (62) involves trigonometric functions of $[kx_n(\cos\theta_i - \cos\theta_b)]$. Thus we need only consider the mod-2π version of this quantity, assume both θ_i and θ_b are near $\frac{\pi}{2}$ rad (both beacon and interferer are near broadside and $\theta_i - \theta_b \sim \frac{1}{20}$). Then

$$\cos\theta_i - \cos\theta_b = \sin(\tfrac{\pi}{2} - \theta_i) - \sin(\tfrac{\pi}{2} - \theta_b)$$

$$\simeq \theta_b - \theta_i \simeq \frac{1}{20} .$$

Assume an array of 10 elements with array size $\simeq$ 500 wavelengths, the average spacing between elements is 50 wavelengths. Then

$$k\Delta x\Delta\theta \simeq 2\pi \cdot 2.5$$

Adjacent elements will therefore differ by the order of 5π radiuses and the modulo 2π phase differently will tend to be random. With non-uniform spacing the modulo 2π phase differences will be further randomized. Therefore ψ_n may approximately be treated as a random variable with zero mean and variance

$$\begin{aligned}
\sigma_{\psi_n}^2 &= \langle\psi_n^2\rangle \text{ (take expectation over } x_n) \\
&= \langle\gamma_{Re}^2\sin^2[kx_n(\cos\theta_i - \cos\theta_b)] + \gamma_{Im}^2\cos^2[kx_n(\cos\theta_i - \cos\theta_b)] \\
&\quad + 2\gamma_{Re}\gamma_{Im}\sin[kx_n(\cos\theta_i - \cos\theta_b)]\cos[kx_n(\cos\theta_i - \cos\theta_b)]\rangle \\
&= \frac{1}{2}\gamma_{Re}^2 + \frac{1}{2}\gamma_{Im}^2 \\
&= \frac{1}{2}|\gamma|^2
\end{aligned} \tag{65}$$

In (65) mod $(kx_n(\cos\theta_i - \cos\theta_b))$ is assumed to be uniformly distributed between $[0, 2\pi]$.

If the integration time in estimating is finite, the estimated beacon phase vector is given by (52)

$$\hat{\underline{S}}_b = \underline{S}_b + \frac{b^*\beta^2 + C_2}{a^*\alpha^2}\ \underline{S}_I + \begin{bmatrix} v_1 e^{jw_1} \\ v_2 e^{jw_2} \\ \vdots \\ v_N e^{jw_N} \end{bmatrix} \tag{66}$$

where C_2 is zero mean with variance

$$\sigma_{C_2}^2 = \frac{\tau}{T}\beta^2\alpha^2|a|^2 + \frac{\tau_1}{2T}\beta^2\sigma_r^2 \quad , \tag{67}$$

and where $v_1, v_2, \ldots v_N$ are independent random variable with zero mean and variance

$$\sigma_{v_n}^2 = \frac{1}{|a|^2\alpha^4}\left[\frac{\tau_1}{2T}\alpha^2|a|^2\sigma_n^2 + \frac{\tau_1}{2T}\beta^2|b|^2\sigma_n^2 + \frac{\tau_1}{2T}\sigma_n^2\sigma_r^2\right] \tag{68}$$

$w_1, w_2, \ldots w_N$ are independent random variables uniformly distributed between $[o, 2\pi]$. The v_n's are independent of the w_n's.

$$\text{Define} \quad \frac{C_2}{a^*\alpha^2} = \lambda = \lambda_{re} + j\lambda_{Im} \tag{69}$$

λ is zero mean with variance

$$\sigma_\lambda^2 = \frac{\sigma_{C_2}^2}{|a|^2\alpha^4}$$

$$= \frac{1}{|a|^2\alpha^4}\left[\frac{\tau}{T}\beta^2\alpha^2|a|^2 + \frac{\tau_1}{2T}\rho^2\sigma_r^2\right] \tag{70}$$

using (55) and (69), (66) becomes

$$\hat{\underline{S}}_b = \underline{S}_b + (\gamma+\lambda)\underline{S}_I + \begin{bmatrix} v_1 e^{jw_1} \\ v_2 e^{jw_2} \\ \vdots \\ v_N e^{jw_N} \end{bmatrix} \tag{71}$$

The nth element of $\hat{\underline{S}}_b$ is

$$e^{jkx_n\cos\theta_b} + (\gamma+\lambda)e^{jkx_n\cos\theta_i} + v_n e^{jw_n}$$

$$= e^{jkx_n\cos\theta_b}\left[1 + (\gamma+\lambda)e^{jkx_n(\cos\theta_i - \cos\theta_b)} + v_n e^{j(w_n - kx_n\cos\theta_b)}\right] \tag{72}$$

Let $v_n = v_{nRe} + jv_{nIm}$ and define

$$A'_n e^{j\psi'_n} = 1 + (\gamma+\lambda)e^{jkx_n(\cos\theta_i - \cos\theta_b)} + v_n e^{j(w_n - kx_n\cos\theta_b)} \tag{73}$$

Proceeding as was done in going from (7) to (9) we have

$$\psi'_n \simeq (\gamma_{Re} + \lambda_{Re})\sin[kx_n(\cos\theta_i - \cos\theta_b)]$$

$$+ (\gamma_{Im} + \lambda_{Im})\cos[kx_n(\cos\theta_i - \cos\theta_b)]$$

$$+ v_{nRe}\sin(w_n - kx_n\cos\theta_b) + v_{nIm}\cos(w_n - kx_n\cos\theta_b) \tag{74}$$

The normalized beacon phase vector estimated is

$$\hat{\underline{S}}_b = \begin{bmatrix} e^{j(kx_1\cos\theta_b + \psi'_1)} \\ e^{j(kx_2\cos\theta_b + \psi'_2)} \\ \vdots \\ e^{j(kx_N\cos\theta_b + \psi'_N)} \end{bmatrix} \tag{75}$$

As in the case of ψ_n we can argue that ψ'_n can be treated as a random error. ψ'_n is zero mean with variance

$$\sigma_{\psi'_n}^2 = \langle (\psi'_n)^2 \rangle$$

$$= \frac{1}{2}\gamma_{Re}^2 + \frac{1}{2}\gamma_{Im}^2 + \frac{1}{2}\langle \lambda_{Re}^2 \rangle + \frac{1}{2}\langle \lambda_{Im}^2 \rangle$$

$$+ \frac{1}{2}\langle v_{n_{Re}}^2 \rangle + \frac{1}{2}\langle v_{n\,Im}^2 \rangle$$

$$= \frac{1}{2}|\gamma|^2 + \frac{1}{2}\sigma_\lambda^2 + \frac{1}{2}\sigma_{v_n}^2$$

$$= \frac{1}{2}\,\frac{b^2\beta^4}{|a|^2\alpha^4}$$

$$+ \frac{1}{2|a|^2\alpha^4}\left[\frac{\tau}{T}\beta^2\alpha^2|a|^2 + \frac{\tau_1}{2T}\beta^2\sigma_r^2\right]$$

$$+ \frac{1}{2|a|^2\alpha^4}\left[\frac{\tau_1}{2T}\alpha^2|a|^2\sigma_n^2 + \frac{\tau_1}{2T}\beta^2|b|^2\sigma_n^2\right.$$

$$\left. + \frac{\tau_1}{2T}\sigma_n^2\sigma_r^2\right] \tag{76}$$

In (76), the dominant terms are

$$\frac{1}{2}\frac{b^2\beta^4}{|a|^2\alpha^4} + \frac{1}{2|a|^2\alpha^4}\frac{\tau}{T}\beta^2\alpha^2|a|^2$$

In order to form a beam in the direction of the beacon station, the array processor will put a phase shifting vector which is the conjugate of the estimated vector, i.e. $\hat{\underline{S}}_b^*$.

$$\hat{\underline{S}}_b^* = \begin{bmatrix} e^{-j(kx_1\cos\theta_b + \psi'_1)} \\ e^{-j(kx_2\cos\theta_b + \psi'_2)} \\ \vdots \\ e^{-j(kx_N\cos\theta_b + \psi'_N)} \end{bmatrix} \tag{77}$$

We now turn to the problem of steering the pointing vector from the beacon to the desired source. The basis for this approach is developed in Steinberg [1] pp. 246-249.

Assume we have a linear array on the X axis with element positions imperfectly known. The beacon station is in the direction θ_b as shown in the figure below.

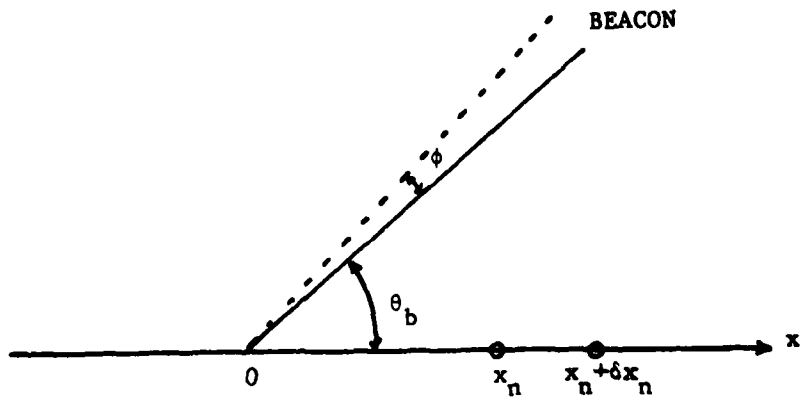

The steering vector for forming a beam on the beacon is given by (77); the nth element phase shift is given by $-kx_n\cos\theta_b-\psi'_n$. We now want to move the beam through an angle ϕ from θ_b. A phase shift Ψ_n needs to be added to $-kx_n\cos\theta_b-\psi'_n$, Ψ_n being determined in the following way.

The array processor imperfectly knows that the location of the nth element is $x_n + \delta x_n$ where δx_n is the location error. To form a beam in θ_b, the phase shift calculated by the array processor is $-k(x_n+\delta x_n)\cos\theta_b$. to form a beam in $\theta_b + \phi$, the phase shift calculated by processor is $-k(x_n+\delta x_n)\cos(\theta_b + \phi)$. The phase increment determined by array processor is, therefore,

$$\Psi_n = -k(x_n + \delta x_n)\cos(\theta_b + \phi) + k(x_n + \delta x_n)\cos\theta_b \tag{78}$$

The total phase shift when pointing at angle $(\theta_b + \phi)$ is the sum of the phase determined by focusing on the beacon (the phase in the exponent in (77)) plus the increment in (78); i.e.,

$$\begin{aligned}\Delta\phi_n &= -kx_n\cos\theta_b - \psi'_n + \Psi_n \\ &= -kx_n\cos\theta_b - \psi'_n - k(x_n+\delta x_n)\cos(\theta_b+\phi) + k(x_n+\delta x_n)\cos\theta_b \\ &= -kx_n\cos(\theta_b + \phi) - \psi'_n - k\delta x_n\cos(\theta_b+\phi) + k\delta x_n\cos\theta_b \end{aligned} \tag{79}$$

In (79) $-kx_n\cos(\theta_b + \phi)$ is the correct phase shift and $-\psi'_n - k\delta x_n\cos(\theta_b + \phi) + k\delta x_n\cos\theta_b$ is error. Let ψ_{en} denote the error of the nth element.

$$\psi_{en} = -\psi'_n - k\delta x_n \cos(\theta_b + \phi) + k\delta x_n \cos\theta_b$$

$$= -\psi'_n - k\delta x_n \cos\theta_b \cos\phi + k\delta x_n \sin\theta_b \sin\phi + k\delta x_n \cos\theta_b \qquad (80)$$

If the scanning angle ϕ is small, $\cos\phi \approx 1$ and $\sin\phi \approx \phi$. (80) is then approximated by

$$\psi_{en} = -\psi'_n + k\phi\delta x_n \sin\theta_b \qquad (81)$$

ψ_{en} is a function of θ_b. If the array is being used for near broadside reception $\theta_b \approx 90^\circ$ and $\sin\theta_b$ can be set equal to unity. If δx_n is zero mean variance $\sigma_{\delta x}^2$, ψ_{en} is also zero mean with variance

$$\sigma^2_{\psi_{en}} = \sigma_{\psi'_n}^2 + k^2\phi^2 \sin^2\theta_b \sigma_{\delta x}^2 \qquad (82)$$

where $\sigma_{\psi'_n}^2$ is given by (76).

Example:

We assume a reference dish antenna with, (1) a 30dB mainlobe to sidelobe ratio, (2) signal and interference of equal level, both 20dB above the noise of each element, and (3) equal noise generated in the array elements and the reference antenna amplifers. Thus

$$a^2 = 1000. \quad b^2 = 1. \quad \alpha^2 = \beta^2 = 100\sigma_n^2 = 100\sigma_r^2.$$

The variance due to estimation is given by (76)

$$\sigma_{\psi'_n}^2 = \frac{b^2\beta^4}{2|a|^2\alpha^4}$$

$$+ \frac{1}{2|a|^2\alpha^4}\left[\frac{\tau}{T}\beta^2\alpha^2|a|^2 + \frac{\tau_1}{2T}\beta^2\sigma_r^2\right]$$

$$+ \frac{1}{2|a|^2\alpha^4}\left[\frac{\tau_1}{2T}\alpha^2|a|^2\sigma_n^2 + \frac{\tau_1}{2T}\beta^2|b|^2\sigma_n^2\right.$$

$$\left. + \frac{\tau_1}{2T}\sigma_n^2\sigma_r^2\right]$$

Using the number assumed, the terms in $\sigma_{\psi_n}^2$ are then

$$b^2\beta^2 = \alpha^4$$

$$\frac{\tau}{T}\beta^2\alpha^2|a|^2 = \frac{\tau}{T}|a|^2\alpha^4 = \frac{\tau}{T}1000\alpha^4$$

$$\frac{\tau_1}{2T}\beta^2\sigma_r^2 = \frac{\tau_1}{2T}\frac{1}{100}\alpha^4$$

$$\frac{\tau_1}{2T}\alpha^2|a|^2\sigma_n^2 = \frac{\tau_1}{2T}\frac{|a|^2}{100}\alpha^4 = \frac{\tau_1}{T}5\alpha^4$$

$$\frac{\tau_1}{2T}\beta^2|b|^2\sigma_n^2 = \frac{\tau_1}{2T}\frac{1}{100}\alpha^4$$

$$\frac{\tau_1}{2T}\sigma_n^2\sigma_r^2 = \frac{\tau_1}{2T}\frac{1}{10000}\alpha^4$$

Therefore the variance due to estimation is dominated by

$$\frac{b^2\beta^4}{2|a|^2\alpha^4} + \frac{1}{2|a|^2\alpha^4}\frac{\tau}{T}\beta^2\alpha^2|a|^2$$

$$= \frac{4}{2|a|^2\alpha^4} + \frac{1}{2|a|^2\alpha^4}\frac{\tau}{T}1000\,\alpha^4$$

$$= \frac{1}{2000} + \frac{\tau}{2T}$$

Therefore, with T large enough ($T >> 10^3\tau$ insures this result).

$$\sigma_{\psi_n}^2 = \frac{1}{2000} = 5 \times 10^{-4}$$

The total variance $\sigma^2_{\psi_{en}}$ is

$$\sigma^2_{\psi_{en}} = \sigma_{\psi_n}^2 + k^2\phi^2\sin^2\theta_b\sigma_{\delta x}^2$$

with $\sin\theta_b = 1$, $\phi = \frac{1}{20}$, and $\sigma_{\delta x}$ in wavelengths

$$\sigma^2_{\psi_{en}} = \sigma_{\psi_n}^2 + \frac{(2\pi)^2}{(20)^2}\sigma_{\delta x}^2$$

$$\simeq 5\times10^{-4} + \frac{\sigma_{\delta x}^2}{10}$$

For $F_s = 0.95e^{-j10^o}$, N = 7, and $Y_d = 10$, the standard deviation for 1 dB loss is about 2^o or 0.04 radians. Let $\sigma^2_{\psi_{en}} = 0.04^2 = 0.0016$ then $\sigma_{\delta x} \simeq 0.1\lambda$; this is a fairly tight tolerance requirement. However, for $F_s = 0.95$, N = 7 and $Y_d = 10$, the standard deviation for 1 dB loss is about 7^o or 0.14 radians. The tolerance of element positions is, in this case, $\sigma_{\delta x} \simeq 0.44\lambda$; the tolerance demands are more relaxed in this case.

We point out that in these examples the dominant contribution to the total pointing phase error is the error induced by steering from beacon to ground station. That is, if the values chosen for reference antenna sidelobe levels are, in fact, realistic, the method is shown by these examples to result in adequate estimates of the beacon pointing phases. The adequacy of the final estimates of pointing phases to the ground station depends now mainly on the scanning range, and the un-

certainty in element position. If the error induced by the scanning process were totally eliminated the pointing vector would be left with an error variance of $\sigma^2_{\psi_{en}} = 5x10^{-4}$ (a standard deviation of about 1^o) which, even with $F_s = 0.95e^{-j10^o}$, causes a loss in SINR is negligible.

References

1. B. D. Steinberg, Principles of Aperture and Array System Design: Including Random and Adaptive Arrays, John Wiley & Sons, 1976.

List of Symbols - Appendix D

a	gain of reference antenna to beacon
b	gain of reference antenna to interferer
C_1	random variable
C_2	random variable
$E[\ ]$	expectation of [ ]
$\underline{I}_1$	N x 1 all 1's vector
k	wave number
$n_n(t)$	noise at the n^{th} array element
$n_r(t)$	noise at the reference antenna
$\underline{N}(t)$	noise vector of the array elements
$r(t)$	output of the reference antenna
$R_n(t)$	autocorrelation function, array element noise
$R_r(t)$	autocorrelation function, reference noise
$\underline{S}_b$	arrival phase vector of the beacon
$\hat{\underline{S}}_b$	estimator of $\underline{S}_b$
$\underline{S}_I$	arrival phase vector of the interferer
T	integration time
u_n	random variables with zero mean and variance σ^2_{rf}, $n = 1, 2, \ldots N$
w_n	random variables uniformly distributed between $[0, 2\pi]$, $n = 1, \ldots N$
x_n	n^{th} element position
$\underline{X}(t)$	input vector of the array
α^2	$<\alpha^2(t)>$
$\alpha(t)$	beacon signal waveform
$<\alpha^2(t)>$	expectation of $\alpha^2(t)$
β^2	$<\beta^2(t)>$
$\beta(t)$	interferer waveform

(Continued)

List of Symbols - Appendix D
(Continued)

γ	random variable
γ_{Im}	imaginary part of γ
γ_{Re}	real part of γ
δx_n	position error of the n^{th} array element
$\Delta\phi_n$	total phase shift of the n^{th} array element when pointing at angle $(\theta_b + \phi)$
θ_b	beacon arrival angle
θ_i	interferer arrival angle
λ	random variable
λ_{Im}	imaginary part of λ
λ_{Re}	real part of λ
$\sigma^2_{C_1}$	variance of C_1
$\sigma^2_{C_2}$	variance of C_2
σ^2_n	noise power at array elements
σ^2_r	noise power at the dish antenna
σ^2_{rf}	variance contributed by the random terms in estimating $\underline{S}_b$
$\sigma^2_{\delta x}$	variance of the error of array element locations
σ^2_λ	variance of λ
$\sigma^2_{\psi_n}$	variance of ψ_n
$\sigma^2_{\psi_{en}}$	variance of ψ_{en}
$\sigma^2_{\psi'_n}$	variance of ψ'_n
τ	duration of signal chips
τ_1	inverse of the bandwidth of $\phi_n(f)$
τ_2	inverse of the bandwidth of $\phi_r(f)$

(Continued)

List of Symbols - Appendix D
(Continued)

ϕ	scanning angle
ϕ_b	electrical phase angle of the beacon signal at the origin
ϕ_i	electrical phase angle of the interferer at the origin
$\phi_n(f)$	power spectral density of noise at array elements
$\phi_r(f)$	power spectral density of noise at the dish antenna
ψ_{en}	total phase error of the n^{th} array element
ψ_n	phase error in the n^{th} element of $\langle \hat{S}_b \rangle$
ψ_n'	phase error in the n^{th} element of $\hat{S}_b$
Ψ_n	phase increment of the n^{th} array element in order to scan the beam

Appendix E

LMS INTERFERENCE CANCELLER ARRAY WITH REFERENCE GENERATING LOOP

by

Y. Bar-Ness

Drexel University

Electrical and Computer Engineering Department

Philadelphia, Pa. 19104

&

F. Haber

Valley Forge Research Center

Moore School of Electrical Engineering

University of Pennsylvania

Philadelphia, Pa. 19104

I. INTRODUCTION

Adaptive Arrays for Communication based on the LMS algorithm of Widrow [1], but utilizing a self-generated reference, have been subjects of study in the past [2]. These methods are based on the exploitation of a distinguishing characteristic of the desired signal which enables it to be separated from unwanted signals. Typically, the desired signal is viewed as being spectrum spread by a known code so that with despreading a moderately clean replica of the desired signal is derived from the array output. With this as the reference, array focusing toward the desired signal is improved, in turn improving the reference. The scheme proposed and analyzed heretofore is shown in Figure 1 [3], and is here called the "LMS adaptive array with coded reference signal loop." Each array element is seen to be weighted, the weight being determined via an LMS loop driven by the correlation between element output and array output with reference subtracted. The limiter functions, in part, to prevent the weights from converging to zero. A difficulty observed with this arrangement is that incidental phase shift in the band-pass circuitry of the reference generating loop will cause the weights to cycle indefinitely with cycling amplitude range and frequency depending on the main feedback loop gain and on the magnitude of the reference loop phase shift [4,5]. Methods of adaptive compensation to overcome this effect have been pursued [6]; non-adaptive correction is not apt to work because of uncertainty of the center frequency caused by doppler shifts and oscillator frequency errors.

An alternative circuit in which one element is left unweighted and the limiter omitted is shown in Figure 2. To distinguish this from the previous circuit we refer to this as the "LMS interference canceller with coded reference signal loop".

Constraining the weight of one element to be constant, the all zero array weight condition cannot arise making the limiter unnecessary on this account. Now, however, operation will be affected by both phase and amplitude differences between reference and signal component of the array output. The analysis presented below is intended to reveal the properties of this circuit with particular attention to the weight convergence and the output signal-to-noise ration (SNR). It is shown that under simple attainable conditions the weights do converge to a constant final value. The configuration of Figure 2, however, generates a variable SNR at the summer output, the SNR possibly being as low as that of a single array element depending on the reference loop gain and phase shift. Because this may be troublesome to the reference generator a variant of this circuit, in which the signal to the reference generator is the sum of weighted element outputs only (see Figure 6), is also analyzed. The SNR at the reference generator input is, in this case, the full value expected out of (N-1) coherently combined elements. Finally, the SNR at the point from which signal output is to drawn is obtained.

II. N-Element LMS Interference Canceler

An N-element interference canceler is shown in Fig. 3. The signal from each antenna auxiliary element $y_i(t)$, $i = 0,1...N-1$, is passed through a quadrature hybrid forming pairs of components $y_{iI}(t) = y_i(t)$ and $y_{iQ}(t) = \hat{y}_i(t)$, $i = 1,2,..N-1$, where the caret stands for the Hilbert transform (90° phase shift). Each of these quadrature signals is weighted by real factors $W_{iI}(t)$ and $W_{iQ}(t)$, respectively, and then summed together with the signal from the main element $y_N(t)$ to produce the actual array output $v_a(t)$. The difference between the array output and the reference signal d(t) is the error signal e(t). Utilizing e(t), the feedback loops adjust the weights $W_{iI}(t)$ and $W_{iQ}(t)$ so that the mean-square error $\overline{|e(t)|^2}$ is minimized.

The operations performed in Fig. 3 are represented by the following: The pairs of signals $y_i(t)$ and $y_i(t)$ are used to express the analytic signal,

$$x_i(t) = [y_i(t) - j\hat{y}_i(t)]/\sqrt{2} \tag{1}$$

The complex weights $W_i(t)$ $W_{iI}(t) + jW_{iQ}(t)$ $i = 1,2...N-1$ act on the $x_i(t)$ to generate an output which, in analytic signal form, is given by,

$$v(t) = \underset{\sim}{x}^{\tau}(t)\underset{\sim}{W}(t) + x_N(t) \tag{2}$$

where $\underset{\sim}{W}^{\tau}(t) = \{W_1(t), W_2(t),...W_{N-1}(t)\}$, $x^{\tau}(t) = \{x_1(t),...x_{N-1}(t)\}$, τ stands for transpose, and $x_N(t) = [y_N(t) - j\hat{y}_N(t)]/\sqrt{2}$ is the analytic signal representation associated with the signal from the main (unweighted) element. The actual signal at the output of the array is given by

$$v_a(t) = \mathrm{Re}\{v(t)\} \tag{3}$$

and

$$e(t) = d(t) - v(t), \tag{4}$$

where e(t) and d(t) are the analytic signal representations associated with the error and reference signals, respectively.

The weight are assumed to be adjusted using the steepest descent algorithm [1]; that is, they are determined by

$$d\underset{\sim}{W}(t)/dt = -k\underset{\sim}{\Delta}_{\underset{\sim}{W}} E[e(t)^2] \tag{5}$$

where $\underset{\sim}{\Delta}_{\underset{\sim}{W}}$ is the gradient with respect to $\underset{\sim}{W}$, and is understood to be a complex vector whose components are the gradients with respect to the real and imaginary parts of $\underset{\sim}{W}$, respectively, and k is the main feedback loop gain. $E(\cdot)$ denotes mathematical expectation. Following the derivation in [1], (5) reduces to

$$dW(t)/dt = 2kE[\underset{\sim}{x}^*(t)e(t)] \tag{6}$$

where the asterisk denote complex conjugate.

Using (6) with the instantaneous product $[\underset{\sim}{x}^*(t)e(t)]$ as an estimate of the corresponding expected value this becomes the complex LMS algorithm whose equivalent network for one antenna element is displayed in Fig. 4. Substituting for e(t) using (2) and (4) we get the differential equation that governs the weight vector $\underset{\sim}{W}(t)$

$$d\underset{\sim}{W}(t)/dt + 2k\underset{\sim}{R}_{\underset{\sim}{x}}\underset{\sim}{W}(t) = 2k\underset{\sim}{R}_{\underset{\sim}{x}d} - 2kE[\underset{\sim}{x}^*(t)x_N(t)] \tag{7}$$

where $\underset{\sim}{R}_{\underset{\sim}{x}} = E[\underset{\sim}{x}^*(t)\underset{\sim}{x}^T(t)]$ is the input covariance matrix and $R_{xd} = E[\underset{\sim}{x}^*(t)d(t)]$.

In obtaining (7), using the network of Fig. 4 as a basis, an assumption commonly made in the analysis of adaptive arrays is used. That is, that the signal and weight processes, the latter now being a random process, are independent. $\underset{\sim}{W}(t)$ in (7) and in the subsequent work should therefore be viewed as an expectation.

For the case of a single CW signal of amplitude A arriving at angle ψ to

broadside we have(†)

$$\underset{\sim}{x}(t) = A\underset{\sim}{P}\exp[j\omega_c t]/\sqrt{2} + \underset{\sim}{N}(t) \tag{8}$$

$$x_N(t) = A\underset{\sim}{P}_N\exp[j\omega_c t]/\sqrt{2} + n_N(t) \tag{9}$$

where $P^\tau = \{e^{-j\alpha_1}, e^{-j\alpha_2} \ldots e^{-j\alpha_{N-1}}\}$, $P_N = e^{-j\alpha_N} = 1$

$$\alpha_i = (2\pi L_i/\lambda_c)\sin\psi \quad i = 1 \ldots N-1 \tag{10}$$

A is the signal amplitude, λ_c is the free space wavelength at frequency ω_c, the L_i are the distances between the ith and the main element, $\underset{\sim}{N}^\tau(t) = \{n_1(t), \ldots n_{N-1}(t)\}$ is the noise process vector and $n_N(t)$ is noise process at the main (unweighted) element. The noise at the ith element is written

$$n_i(t) = n_{iI}(t) - jn_{iQ}(t) \tag{11}$$

with

$$E[n_{iI}^2(t)] = E[n_{iQ}^2(t)] = \sigma_n^2/2. \tag{12}$$

Hence

$$E[n_i(t)n_j^*(t)] = \sigma_n^2 \quad \text{for } i = j, \text{ and every } i$$
$$= 0 \qquad i \neq j \tag{13}$$

The covariance matrix of the element output is therefore

$$\underset{\sim}{R}_x = \underset{\sim}{\Phi} + \sigma_n^2\underset{\sim}{I} \tag{14}$$

where $\underset{\sim}{\Phi} = A^2\underset{\sim}{P}^*\underset{\sim}{P}^\tau/2$.

Therefore (7) can be written as

$$d\underset{\sim}{W}(t)/dt + 2k(\underset{\sim}{\Phi} + \sigma_n^2\underset{\sim}{I})\underset{\sim}{W}(t) = 2k\underset{\sim}{R}_{xd} - kA^2\underset{\sim}{P}^*P_N \tag{15}$$

(†) We assume without loss of generality that x(t) contains no interference. In fact, the interference term will only change the matrix Φ.

III. N-Element Interference Canceler with Reference Signal Loop

a) Solution of the Equation for Expected Array Weights.

When the array output v(t) is processed to produce a reference signal as in Fig. 5, then

$$d(t) = [A\underset{\sim}{P}^{T}\exp[j\omega_c t]/\sqrt{2}\ \underset{\sim}{W}(t) + AP_N\exp[j\omega_c t]/\sqrt{2}]ae^{-j\phi} \tag{16}$$

where a is a positive constant depending on loop gain and filter attenuation and ϕ is a phase shift introduced by the reference loop filter. Noise and interference entering the reference loop will be substantially attenuated following the filter and as a consequence d(t) is represented in (16) as free of these influences.

Using the definition of R_{xd} we have

$$\begin{aligned}\underset{\sim}{R}_{xd} &= E\{\underset{\sim}{x}^{*}(t)(A\underset{\sim}{P}\exp[j\omega_c t]/\sqrt{2}\underset{\sim}{W}(t)+A/\sqrt{2}P_N\exp[j\omega_c t]\}ae^{-j\phi} \\ &= [\underset{\sim}{\phi}\underset{\sim}{W}(t) + A^2\underset{\sim}{P}^{*}P_N/2]ae^{-j\phi}\ . \end{aligned} \tag{17}$$

Thus (15) becomes

$$d\underset{\sim}{W}(t)/dt + 2k[(1-ae^{-j\phi})\underset{\sim}{\phi}+\sigma_n^2\underset{\sim}{I}]\underset{\sim}{W}(t)= -kA^2(1-ae^{-j\phi})P^{*}P_N. \tag{18}$$

The matrix ϕ is Hermitian having rank equal to one.

Therefore there exists a constant unitary matrix $\underset{\sim}{Q}$ such that $\underset{\sim}{Q}'\underset{\sim}{\phi}\underset{\sim}{Q} = \underset{\sim}{\Lambda}$ (the prime denotes transpose conjugate) where $\underset{\sim}{\Lambda}$ is a diagonal matrix with only one non-zero element λ_{N-1}.

Premultiplying (18) by $\underset{\sim}{Q}'$ we get

$$d\underset{\sim}{\Gamma}(t)/dt + 2k[(1-ae^{-j\phi})\underset{\sim}{\Lambda} + \sigma_n^2\underset{\sim}{I}]\underset{\sim}{\Gamma}(t) = -kA^2(1-ae^{-j\phi})\underset{\sim}{Q}'\underset{\sim}{P}^{*}P_N \tag{19}$$

where

$$\underset{\sim}{\Gamma}(t) = \underset{\sim}{Q}'\underset{\sim}{W}(t) \tag{19a}$$

(19) is obtained also using the fact that $\underset{\sim}{Q}'\underset{\sim}{Q} = \underset{\sim}{I}$. It can be easily shown that $\underset{\sim}{Q}'\underset{\sim}{P}^{*}$ is a complex vector with only one non-zero entry which equals $[\sqrt{2\lambda_{N-1}}/A]e^{j\delta}$, where δ is some arbitrary constant. We will choose $\delta = 0$.

With $\Gamma^T(t) = [\gamma_1(t),\ldots\ldots,\gamma_{N-1}(t)]$ (19) can be written [5]

$$d\gamma_i(t)/dt + 2k\sigma_n^2\gamma_i(t) = 0 \qquad i = 1,2,\ldots,N-2 \tag{20}$$

$$d\gamma_{N-1}(t)/dt+2k[(1-ae^{-j\phi})\lambda_{N-1}+\sigma_n^2]\ \gamma_{N-1}(t) = -2kA\sqrt{\lambda_{N-1}/2}(1-ae^{-j\phi}) \tag{21}$$

Note that in (20) we have used the fact that $\lambda_i = 0$ for $i = 1,2\ldots N-2$.

The solution to (20) is given by

$$\gamma_i(t) = \gamma_i(0)\ \exp[-2k\sigma_n t] \qquad i = 1,2\ldots N-2 \tag{22}$$

(21) is solved by decomposing it into its real and imaginary parts which are given by

$$d\gamma_{N-1}^r(t)/dt+2k[(1-a\cos\phi)\lambda_{N-1}+\sigma_n^2]\ \gamma_{N-1}^r(t)+2ka\sin\phi\lambda_{N-1}\gamma_{N-1}^i(t) = -2kA\sqrt{\lambda_{N-1}/2}[1-a\cos\phi] \tag{23}$$

$$d\gamma_{N-1}^i(t)/dt-2ka\sin\phi\lambda_{N-1}\gamma_{N-1}^r(t)+2k[(1-a\cos\phi)\lambda_{N-1}+\sigma_n^2]\gamma_{N-1}^i(t) = -2kA\sqrt{\lambda_{N-1}/2}[a\sin\phi] \tag{24}$$

where $\gamma_{N-1}(t) = \gamma_{N-1}^r(t) + j\gamma_{N-1}^i(t)$

These two equations can be written in matrix form as,

$$\begin{bmatrix} d\gamma_{N-1}^r(t)/dt \\ d\gamma_{N-1}^i(t)/dt \end{bmatrix} + 2k\lambda_{N-1}\begin{bmatrix} (1-a\cos\phi)+c & a\sin\phi \\ -a\sin\phi & (1-a\cos\phi)+c \end{bmatrix}\begin{bmatrix} \gamma_{N-1}^r(t) \\ \gamma_{N-1}^i(t) \end{bmatrix} = -2kA\sqrt{\lambda_{N-1}/2}\begin{bmatrix} 1-a\cos\phi \\ a\sin\phi \end{bmatrix} \tag{25}$$

where

$$c = \sigma_n^2/\lambda_{N-1} \tag{26}$$

Using a diagonalization transformation (see Appendix A-1) we find the solution to (25) to be (see Appendix A-1)

$$\gamma_{N-1}^r(t) = \{[\gamma_{N-1}^r(0)-C_r(\phi)]\cos(2k\lambda_{N-1}\ a\sin\phi)t - \{\gamma_{N-1}^i(0)-C_i(\phi)]\ \sin(2k\lambda_{N-1}a\sin\phi)t\}\ \exp.[-2k\lambda_{N-1}(1-a\cos\phi+c)t]+C_r(\phi)$$

$$\gamma_{N-1}^{i}(t) = \{[\gamma_{N-1}^{i}(0)-C_i(\phi)]\cos(2k\lambda_{N-1}\,a\sin\phi)t + [\gamma_{N-1}^{r}(0)-C_r(\phi)]\sin(2k\lambda_{N-1}\,a\sin\phi)t\}\exp[-2k\lambda_{N-1}(1-a\cos\phi+c)t] + C_i(\phi) \quad (27)$$

where

$$C_r(\phi) = -\frac{A}{\sqrt{2\lambda_{N-1}}}\,\frac{(1-a\cos\phi)(1-a\cos\phi+c) - a^2\sin^2\phi}{(1-a\cos\phi+\ )^2 + a^2\sin^2\phi} \quad (28)$$

$$C_i(\phi) = -\frac{A}{\sqrt{\lambda_{N-1}}}\,\frac{a\sin\phi(2 - 2a\cos\phi + c)}{(1-a\cos\phi+\ )^2 + a^2\sin^2\phi} \quad (29)$$

b) Stability Condition

Stability is viewed as requiring the expected value of the weight vector $\underset{\sim}{W}(t)$ to converge to a constant steady state value. This, in turn, requires the vector $\underset{\sim}{\Gamma}$ given by (19a) to approache a constant. The components of $\underset{\sim}{\Gamma}$, γ_i, $i = 1,2...N-1$, must therefore converge. The first (N-2) components given by (22) will converge for $k > 0$. For $\gamma_{N-1}^{r}(t)$ and $\gamma_{N-1}^{i}(t)$ to converge to the final values $C_r(\phi)$ and $C_i(\phi)$ respectively, it is necessary and sufficient that

$$1 - a\cos\phi > -c$$

be satisfied. Furthermore, one can show that $\lambda_{N-1} = (N-1)A^2/2$ and therefore using (26) this condition becomes

$$1 - a\cos\phi > -2\sigma_n^2/A^2(N-1) \quad (30)$$

For this to be satisfied for any signal-to-noise ratio $(A^2/2\sigma_n^2)$ it is sufficient to require that

$$a\cos\phi < 1 \quad (31)$$

In particular if we choose $a<1$ the system converges to the steady state regardless of the input SNR and/or the amount of phase shift in the reference loop.

c) Array Output SNR

The complex envelope of the desired signal at the array output is given by

$$s(t) = (A/\sqrt{2})\ [\underset{\sim}{P}^T\underset{\sim}{W}(t) + P_N]$$

$$= (A/\sqrt{2})\ [\underset{\sim}{P}^T\underset{\sim}{Q}\underset{\sim}{\Gamma}(t) + P_N]$$

By using (20) we get in the steady state

$$\lim_{t\to\infty} s(t) = (A/\sqrt{2})\ [\underset{\sim}{P}^T q_1 \gamma_{N-1}(\infty) + P_N]$$

where q_1 is the last column of the matrix Q. By definition $\underset{\sim}{Q}'\underset{\sim}{\phi}\underset{\sim}{Q} = (A^2/2)\underset{\sim}{Q}'\underset{\sim}{P}^*\underset{\sim}{P}^T\underset{\sim}{Q} = \underset{\sim}{\Lambda}$, therefore $(A/\sqrt{2})P^T q_1 = \sqrt{\lambda_{N-1}}$ and

$$\lim_{t\to\infty} s(t) = \gamma_{N-1}(\infty)\ \sqrt{\lambda_{N-1}} + A/\sqrt{2} \tag{31a}$$

If the stability condition is satisfied then $\lim_{t\to\infty} s(t)$ exist and the output desired signal power S_o is given by

$$S_o = |\gamma_{N-1}(\infty)\ \sqrt{\lambda}_{N-1} + A/\sqrt{2}|^2 \tag{31b}$$

With $\gamma_{N-1}(\infty) = C_r(\phi) + jC_i(\phi)$, and using (28) and (29), we obtain

$$S_o = A^2[(1 + \alpha_r^2(\phi) + \alpha_i^2(\phi)]/2 \tag{32}$$

where

$$\alpha_r(\phi) = -C_r(\phi)\sqrt{2\lambda_{N-1}}/A \tag{33}$$

$$\alpha_i(\phi) = -C_i(\phi)\sqrt{2\lambda_{N-1}}/A \tag{34}$$

Also the noise power is given by

$$N_o = \sigma_n^2(|\gamma_{N-1}(\infty)|^2 + 1)$$

$$= \sigma_n^2[A^2/2\lambda_{N-1}(\alpha_r^2(\phi) + \alpha_i^2(\phi) + 1]$$

Since $\lambda_{N-1} = (N-1)A^2/2$, we have

$$N_o = \sigma_n^2[(1/N-1)(\alpha_r^2(\phi) + \alpha_i^2(\phi) + 1] \tag{35}$$

From (32) and (35) we finally write for the output SNR

$$\frac{S_o}{N_o} = \frac{A^2(N-1)}{2\sigma_n^2}\ \left[\frac{\alpha_r^2(\phi) + \alpha_i^2(\phi) + 2\alpha_r(\phi) + 1}{\alpha_r^2(\phi) + \alpha_i^2(\phi) + N-1}\right]$$

$$= \frac{A^2(N-1)}{2\sigma_n^2}\ \frac{(2-2a\cos\phi + c)^2}{N[(1-a\cos\phi+c)^2 + a^2\sin^2\phi)-c(2-2a\cos\phi+c)]} \tag{36}$$

The last step is obtained in (E.13) of Appendix A-2. Note that in contrast to the LMS adaptive array with coded reference loop as treated by Compton and DiCarlo, here the output signal-to-noise power ratio depends on the reference loop phase shift and gain. This ratio is less than $A^2(N-1)/2\sigma_n^2$ for most practical cases (see Appendix A-3) if we choose a to be less than one. The output SNR may even fall to the output SNR of a single element, $A^2/2\sigma_n^2$ (see Appendix A-4).

From these results it is evident that in the network of Fig. 2. The array element outputs are not being maximally combined to give the expected array gain of an N element array. In particular, the variability of the SNR at this point is apt to affect the performance of the reference generating loop. However, we now show that utilizing only the weighted element outputs as reference loop input one gets an SNR close to the maximum and not dependent on the parameters of the reference generating loop.

The sum of the weighted array element outputs (auxiliary output) alone is

$$v_{au}(t) = \underset{\sim}{x}^T(t)\underset{\sim}{W}(t)$$

and the signal component is

$$s_{au}(t) = A\underset{\sim}{P}^T\underset{\sim}{W}(t)/\sqrt{2}$$

This can be expressed in a form similar to (31a) with the component contributed by the unweighted element deleted. Thus

$$\lim_{t\to\infty} s_{au}(t) = \gamma_{N-1}(\infty)\sqrt{\lambda_{N-1}},$$

and the power of the desired signal at the auxiliary output is

$$S_{oau} = |\gamma_{N-1}(\infty)|^2\lambda_{N-1} \tag{37}$$

The corresponding noise power is similar to (34a) with the contribution by the unweighted element deleted. Thus

$$N_{oau} = \sigma_n^2|\ \gamma_{N-1}(\infty)|^2 \tag{38}$$

and the signal-to-noise power ratio

$$(S_o/N_o)_a = \lambda_{N-1}/\sigma_n^2 = A^2(N-1)/2\sigma_n^2 \tag{39}$$

The array gain of the (N-1) unweighted elements is therefore realized; that is, the weights adjust themselves to coherently combine the output of the weighted elements and to provide maximum SNR. However, the resultant weighted output is not coherently combined with the output of the unweighted element; the SNR of the combination depends on the parameters of the reference generating loop and has a value generally well below that of the combined unweighted elements.

We now propose a modified circuit which takes advantage of the foregoing to provide constant SNR to the reference loop, but which also combines the weighted and unweighted element outputs to give a good final output SNR.

IV. Alternative Arrangement for Extracting the Reference Signal

The system arrangement depicted in Fig. 6. is proposed to overcome the problem discussed above. Here the reference signal $d_1(t)$ is given by

$$d_1(t) = a\, \underset{\sim}{x}^T(t)\underset{\sim}{W}(t)e^{-j\phi}$$

where a and ϕ are gain and phase shift in the reference loop. Consequently,

$$\begin{aligned}\underset{\sim}{R}_{xd1} &= E\,[\underset{\sim}{x}^*(t)\ \underset{\sim}{x}^T(t)\underset{\sim}{W}(t)]\ ae^{-j\phi} \\ &= \underset{\sim}{\phi}\underset{\sim}{W}(t)ae^{-j\phi} \qquad (40)\end{aligned}$$

Instead of (18) the weight vector W(t) will be governed by

$$d\underset{\sim}{W}(t)/dt + 2k[(1-ae^{-j\phi})\underset{\sim}{\phi} + \sigma_n^2\underset{\sim}{I}]\underset{\sim}{W}(t) = -kA^2\underset{\sim}{P}^*P_N$$

where, $\underset{\sim}{P}$ and P_N and $\underset{\sim}{\phi}$ were defined in connection with (8), (9) and (14). Following the same procedure as used earlier two equations in $\gamma^r_{N-1}(t)$ and $\gamma^i_{N-1}(t)$ similar to (25) are obtained with the right hand side being $-2kA\sqrt{\lambda_{N-1}}/2\begin{bmatrix}1\\0\end{bmatrix}$. The solution to these equations is given by (27) with

$$C_{r1}(\phi) = -\frac{A}{\sqrt{\lambda_{N-1}}}\ \frac{(1 - a\cos\phi + c)}{(1 - a\cos\phi + c)^2 + a^2\sin^2\phi} \tag{41}$$

$$C_{i1}(\phi) = -\frac{A}{\sqrt{2\lambda_{N-1}}}\ \frac{a\sin\phi}{(1 - a\cos\phi + c)^2 + a^2\sin^2\phi} \tag{42}$$

The stability condition remains exactly the same (eqs. (30) and (31)). Even though the final weights different from what they were in the previous system set up, the output desired signal and noise powers remain as they are given by (37) and (38), respectively. Therefore the SNR of the weighted element output, which is also SNR fed through the reference loop, equals $A^2(N-1)/2\sigma^2$.

a) Output SNR

Signal output in the configuration of Fig. 6 is taken from the point where weighted and unweighted elements are summed, as shown.

The desired signal and noise power output at this point are given by (32) and (35) respectively, with $\alpha_{r1}(\phi)$ and $\alpha_{i1}(\phi)$ used instead of $\alpha_r(\phi)$ and $\alpha_i(\phi)$, and with

$$\alpha_{r1}(\phi) = -C_{r1}(\phi)\sqrt{2\lambda_{N-1}}/A \tag{43}$$

$$\alpha_{i1}(\phi) = -C_{i1}(\phi)\sqrt{2\lambda_{N-1}}/A \tag{44}$$

$C_{r1}(\phi)$ and $C_{i1}(\phi)$ are given by (41) and (42). Using appendix (A-5) we write for the output SNR

$$\begin{aligned}\left(\frac{S_o}{N_o}\right)_1 &= \frac{A^2(N-1)}{2\sigma_n^2}\left[\frac{\alpha_{r1}^2(\phi) + \alpha_{i1}^2(\phi) + 2\alpha_{r1}(\phi) + 1}{\alpha_{r1}^2(\phi) + \alpha_{i1}^2(\phi) + N-1}\right] \\ &= \frac{A^2(N-1)}{2\sigma_n^2}\left[\frac{(2 - a\cos\phi + c)^2 + a^2\sin^2\phi}{(N-1)((1 - a\cos\phi + c)^2 + a^2\sin^2\phi)}\right]\end{aligned} \tag{45}$$

As in the case of the configuration of Fig. 2, with the configuration of Fig. 6 the output SNR depends on the reference loop phase shift and gain. This ratio

exhibits a maximum value when the phase shift is the smallest, $\phi = 0$ (provided that $N > 3$, or else for $N = 2$, $A^2/2\sigma_n^2 < 2.5$ is necessary). If furthermore $a = 1$ then for most practical cases the output SNR is approximately equal to its optimal value $A^2(N-1)/2\sigma_n^2$ (see Appendix A-6). Therefore, from the point of view of output SNR the configuration of Fig. 6 is preferable to that of Fig. 2.

V. Conclusion

We have here reported an analysis of the properties of an adaptive array based on the LMS algorithm with a self-generated reference. Circuits heretofore proposed, analyzed, and tested had been reported to suffer oscillatory weight instability when the reference generating loop shifts the phase of the signal component of the array output. The scheme examined here is a variant of the earlier scheme in which one array element is left unweighted and the reference generating loop is operated without a limiter. As a consequence the signal output of the reference generating loop is not fixed in amplitude and may differ from the signal at the loop input in both amplitude and phase.

It was found that in this mode of operation, stable nonoscillatory weights are obtained in the steady state provided certain mild conditions are satisfied on the gain and phase shift of the reference generating loop. Two alternative ways of driving the reference generating loop were examined. In the first, the sum of all array element outputs were used to drive the loop. Here it was found that the SNR entering the loop was highly variable being, under some conditions, nearly equal to the SNR of a single array element. This result was not viewed as a desirable one and an alternative in which the reference generating loop was driven by the weighted elements alone was then studied. Here a constant high SNR to the loop is obtained and, under reasonable conditions of loop gain and phase shift, a high (though moderately variable) signal output SNR.

Arrays of the sort here discussed are used where adaptive interference cancelling is sought. The analysis reported here as well as that reported earlier on other circuits with a self-generated reference signal deal only with desired signal plus noise. Clearly, all candidate schemes ought to also be examined with interference present and the output ratio of signal to interference plus noise determined. This will undoubtedly be done. As an interim measure we have also determined the component of signal power in the residue entering the array control processor. The details are not reported here but the analysis showed that the first circuit resulted in somewhat less signal power at this point than the second circuit. The reason for concentrating on this quantity is the expectation that the scheme generating a smaller signal power residue will be a more effective interference canceller; the desired signal would then not mask the interference and it would be the latter which mainly influences the weights generated.

Appendices

A-1 By using the following information

$$\begin{bmatrix}\rho_1(t)\\ \rho_2(t)\end{bmatrix} = \begin{bmatrix}1 & j\\ j & 1\end{bmatrix} \begin{bmatrix}\gamma^r_{N-1}(t)\\ \gamma^i_{N-1}(t)\end{bmatrix} \tag{E.1}$$

(25) becomes

$$\begin{bmatrix}d\rho_1(t)/dt\\ d\rho_2(t)/dt\end{bmatrix} + 2k\lambda_{N-1} \begin{bmatrix}1-a\cos\phi+c-ja\sin\phi & 0\\ 0 & 1-a\cos\phi+c+ja\sin\phi\end{bmatrix} \begin{bmatrix}\rho_1(t)\\ \rho_2(t)\end{bmatrix}$$

$$= -2kA\sqrt{\lambda_{N-1}}/2 \begin{bmatrix}1-a\cos\phi+ja\sin\phi\\ j(1-a\cos\phi)+a\sin\phi\end{bmatrix} \tag{E.2}$$

(E.2) yields two disjoint differential equation in $\rho_1(t)$ and $\rho_2(t)$. The solution of which is given by

$$\rho_1(t) = [\rho_1(0)-C_1(\phi)]\ \exp[-2k\lambda_{N-1}(1-a\cos\phi+c-ja\sin\phi)t] + C_1(\phi) \tag{E.3}$$

$$\rho_2(t) = [\rho_2(0)-C_2(\phi)]\ \exp[-2k\lambda_{N-1}(1-a\cos\phi+c+ja\sin\phi)t] + C_2(\phi) \tag{E.4}$$

where

$$C_1(\phi) = -\frac{A}{\sqrt{2}\lambda_{N-1}} \frac{1 - a\cos\phi + ja\sin\phi}{1 - a\cos\phi + c - ja\sin\phi} \tag{E.5}$$

$$C_2(\phi) = -\frac{A}{\sqrt{2}\lambda_{N-1}} \frac{j(1 - a\cos\phi) + a\sin\phi}{1 - a\cos\phi + c + ja\sin\phi} \tag{E.6}$$

Transforming back by using the transformation of (E.1) we get

$$\gamma_{N-1}^{r}(t) = \{[\gamma_{N-1}^{r}(0) - C_r(\phi)]\cos(2k\lambda_{N-1}a\sin\phi)t - [\gamma_{N-1}^{i}(0) - C_i(\phi)]\sin(2k\lambda_{N-1}a\sin\phi)t\}$$
$$\exp[-2k\lambda_{N-1}(1 - a\cos\phi+c)t] + C_r(\phi) \qquad (E.7)$$

$C_r(\phi)$ is given by (28).

A-2 From (33) and (34) together with (28) and (29) we write

$$\alpha_r(\phi) = \frac{b_1^2(\phi) - b_2^2(\phi) + cb_1(\phi)}{b_1^2(\phi) + b_2^2(\phi) + 2cb_1(\phi) + c^2} \qquad (E.8)$$

$$\alpha_i(\phi) = \frac{2b_1(\phi)b_2(\phi) + cb_2(\phi)}{b_1^2(\phi) + b_2^2(\phi) + 2cb_1(\phi) + c^2} \qquad (E.9)$$

where

$$b_1(\phi) = 1-a\cos\phi \qquad (E.10)$$

$$b_2(\phi) = a\sin\phi \qquad (E.11)$$

Thus

$$\alpha_r^2(\phi) + \alpha_i^2(\phi) = \frac{(b_1^2(\phi) - b_2^2(\phi))^2 + c^2(b_1^2(\phi) + b_2^2(\phi))}{b_1^2(\phi) + b_2^2(\phi) + 2cb_1(\phi) + c^2} + \frac{2cb_1(\phi)(b_1^2(\phi) + b_2^2(\phi))}{b_1^2(\phi) + b_2^2(\phi) + 2cb_1(\phi) + c^2}$$
$$= \frac{b_1^2(\phi) + b_2^2(\phi)}{b_1^2(\phi) + b_2^2(\phi) + 2cb_1(\phi) + c^2} \qquad (E.12)$$

Also

$$2\alpha_r(\phi) + 1 = \frac{3b_1^2(\phi) - b_2^2(\phi) + 4cb_1(\phi) + c^2}{b_1^2(\phi) + b_2^2(\phi) + 2cb_1(\phi) + c^2}$$

so that

$$\alpha_r^2(\phi) + \alpha_i^2(\phi) + 1 = \frac{(2b_1(\phi) + c)^2}{b_1^2(\phi) + b_2^2(\phi) + 2cb_1(\phi) + c^2}$$

Finally

$$\frac{\alpha_r^2(\phi) + \alpha_i^2(\phi) + 2\alpha_r(\phi) + 1}{\alpha_r^2(\phi) + \alpha_i^2(\phi) + N-1}$$

$$= \frac{(2b_1(\phi) + c)^2}{N(b_1^2(\phi) + b_2^2(\phi) + 2cb_1(\phi) + c^2) - c(2b_1(\phi) + c)}$$

$$= \frac{(2 - 2a\cos\phi + c)^2}{N((1-a\cos\phi+c)^2 + a^2\sin\phi) - c(2-a\cos\phi+c)} \qquad \text{(E.13)}$$

where in the last step we used (E.10) and (E.11).

A-3 To examine the dependence of S_o/N_o on the reference loop phase shift, of the circuit of Fig. 2 we rewrite (36)

$$\frac{S_o}{N_o}(a,\phi) = \frac{1}{c}\left(\frac{(2 - 2a\cos\phi + c)^2}{N((1-a\cos\phi+c)^2 + a^2\sin^2\phi) - c(2-2a\cos\phi + c)}\right) \qquad \text{(E.14)}$$

where $c = 2\sigma_n^2/A^2(N-1)$

Setting $c\partial S_o/N_o(a,\phi)/\partial\phi = 0$, yields the equation

$$2(2 - 2a\cos\phi+c)2a\sin\phi[N((1-a\cos\phi+c)2 + a2\sin2\phi) - c(2 - 2a\cos\phi+c)]$$

$$- 2(2 - 2a\cos\phi+c)^2[N(2(1 - a\cos\phi+c)a\sin\phi + 2a^2\sin\phi\cos\phi) -2ac\sin\phi]$$

$$= 0 \qquad \text{(E.15)}$$

The stationary points, therefore occur under one or more of the following conditions.

1) $2-2a\cos\phi + c + 0$ (E.16)

or, $a\cos\phi = (c+2)/2$. This condition cannot hold for $a < 1$ and $c \neq 0$

2) $2a \sin\phi = 0$

or, $\phi = 0$ since $a \neq 0$ (E.17)

3) $2N((1-a\cos\phi+c)^2 + a^2\sin^2(\phi)) - 2c(2-2a\cos\phi+c)$

$$= (2-2a\cos\phi+c)\,(N+c(N-1))$$

which implies

$$2-2a\cos\phi+c = 2N(1-a^2+c)/(N+cN-c) \qquad \text{(E.18)}$$

The values of S_o/N_o at these points are, respectively

1) $S_o/N_o = 0$

2) $$S_o/N_o = \frac{1}{c}\ \frac{(2-2a+c)^2}{N(1-a+c)^2 - c(2-2a+c)}$$

$$= \frac{A^2(N-1)}{2\,\sigma_{n2}}\ \frac{(2-2a+c)^2}{N(1-a+c)^2 - c(2-2a+c)} \qquad \text{(E.19)}$$

It is possible to show that if we choose $a < 1$ for this case; (i.e., $\phi = 0$), then the second factor of (E.19) decreases with c. Therefore S_o/N_o is upper bounded by

$$S_o/N_o < \frac{A^2(N-1)}{2\sigma_n^2}\ \frac{4(1-a)^2}{N(1-a)^2}$$

$$= \frac{A^2}{2\sigma_n^2}\,(N-1 + \frac{(4-N)(N-1)}{N}) \qquad \text{(E.20)}$$

The upper bound is larger than $A^2(N-1)/2\sigma_n^2$ only if $N < 4$. It equals $A^2N/2\sigma_n^2$ when $N = 2$, and approaches $A^2/2\sigma^2.4$ for a very large N

$$3)\ S_o/N_o = \frac{A^2(N-1)}{2\sigma_n^2}\ [\frac{4N(1-a^2+c)}{(N+cN-c)^2}] \qquad \text{(E.21)}$$

Again, it is possible to show that if we choose $a < 1$ then the second factor of (E.21) decreases with c and hence

$$S_o/N_o < [A^2(N-1)/2\sigma_n^2]4(1-a^2)/N$$

The upper bound can be greater than $A^2(N-1)/2\sigma_n^2$ only when $N < 4$, and equals $A^2N/2\sigma_n^2$ when $N < 2$. This upper bound is attained when c is very small. To conclude we notice that the output signal-to-noise ratio depends

on ϕ and it is less than $A^2(N-1)/2\sigma_n^2$ for most cases of practical interest.

A-4 To examine the dependence of S_o/N_o on the reference loop gain in the circuit of Fig. 2 use (E.14) to write

$$\partial(S_o/N_o)/\partial a = 2[2-2a\cos\phi+c)(-c\cos\phi(N+Nc-c-2) + 2a(\cos^2\phi(N+Nc-c)-N-Nc/2]$$

Stationary points occur under one of the following conditions

1) $(2-2a\cos\phi+c) = 0$ (E.22)

or $a\cos\phi = (c+2)/2$. Again, this is not valid for $a < 1$ and $c \neq 0$

2) $$a = \frac{-c\cos\phi[(N-2)+c(N-1)]}{[(1-\cos^2\phi)(N+cN/2)+(c-cN/2)\cos^2\phi]} \quad \text{(E.23)}$$

This point is a maximum or minimum depending on whether $\cos^2\phi$ is less or greater than $(N+Nc/2)/(N+Nc-c)$ respectively. But

$$1/2 < \frac{N+Nc/2}{N+Nc-C} < 1 \quad \text{(E.24)}$$

for $N > 2$ and any c. Therefore for $\cos\phi = 1$, the minimum point occurs at $a = 2$ if we assume c is small. From (E.14) for $\phi = 0$ and $a = 1$ $S_o/N_o = A^2/2\sigma_n^2$, while for $\phi = 0$ $a \simeq 0$ $S_o/N_o = A^2(N-1)/2\sigma_n N$.

A-5 Using (43) and (44) together with (41) and (42) we write

$$\alpha_{r1}(\phi) = \frac{b_1(\phi) + c}{b_1^2(\phi) + b_2^2(\phi) + 2cb_1(\phi) + c^2}$$

$$\alpha_{i1}(\phi) = \frac{b_2(\phi)}{b_1^2(\phi) + b_2^2(\phi) + 2cb_1(\phi) + c^2}$$

where $b_1(\phi)$ and $b_2(\phi)$ were defined in (E.10) and (E.11). As in Appendix A-2 we now have

$$\alpha_{i1}^2(\phi) + \alpha_{i1}^2(\phi) = \frac{1}{b_1^2(\phi) + b_2^2(\phi) + 2cb_1(\phi) + c^2}$$

Also

$$2\alpha_{r1}(\phi) + 1 = \frac{(b_1(\phi)+c)(b_1(\phi)+c+2) + b_2^2(\phi)}{b_1^2(\phi) + b_2^2(\phi) + 2cb_1(\phi) + c^2}$$

so that

$$\alpha_{r1}^2(\phi) + \alpha_{i1}^2 + 2\alpha_{r1}(\phi) + 1$$

$$= \frac{(b_1(\phi) + c+1)^2 + b_2^2(\phi)}{(b_1^2(\phi) + b_2^2(\phi) + 2cb_1(\phi) + c^2}$$

Finally

$$\frac{\alpha_{r1}^2(\phi) + \alpha_{i1}^2(\phi) + 2\alpha_{r1}(\phi) + 1}{\alpha_{r1}^2(\phi) + \alpha_{i1}^2(\phi) + N-1}$$

$$= \frac{(b_1(\phi) + c+1)^2 + b_2^2(\phi)}{(N-1)[b_1^2(\phi) + b_2^2(\phi) + 2cb_1(\phi)+c^2] + 1}$$

$$= \frac{(2-2a\cos\phi+c)^2 + a^2\sin^2\phi}{(N-1)[(1-a\cos\phi+c)^2 + a^2\sin^2\phi] + 1} \qquad \text{(E.25)}$$

A-6 To examine the dependence of $(S_o/N_o)_1$ on the reference loop phase shift ϕ of the circuit of Fig. 6, we write (45)

$$(S_o/N_o)_1(a,\phi) = \frac{1}{c}\left(\frac{(2-a\cos\phi+c)^2 + a^2\sin^2\phi}{(N-1)[(1-a\cos\phi+c)^2 + a^2\sin^2\phi] + 1}\right.$$

Hence $c\partial(S_o/N_o)_1(a,\phi)/\partial\phi = 0$ implies that

$$2(c+2)\ a\sin\phi[(N-1)((1-a\cos\phi+c)^2 + a^2\sin^2\phi) + 1]$$

$$-(c+1)(N-1)a\sin\phi[(2-a\cos\phi+c)^2 + a^2\sin^2\phi] = 0 \qquad \text{(E.25)}$$

After some manipulation one can show that (E.25)is equivalent to

$$2a\sin\phi[(N-1)a^2 - N(c+1)(c+2) + (c+2)^2] = 0 \qquad \text{(E.26)}$$

A solution to (E.26) is given by

$$a\sin\phi = 0$$

which implies $\phi = 0$ since $a \neq 0$ (E.27)

For this value to be maximum it is necessary and sufficient to have

$$a^2 < [N(c+1)(c+2) - (c+2)2]/(N-1) \qquad \text{(E.28)}$$

The right hand term of (E.28) is increasing with c. To make this term greater than or equal to one and consequently (E.28) to be satisfied for every $a < 1$, it sufficient to require

$$3 < N + (N-2)(c^2+3c) + c^2 + 2c \qquad \text{(E.29)}$$

This is satisfied for every c if $N > 3$ or when $N = 2$ provided that $c>0.4$ (or $A^2/3\sigma_n^2<2.5$).

The value of $(S_o/N_o)_1$ at $\phi = 0$ is given by

$$(S_o/N_o)_1 = \frac{1}{c}\left[\frac{(2-a+c)^2}{(N-1)(1-a+c)^2+1}\right]$$

If c is small enough then

$$(S_o/N_o)_1 = \frac{A^2(N-1)}{2\sigma_n^2}\left[\frac{(2-a)^2}{(N-1)(1-a)^2+1}\right] \qquad \text{(E.30)}$$

If c is very large then

$$(S_o/N_o)_1 \approx A^2/2\sigma_n^2 \qquad \text{(E.31)}$$

However, c large is not a practical alternative. If a is close to unity then

$$(S_o/N_{o)1} = (A^2(N-1)/2\sigma_n^2)[(1+c)^2/(N-1)c^2+1)]$$

$(N-1)c^2 = (2\sigma_n/A^2)^2/(N-1)$ which is much smaller than unity for reasonably large N and practical value of noise-to-signal power ratio of a single array element. Therefore $(S_o/N_o)_1$ is approximately equal the optimal signal-to-noise ratio $A^2(N-1)/2\sigma_n^2$

To conclude we notice that the output signal-to-noise ratio of this configuration also depends on the reference signal loop parameters, a and ϕ. However, for $\phi \approx 0$ and $a \approx 1$ the output signal-to-noise power ratio approaches the optimum value $A^2(N-1)/2\sigma_n^2$ for most of the practical cases.

VII. References

1. B. Widrow, J. McCool and J. Ball, "The Complex LMS Algorithm", Proc. IEEE, Vol. 63, pp. 719-720, April 1975.
2. R.L. Reigher and R.T. Compton, Jr., "An Adaptive Array for Interference Rejection", Proc. IEEE, Vol. 61, p. 748, June 1973.
3. R. Compton, Jr., "An Adaptive Array in Spread Spectrum Communication", Proc. IEEE, Vol. 66, p. 289, March 1978.
4. D.M. DiCarlo, R.T. Compton, Jr., "Reference Loop Phase Shift in Adaptive Arrays", IEEE Trans. on Aerosp. Electron Systems, Vol. AES-14, pp. 599-607, July 1978.
5. D.M. DiCarlo, "Reference Loop Phase Shift in an N-Element Adaptive Array", IEEE Trans. on Aerosp. Electron Systems, Vol. AES-15, pp. 576-582, July 1979.
6. Y. Bar-Ness, "Eliminating Reference Loop Phase Shift in Adaptive Arrays", IEEE Trans. on aerosp. Electron. Systems, Vol. AES-18, pp 115-123 Jan. 1982.

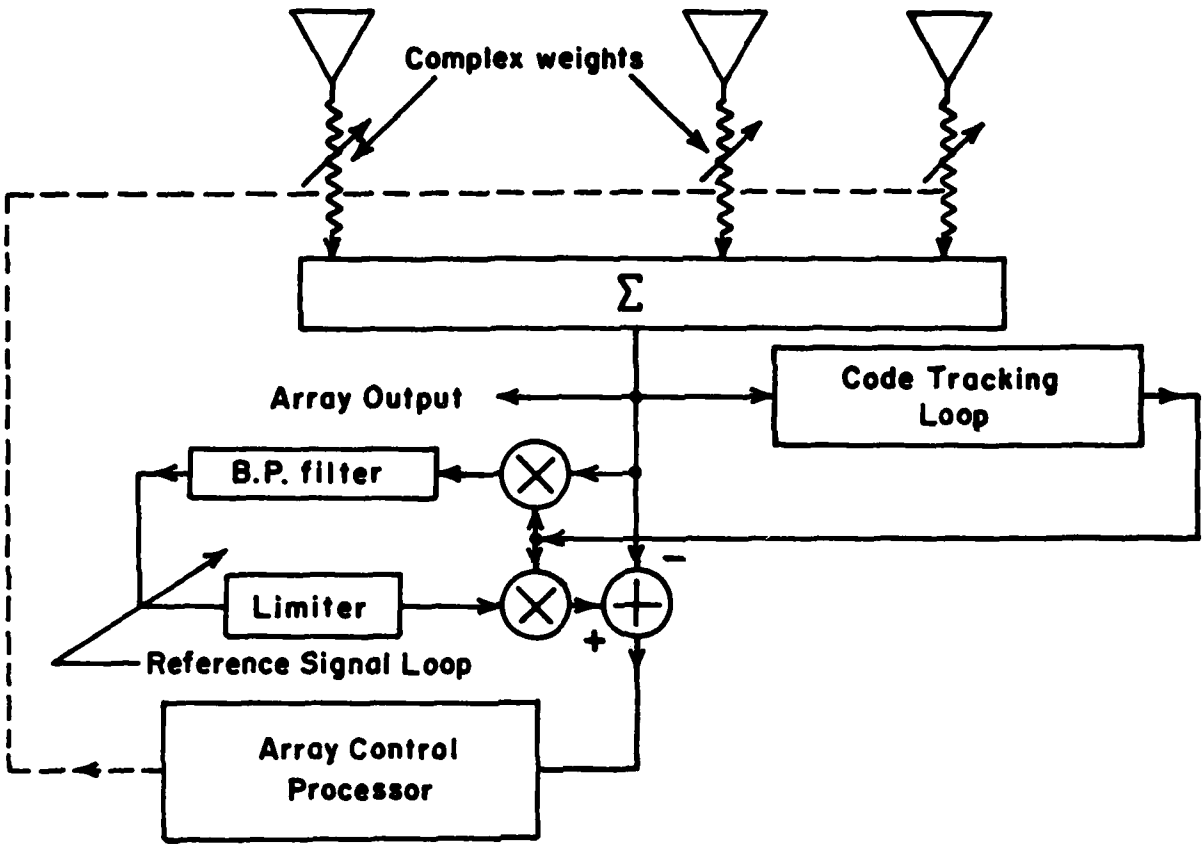

Figure 1 The LMS Adaptive Array with Coded Reference Signal Loop for Sp. Sp. Communication

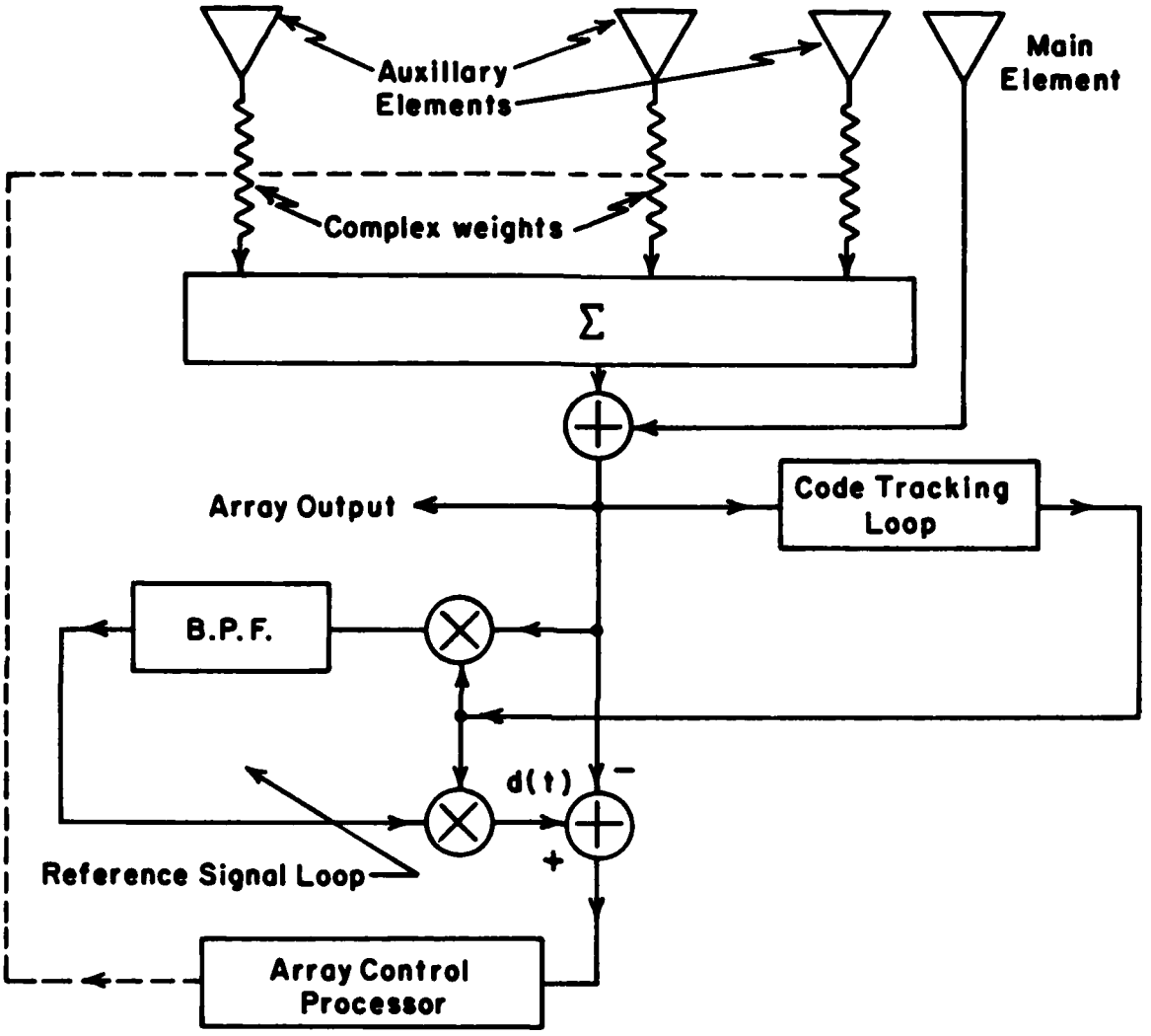

Figure 2 The LMS Interference Canceler with Coded Reference Signal Loop for Sp. Sp. Communications

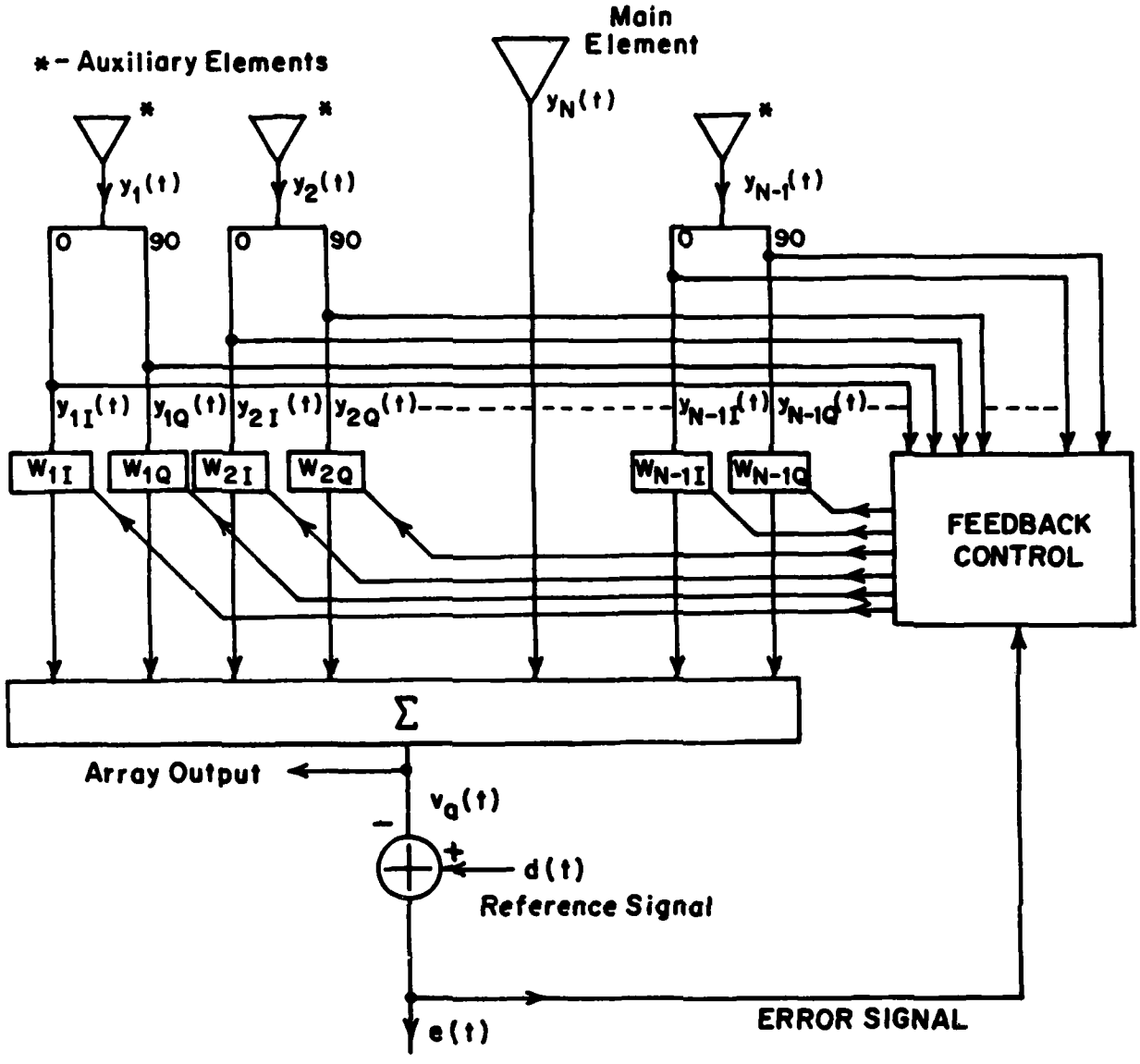

Figure 3 Quadrature Weighted LMS Interference Canceler

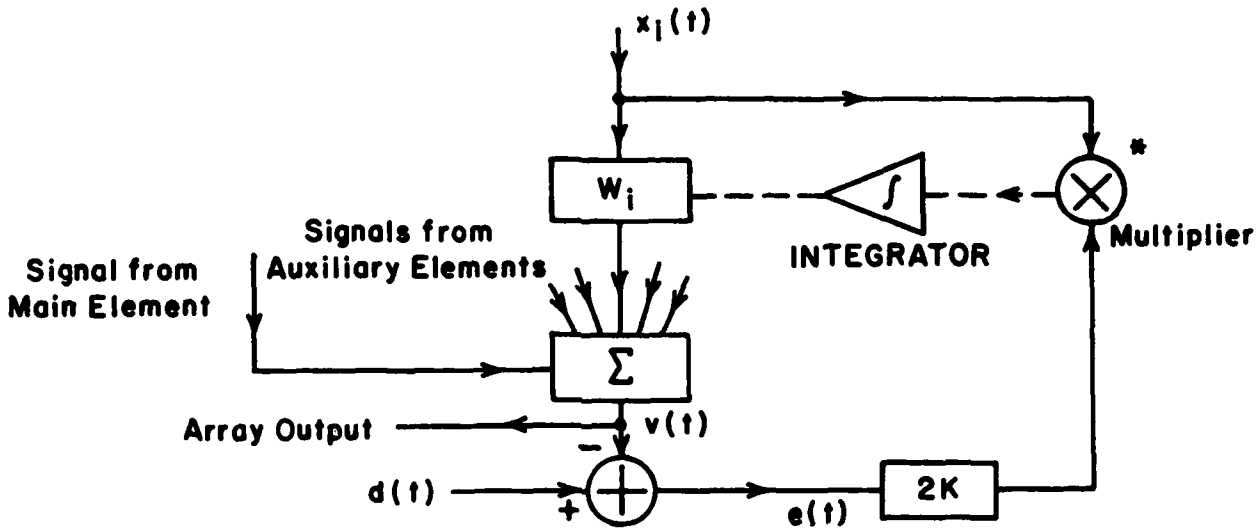

Figure 4 Main Feedback Loop for LMS Algorithm Realization

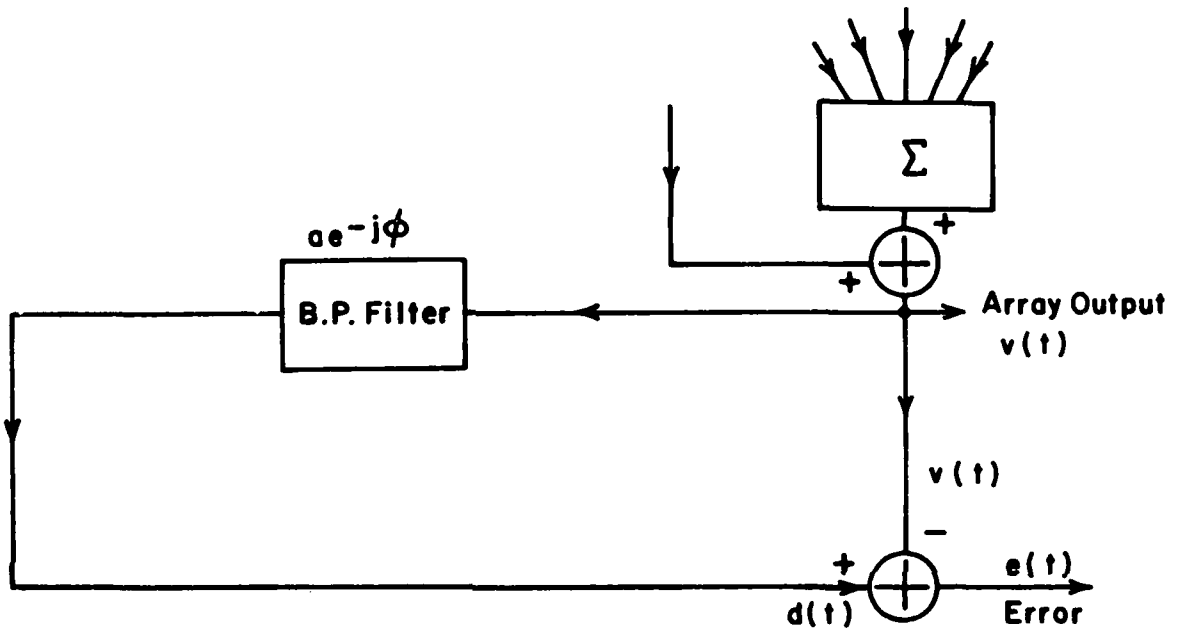

Figure 5 Reference Signal Loop

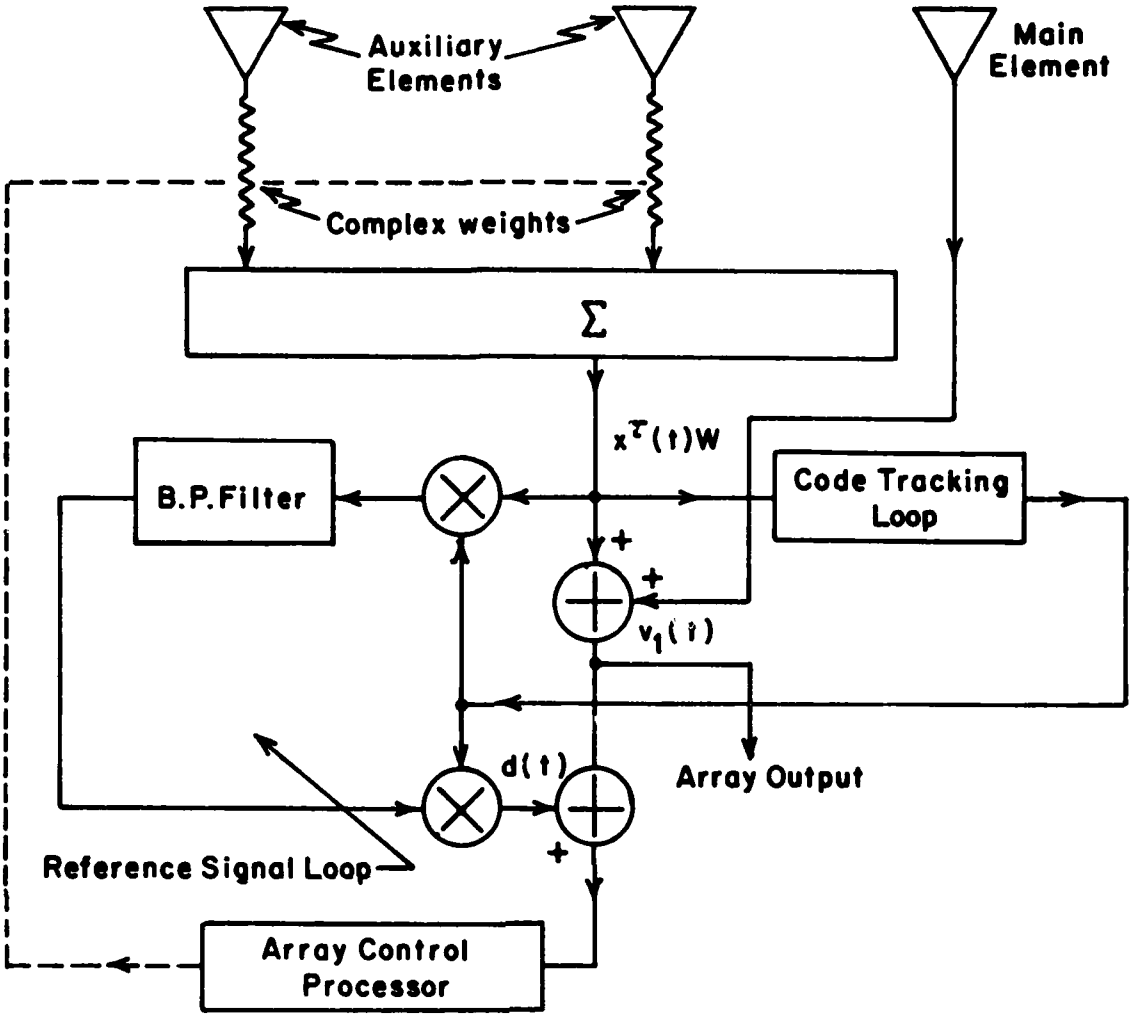

Figure 6 The LMS Interference Canceler With Different Arrangement for Extracting the Reference Signal

AD-A133 733 RESEARCH IN ADAPTIVE BEAMFORMING FOR SATELLITE COMMUNICATIONS(U) PENNSYLVANIA UNIV PHILADELPHIA F HABER ET AL. MAY 83 RADC-TR-83-54 F30602-81-K-0211 F/G 17/2 NL

3/3

UNCLASSIFIED

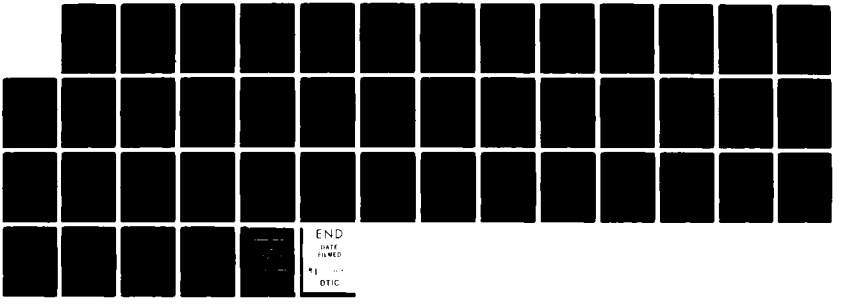

END

DATE FILMED

DTIC

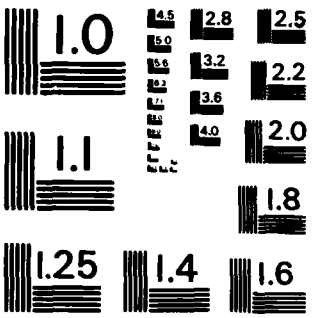

List of Symbols - Appendix E

A	desired signal amplitude
a	constant dependant on the limited level and filter attenuation of the reference extraction loop
c	defined to be σ_n^2/λ_{N-1}
d(t)	reference signal
$d_1(t)$	reference signal for alternative arrangement
E[ ]	denotes expected values
e(t)	minimized error signal for LMS algorithm
I	identity matrix
k	gain constant for LMS algorithm
N	number of elements
$N^t(t)$	noise process vector (1 x N)
N_o	noise power at array output
$N_{o_{a\mu}}$	noise power in $v_{a\mu}$
$n_N(t)$	noise process at main element
P^t	input signal's phase vector (1 x N)
P_N	phase at main element
Q	unitary diagonalizing matrix
R_x	input signal autocorrelation matrix (N x N)
R_{xd}	input-reference signal cross-correlation matrix (N x N)
R_{xd_1}	input-reference signal cross-correlation matrix for alternative arrangement (N x N)
S_o	output desired signal power
S(t)	desired signal at array output
S(t)	desired signal at array output
$S_{a\mu}(t)$	signal component of $v_{a\mu}$

(Continued)

List of Symbols - Appendix E
(Continued)

$v(t)$	array output
$v_a(t)$	real part of $v(t)$
$v_{a\mu}(t)$	sum of the weighted array element outputs
$w^t(t)$	array weight vector (1 x N-1)
$w_{iI}(t)$	weighting factor for $y_{iI}(t)$
$w_{iQ}(t)$	weighting factor for $y_{iQ}(t)$
$x^t(t)$	the system's input vector (1 x N)
$y_i(t)$	signal at i^{th} antenna element
$y_{iI}(t)$	equivalent to $y_i(t)$
$y_{iQ}(t)$	Hilbert transform of $y_i(t)$
$y_N(t)$	signal at unweighted main element
α_i	incoming phase of input signal at the i^{th} element
$\Gamma^t(t)$	Q' $w(t)$ uncoupled complex array weight vector (1 x N)
$\gamma_i(t)$	elements of $\Gamma^t(t)$
$\gamma_i{}^r(t)$	real part of the i^{th} uncoupled weight $\gamma_i(t)$
$\gamma_i{}^t(t)$	imaginary part of the i^{th} uncoupled weight $\gamma_i(t)$
Λ	uncoupled signal autocorrelation matrix (N x N)
λ_c	free space wavelength at frequency ω_c
λ_{n-1}	the only nonzero element of Λ
σ_n^2	noise power present at each element
ψ	arrival angle of input signal
ω_c	narrowband center frequency of input signal
$\lvert\ \rvert$	denotes magnitude

(Continued)

List of Symbols - Appendix E
(Continued)

$\hat{}$	denotes Hilbert transform
*	denotes conjugate
t	denotes transpose
'	denotes conjugate transpose

Appendix F

EFFECT OF INTERFERENCE ON THE BEHAVIOR OF AN LMS ADAPTIVE ARRAY WITH REFERENCE SIGNAL LOOP

by

Yeheskel Bar-Ness

and

Charles A. Bono

Drexel University
Electrical and Computer Engineering Department
Philadelphia, Pa. 19104

Effect of Interference on the Behavior of an LMS Adaptive Array with Reference Signal Loop

Abstract

A phase shift in the reference loop extraction scheme of adaptive arrays utilizing the Widrow LMS algorithm has been shown to cause cycling of the array weights in an interference free environment. Under the same conditions a compensation scheme proposed by Bar-Ness [3] was shown to force the weights to converge to a steady-state value. This paper investigates the compensated scheme in a multiple and single interference environment. For the case of single interference, it is shown that the array weights of the compensation scheme will converge to a steady state constant value while those of the uncompensated scheme will continue to oscillate.

I. Introduction:

Recently adaptive arrays have been attracting much attention. One reason is that these arrays can be used to null an undesired signal coming from a different source location than a desired signal. By doing this, adaptive arrays can be used as automatic beam steerers as well as interference cancellers.

One popular scheme used in adaptive array systems utilizes the least mean square (LMS) algorithm proposed by Widrow et al [1]. The scheme, however, requires a reference signal which correlates with the desired signal to be extracted. Obviously, the reference signal cannot be available apriori to the receiver and must somehow be extracted from the incoming inputs to the system.

One way of extracting a reference signal is by using a narrowband signal while having broadband interference. Then by use of a narrowband filter the interference is attenuated while the desired signal passes through and is used as a reference signal. This condition can be met by use of spread spectrum

methods. By this method, the desired signal's spectrum is spread by multiplying the signal by a pseudo-random code at the transmitter. Then at the receiver the incoming signals are multiplied by the same pseudo-random code. This process despreads the desired signal making it narrowband and at the same time spreads the interference making it broadband. Thus the reference signal can be extracted by use of a narrow band filter.

One problem with this scheme was first shown by Compton and DiCarlo [2]. They demonstrated using an interference free input that a phase shift introduced by the narrow band filter in the reference signal extraction loop causes the array weights to cycle. This work used a single array element and, DiCarlo [4] later extended the analysis to an N-element array and was able to attain the same results. Here a basic problem lies in the fact that the reference loop phase shift is a function of the incoming signals center frequency and cannot be known apriori. Thus, it cannot be compensated for all incoming signals, and under a wide range of nonstationary environments.

With the weight cycling problem in mind, Bar-Ness [3] added an adaptively controlled complex weight into the reference loop (Fig.5). This complex weight was shown by Bar-Ness to effectively compensate for the reference loop phase shift. Bar-Ness also showed in his analysis that with an interference free input this extraction scheme causes the array weights to converge on a steady--state value.

It is the purpose of this paper to examine the effect of interference on Bar-Ness's results. This first will be done for the general case of a multiple interference environment, then we consider the special case of a single interference.

For the multiple interference case it is shown that the reference loop phase shift is compensated for, however, a general condition for weight conver-

gence has not yet been found. For the single interference case a sufficient condition for convergence is found. The uncompensated case of Compton's array will also be examined and it is concluded that the existence of interference will still result in weight cycling.

II. Array Element Weight Controlling Equations:

A basic schematic of the narrowband adaptive array processor is shown in Fig. 1. The incoming signal to each of the N antenna elements is split into its in-phase (X_{iI}) and quadrature phase (X_{iq}) components giving 2N inputs to the system. Each input is weighted by a real factor w_{iI} or w_{iQ} and then summed to produce the array output v(t). An error signal $\varepsilon(t)$ is produced by taking the difference between a reference signal d(t) and the array output v(t). The weights are controlled such that the mean square of the error ($\overline{e^2(t)}$) is minimized.

Following the results first made by Widrow [1] the weights are controlled according to the equation:

$$\frac{dw_i(t)}{dt} = - k \frac{\partial}{\partial w_i} [\overline{e^2(t)}] \tag{1}$$

where k is the main feedback loop gain, and the overbar stands for expected value.

Realizing that we represent the array output analytically be

$$v(t) = X^t(t)\, w(t) \tag{2}$$

where:

$$w^t(t) = \{w_1(t),\ w_2(t),\ldots,\ w_n(t)\} \tag{3}$$

$$w_i(t) = w_{iI}(t) + jw_{iQ}(t)$$

$$X^t(t) = \{X_1(t),\ X_2(t),\ldots,\ X_N(t)\} \tag{4}$$

$$X_i(t) = X_{iI}(t) + jX_{iQ}(t)$$

t - indicates transpose

Using (2) we can define the error signal as

$$e(t) = d(t) - v(t) = d(t) - x^t(t)w(t) \tag{5}$$

Substituting (5) into (1) and evaluating the partial derivative we get from Widrow [1]

$$dw(t)/dt = 2k\ (\overline{x^*(t)e(t)}) \tag{6}$$

$$= 2k\ (\overline{x^*(t)d(t)} - \overline{x^*(t)x^t(t)}w(t)) \tag{7}$$

or

$$dw(t)/dt + 2k\ R_x\ w(t) = 2k\ R_{xd} \tag{8}$$

where:

$$R_x = E[x^*(t)\ x^t(t)] \tag{9}$$

$$R_{xd} = E[x^*(t)\ d(t)] \tag{10}$$

and E[ ] denotes the expected value.

Notice that R_x is the input auto correlation matrix and R_{xd} is the input-reference signal cross correlation matrix. Also, using eq. (6) we see that the feedback network of Fig. (2) can be implemented as a weight controller.

For the case of one continuous wave (CW) signal and m-interference signals arriving at angles ψ and $X(_i(i=1,..m)$ respectively with reference to broadside (Fig. (3)), we can represent the input vector of eq. (4) as

$$x(t) = A/\sqrt{2}\ P_s + \sum_{i=1}^{m} B_i/\sqrt{2}\ P_{I_i} + N(t) \tag{11}$$

where, $N^t(t) = [n_1(t), n_2(t), .., n_N(t)]$ is the noise process. A is the desired signal amplitude. B_i is the amplitude of the i^{th} interferer. And assuming a nonlinear array

$$P_s^t = e^{-j\rho_s(t)}[1,\ e^{-j\alpha_2},\ e^{-j\alpha_3},\ \ldots\ .\ e^{-j\alpha_n}] \tag{12}$$

$$P_{I_i}^t = e^{-j\rho_i(t)}[1,\ e^{-jb_{i_2}},\ e^{-jb_{i_3}}\ \ldots\ .\ e^{-jb_{i_n}}] \tag{13}$$

where $\alpha_j = 2\pi L_j/\lambda_c \sin\psi$ and $b_{ij} = 2\pi L_j/\lambda_c \sin X_i$, and ρ_s and ρ_i are the incoming phases of the complex envelope of the desired signal

and the i^{th} interferer respectively. L_j is the distance between the first and j^{th} input element. λ_c is the free space wavelength of the centerband frequency of the input.

Using (11) in the definition of the input autocorrelation maxtrix (R_x) and assuming that the noise, signal and the m-interferers are uncorrelated we can say that

$$R_x = \Phi_s + \sum_{i=1}^{m} \Phi_{I_i} + \sigma_n^2 I \tag{14}$$

where σ_n^2 is the noise power, I is the identity matrix, and Φ_s and Φ_{I_i} are defined as

$$\Phi_s = \frac{A^2}{2} P_s^* P_s^t \tag{15}$$

$$\Phi_{I_i} = \frac{B_i^2}{2} P_{I_i}^* P_{I_i}^t \tag{16}$$

Using the definition of R_x (14) in (8) we get

$$dw(t)/dt + 2k(\Phi_s + \sum_{i=1}^{m} \Phi_{I_i} + \sigma_n^2 I)w(t) = 2kR_{xd} \tag{17}$$

Equation (17) describes the controlling equation for each of the element weights.

Using the scheme of Fig. (4) to extract a reference signal (d(t)) from the array output (v(t)), and assuming wide band interference with a narrow band desired signal, it can be easily shown [2] that the reference signal is given by

$$d(t) = \frac{a(P_s^t w(t))}{|P_s^t w(t)|} e^{-j\phi} \tag{18}$$

where, a is a constant depending on the limiter level and filter attenuation of Fig. (4). ϕ is the phase shift introduced by the reference loop and is dependent on the frequency of the incoming desired signal.

Investigating the system described by equations (18) and (17) with no interferences ($\Phi_{I_i} = [0]$), DiCarlo [4] demonstrated that the weights would os-

cillate at a radial frequency dependent upon the reference loop phase shift (ϕ), the signal and noise powers, the feedback loop gain (k) and the number of array elements.

III. Phase Compensation Scheme

To contend with the problem of weight cycling caused by the non-zero phase shift of the reference loop extraction scheme (Fig. 4), Bar-Ness [3] proposed the adaptively controlled phase compensation scheme of Fig. (5). This scheme introduces a complex weight w_r to the reference extraction loop, where w_r is adaptively controlled so that it minimizes the phase difference at point 1 and 2 of Fig. (5). As seen this controlling is done by the use of an integrator and a multiplier which together form a correlation loop between $e_1(t)$ and the original reference signal now renamed y(t). From Fig. (5) we see that $e_1(t)$ is the difference between the compensated reference signal and the array output v(t). Thus as the correlation loop minimizes the mean-square of $e_1(t)$ the phase difference between the reference signal and the array output is also minimized.

Analysis of Phase Compensation Scheme:

Following Bar-Ness's analysis, it is seen from Fig. (5) that the governing equation for the added complex weight $w_r(t)$ is

$$\frac{dw_r(t)}{dt} = -2k_r\overline{y^*(t)e_1(t)} \tag{19}$$

where from (18)

$$y(t) = \frac{a(P_s{}^t w(t))}{|P_s{}^t w(t)|} e^{-j\phi} \tag{20}$$

and from Fig. 5.

$$e_1(t) = cy(t)w_r(t) - x^T(t)w(t) \tag{21}$$

Noticing that the newly defined reference signal d(t) is equal to the sum of

the product $[y_1(t)w_r(t)]$ and an amplitude limited version of $[y_1(t)w_r(t)]$ we get

$$d(t) = y(t)w_r(t) + b_1 \frac{y(t)\, w_r(t)}{|y(t)w_r(t)|} \tag{22}$$

But $|y(t)| = a$ which is the first limiter level. Thus (22) becomes

$$d(t) = y(t)\, [w_r(t) + \frac{b_1\, w_r(t)}{a|w_r(t)|}] \tag{23}$$

Now that the reference signal (d(t)) is defined for our system we can use it to describe the input-reference cross correlation matrix ($R_{xd} = E[x^*(t)\, d(t)]$). Substituting from (23)

$$R_{xd} = E[x^*(t)\, y(t)[w_r(t) + \frac{b_1\, w_r(t)}{a|w_r(t)|}]] \tag{24}$$

Substituting for y(t) from (20), (24) becomes

$$R_{xd} = E[x^*(t)\, \frac{P_s^t w(t)}{|P_s^t w(t)|}\, [a\, w^r(t) + \frac{b_1 w_r(t)}{|w_r(t)|}] e^{-j\phi}] \tag{25}$$

Using the assumption that the incoming signals are uncorrelated with one another we see that

$$E[x^*(t)P_s^t] = \frac{A}{\sqrt{2}} P_s^* P_s^t = \frac{\sqrt{2}}{A}\, \Phi_s \tag{26}$$

Using this in (25) we get

$$R_{xd} = \frac{\sqrt{2}}{A}\, [\frac{\Phi_s w(t)}{|P_s^t w(t)|}][a w_r(t) + \frac{b_1 w_r(t)}{|w_r(t)|}] e^{-j\phi} \tag{27}$$

Now having R_{xd} defined by (27), the element weight equation (17) becomes

$$\frac{dw(t)}{dt} + 2k(\Phi_s + \sum_{i=1}^{m} \Phi_{I_i} + \sigma_n^2 I)\, w(t) = \tag{28}$$

$$\frac{2\sqrt{2}k}{A}\, [\frac{\Phi_s w(t)}{|P_s^t w(t)|}][a\, w_r(t) + \frac{b_1 w_r(t)}{|w_r(t)|}] e^{-j\phi}$$

Having the element weights defined by (28) we turn our attention back to the phase compensation weight $w_r(t)$. By substituting equaiton (21) into (19) we get

$$dw_r(t)/dt = -2k_r E[y^*(t)(cy(t)w_r(t) - x^T(t)w(t))] \tag{29}$$

But $y^*(t)\, y(t) = |y(t)|^2 = a^2$ (29a)

And by using the definition of y(t) from (20), (29) becomes

$$dw_r(t)/dt = -2k_r[ca^2 w_r(t) - E[(aP_s'w^*(t)/|P_s^t w(t)|)x^t(t)w(t)e^{j\phi}] \tag{29b}$$

where: ' stands for transpose conjugate

Since $P_s'w^*(t)$ is a scalar we can see

$$P_s'w^*(t) = w'(t)P_s^* \tag{29c}$$

and using (16) we can rewrite (29b) as

$$dw_r(t)/dt = -2k_r[ca^2 w_r(t) - a\sqrt{2}/A\ (w'(t)\Phi_s w(t)/|P_s^t w(t)|)e^{j\phi}] \tag{30}$$

or

$$dw_r(t)/dt + 2k_r ca^2 w_r(t) = \frac{2\sqrt{2}k_r a}{A}\left[\frac{w'(t)\Phi_s w(t)}{|P_s^t w(t)|}\right]e^{j\phi} \tag{30a}$$

Using the fact that Φ_s and Φ_{I_i} (i=1 to m) are all of rank 1 and complex Hermetian matrices, we see that $\sum_{i=1}^{m} \Phi_{I_i}$ is of rank $\leq m$ and using Appendix A we can find a unitary matrix Q such that

$$\Lambda_s = Q'\,\Phi_s Q = \begin{bmatrix} \lambda_1 & \cdots & 0 \\ \vdots & 0 & \\ \vdots & & \\ 0 & & 0 \end{bmatrix} \tag{31}$$

$$\Lambda_I = Q' \sum_{i=1}^{m} \Phi_{I_i} Q = \begin{bmatrix} \begin{bmatrix} q_{ij} & \cdots & \\ \vdots & & \\ \vdots & \cdots & \end{bmatrix}_{m+1 \times m+1} & \begin{matrix} 0 \\ \vdots \\ \vdots \end{matrix} \\ \begin{matrix} 0 & \cdots & 0 \end{matrix} & 0 \end{bmatrix} \tag{32}$$

where

$$q_{ij} \text{ - positive, real} \qquad i = j \tag{33}$$

$$q_{ij} = q_{ij}^{+} e^{-j\rho_{ij}} \qquad i \neq j \tag{34}$$

Premultiplying (28) by Q' we get

$$Q'\frac{dw(t)}{dt} + 2k\ Q'(\Phi_s + \sum_{i=1}^{m} \Phi_{I_i} + \sigma_n^2 I)Q\ Q'\ w(t)$$

$$= \frac{2\sqrt{2}k}{A} \frac{Q'\Phi_s Q\ Q'w(t)}{|P_s^t w(t)|} [a\ w_r(t) + \frac{b_1 w_r(t)}{|w_r(t)|}]e^{-j\phi} \tag{35}$$

Defining $\Gamma(t) = Q'w(t) = [\gamma_1, \gamma_2, \ldots \gamma_n]$ (36)

Using (31), (32), and (35), (36) becomes

$$d\Gamma(t)/dt + 2k[\Lambda_s + \Lambda_I + \sigma_n^2 I]\Gamma(t)$$

$$= \frac{2\sqrt{2}k}{A} \frac{\Lambda_s}{|P_s^t w(t)|} \Gamma(t)[a\ w_r(t) + \frac{b_1 w_r(t)}{|w_r(t)|}]e^{-j\phi} \tag{37}$$

Evaluating $|P_s^t w(t)|$ we get

$$|P_s^t w(t)| = [[P_s^t w(t)]'[P_s^t w(t)]]^{1/2} = [w'(t)P_s^* P_s^t w(t)]^{1/2} \tag{38}$$

or

$$|P_s^t w(t)| = [w'(t)Q\ Q'P_s^* P_s^t Q\ Q'w(t)]^{1/2} = [\Gamma'(t)\frac{2}{A^2}\Phi_s\ \Gamma(t)]^{1/2}$$

$$= \frac{\sqrt{2}}{A} [\Gamma'(t)\Lambda_s\ \Gamma(t)]^{1/2} \tag{39}$$

Using the definition of Λ_s [(31)] and (36), (39) becomes

$$|P_s^t w(t)| = \frac{\sqrt{2}}{A} [|\gamma_1|^2\ \lambda_1]^{1/2} = \frac{\sqrt{2}}{A}|\gamma_1|\sqrt{\lambda_1} \tag{40}$$

And (37) becomes

$$d\Gamma(t)/dt + 2k[\Lambda_s + \Lambda_I + \sigma_n^2 I]\ \Gamma(t)$$

$$= 2k\frac{\Lambda_1}{\sqrt{\lambda_1}|\gamma_1|}\ \Gamma(t)[a\ w_r(t) + \frac{b_1 w_r(t)}{|w_r(t)|}]e^{-j\phi} \tag{41}$$

From (31) and (32) we see that (41) can be written in the form

$$d\gamma_i(t)/dt + 2k\ \sigma_n^2\ \gamma_i(t) = 0 \qquad i=M+2, \ldots\ N \tag{42}$$

$$d\gamma_1(t)/dt + 2k[\sum_{j=1}^{m+1} q_{1j}\gamma_j + \sigma_n^2\ \gamma_1] = 0 \qquad i=2, \ldots\ M+1 \tag{43}$$

$$d\gamma_1(t)/dt + 2k[\sum_{j=1}^{m+1} q_{1j}\gamma_j + (\lambda_1 + \sigma_n^2)\gamma_1]$$

$$= 2k\sqrt{\lambda_1}\,[\frac{\gamma_1(t)}{|\gamma_1(t)|}]\,[aw_r(t) + \frac{b_1 w_r(t)}{|w_r(t)|}]e^{-j\phi} \qquad (44)$$

Turning our attention back to the reference loop weight $w_r(t)$, we see that by substituting (40) into (30) and using (36) we get

$$dw_r(t)/dt + 2k_r ca^2 w_r(t) = 2a\,k_r\,\frac{\Gamma'(t)\Lambda_s\Gamma(t)}{|\gamma_1|\sqrt{\lambda_1}}\,e^{j\phi} \qquad (45)$$

or

$$dw_r(t)/dt + 2k_r ca^2 w_r(t) = 2a\,k_r\,\sqrt{\lambda_1}|\gamma_1|e^{j\phi} \qquad (46)$$

At this point it is noticed that eqs. (42),(43),(44), and (46) are a set of N-complex nonlinear differential equations which describe the response of the system weights. Looking at (42) we see that [N-(m+1)] of the weights will exponentially decay to a steady state value of zero. Or solving (42) we see that

$$\gamma_i(t) = \gamma_i(0)\,e^{-2k\sigma_n^2 t} \qquad i = M+2, \ldots N \qquad (47)$$

To solve for the remaining M+1 weights plus the complex weight $w_r(t)$ we define:

$$\gamma_i(t) = P_i(t)e^{-j\theta_i(t)} \qquad (48)$$

$$w_r(t) = P_r(t)e^{-j\psi(t)} \qquad (49)$$

where $P_i(t)$ and $P_r(t)$ are assumed non-negative. Using (48), (49), along with (33),(34) we can rewrite the system weights equations [(43),(44),(46)] as

$$d[P_i(t)e^{-j\theta_i(t)}]/dt + 2k[\sum_{j=1}^{m+1} q_{ij}^{+}\,P_j(t)e^{-j(\theta_j(t)+\rho_{ij})} + \sigma_n^2 P_i(t)e^{-j\theta_i(t)}] = 0 \qquad i=2, \ldots M+1 \qquad (50)$$

$$d[P_1(t)e^{-j\theta_1(t)}]/dt + 2k[\sum_{j=1}^{m+1} q_{1j}^{+}P_j(t)e^{-(\theta_j(t)+\rho_{1j})} + (\lambda_n + \sigma_n^2)P_1(t)e^{-j\theta_1(t)}] = 2k\sqrt{\lambda_1}e^{-j\theta_1(t)}\,[aP_r(t) + b_1]e^{-j(\phi+\psi)} \qquad (51)$$

$$d[P_r(t)e^{-j\psi(t)}]/dt + 2k_r ca^2 P_r(t)e^{-j\psi(t)} = 2ak_r\sqrt{\lambda_1}P_1(t)e^{j\phi} \tag{52}$$

Evaluating the derivatives of (50), (51), (52) we get

$$\frac{dP_i(t)}{dt}e^{-j\theta_i(t)} - jP_i(t)e^{-j\theta_i(t)}[\frac{d\theta_i(t)}{dt}] + 2k[\sum_{j=1}^{m+1} q_{ij}^{+}P_j(t)e^{-(\theta_j+\rho_{ij})}$$

$$+ \sigma_n^2 P_i(t)e^{-j\theta_i(t)}] = 0 \qquad i=2, \ldots. M+1 \tag{53}$$

$$\frac{dP_1(t)}{dt}e^{-j\theta_1(t)} - jP_1(t)e^{-j\theta_1(t)}[\frac{d\theta_1(t)}{dt}] + 2k[\sum_{j=1}^{m+1} q_{1j}^{+}P_j(t)e^{-(\theta_j+\rho_{1j})}$$

$$+ (\lambda_1 + \sigma_n^2)P_1(t)e^{-j\theta_1(t)}]$$

$$= 2k\sqrt{\lambda_1}[e^{-j\theta_1(t)}][aP_r(t) + b_1]e^{-j(\phi+\psi)} \tag{54}$$

$$\frac{dP_r(t)}{dt}e^{-j\psi(t)} - jP_r(t)e^{-j\psi(t)}[\frac{d\psi(t)}{dt}] + 2k_r ca^2 P_r(t)e^{-j\psi(t)}$$

$$= 2ak_r\sqrt{\lambda_1}P_1(t)e^{j\phi} \tag{55}$$

Multiplying both sides of (53),(54) and (55) by $e^{j\theta_i(t)}$, $e^{j\theta_1(t)}$ and $e^{j\psi(t)}$ respectively and equating the real and imaginary parts of each we get

$$dP_i(t)/dt + 2k[\sum_{j=1}^{m+1} q_{ij}^{+}P_j(t)\cos(\theta_i - \theta_j - \rho_{ij}) + \sigma_n^2 P_i(t)] = 0$$

$$i = 2, \ldots M+1 \tag{56}$$

$$dP_1(t)/dt + 2k[\sum_{j=1}^{m+1} q_{1j}^{+}P_j(t)\cos(\theta_1 - \theta_j - \rho_{1j}) + (\lambda_1 + \sigma_n^2)P_1(t)]$$

$$= 2k\sqrt{\lambda_1}[aP_r(t) + b_1]\cos(\phi + \psi) \tag{57}$$

$$dP_r(t)/dt + 2k_r ca^2 P_r(t) = 2ak_r\sqrt{\lambda_1}P_1(t)\cos(\phi + \psi) \tag{58}$$

$$P_i(t)\frac{d\theta_i(t)}{dt} - 2k[\sum_{j=1}^{m+1} q_{ij}^{+}P_j(t)\sin(\theta_i - \theta_j - \rho_{ij})] = 0$$

$$i = 2, \ldots M+1 \tag{59}$$

$$P_1(t)\frac{d\theta_1(t)}{dt} - 2k[\sum_{j=1}^{m+1} q_{1j}^{+}P_j(t)\sin(\theta_1 - \theta_j - \rho_{1j})]$$

$$= 2k\sqrt{\lambda_1}[aP_r(t) + b_1]\sin(\phi + \psi) \tag{60}$$

$$P_r(t)\frac{d\psi(t)}{dt} = -2ak_r\sqrt{\lambda_1}P_1(t)\sin(\phi + \psi) \tag{61}$$

Looking at equations (58) and (61) we see that the compensation weights ($w_r(t) = P_r(t)e^{-j\psi(t)}$) controlling equation is not affected by the interference. Thus we get from Bar-Ness [3]

$$\cot[\phi(t)+\psi(t)] = \frac{P_r(0)\cos(\phi_{10}+\psi_0)+2k_r a\sqrt{\lambda_n}\int_0^t P_1(t)\exp(2k_r ca^2\tau)d\tau}{P_r(0)\sin(\phi_{10} + \psi_0)} \tag{62}$$

Also, if $P_1(t)$ is bounded away from zero, and assuming it is positive then for sufficiently large t we have

$$\phi(t) \equiv -\psi(t) \tag{63}$$

Thus the refernece loop phase shift is compensated for and the weight equations (56), (57), (58), (59), (60) and (61) reduce to

$$\frac{dP_1(t)}{dt} + 2k[\sum_{j=1}^{m+1} q_{1j}^{+}P_j(t)\cos(\theta_1 - \theta_j - \rho_{1j}) + (\lambda_1 + \sigma_n^2)P_1(t)$$

$$= 2k\sqrt{\lambda_1}[aP_r(t) + b_1] \tag{64}$$

$$\frac{dP_i(t)}{dt} + 2k[\sum_{j=1}^{m+1} q_{ij}^{+}P_j(t)\cos(\theta_i - \theta_j - \rho_{ij}) + (\sigma_n^2)P_i(t) = 0$$

$$i = 2,\ldots M+1 \tag{65}$$

$$\frac{dP_r(t)}{dt} + 2k_r ca^2P_r(t) = 2ak_r\sqrt{\lambda_1}P_1(t) \tag{66}$$

$$P_i(t)\frac{d\theta_i(t)}{dt} - 2k[\sum_{j=1}^{m+1} q_{ij}^{+}P_j(t)\sin(\theta_i - \theta_j - \rho_{ij})] = 0$$

$$i = 2,\ldots M+1 \tag{67}$$

$$P_1(t)\frac{d\theta_1(t)}{dt} - 2k[\sum_{j=1}^{m+1} q_{1j}^{+}P_j(t)\sin(\theta_1 - \theta_j - \rho_{1j})] = 0 \tag{68}$$

$$P_r(t)\frac{d\psi(t)}{dt} = 0 \tag{69}$$

At this point we have shown that the added weight $w_r(t)$ effectively compensated for the reference loop phase shift ϕ. However, we have not as yet been able to find a general solution for the weight equations (64-69). In the next section we investigate the special case of a single interference and give a sufficient condition for convergence of the array weights.

IV. Special Case: Single Interference in an N Element Array

With the number of interferers (m) reduced to 1 the input vector (eq.(11)) becomes

$$x(t) = \frac{A}{\sqrt{2}} P_s + \frac{B}{\sqrt{2}} P_I + N(t) \tag{71}$$

where A and B are the amplitudes of the signal and interference respectively. P_s and P_I are their respective direction vectors and are defined in equations (12) and (13).

Following the derivation for the multiple interference case we see that we must diagonalize the desired signal autocorrelation matrix ($\phi_s = \frac{A^2}{2} P_s^* P_s^t$) as in (31). Also, we must use the same unitary diagonalizing matrix Q in order to transform the interference autocorrelation matrix ($\phi_I = \frac{B^2}{2} P_I^* P_I^t$) to the form of (32) where m=1. Using the definitions of Appendix A (A5), let

$$Q' = \begin{bmatrix} - & v'_1 & - \\ - & v'_2 & - \\ & \vdots & \\ - & v'_n & - \end{bmatrix} \tag{72}$$

where: v_1 is the eigenvector corresponding to the only non zero eigenvalue of ϕ_s

$v_2 - v_n$ are the eigenvectors corresponding to the n-1 zero eigenvalues of ϕ_s

' denotes the transpose conjugate of the vector

By inspection we can see that a proper choice for v_1 is:

$$v_1' = P_s^t / |P_s| = 1/\sqrt{N} \, [1 \quad e^{-j\alpha_2} \quad \ldots \quad e^{-j\alpha_n}] \tag{73}$$

Using this knowledge, we get from (31)

$$\Lambda s = Q' \Phi_s Q = \frac{A^2}{2} Q' P_s^* P_s^t Q \tag{74}$$

$$= \frac{A^2}{2} \begin{bmatrix} \text{---} & v'_1 & \text{---} \\ \text{---} & v'_2 & \text{---} \\ & \vdots & \\ \text{---} & v'_n & \text{---} \end{bmatrix} \begin{bmatrix} 1 \\ e^{j\alpha_2} \\ \vdots \\ e^{j\alpha_n} \end{bmatrix} [1 \quad e^{-j\alpha_2} \quad \cdots \quad e^{-j\alpha_n}] \begin{bmatrix} \cdot & \cdot & \cdot \\ \cdot & \cdot & \cdot \\ \cdot & \cdot & \cdot \\ v_1 & v_2 & \cdots & v_n \\ \cdot & \cdot & \cdot \\ \cdot & \cdot & \cdot \\ \cdot & \cdot & \cdot \end{bmatrix} \tag{75}$$

Combining (72), (73), and (75) we see that

$$\Lambda_s = \begin{bmatrix} \lambda_1 & 0 & \cdot & \cdot & \cdot \\ 0 & 0 & & & \\ \cdot & & \cdot & & \\ \cdot & & & \cdot & \\ 0 & & & & 0 \end{bmatrix} \tag{76}$$

where from Appendix A (A4) we know

$$\lambda_1 = \frac{NA^2}{2} \tag{77}$$

Using Appendix A we see that we now can place a restriction on Q such that

$$\Lambda_I = Q' \Phi_I Q = \frac{B^2}{2} Q' P_I^* P_I^t Q = \frac{B^2}{2} Z^* Z^t \tag{78}$$

$$= \left[\begin{array}{cc|c} q_{11} & q_{12} & 0 \quad \cdots \quad 0 \\ & & \vdots \\ q_{21} & q_{22} & 0 \quad \cdots \quad \cdot \\ \hline 0 & 0 & 0 \quad \cdots \quad \cdot \\ \vdots & & \vdots \\ 0 \quad \cdots & & \cdots \quad 0 \end{array}\right] \tag{79}$$

where:

$$Z^t = [\langle v_1 P_I^* \rangle \ \langle v_2 P_I^* \rangle \ \langle v_3 P_I^* \rangle \ \ldots \ \langle v_n P_I^* \rangle] \tag{80}$$

From Appendix A we know that this can be accomplished if we let v_1 and v_2 span the plane defined by P_s^* and P_I^* and making the other n-2 eigenvector orthonormal to the space spanned by v_1 and v_2. Thus using the diagram below

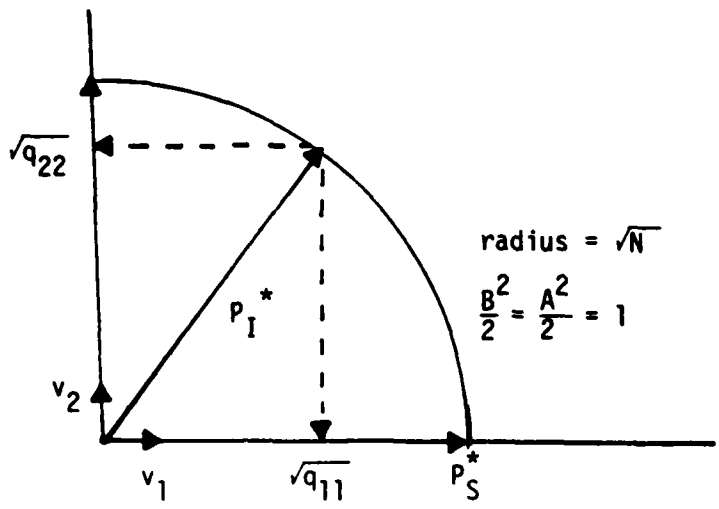

we see that

$$v_2 = \frac{P_I^* - \langle P_I^*, v_1 \rangle v_1}{|P_I^* - \langle P_I^* v_1 \rangle v_1|} \tag{81}$$

Using (79) and (80) we get

$$q_{11} = \frac{B^2}{2} |\langle P_I^*, v_1 \rangle|^2 = \frac{B^2}{2N} |\langle P_I^*, P_s^* \rangle|^2 \tag{82}$$

where we have also used the fact that $|P_s|^2 = P_s^t P_s^* = N$.

Furthermore, using (79) and (80) in conjunction with Appendix B we get

$$q_{22} = \frac{B^2}{2} |\langle P_I^*, v_2 \rangle|^2 = \frac{NB^2}{2} - q_{11} \tag{83}$$

$$q_{21} = q_{12}^* = \frac{B^2}{2} \langle P_I^*, v_2 \rangle \langle v_1, P_I^* \rangle \tag{84}$$

From Appendix C we know that $\langle P_I^*, v_2 \rangle$ is real and thus (84) is seen as

$$|q_{21}| = |q_{12}| = \frac{B^2}{2} \langle P_I^*, v_2 \rangle \; |\langle v_1, P_I^* \rangle| \tag{85}$$

$$\underline{/q_{21}} = \underline{/q_{12}} = \underline{/\arg \langle v_1, P_I^* \rangle} \tag{86}$$

Noting that we can make Λ_I a real matrix if we eliminate the angle introduced in (86), by inspection using (79) we see that we can define a new Q such that

$$Q_n' = A'Q' \tag{87}$$

where

$$A' = \begin{bmatrix} \underline{1/\arg(\langle v_1, P_I^* \rangle)} & & 0 \\ & 1 & \\ & & 1 \\ 0 & & \end{bmatrix} \quad (88)$$

Now using Q'_n we define Λ_I as

$$\Lambda_{nI} = Q_n' \Phi_I Q_n$$

$$= \left[\begin{array}{cc|c} q_{n11} & q_{n12} & \\ q_{n21} & q_{n22} & 0 \\ \hline & 0 & 0 \end{array}\right] \quad (89)$$

where

$$q_{n11} = q_{11} = \frac{B^2}{2N} |\langle P_I, P_s^* \rangle|^2 \quad (90)$$

$$q_{n22} = q_{22} = \frac{B^2}{2} |\langle v_2, P_I^* \rangle|^2 = \frac{NB^2}{2} - q_{11} \quad (91)$$

$$q_{n21} = q_{n12} = \sqrt{q_{11} q_{22}} = |q_{12}| \quad (92)$$

Obviously Λ_{nI} as defined in (89) is a positive real symmetric matrix.

Also we realize from (75) that

$$\Lambda_{ns} = Q_n' \Phi_s Q_n = Q' \Phi_s Q = \Lambda_s \quad (94)$$

As we did in the multiple interference case we let $\Gamma = Q_n' w(t)$. And, using (90)-(94) we see that one interference causes the multiple interference system's weight equations (64)-(69) to become

$$\frac{dP_1(t)}{dt} + 2k[(q_{11} + \lambda_1 + \sigma_n^2)P_1(t) + \sqrt{q_{11} q_{22}} \cos(\theta_1 - \theta_2) P_2(t)]$$

$$= 2k \sqrt{\lambda_1} [a P_r(t) + b_1] \quad (95)$$

$$\frac{dP_2(t)}{dt} + 2k[\sqrt{q_{11} q_{22}} P_1(t) \cos(\theta_2(t) - \theta_1(t))$$

$$+ (q_{22} + \sigma_n^2) P_2(t)] = 0 \quad (96)$$

$$\frac{dP_r(t)}{dt} + 2k_r ca^2 P_r(t) = 2a\, k_r \sqrt{\lambda_1}\, P_1(t) \tag{97}$$

$$P_1(t)\frac{d\theta_1(t)}{dt} + 2k[\sqrt{q_{22}q_{11}}\sin(\theta_2(t) - \theta_1(t))P_2(t)] = 0 \tag{98}$$

$$P_2(t)\frac{d\theta_2(t)}{dt} - 2k[\sqrt{q_{11}q_{22}}\sin(\theta_2(t) - \theta_1(t))P_1(t)] = 0 \tag{99}$$

$$P_r(t)\frac{d\psi(t)}{dt} = 0 \tag{100}$$

Trying to analyze the convergence of $\theta_1(t)$ and $\theta_2(t)$ we can premultiply (98) and (99) by $P_2(t)$ and $P_1(t)$ respectively and substract to get

$$P_1(t)P_2(t)\frac{d(\theta_2-\theta_1)}{dt} - 2k\sqrt{q_{11}q_{22}}[P_1^2(t)+P_2^2(t)]\sin(\theta_2-\theta_1) = 0 \tag{101}$$

or

$$\frac{d(\theta_2-\theta_1)}{dt} = + \frac{2k\sqrt{q_{11}q_{22}}[P_1^2(t) + P_2^2(t)]}{P_1(t)\, P_2(t)} \sin(\theta_2-\theta_1) \tag{102}$$

Assuming that $P_1(t)$ or $P_2(t)$ cannot attain a valve of zero over a finite time interval then the phase difference $\theta_2(t) - \theta_1(t)$ will converge on

$$\theta_2(t) - \theta_1(t) = \pi. \tag{103}$$

Using (103) in (98) and (99) we get

$$P_2(t)\, d\theta_2(t)/dt = 0 \quad \text{or} \quad d\theta_2/dt = 0 \tag{104}$$

$$P_1(t)\, d\theta_1(t)/dt = 0 \quad \text{or} \quad d\theta_1/dt = 0 \tag{105}$$

It can be shown from (95), (96), (97) by inspection that in fact $P_1(t)$, $P_2(t)$, $P_r(t)$ can never attain a steady state value of zero and thus equations (100), (104), (105) hold.

At this point we have shown that the phases of the weights $\psi(t)$, $\theta_1(t)$, $\theta_2(t)$ converge on a steady state value. Now using equation (103) in (95), (96), and (97) we get a linear set of equations for the magnitude of the weights.

$$\frac{dP_1(t)}{dt} + 2k[(q_{11} + \lambda_1 + \sigma_n^2)P_1(t) - \sqrt{q_{11}q_{22}}P_2(t)$$
$$= 2k\sqrt{\lambda_1}[aP_r(t) + b_1] \tag{106}$$

$$\frac{dP_2(t)}{dt} - 2k[\sqrt{q_{11}q_{22}}P_1(t) + [q_{22} + \sigma_n^2]P_2(t) = 0 \tag{107}$$

$$\frac{dP_r(t)}{dt} + 2k_r ca^2 P_r(t) = 2ak_r\sqrt{\lambda_1}P_1(t) \tag{108}$$

or

$$\begin{bmatrix} \dot{P}_1(t) \\ \dot{P}_2(t) \\ \dot{P}_3(t) \end{bmatrix} = \begin{bmatrix} -2k[(q_{11} + \lambda_1 + \sigma_n^2)] & +2k[\sqrt{q_{11}q_{22}}] & -2ka\sqrt{\lambda_1} \\ +2k\sqrt{q_{11}q_{22}} & -2k(q_{22} + \sigma_n^2) & 0 \\ -2ak_r\sqrt{\lambda_1} & 0 & -2k_r ca^2 \end{bmatrix} \begin{bmatrix} P_1(t) \\ P_2(t) \\ P_3(t) \end{bmatrix}$$
$$+ \begin{bmatrix} 2k\sqrt{\lambda_1}\, b_1 \\ 0 \\ 0 \end{bmatrix} \tag{109}$$

The eigenvalues of the matrix in (109) can be obtained by solving the equation

$$(\lambda + 2k_r ca^2)[(\lambda + 2k(\lambda_1 + \sigma_n^2 + q_{11}))(\lambda + 2k(\lambda_2 + \sigma_n^2 - q_{11}))$$
$$- 4k^2 q_{11}(\lambda_2 - q_{11})]$$
$$- 4kk_r\lambda_1 a^2(\lambda + 2k(\lambda_2 + \sigma_n^2 - q_{11})) = 0 \tag{110}$$

when we used the fact that $q_{22} = \frac{NB^2}{2} - q_{11}$ and defined $\lambda_2 = \frac{NB^2}{2}$. (110) can be rearranged to get

$$(\lambda + 2k(\lambda_2 + \sigma_n^2))[(\lambda + 2k_r ca^2)(\lambda + 2k(\lambda_1 + \sigma_n^2)) - 4kk_r\lambda_1 a^2]$$
$$- 4k^2 q_{11}\lambda_1(\lambda + 2k_r a^2(c-1)) = 0 \tag{111}$$

(111) can be looked upon as an equation for the loci of the three eigenvalues when q_{11} varies from 0, when the interference direction is orthogonal to the desired signal direction, to a value equals λ_2, when both direction are the

same. Notice that with no interference $\lambda_2 = \frac{NB^2}{2} = 0$ then by (82) q_{11} is also zero and (111) reduces to

$$(\lambda + 2k\sigma_n^2)[(\lambda + 2k_r ca^2)(\lambda + 2k(\lambda_1 + \sigma_n^2)) - 4kk_r\lambda_1 a^2] = 0 \tag{112}$$

This is exactly what we had in [3]. Also if for the orthogonal case $q_{11} = 0$ but $\lambda_2 \neq 0$ then from (111)

$$(\lambda + 2k(\lambda_2 + \sigma_n^2))[(\lambda + 2k_r ca^2)(\lambda + 2k(\lambda_1 + \sigma_n^2)) - 4kk_r\lambda_1 a^2] = 0 \tag{113}$$

so that for this case the interference has the effect of changing one of the eigenvalues from $-2k\sigma_n^2$ to $-2k(\lambda_2 + \sigma_n^2)$. One can easily show that the other two eigenvalues an unconditionally real and they are both negative when $\frac{c(\lambda_1 + \sigma_n^2)}{\lambda_1} > 1$. For $q_{11} = \lambda_2$ we get after rearranging the terms of (111). (See Appendix D).

$$(\lambda + 2k\sigma_n^2)[(\lambda + 2k_r ca^2)(\lambda + 2k(\lambda_1 + \lambda_2 + \sigma_n^2)) - 4kk_r\lambda_1 a^2] = 0 \tag{114}$$

Again it can be easily shown that the two eigenvalues that correspond to the second factor are unconditionally real and both are negative if

$$c\left(\frac{\lambda_1 + \lambda_2 + \sigma_n^2}{\lambda_1}\right) > 1 \tag{115}$$

The condition is obviously easier to satisfy than the previous condition we obtained with $q_{11} = 0$. Comparing (113) with (114) we notice the difference in the second factor of the first term in the square parenthesis where we have $\lambda_1 + \lambda_2$ representing the sum of power of both the interference and the design signal instead of λ_1 representing the power of the desired signal only. The first terms in the parenthesis remain unchanged since the reference generating loop is not affected by the interference.

In order to get an idea of what happens to the eigenvalues as the interference direction varies between the orthogonal and colinear directions of the desired signal we can plot the root loci of (111) keeping in mind that q_{11}

increases from zero to λ_2 as the direction of the interference moves from an orthogonal to a colinear direction. Doing this we can prove that the eigenvalues will always have a negative real part as long as $\frac{c(\lambda_1 + \sigma_n^2)}{\lambda_1} > 1$. The proof is given in Appendix E.

The steady state values of the weights are derived by setting the left-hand side of (109) to zero and evaluating. Doing this

$$\lim_{t\to\infty} \begin{bmatrix} P_1(t) \\ P_2(t) \\ P_3(t) \end{bmatrix} = \frac{-1}{2k[q_{22}(c(\sigma_n^2 + \lambda_1) - \lambda_1) + \sigma_n^2(c(q_{11} + \sigma_n^2 + \lambda_1) - \lambda_1)]}$$

$$\begin{bmatrix} c[q_{22} + \sigma_n^2] & +c\sqrt{q_{11}q_{22}} & \frac{k}{k_r a}\sqrt{\lambda_1}[q_{22} + \sigma_n^2] \\ +c\sqrt{q_{11}q_{22}} & [c(\lambda + \sigma_n^2 + q_{11}) - \lambda_1] & \frac{k}{k_r a}\sqrt{\lambda_1 q_{11} q_{22}} \\ \frac{\sqrt{\lambda_1}}{a}[q_{22} + \sigma_n^2] & \frac{1}{a}\sqrt{\lambda_1 q_{11} q_{22}} & \frac{k}{k_r a^2}[(q_{22} + \sigma_n^2)(\lambda_1 + \sigma_n^2) + \sigma_n^2 q_{22}] \end{bmatrix}$$

$$\begin{bmatrix} -2k\sqrt{\lambda_1}b_1 \\ 0 \\ 0 \end{bmatrix} \tag{121}$$

or

$$\lim_{t\to\infty} P_1(t) = \frac{+\sqrt{\lambda_1}b_1 c[q_{22} + \sigma_n^2]}{G} \tag{122}$$

$$\lim_{t\to\infty} P_2(t) = \frac{\sqrt{\gamma_1}cb_1\sqrt{q_{11}q_{22}}}{G} \tag{123}$$

$$\lim_{t\to\infty} P_r(t) = \frac{\frac{\lambda_1 b_1}{a}[q_{22} + \sigma_n^2]}{G} \tag{124}$$

where

$$G = q_{22}[c(\sigma_n^2 + \lambda_1) - \lambda_1] + \sigma_n^2[c(q_{11} + \sigma_n^2 + \lambda_1) - \lambda_1] \quad (125)$$

To conclude we notice that under the conditions specified the added complex weight $w_r(t)$ convergeson a steady state value which cancels the reference loop phase shift ϕ. By doing this we have shown that the result is the elimination of the weight cycling.

We have also shown that an increase in the interference power will make one of the eigenvalues more negative, thus giving a stabilizing effect to the system. In general, we see that the array weight's convergence rates depend on the power as well as the relative directions of the interference and desired signal.

V. The Uncompensated Scheme With Single Interference

The uncompensated scheme will be considered as a special case of the compensated scheme with $P_r(t) = 1$ and $\psi(t) = 0$. Using this in (56) and (57) respectively we get

$$\frac{dP_1(t)}{dt} + 2k(q_{11} + \lambda_1 + \sigma_n^2)P_1(t) + 2kq_{12}P_2(t)\cos(\theta_1(t) - \theta_2(t)) = 2ka\sqrt{\lambda_1}\cos\phi \quad (126)$$

$$\frac{dP_2(t)}{dt} + 2kq_{21}P_1(t)\cos(\theta_2(t) - \theta_1(t)) + 2k(q_{22} + \sigma_n^2)P_2(t) = 0 \quad (127)$$

Similarly (60) and (59) become

$$P_1(t)\frac{d\theta_1(t)}{dt} + 2kq_{12}P_2(t)\sin(\theta_1(t) - \theta_2(t)) = 2ka\sqrt{\lambda_1}\sin\phi \quad (128)$$

$$P_2(t)\frac{d\theta_2(t)}{dt} - 2kq_{21}P_1(t)\sin(\theta_1(t) - \theta_2(t)) = 0 \quad (129)$$

A general solution for the differential equations of (126),(127),(128), and (129) has not yet been found. However, for the case when the direction vector

of the interferer and the desired signal are othogonal (i.e., $\langle P_I P_s \rangle = 0$) we can reduce the problem. For this case we get from (82), (83), and (84) that

$$q_{11} = q_{21} = q_{12} = 0 \tag{130}$$
$$q_{22} = \frac{NB^2}{2}$$

Substituting (130) and (131) into (126), (127), (128), and (129) we get

$$\frac{dP_1(t)}{dt} + 2k(\lambda_1 + \sigma_n^2)P_1(t) = 2ka\sqrt{\lambda_1}\cos\phi \tag{131}$$

$$\frac{dP_2(t)}{dt} + 2k(q_{22} + \sigma_n^2)P_2(t) \tag{133}$$

$$P_1(t)\frac{d\theta_1(t)}{dt} = 2ka\sqrt{\lambda_1}\sin\phi \tag{134}$$

$$P_2(t)\frac{d\theta_2(t)}{dt} = 0 \tag{135}$$

From the solution of (133) we see that the weight $\gamma_2(t) = P_2(t)\exp[-j\theta_2(t)]$ will exponentially decay to a steady state value of zero. Also we note that (132) and (134) are the equivalent to the weight equations derived by DeCarlo [4] for the interference free case. (n.b. equations (30) and (33) of reference [4]). In his solution DeCarlo showed that the magnitude of the weight ($|\gamma_1(t)| = P_1(t)$) would converge on a steady state value proportional to the cosine of the phase offset ϕ. However the phase of the weight ($\arg(\gamma_1(t)) = \theta_1(t)$) will oscillate at a radian frequency proportional to the tangent of the phase offset ϕ.

To conclude we see that when the direction vector of the interference is orthogonal to that of the desired signal, the interference will have no effect on the system weights. And we see that the weights will approach a limit cycle in exactly the same fashion as DiCarlo [4] predicted for the no interference case.

VI. Conclusion

In this paper we have devised a method by which we have been able to better study the effects of interference on the array weights of an adaptive array system. Using this method we have further analyzed Bar-Ness's compensation scheme [3] and have shown that for a multiple interference case the reference loop phase shift is effectively compensated for. We have also been able to show that for the single interference case the array weights will converge on a steady-state value. For the uncompensated Compton scheme [2] it was demonstrated that the array weights will cycle for the special case of one interference with a direction vector orthogonal to that of the desired signal. Future work is planned for the study of a general solution for the multiple interference case with Bar-Ness's Compensation Scheme as well as a general solution for the single interfernece case with Compton's scheme. Furthermore, analysis is planned for the signal to noise plus interference ratio of Bar-Ness's scheme in a single interference environment.

Appendix A

The desired signal's auto correlation matrix Φ_s is defined in (15) as

$$\Phi_s = \frac{A^2}{2} P_s^* P_s^t = \frac{A^2}{2} \begin{bmatrix} 1 & e^{-j\alpha_2} & \cdots & e^{-j\alpha_n} \\ e^{j\alpha_2} & & & \\ \vdots & & & \\ e^{j\alpha_n} & & & 1 \end{bmatrix}_{n \times n} \tag{A1}$$

Φ_s is Hermetian having rank equal to one. Therefore, a unitary matrix exists such that $\Lambda_s = Q'\Phi_s Q$ is a diagonal matrix with only one non zero element. Thus

$$\Lambda_s = Q'\Phi_s Q = \begin{bmatrix} \lambda_1 & 0 & \cdots & 0 \\ 0 & & & \\ \vdots & & & \\ 0 & & & 0 \end{bmatrix} \tag{A2}$$

Since we have used a similarity transformation to obtain Λ_s, we see that:

$$\text{Trace}[\Phi_s] = \text{Trace}[\Lambda_s] \tag{A3}$$

Thus by inspection of (A1) and (A2) we get

$$\lambda_1 = \frac{NA^2}{2} \tag{A4}$$

We can more formally define the diagonalizing matrix Q as

$$Q' = \begin{bmatrix} \_\_ v_1' \_\_ \\ \_\_ v_2' \_\_ \\ \vdots \\ \_\_ v_n' \_\_ \end{bmatrix} \tag{A5}$$

Where since Φ_s is Hermetian, v_i(i=1 to n) form an orthonormal set of

eigenvectors where v_1 is the eigenvector corresponding to the one nonzero eigenvalue of Φ_s and

$$v_1 = P_s/|P_s|. \tag{A6}$$

Also, v_i(i=2 to N) are the eigenvectors corresponding to the N-1 zero eigenvalues of Φ_s.

Now, turning our attention to the M interferers, we see that the autocorrelation matrix Φ_{I_i}(i = 1 to M) of each interference is defined in (16) as

$$\Phi_{I_i} = \frac{B_i^2}{2} P_{I_i} P_{I_i}^* = \begin{bmatrix} 1 & e^{-jb_{i_2}} & \cdots & e^{-jb_{i_n}} \\ e^{jb_{i_2}} & \ddots & & \\ \vdots & & \ddots & \\ e^{jb_{i_n}} & & & 1 \end{bmatrix} \tag{A7}$$

Each matrix Φ_{I_i}(i = 1 to M) is Hermetian of rank 1. Thus we see that a matrix defined by $\sum_{i=1}^{M} \Phi_{I_i}$ will also be Hermetian and have rank $\leq$ M. Now leaving v_1 alone so that (A2) is always satisfied we can see that the vectors v_i (i = 2 to M+1) can always be made so that v_j(j = 1 to M+1) will span the M-space spanned by $\sum_{i=1}^{M} \Phi_{I_i}$. And, the eigenvectors v_k(k = M+2 to N) can be made orthogonal to that M-space as well as the direction of v_1. By doing this we can get a transformation of the matrix $\sum_{i=1}^{M} \Phi_i$ such that

$$\Lambda_I = Q' \sum_{i=1}^{M} \Phi_i Q = \begin{bmatrix} \begin{bmatrix} q_{i_j} & \cdots \\ \vdots & \ddots \end{bmatrix}_{M+1,M+1} & 0 \\ 0 & 0 \end{bmatrix} \tag{A8}$$

where since this a similarity transformation Λ_I must be Hermetian and therefore

$$q_{ij} \text{ - positive and real} \qquad i = j \tag{A9}$$

$$q_{ij} = q_{ji}^{*} \text{ - complex} \qquad i \neq j \tag{A10}$$

For $i \neq j$ we can write q_{ij} in the form

$$q_{ij} = q_{ij}^{+} \, e^{-j\rho_{ij}} \tag{A11}$$

where

$$q_{ij}^{+} = |q_{ij}| \tag{A12}$$

$$\rho_{ij} = \arg[q_{ij}] \tag{A13}$$

Appendix B

From (83)

$$q_{22} = \frac{B^2}{2} |\langle P_I^*, v_2\rangle|^2 \tag{B1}$$

Substituting for v_2 from (81)

$$q_{22} = \frac{B^2}{2} |\langle P_I^*, \frac{P_I^* - \langle P_I^*, v_1\rangle v_1}{|P_I^* - \langle P_I^*, v_1\rangle v_1|} \rangle|^2 \tag{B2}$$

or

$$q_{22} = \frac{B^2}{2} \frac{\langle P_I^*, P_I^*\rangle - \langle P_I^*, v_1\rangle^* \langle P_I^* v_1\rangle}{|P_I^* - \langle P_I^*, v_1\rangle v_1|}|^2 \tag{B3}$$

Evaluating the demoninator

$$|P_I^* - \langle P_I^*, v_1\rangle v_1| = [\langle P_I^* - \langle P_I^*, v_1\rangle v_1, P_I^* - \langle P_I^*, v_1\rangle v_1\rangle]^{\frac{1}{2}} \tag{B4}$$

$$= [\langle P_I^*, P_I^*\rangle - \langle P_I^*, v_1\rangle\langle v_1, P_I^*\rangle - \langle P_I^*, v_1\rangle^*\langle P_I^*, v_1\rangle + \langle P_I^*, v_1\rangle\langle P_I^*, v_1\rangle]^{\frac{1}{2}} \tag{B5}$$

or

$$|P_I - \langle P_I^*, v_1\rangle v_1| = [\langle P_I^*, P_I^*\rangle - \langle P_I^*, v_1\rangle\langle v_1, P_I^*\rangle]^{\frac{1}{2}} \tag{B6}$$

Substituting (B6) into (B3) we get

$$q_{22} = \frac{B^2}{2} [\langle P_I^*, P_I^*\rangle - \langle P_I^*, v_1\rangle^* \langle P_I^* v_1\rangle] \tag{B7}$$

$$= \frac{B^2}{2} [\langle P_I^*, P_I^*\rangle - |\langle P_I^*, v_1\rangle|^2] \tag{B8}$$

But $\langle P_I^*, P_I^*\rangle = N$ (B9)

and from (82)

$$\frac{B^2}{2} |\langle P_I^*, v_1\rangle|^2 = q_{11} \tag{B10}$$

Thus (B8) becomes

$$q_{22} = \frac{NB^2}{2} - q_{11} \tag{B11}$$

Appendix C

Using the definition of v_2 from (82) we get

$$\langle P_I^*, v_2 \rangle = \langle P_I^*, \frac{P_I^* - \langle P_I^*, v_1 \rangle v_1}{|P_I^* - \langle P_I^*, v_1 \rangle v_1|} \rangle \tag{C1}$$

or

$$\langle P_I^*, v_2 \rangle = \frac{\langle P_I^*, P_I^* \rangle - \langle P_I^*, v_1 \rangle^* \langle P_I^*, v_1 \rangle}{|P_I^* - \langle P_I^*, v_1 \rangle v_1|} \tag{C2}$$

Substituting for the demoninator from (B6) and using (B10) we get

$$\langle P_I^*, v_2 \rangle = [\langle P_I^*, P_I^* \rangle - \langle P_I^*, v_1 \rangle^* \langle P_I^*, v_1 \rangle]^{\frac{1}{2}} \tag{C3}$$

$$= [N - |\langle P_I^*, v_1 \rangle|^2]^{\frac{1}{2}} \tag{C4}$$

Thus from (C4) we see that $\langle P_I^*, v_2 \rangle$ will always be a real number.

Appendix D

Substituting $q_{11} = \lambda_2$ in (111), we get after rearranging terms

$$(\lambda + 2k_r ca^2)[(\lambda + 2k(\lambda_2 + \sigma_n^2))(\lambda + 2k(\lambda_1 + \sigma_n^2)) + 4k^2\lambda_1\lambda_2]$$
$$- 4kk_r\lambda_1 a^2(\lambda + 2k(\lambda_2 + \sigma_n^2)) + 8k^2\lambda_1\lambda_2 k_r a^2 = 0 \qquad \text{(D1)}$$

or

$$(\lambda + 2k_r ca^2)[\lambda^2 + 2k(\lambda_1 + \lambda_2 + 2\sigma_n^2)\lambda + 4k^2\sigma_n^2(\lambda_1 + \lambda_2)$$
$$+ 4k^2(\sigma_n^2)^2] - 4kk_r\lambda_1 a^2(\lambda + 2k\sigma_n^2) = 0 \qquad \text{(D2)}$$

Factoring the first and rearranging we finally get

$$(\lambda + 2k\sigma_n^2)[(\lambda + 2k_r ca^2)(\lambda + 2k(\lambda_1 + \lambda_2 + \sigma_n^2)) - 4kk_r\lambda_1 a^2] = 0 \qquad \text{(D3)}$$

Appendix E

We know by solving (113) that the roots of (111) for $q_{11} = 0$ are unconditionally real and negative if $c(\lambda_1 + \sigma_n^2)/\lambda_1 > 1$. Thus under this condition the root loci of (111) has 3 poles and one zero all on the negative real axis. We are only interested in the roots for $0 < q_{11} < \lambda_2$ and we realize from (114) that the roots of (111) as q_{11} approaches λ_2 will be unconditionally real and negative under the previous specified condition. Below are the 4 possible paths which the root loci of (111) can follow according to the above specifications

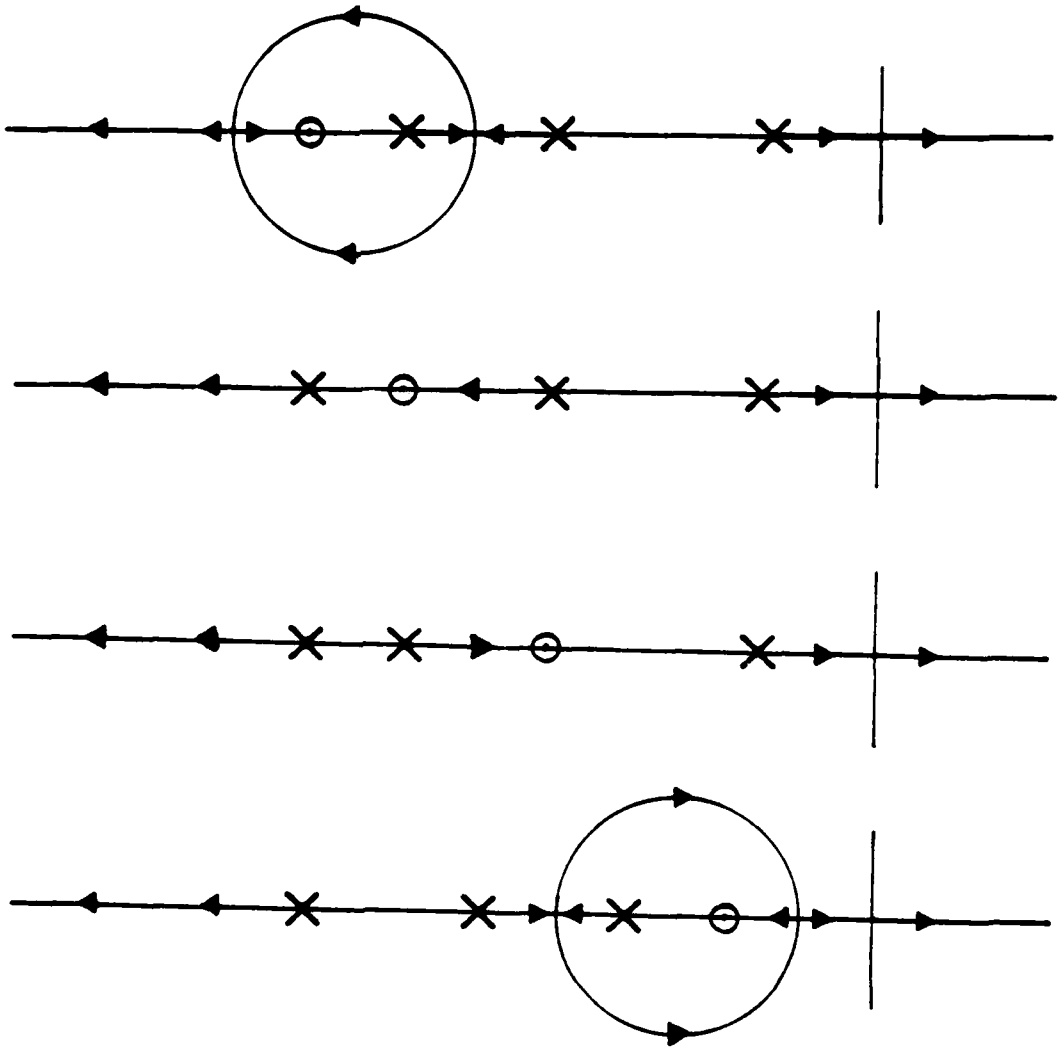

where the arrows point in the direction of increasing q_{11}. The poles for $q_{11} = 0$ are defined by the roots of (113) and from (111) the zero is at $-2k_r a^2(c - 1)$.

Obviously since we see from the above root loci that if for the maximum value of $q_{11} = \lambda_2$ the roots of (111) are negative and real so that for any value of $q_{11} < \lambda_2$ the root must always have a negative real part.

As an example let's assume the following values

$c = 1.2$ $\quad k = 50$ $\quad \sigma_n^2 = .001$

$a = 8.33$ $\quad k_r = 25$

$b = 1.6262$ $\quad \lambda_1 = 1$ $\quad \lambda_2 = 1/2$

From (113) the equation for the roots when $q_{11} = 0$ is:

$$(\lambda - 50.1)[(\lambda + 4166.33)(\lambda + 100.1) - 347{,}194.45] \qquad \text{(E1)}$$

which has roots at

$\lambda = -50, -16.4, -4249.9$

Notice also that the zero for this root loci is found from (111) to be -694.43.

As we increase q_{11} to $\lambda_2 = 1/2$ from (114) we get roots at $\lambda = -.1, -65.4, -4251$.

The root loci is plotted as

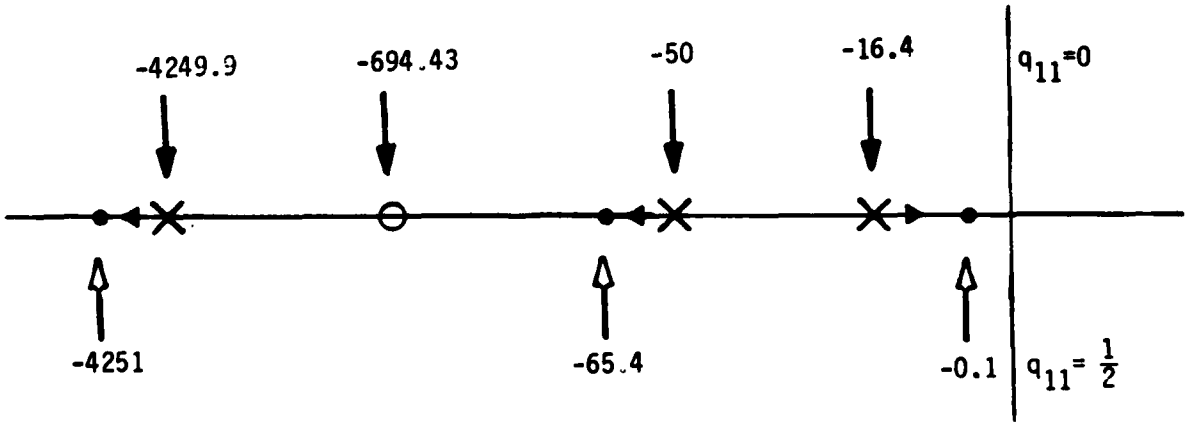

Notice from (113) and (E1) that an increase in interference power will only affect the eigenvalue at $\lambda = -50$. In fact an increase in power will cause this eigenvalue to become more negative, thus helping to stabilize the system.

References

[1] Widrow, B., McCool, J. and Ball, J. (1975), "The Complex LMS Algorithm", Proceedings of the IEEE, April 1975.

[2] DiCarlo, D.M., and Compton, R.T., Jr., (1978), "Reference Loop Phase Shift in Adaptive Arrays", IEEE Transactions on Aerospace and Electronic Systems, July 1978, AES-14.

[3] Bar-Ness, Y., (1982), "Eliminating Reference Loop Phase Shift in Adaptive Arrays", IEE Transactions on Aerospace and Electronic Systems, January, 1982, AES-18.

[4] DiCarlo, D.M., (1979), "Reference Loop Phase Shift in a N-element Adaptive Array", IEEE Transactions on Aerospace and Electronic Systems, July, 1979, AES-15.

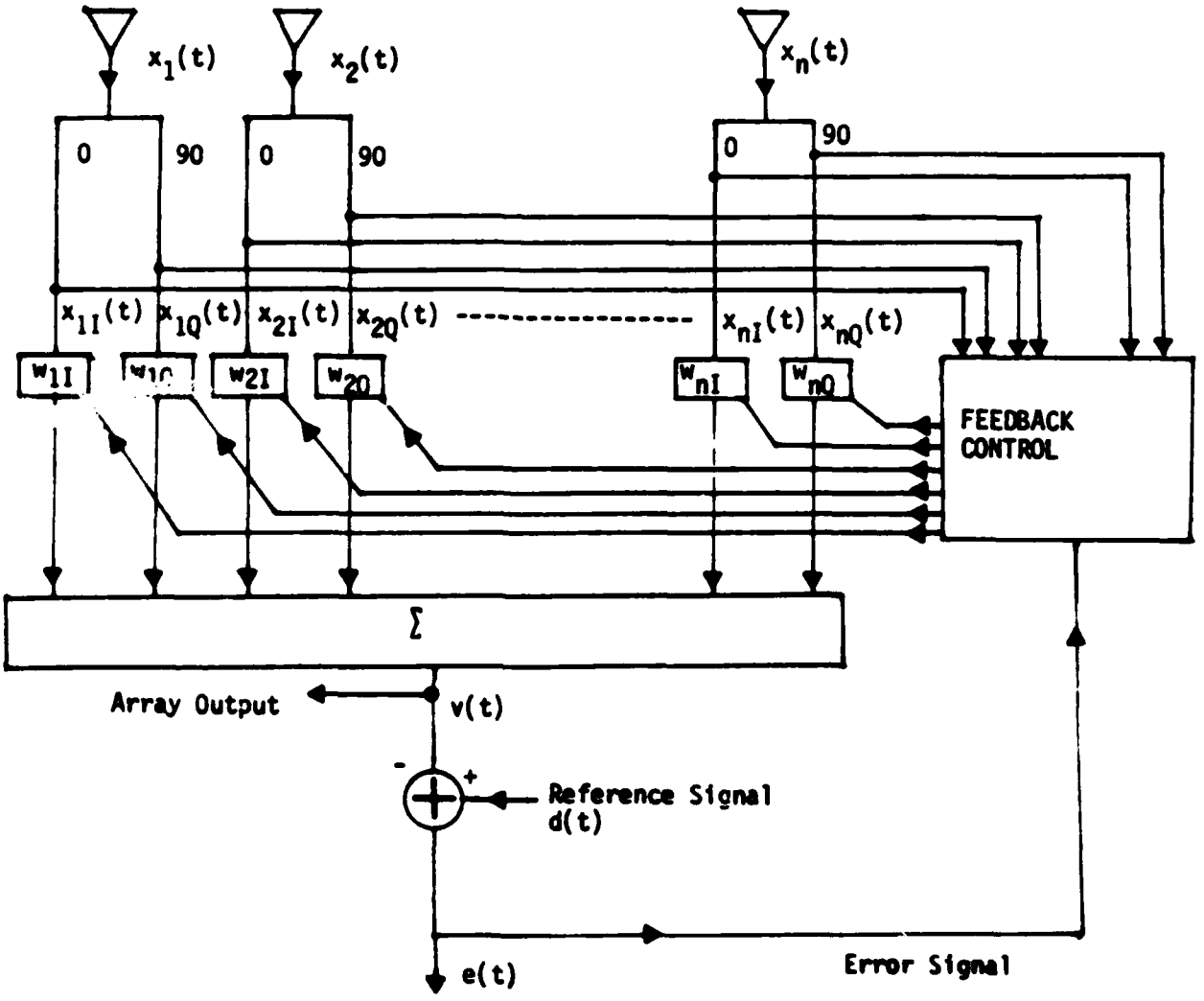

Figure 1 Quadrature Weighted Adaptive Array

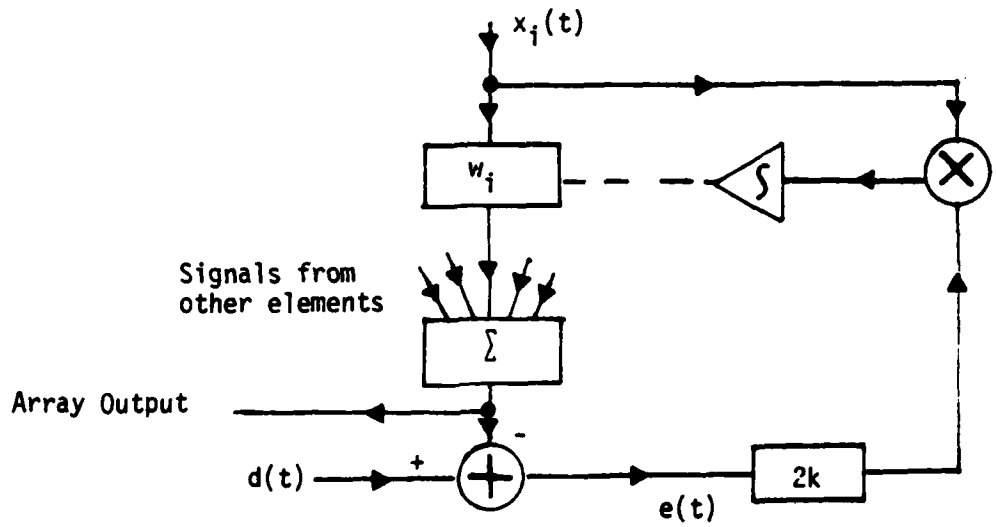

Figure 2 Main Feedback Loop for LMS Algorithm Realization

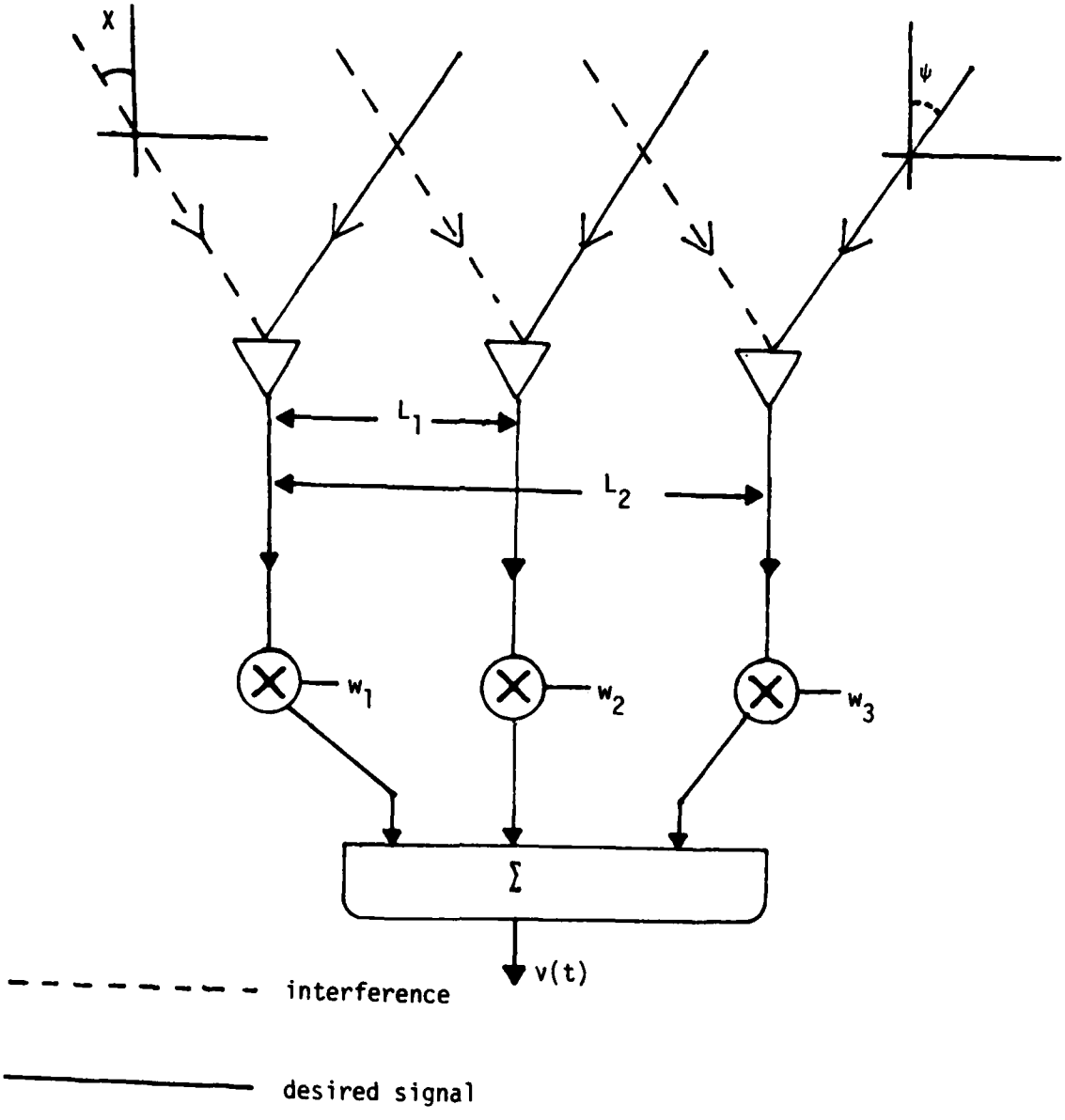

Figure 3 Arrival of desired signal and interference for 3 element array

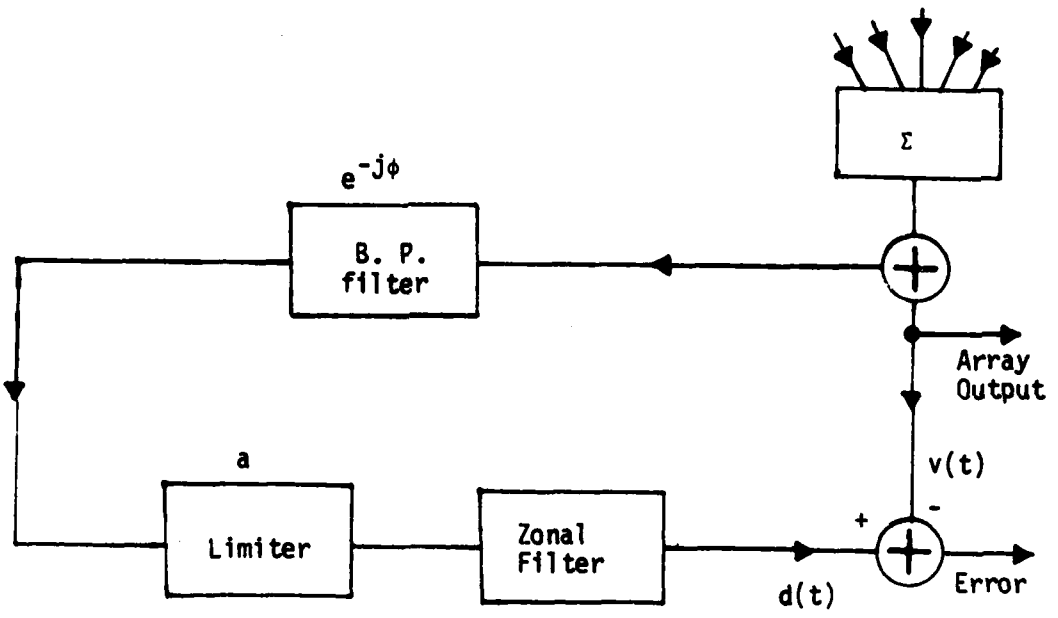

Figure 4 Reference Signal Loop

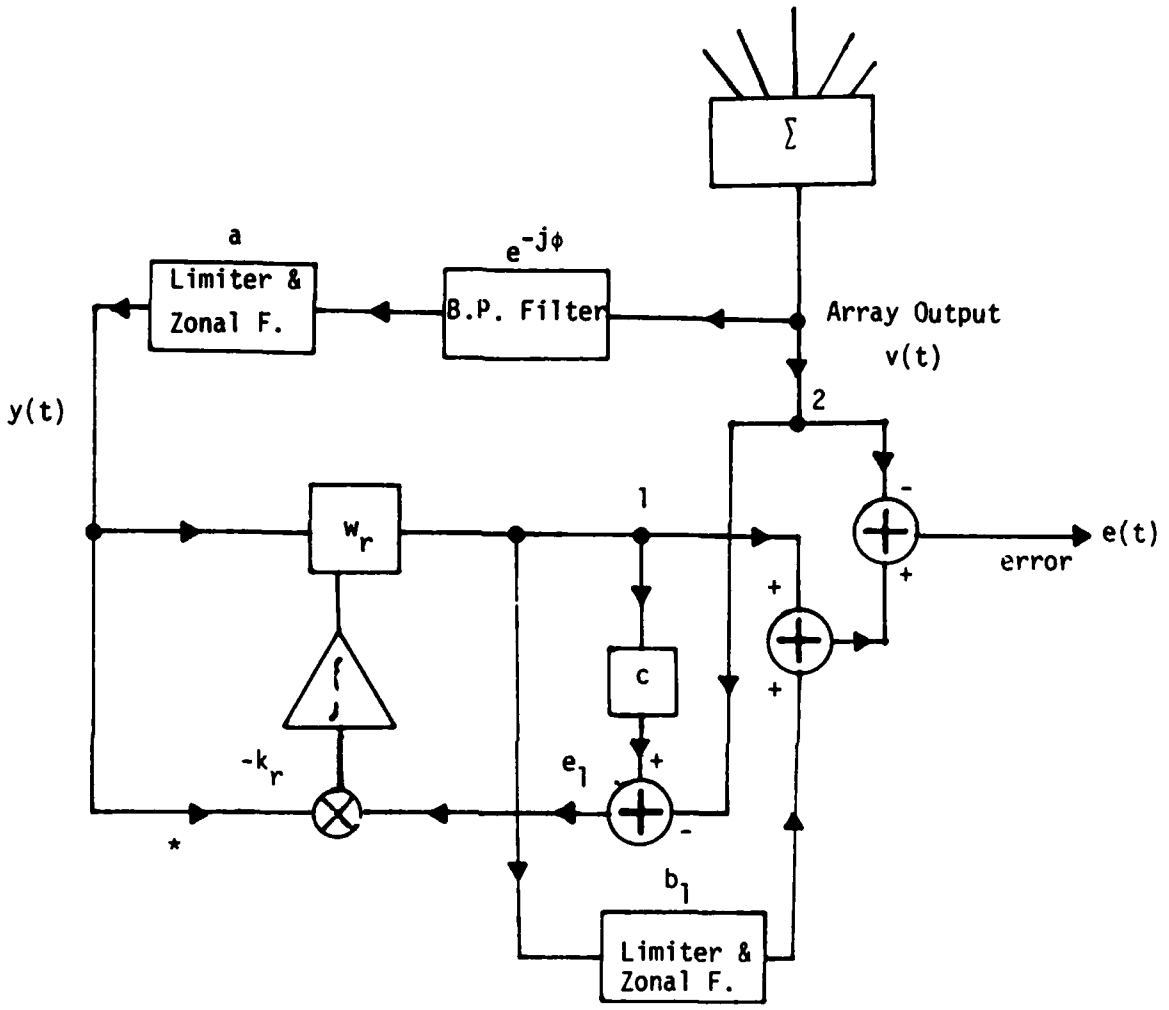

Figure 5 Phase-Compensated Reference Signal Loop

List of Symbols - Appendix F

A	desired signal's amplitude
a	constant dependent on the limiter level and filter attenuation of the reference extraction loop
B_i	i^{th} interference amplitude
b_l	compensation scheme limiter level
b_{ij}	phase of the i^{th} interference at the j^{th} element
c	compensation loop weighting factor
d(t)	reference signal
E[ ]	denotes expected value
e(t)	error signal for array LMS algorithm
$e_l(t)$	error signal of compensation scheme
k	gain constant for LMS algorithm in array weights
k_r	gain constant for LMS algorithm in compensation loop
L_j	distance between 1^{st} and j^{th} antenna element
M	number of interferers
N	number of array elements
$P_i(t)$	magnitude of linear transformed array weights
$P_{Ii}{}^T$	i^{th} interference incoming phase vector (1 x N)
$P_r(t)$	magnitude of the complex compensation weight $w_r(t)$
$P_S{}^T$	desired signal's phase vector (1 x N)
Q	diagonalizing matrix [N x N]
q_{ij}	components of Λ_I
q^+_{ij}	magnitude of q_{ij}
R_x	input signal autocorrelation matrix
R_{xd}	input-reference signal cross-correlation matrix
t	denotes transpose

(Continued)

v_i - eigenvectors of Φ_s used as vector components of Q

$w^T(t)$ - complex antenna element weight vector (1 x N)

$w_i(t)$ - components of $w^T(t)$ corresponding to the i^{th} complex array weight

$w_r(t)$ - complex reference extraction loop compensation weight

$x^T(t)$ - system's input vector (1 x N)

$x_{iI}(t)$ - inphase component of the i^{th} array element input

$x_{iQ}(t)$ - quadrature component of the i^{th} array element input

$y(t)$ - input to the compensation scheme

α_j - phase of desired signal at the j^{th} element

$\Gamma^T(t) = Q'w(t)$

- uncoupled complex array weight vector (1 x N)

γ_i - components of $\Gamma^T(t)$ corresponding to the i^{th} complex transformed array weight

θ_i - phase of linear transformed array weight

$\Lambda_s = Q' \Phi_s Q$

- diagonalized desired signal's autocorrelation matrix (N x N)

$\Lambda_I = \sum_{i=1}^{M} Q' \Phi_{Ii} Q$

- sum of the diagonalized interference signals autocorrelation matrices (N x N)

$\lambda_1 = NA^2/2$; only nozero component of Λ_s

$\lambda_2 = NB^2/2$; trace of Λ_I

ρ_{ij} - angle of the complex value q_{ij}

ϕ - phase shift introduced by uncompensated reference signal loop

Φ_{Ii} - i^{th} interference autocorrelation matrix (N x N)

Φ_s - desired signal's autocorrelation matrix (N x N)

$\psi(t)$ - phase of the complex compensation weight $w_r t$

(Continued)

List of Symbols - Appendix F
(Continued)

$\|\ \|$	denotes magnitude
$<\ >$	denotes inner produce
$*$	denotes conjugate
$'$	denotes transponse conjugate

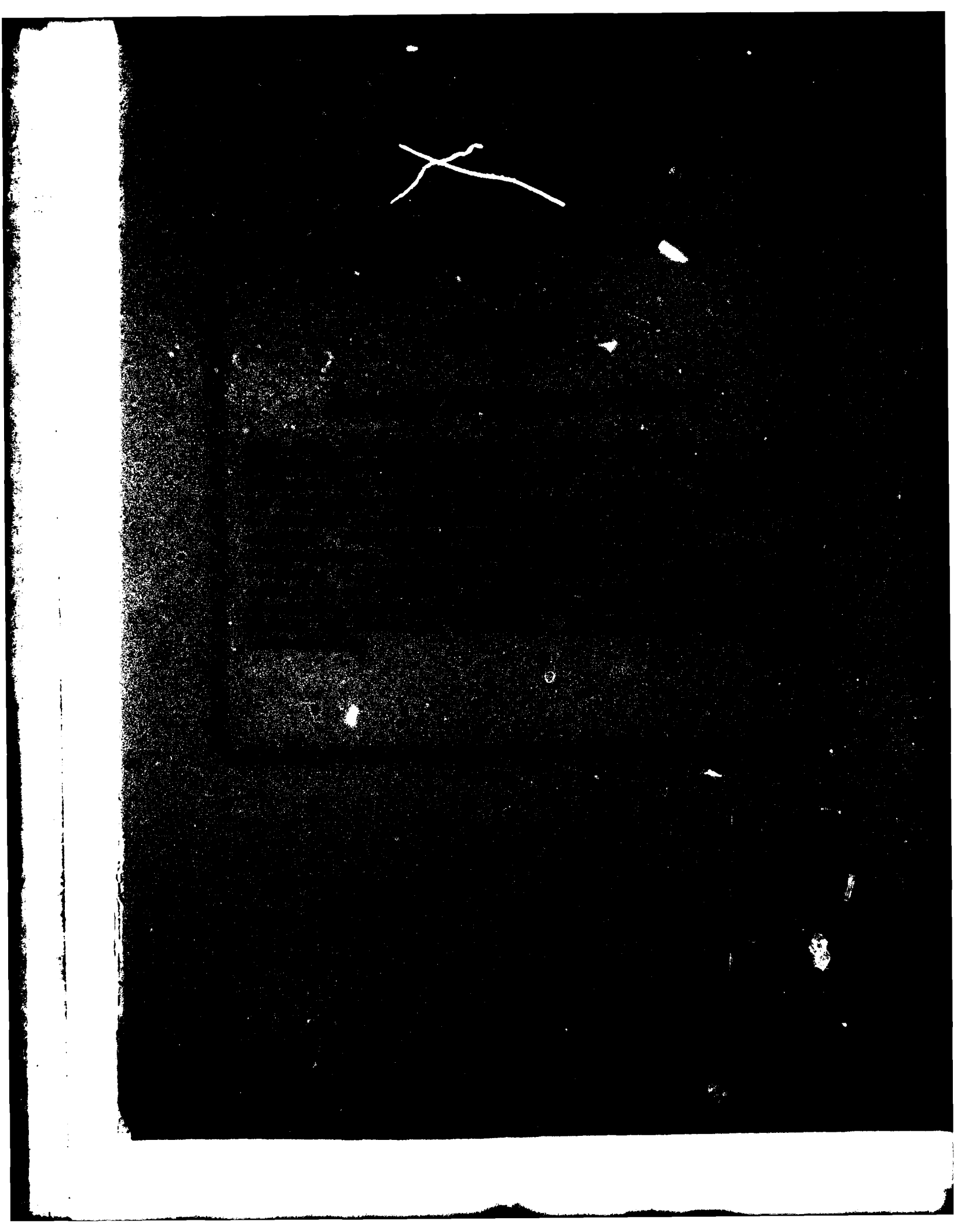

END

DATE
FILMED

11-83

DTIC